"Jaszowiec" 2016

45th International School & Conference on the Physics of Semiconductors

Hotel Klimczok, Szczyrk, Poland, June 18th - 24th, 2016

Institute of Physics, Polish Academy of Sciences
Faculty of Physics, University of Warsaw, Institutes of Experimental and Theoretical Physics
Institute of High Pressure Physics, Polish Academy of Sciences
Divisions of Experimental and Theoretical Physics, Wrocław University of Science and Technology
Institute of Electron Technology
The Foundation "Pro Physica"
Ministry of Science and Higher Education (Republic of Poland)
Polish Academy of Sciences

"Jaszowiec" 2016

45th International School & Conference
on the Physics of Semiconductors
SZCZYRK, POLAND
June 18th – 24th, 2016

Organized by:

- Institute of Physics, Polish Academy of Sciences
- Faculty of Physics, University of Warsaw
  (Institute of Experimental Physics and Institute of Theoretical Physics)
- Institute of High Pressure Physics, Polish Academy of Sciences
- Divisions of Experimental and Theoretical Physics,
  Wrocław University of Science and Technology
- Institute of Electron Technology
- Polish Academy of Sciences
- Foundation „Pro-Physica"
- Ministry of Science and Higher Education, Republic of Poland

---

www.jaszowiec.edu.pl

Warsaw, 2016

International Advisory Committee

Günther Bauer, *Linz*
Laurence Eaves, *Nottingham*
Jacek K. Furdyna, *Notre Dame*
David Gershoni, *Haifa*
Paweł Hawrylak, *Ottawa*
Detlef Hommel, *Wrocław*
Hideo Ohno, *Sendai*
Marek Potemski, *Grenoble*
Denis Scalbert, *Montpellier*
Maurice S. Skolnick, *Sheffield*
Wladek Walukiewicz, *Berkeley*
Dmitri Yakovlev, *Dortmund*

Program Committee

Adam Babiński
Witold Bardyszewski
Piotr Bogusławski
Łukasz Cywiński
Marta Gryglas-Borysiewicz - *Chair of the Tutorial Session*
Izabella Grzegory
Krzysztof Korona
Piotr Kossacki
Jacek Kossut
Bogdan Kowalski
Jerzy Łusakowski
Paweł Machnikowski
Anna Piotrowska
Maciej Sawicki - *Chair*
Grzegorz Sęk
Czesław Skierbiszewski
Tomasz Story
Bartłomiej Witkowski – *Secretary*

Organizing Committee

Martyna Cinak-Modzelewska
Marta Gryglas-Borysiewicz
Maciej Sawicki
Bartłomiej Witkowski
Maciej Zajączkowski

Sponsoring organizations and companies:

- Ministry of Science and Higher Education, Republic of Poland
- U.S. Navy - Office of Naval Research
- US Army International Technology Center-Atlantic

Exhibitors:

Partner:

WELCOMING ADDRESS

It is my great honor to welcome each and every one of you to the 45th "Jaszowiec" International School and Conference on the Physics of Semiconductors, which this year makes another quantum hop - to Szczyrk. I hope that you will find the new location well suited for exchanging scientific ideas both at the venue facilities and in the gorgeous surrounding. The Conference follows the nearly half a century long tradition of gathering representatives of the semiconductor community from all over the world to present their recent achievements, to be inspired by new ideas and to find responses to relevant scientific questions. The daily schedule recovers this year the old good custom of providing the participants with free afternoons to foster the discussions with old friends and to build new scientific cooperation and friendships.

The scope of the Conference covers, in particular, topics like low-dimensional and layered semiconductor structures, topological matter, wide gap semiconductors, and spintronics. This year a new theme has been introduced, namely the physics of phase separated materials. All topics are considered from various perspectives including technological applications, experiment, theory, and modeling.

Like in a half of the previous meetings also this Conference is preceded by a School, specifically, a two-day tutorial session, during which five outstanding teachers and scientists will introduce some of the hottest subjects relevant to today's semiconductor physics. The event targets primarily young scientists, undergraduate and postgraduate students, but all the Conference attendees are warmly welcome! Both the School lecturers and Marta Gryglas-Borysiewicz, who chairs this event for the first time, truly deserve our special acknowledgment!

I wish also to express my gratitude to the members of the Program and Advisory Committees who took the responsibility of shaping the scientific schedule of "Jaszowiec" 2016. I wish also to acknowledge the tremendous effort put forward by the Organizing Committee: Batłomiej Witkowski, the Secretary of the Conference and Martyna Cinak-Modzelewska and Maciej Zajączkowski who all made the leap to a new venue possible and who will continue to work hard to support our scientific meeting here in Szczyrk.

I also gratefully acknowledge the financial support of the Eight Organizing Institutions and our local and overseas sponsors. Without them "Jaszowiec" 2016 would not have assumed the form it takes now.

Finally, there would be no conference without you, the Participant. To you goes my final address of gratitude. Many thanks for choosing "Jaszowiec" this year! And for your effort in preparing a contribution which will be essential for the success of the event. I hope you will profit from the time spent here and you will leave the Conference with nice and lasting memories. So, enjoy your stay in Szczyrk, enjoy the Conference!

Your Chairman of the Conference
Maciej (Mike) Sawicki

Artur Ginalski
Edwards
Manor Royal
Crawley, West Sussex
RH10 9LW United Kingdom
Mobile: +48 734 474 189
Tel: +48 22 572 68 00
Email: artur.ginalski@edwardsvacuum.com
Web: www.edwardsvacuum.com

Edwards Vacuum

Edwards is a leading developer and manufacturer of sophisticated vacuum products, abatement solutions and related value-added services.
Our products are integral to manufacturing processes for semiconductors, flat panel displays, LEDs and solar cells; are used within an increasingly diverse range of industrial processes including power, glass and other coating applications, steel and other metallurgy, pharmaceutical and chemical; and for both scientific instruments and a wide range of R&D applications.

Our Technology Leadership

As a trusted partner, we have well-established customer relationships with many of the world's leading manufacturers and a deep understanding of their key process challenges. Our technology know-how and application experience foster innovative solutions which help optimize processes through long-standing collaboration and partnerships.

- ***Innovation*** We convert our industry knowledge and product technology insight into innovative product solutions that create customer advantage and value.
- ***Application*** Every day we work with more customers that our competitors to better understand their needs and ensure we deliver optimized total vacuum solutions.
- ***Partnerships*** We collaborate with customers and across industries to develop products on some of the most demanding applications.

Ultra High Vacuum Pump Products For Research & Development Labs

We offer a broad range of vacuum products to meet the challenges of today's research and development laboratories. Collaboration with major scientific instrument manufacturers, universities and major research institutes ensures a deep understanding of research and the role that vacuum plays. Our focus on technological advancement in vacuum as well as investment in R&D enables us to develop the innovative products that meet your specific application requirements.

- **Single Supplier:**
  Wide Portfolio of Class Leading Products Under One Roof
- **Best Solution Based on Optimum Technologies:**
  From UHV (Ultra High Vacuum) to Atmosphere
- **Peace of Mind:**
  Experience to Help You Choose the Best Solution

Semiconductor Processing

We continue to innovate leading technology solutions which will improve your process up-time, yield, throughput and safety compliance whilst striving to balance the often conflicting requirements of lower cost of ownership through reduced environmental emissions and extended product lifetimes with a reduction in on-going service costs.

Serving all leading process tool OEMs and with a presence at every major semiconductor fab in the world, our systems are designed to meet the specific requirements of existing and developing processes. A variety of systems, such as dry vacuum pumps, turbomolecular pumps and point-of-use abatement systems are offered to optimise performance across the range of applications, from light duty to the heaviest duty processes.

Pawel Wrona, *Labis*
Oleksiy Soroka, *Oxford Instruments Nanoscience*
www.labis.pl

LABIS, with its headquarters in Warsaw, is a modern and innovative private enterprise providing professional support, sales and service for advanced tools and systems to physics institutes and applied science. Since August 2010 we have been an **Oxford Instruments, UK** official distributor for Poland. Since that time we achieved success in the delivery and installation of Oxford Instruments **NanoScience** products to almost all Universities in our country. We are proud to promote and offer a full range of products, many of which are already installed in Poland:

- Optical Nitrogen Cryostats – 5 systems delivered.
- Helium Flow Cryostats – 7 systems delivered.
- Cryogen Free Cryostats – 6 systems delivered.
- Dilution Refrigerators – 2 dry systems and 1 wet system delivered.
- 3He Refrigerators – 1 system delivered.
- Superconducting Magnets – 11 systems delivered.
- Cryospares and Electronics – several dozen delivered.

Oxford Instruments NanoScience designs, supplies and supports market-leading research tools that enable quantum technologies, new materials and device development in the physical sciences. Our tools support research down to the atomic scale through creation of high performance, cryogen free low temperature and magnetic environments, based upon our core technologies in low and ultra-low temperatures, high magnetic fields and system integration, with ever-increasing levels of experimental and measurement readiness. Oxford Instruments NanoScience is a part of the Oxford Instruments plc group.

Our second technology business is to provide scientific tools and systems from our partners, working on a non-exclusive bases. Some systems we have successfully delivered are Microworld - France, Demaco - The Netherlands, Attocube - Germany, AA Optoelectronics - France, Oxford Instruments Plasma Technology and Oxford Instruments Industrial Analysis.

Our third technology business is to design and produce optoelectronic UVLAB devices for authenticating documents, banknotes and general fluorescents study. Our UVLAB products includes:

- Ultraviolet LED Illuminators
- Ultraviolet LED Flashlights
- Ultraviolet LED Fiber Illuminators
- Ultraviolet LED Optoelectronics

We hope to see you at our exhibitor booth at 45th International School and Conference on the Physics of Semiconductors, Jaszowiec 2016 here in Szczyrk.

Cryotechnology & Magnetometry at its best

PPMS®-DynaCool™

A cryogen-free, user-friendly and automated low-temperature platform equipped with a superconducting magnet for the measurement of materials properties

- Specific heat
- Magnetic AC susceptibility and DC moment
- Electrical AC and DC transport properties
- Thermal transport properties
- Temperature range: 1.8 K – 400 K
- 9 or 14 Tesla magnetic field

Helium liquefiers for your lab

- Liquid helium at any time with the ATL (Advanced Technology Liquefier)
- Easy to use
- Automated operation
- Portable system
- Liquefaction rates up to 27 liters per day
- Excellent energy efficiency

Recycling of helium

- Modular helium recovery customized to your experiment
- Collect, store and purify helium

lot-qd.pl

LOT-QD Group Europe. ul. Sztygarska 12/3. 41-500 Chorzow

Phone: +48 32 2482048. E-mail: info@lot-qd.pl

OCI Vacuum Microengineering Inc.

Nano-Science Analytical Instruments and Technology

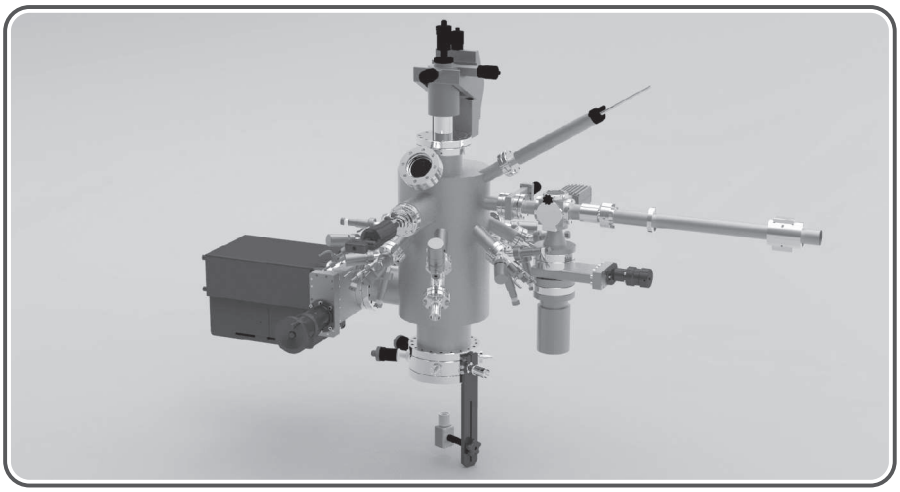

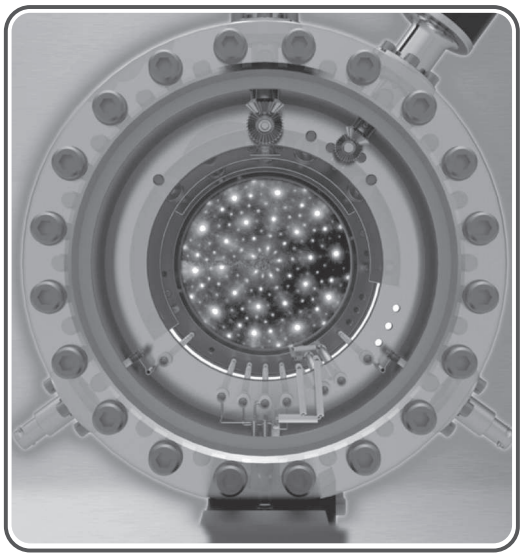

- Compact MBE-LEED system based on Medium Energy Electron Diffraction, LEED, and AES during growth
- LEED - Low Energy Electron Diffraction
- AES - Auger Electron Spectroscopy
- Electron and Ion Sources
- Effusion Cells

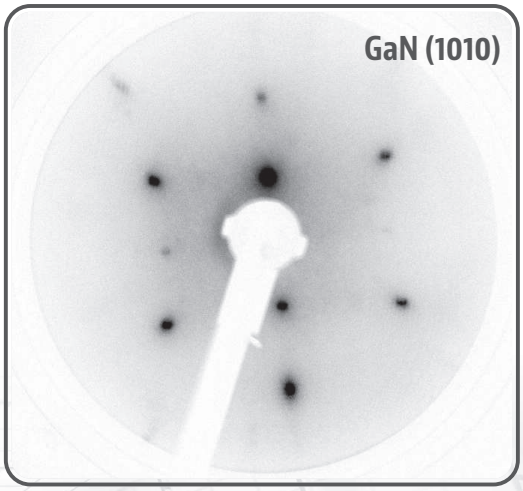

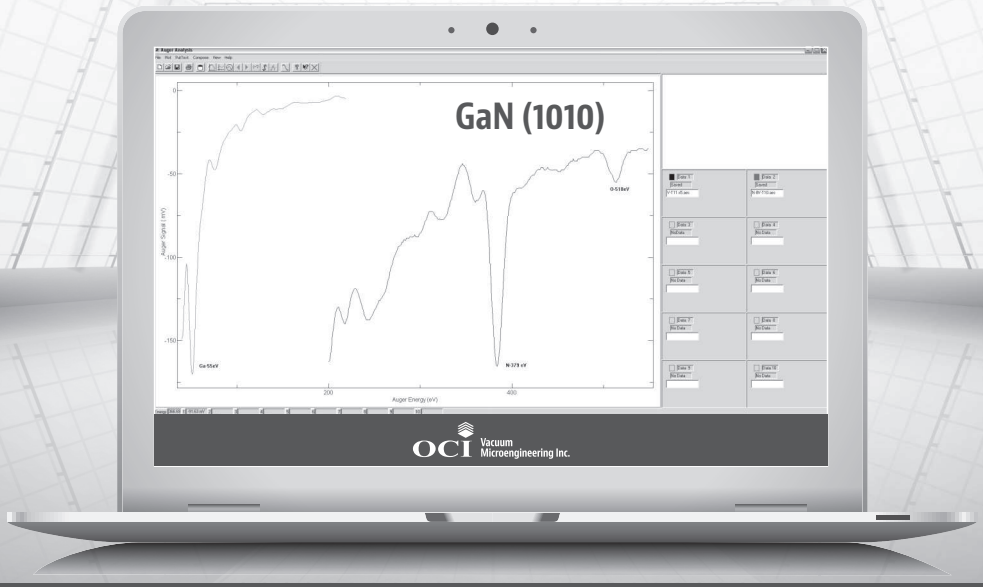

TEL. (519) 457-0878, FAX (519) 457-0837 · 200 Stronach Crescent, London, Ontario, Canada N5V 3A1

E-mail: info@ocivm.com, Website: **www.ocivm.com**

45th International School & Conference on the Physics of Semiconductors "Jaszowiec" 2016

Saturday, June 18th, 2016

14:20 – 14:30 **Marta Gryglas-Borysiewicz – School opening address**

14:30 – 16:15 **Steven Blundell** (University of Oxford, United Kingdom)
Magnetism: from molecules to materials (SaI1)

16:15 – 16:45 Coffee Break

16:45 – 18:30 **Krzysztof Dybko** (Institute of Physics Polish Academy of Sciences, Poland)
Electrical transport in topological insulators (SaI2)

18:30 **Barbecue**

Sunday, June 19th, 2016

11:45 – 13:30 **Eugenio Coronado** (University of Valencia, Spain)
Molecular Spintronics (SuI1)

13:30 – 14:30 Lunch break

14:30 – 16:15 **Ermin Malic** (Chalmers University of Technology, Sweden)
Microscopic view on the ultrafast carrier dynamics in grapheme (SuI2)

16:15 – 16:45 Coffee Break

16:45 – 18:30 **Darell Schlom** (Cornell University, United States)
Thin-Film Alchemy: Using Strain and Dimensionality to Unleash the Hidden Properties of Oxides (SuI3)

20:00 – 21:00 **Concert in the memory of prof. Jan Gaj - chamber music performed by the outstanding, talented children supported by the Polish Children's Fund**

21:00 **Welcoming glass of wine**

Monday, June 20th, 2016

8:50 – 9:00 **Maciej Sawicki – Conference opening address**

9:00 – 9:45 **Peter Wadley** (University of Nottingham, United Kingdom)
Current induced switching of an antiferromagnet (MoI1)

9:45 – 10:00 **M.J. Grzybowski**, P. Wadley, K.W. Edmonds, R. Beardsley, V. Hills, R.P. Campion, F. Maccherozzi, S.S. Dhesi, C. Andrews, J.S. Chauhan, V. Novak, B.L. Gallagher, T. Jungwirth
Imaging of Current-Induced Switching of an Antiferromagnet (MoO1)

10:00 – 10:15 **K. Oreszczuk**, M. Goryca, W. Pacuski, T. Smoleński, T. Kazimierczuk, M. Nawrocki, P. Kossacki
Individual CdSe/ZnSe quantum dots with a few Mn^{2+} ions (MoO2)

10:15 – 10:30 T. Smoleński, T. Kazimierczuk, J. Kobak, **M. Goryca**, A. Golnik, P. Kossacki, W. Pacuski
Optical spin orientation of an individual Fe^{2+} ion in a quantum dot (MoO3)

10:30 – 10:45 **F. Heisterkamp**, E. Kirstein, A. Greilich, E.A. Zhukov, T. Kazimierczuk, D.R. Yakovlev, A. Pawlis, M. Bayer
Dynamics of nuclear spin polarization induced and detected by coherently precessing electron spins in fluorine-doped ZnSe (MoO4)

10:45 – 11:15 Coffee Break

11:15 – 12:00 **Daniel Vanmaekelbergh** (Utrecht University, Netherlands)
Semiconductors with honeycomb nanogeometry: importance, synthesis, and opto-electronic properties (MoI2)

12:00 – 12:15 **A. Jamróz**, J.A. Majewski
Role of defects in alloy ordering of honeycomb graphene-like binary C-B, and C-N, and ternary C-N-B structures (MoO5)

12:15 – 12:30 **A. Mreńca-Kolasińska**, S. Heun, B. Szafran
Gate-induced Aharonov-Bohm interferometer in graphene nanoribbon (MoO6)

12:30 – 12:45 **A. Łopion**, L. Stobiński, K. Pakuła, R. Bożek, P. Kaźmierczak, A. Wysmołek, R. Stępniewski
Light Induced Modification of Graphene Oxide Layers on GaN (MoO7)

12:45 – 13:00 **A. Dudek**, N. Gonzalez Szwacki
Will borophene outperform graphene? (MoO8)

13:00 – 14:30 Lunch break

14:30 – 15:30 **MONDAY POSTER SESSION A**

18:30 – 19:30 Dinner

19:30 – 20:15 **Tomasz Dietl** (Institute of Physics Polish Academy of Sciences, Poland)
Topological materials doped with magnetic impurities (MoI3)

20:15 – 20:30 **M. Majewicz**, G. Grabecki, P. Nowicki, Ł. Szyller, J. Wróbel, Ł. Cywiński, M. Zholudev, V. Gavrilenko, N.N. Mikhailov, S.A. Dvoretskii, W. Knap, F. Teppe, T. Dietl
Conductance of µm-long edge channels in HgTe/(Hg,Cd)Te 2D topological insulator (MoO9)

20:30 – 20:45 **M. Galicka**, V. Volobuev, P. Kacman, P. Mandal, J.O. Caha, J. Sanchez-Barriga, O. Rader, G. Bauer, G. Springholz, R. Buczko
Rashba splitting in (111)-oriented PbSnTe:Bi topological crystalline insulators films (MoO10)

20:45 – 21:00 C. Polley, A. Forsman, O. Tjernberg, **R. Buczko**, A. Szczerbakow, P. Dziawa, B.J. Kowalski, T. Story, T. Balasubramanian
ARPES study of the interface states in normal/topological crystalline insulator heterostructures (MoO11)

21:00 – 22:00 **MONDAY POSTER SESSION B**

Tuesday, June 21st, 2016

9:00 – 9:45 **Qihua Xiong** (Nanyang Technological University, Singapore)
Laser cooling of II-VI semiconductor nanostructures: Towards all solid state semiconductor optical cooler (TuI1)

9:45 – 10:00 **K. Gałkowski**, A. Mitioglu, A. Miyata, P. Plochocka, O. Portugall, J. Tse-Wei Wang, T. Stergiopoulos, G.E. Eperon, S.D. Stranks, H.J. Snaith, R.J. Nicholas
Magneto-optical studies of Methylammonium and Formamidinium based organo-lead halide perovskite semiconductors (TuO1)

10:00 – 10:15 **M. Białek**, D. Śnieżek, J. Wróbel, V. Umansky, J. Łusakowski
Geometrically confined magnetoplasmons in a 2DEG (TuO2)

10:15 – 10:30 **S. Grankowska Ciechanowicz**, K.P. Korona, A. Wołoś, A. Drabińska, A. Iwan, B. Boharewicz, I. Tazbir, J. Wojtkiewicz, M. Kamińska
Photo-induced Charge Transfer in Third Generation Solar Cells (TuO3)

10:30 – 10:45 **J. Kaczmarski**, M.A. Borysiewicz, A. Taube, T. Boll, M. Myśliwiec, K. Piskorski, M. Wzorek, K. Stiller, E. Kamińska
Revisiting Ru-Si-O as a nanocrystalline Schottky electrode for oxide semiconductors (TuO4)

10:45 – 11:15 Coffee Break

11:15 – 12:00 **Yasushi Nanishi** (Ritsumeikan University, Japan)
Recent Advancement of Growth of InN and In-rich InGaN by RF-MBE (TuI2)

12:00 – 12:15 **P. Strak**, P. Kempisty, K. Sakowski, A. Kaminska, D. Jankowski, K. Korona, J. Borysiuk, M. Beeler, E. Grzanka, E. Monroy and S. Krukowski
Polarization in Nitrides Determination by Direct Slab Calculations - ab initio Results and Experimental Verification (TuO5)

12:15 – 13:00 **Kensuke Kobayashi** (Osaka University, Japan)
Current Fluctuations in Mesoscopic Systems (TuI3)

13:00 – 14:30 Lunch break

14:30 – 15:30 **TUESDAY POSTER SESSION A**

18:30 – 19:30 Dinner

20:00 – 20:15 **M. Popielska**, M. Marchwiany, M. Kruk, A. Gąsiorowski, J.A. Majewski
Justification of different approaches including Van der Waals interaction on the example of graphene-like-structures on metallic and insulating substrates (TuO6)

20:15 – 20:30 **J. Binder**, F. Withers, M.R. Molas, K. Nogajewski, C. Faugeras, K.S. Novoselov, M. Potemski
Light-Emitting Tunneling Van Der Waals Heterostructures In Magnetic Fields (TuO7)

20:30 – 20:45 **T. Smoleński**, M. Goryca, M. Koperski, C. Faugeras, T. Kazimierczuk, A. Bogucki, K. Nogajewski, P. Kossacki, M. Potemski
Tuning valley polarization in a WSe_2 monolayer with a tiny magnetic field (TuO8)

20:45 – 21:00 **Ł. Kłopotowski**, A. Mitioglu, G. Deligeorgis, L. Kulyuk, D.K. Maude, P. Plochocka
Inter-valley exciton relaxation in strongly excited monolayer WSe_2 (TuO9)

21:00 – 21:15 **J. Jadczak**, L. Bryja, P. Kapuściński, P. Sitarek, A. Wójs, Y.S. Huang
Robust trion emission in two-dimensional $Mo(S_xSe_{1-x})_2$ alloys (TuO10)

21:15 – 21:30 **M.R. Molas**, K. Nogajewski, J. Binder, M. Potemski
Optical study of monolayer, few-layer and bulk tungsten disulfide (TuO11)

21:30 – 22:30 **TUESDAY POSTER SESSION B**

Wednesday, June 22nd, 2016

9:00 – 9:45 **Mariusz Ciorga** (University of Regensburg, Germany)
Spin injection and spin transport in a high mobility 2D electron gas (WeI1)

9:45 – 10:00 **K. Kolasiński**, B. Szafran
Simulations of scanning gate microscopy imaging of the spin-orbit interaction in 2DEG in presence of in-plane magnetic field (WeO1)

10:00 – 10:15 **M. Syperek**, Ł. Dusanowski, J. Misiewicz, A. Somers, J.P. Reithmaier, S. Höfling, G. Sęk
On the spin memory effect in InAs quantum dash emitting at 1.55 µm (WeO2)

10:15 – 10:30 **J. Debus**, T.S. Shamirzaev, D. Dunker, J. Rautert, V.F. Sapega, D.R. Yakovlev, M. Bayer
Spin properties of the indirect exciton in indirect band-gap (In,Al)As/AlAs quantum dot ensembles (WeO3)

10:30 – 10:45 **S. Zhou**, Y. Yuan, M. Sawicki, A.W. Rushforth, K.W. Edmonds, R.P. Campion, B.L. Gallagher, C. Timm, M. Helm
Application of Ion Beams to Fabricate and Tune Properties of Dilute Ferromagnetic Semiconductors (WeO4)

10:45 – 11:15 Coffee Break

11:15 – 12:00 **Yusuke Kozuka** (The University of Tokyo, Japan)
Advances and Prospects of High-Mobility 2D Electrons in ZnO Heterostructures (WeI2)

12:00 – 12:15 **J. Krzywda**, K. Roszak
Phonon - mediated generation of quantum correlations between quantum dot qubits (WeO5)

12:15 – 12:30 T. Smoleński, **T. Kazimierczuk**, M. Goryca, M. Koperski, P. Wojnar, A. Golnik, P. Kossacki
P-shell exciton complexes with neutral-exciton-like exchange interaction in CdTe/ZnTe quantum dots (WeO6)

12:30 – 12:45 **K. Sawicki**, J.G. Rousset, R. Rudniewski, W. Pacuski, J. Suffczyński, M. Nawrocki
Room temperature polariton lasing in a ZnTe based microcavity containing a single CdSe/(Cd,Mg)Se quantum well (WeO7)

12:45 – 13:00 P.L. Ardelt, **K. Gawarecki**, K. Müller, A.M. Waeber, A. Bechtold, K. Oberhofer, J.M. Daniels, F. Klotz, M. Bichler, T. Kuhn, H.J. Krenner, P. Machnikowski, J.J. Finley
Coulomb mediated hybridization of excitons in quantum dot molecules (WeO8)

13:00 – 14:30 Lunch break

14:30 – 15:30 **WEDNESDAY POSTER SESSION A**

18:30 – 19:30 Dinner

19:30 – 20:15 **Jacek Szade** (University of Silesia, Poland)
Local conductance and ultrafast dynamics of MBE grown Bi_2Te_3 films (WeI3)

20:15 – 20:30 **P. Potasz**, J. Jaworowski
Stability of Laughlin type and composite fermion states in Chern insulators (WeO9)

20:30 – 20:45 **R. Rechciński**, J. Tworzydło
Double-Weyl Nodes And Fermi Arcs In Magnetically Doped Cd_3As_2 (WeO10)

20:45 – 21:00 **S.P. Łepkowski**, W. Bardyszewski
Electric field driven topological phase transition in InN/GaN quantum wells (WeO11)

21:00 – 22:00 **WEDNESDAY POSTER SESSION B**

Thursday, June 23rd, 2016

9:00 – 9:45 **Michał Zieliński** (Nicolaus Copernicus University, Poland)
Atomistic Modeling of Excitonic States in Semiconducting Nanostructures: Beyond 10-Million Atoms in Simulation (ThI1)

9:45 – 10:30 **Michał Matuszewski** (Institute of Physics Polish Academy of Sciences, Poland)
Theory of Polariton Condensates (ThI2)

10:30 – 10:45 **N. Bobrovska**, M. Matuszewski
Adiabatic approximation and fluctuations in exciton-polariton condensates (ThO1)

10:45 – 11:15 Coffee Break

11:15 – 12:00 **Alberta Bonanni** (Johannes Kepler University, Austria)
Spin-orbitronics of nitride semiconductors (ThI3)

12:00 – 12:15 D. Sztenkiel, **M. Foltyn**, G.P. Mazur, R. Adhikari, K. Kosiel, K. Gas, M. Zgirski, R. Kruszka, R. Jakieła, T. Li, A. Piotrowska, A. Bonanni, M. Sawicki, T. Dietl
Stretching magnetism with an electric field in a nitride semiconductor (ThO2)

12:15 – 12:30 **I. Beleckaitė**, R. Adomavičius, R. Butkutė, V. Pačebutas, A. Arlauskas, A. Šiušys, A. Reszka, J. Sadowski, A. Krotkus
Terahertz emission from semiconductor nanowires and non-stoichiometric layers: similarities and differences (ThO3)

12:30 – 12:45 **S. Krukowski**, P. Kempisty, P. Strak, K. Sakowski
Intrasurface Electron Transitions Change of Adsorption Energy at Surfaces of Semiconductors - Mechanism and Consequences to Growth and Doping of Crystals and Layers (ThO4)

12:45 – 13:00 **T. Słupiński**, K.P. Korona, J. Borysiuk
Efficient emission from InAlGaAs single quantum dots with low lattice misfit and AlGaAs indirect bandgap barrier (ThO5)

13:00 – 14:30 Lunch break

14:45 – 19:00 **EXCURSION**

20:00 **Conference Banquet**

Friday, June 24th, 2016

10:00 – 10:45 **Tilmann Kuhn** (Westfälische Wilhelms-Universität, Germany)
The Role of Phonons for the Optical Control of Excitons and Biexcitons in Semiconductor Quantum Dots (FrI1)

10:45 – 11:15 Coffee Break

11:15 – 12:00 **Chris Palmstrøm** (University of California, United States)
Self-assembly of Single Crystal Rare-earth Monopnictide Nanostructures in III-V Epilayers (FrI2)

12:00 – 12:45 **Yaniv Gelbstein** (Ben-Gurion University of the Negev, Israel)
Phase Separation in IV-VI Alloys - Generation of Thermodynamically Stable Nano-Features (FrI3)

12:45 – 13:00 **Maciej Sawicki – Conference closing address**

13:00 – 14:30 Lunch

15:00 Departure of conference buses to Bielsko-Biała

MONDAY POSTER SESSION including special session about novel electronic devices for energy production, conversion, storage and monitoring

1. P.A. Dróżdż, M. Sarzyński, K.P. Korona, S. Grzanka, R. Czernecki, E. Grzanka, J. Goss, T. Suski
Carrier Recombination Mechanisms in Multicolor InGaN/GaN Light Emitting Diode

2. M.A. Borysiewicz, M. Wzorek, M. Ekielski, M. Myśliwiec, J. Kaczmarski
MnO2 Nano-films for the Enhancement of Transparent Nanocoral ZnO-Based Supercapacitor Performance

3. M.A. Borysiewicz, S. Chusnutdinow, M. Wzorek, T. Wojciechowski
Dye Aggregation Influence on Dye Sensitized Solar Cell Performance in Nanocoral ZnO-Based Thin Film Cells Sensitized With N-719 and Rose Bengal Dyes

4. M. Masłyk, M.A. Borysiewicz, M. Wzorek, T. Wojciechowski, M. Kwoka, E. Kamińska
Growth Mechanism Of Zn/ZnO Core-Shell Nanostructures Obtained By DC Reactive Magnetron Sputtering With Variable Absolute Gas Flow Values At A Set Ratio

5. E. Zielony, E. Płaczek-Popko, M. Morawski, J. Szatkowski, Z. Gumienny, K. Paradowska, S. Chusnutdinow, G. Karczewski
Identification of Recombination Centers in the CdTe-based Solar Cells by Means of PL-T and PL-V Techniques

6. K.M. Paradowska, E. Przeździecka, E. Płaczek-Popko, K. Gwóźdź, M. Stachowicz, J. Sajkowski, J. Dyczewski, A. Kozanecki
Raman spectroscopy of epitaxial $Zn_xMg_{x-1}O$ layers doped with V-group elements grown by MBE

7. K.M. Paradowska, E. Płaczek-Popko, M.A. Pietrzyk, A. Kozanecki
Optoelectronic properties of PA-MBE ZnO-based heterojunctions

8. S. Ağan
Si, Ge and SiGe Nanocrystals for Memory Device and Solar Cell Applications

9. T. Palutkiewicz, M. Wołoszyn, B.J. Spisak
Transport characteristics of gated core-multishell nanowires: Self-consistent approach

10. J. Binder, R. Stepniewski, W. Strupinski, A. Wysmolek
Controlled Functionalization Of Graphene Based Solution Gated Field-Effect Transistors

11. S. Prucnal, Y. Berencen, W. Skorupa, S. Zhou
Ultra-doped Ge: old material with new functionalities

12. S. Prucnal, Y. Berencen, W. Skorupa, S. Zhou
Band gap engineering in Ge via non-equilibrium thermal processing and Sn doping

13. K. Gwóźdź, E. Płaczek-Popko, E. Zielony, Z. Gumienny, K. Paradowska, R. Pietruszka, B.S. Witkowski, K. Kopalko, M. Godlewski, W. Jacek, L. Chang
Photoconversion of the Plasmonic Solar Cells Based on ZnO Nanorods and Silicon with Silver and Gold Nanoparticles

14. P. Caban, R. Pietruszka, K. Kopalko, B. Witkowski, M. Godlewski, K. Gwóźdź, E. Zielony, E. Płaczek-Popko
ZnO/GaAs heterojunction solar cells fabricated by ALD method

15. A. Bogucki, Ł. Zinkiewicz, P. Wasylczyk, W. Pacuski, P. Kossacki
Single Quantum Dot Spectroscopy in a Standard Macro-photoluminescence Setup

16. P. Scharoch, M.P. Polak, R. Kudrawiec
Ab initio calculations for electronic structure engineering of Bi diluted III-V compounds and $Ge_{1-x}Sn_x$ alloy

17. K. Kucharski, P. Zagrajek, D. Tomaszewski, A. Panas, G. Głuszko, J. Marczewski
An influence of silicon substrate parameters on a responsivity of MOSFET-based THz detectors

18. D. Yavorskiy, K. Karpierz, M. Białek, M. Grynberg, J. Łusakowski
Thermal Emission of THz Radiation from Field Effect Transistors

19. B. Hajduk, B. Jarząbek, J. Jurusik
The study of glass transition temperature measured on P3HT:PCBM thin films using spectroscopic ellipsometry

20. V. Janonis, V. Jakštas, I. Grigelionis, I. Kašalynas
Investigation of Thermal and Plasmonic Emission from Grating-Gated GaN/AlGaN High Electron Mobility Transistors

21. S. Chusnutdinow, M. Szot, L. Kowalczyk, W. Zaleszczyk, V. Kolkovsky, M. Wiater, T. Wojtowicz, G. Karczewski
Photoelectrical properties of p-i-n diodes with PbSe quantum wells

22. T. Groń, M. Bosacka, E. Filipek, A. Pacześna, P. Urbanowicz, B. Sawicki, H. Duda
Electrical properties of $CuInVO_5$

23. T. Groń, E. Filipek, A. Pacześna, P. Urbanowicz, B. Sawicki, H. Duda
Electrical properties of $Sr_2InV_3O_{11}$

24. T. Groń, E. Filipek, G. Dąbrowska, H. Duda, M. Oboz
Influence of Cr-substitution on the magnetic properties of $Fe_{1-x}Cr_xSnSbO_6$

25. K. Ryczko, J. Misiewicz, M. Kamp, G. Sęk
Designing the active region of mode-locked interband cascade lasers

26. A. Rodil, S. Koelling, A. Cavalli, E.P. Bakkers, P.M. Koenraad
Dopant mapping in InP nanowires for solar cell applications

27. D. Ziemkiewicz, S. Zielińska-Raczyńska, G. Czajkowski
Optical Functions of Rydberg Excitons

28. H. Bednarski, B. Hajduk, J. Jurusik, M. Domański, B. Jarząbek, K. Łaba, M. Łapkowski
The influence of PEDOT to PSS ratio on the optical properties of PEDOT:PSS thin solid films-insight from spectroscopic ellipsometry

29. H. Bednarski, B. Hajduk, J. Jurusik, M. Domański, K. Łaba, M. Łapkowski
The influence of morphology on the optical properties of PEDOT:PSS thin solid films - insight from spectroscopic ellipsometry studies

30. H. Bednarski, B. Hajduk, J. Jurusik, M. Domański, H. Janeczek, M. Łapkowski
Studies on the influence of temperature on the optical properties and electrical conductivity changes of PEDOT:PSS thin solid films

31. K. Grodecki, P. Martyniuk, W. Pusz, A. Kowalewski, D. Stępień, A. Kębłowski, J. Piotrowski, D. Stanaszek, W. Gawron, A. Rogalski
Fast response HOT (111) HgCdTe MWIR detectors

32. J. Rosowska, J. Kaszewski, B. Witkowski, Ł. Wachnicki, M. Godlewski
The effect of synthesis pressure on properties of Eu-doped ZnO nanopowders prepared by microwave hydrothermal method

33. M. Szot, K. Dybko, P. Pfeffer, A. Szczerbakow, L. Kowalczyk, P. Dziawa, T. Zayarnyuk, K. Piotrowski, M.U. Gutowska, A. Szewczyk, W. Zawadzki, T. Story
Experimental and theoretical analysis of room temperature thermoelectric and thermal properties of PbTe-CdTe solid solution

34. M. Zięba, B. Taliashvili, P. Dziawa, W. Knoff, W. Wołkanowicz, K. Dybko, R. Minikayev, E. Łusakowska, A. Reszka, T. Story
MBE Growth, Magnetic and Structural Properties of $Sn_{1-x}Mn_xTe$ Layers

35. M. Ściesiek, W. Pacuski, J.G. Rousset, M. Parlińska-Wojtan, A. Golnik, J. Suffczyński
Design and optical properties of micropillars with two vertically coupled ZnTe microcavities

36. R. Kuna, R. Minikayev, M. Trzyna, A. Szczerbakow, K. Gas, J. Łażewski, A. Bosak, W. Szuszkiewicz
Inelastic X-ray Scattering Studies of the Phonon Dispersion in PbTe and (Pb,Cd)Te Solid Solution

37. A. Siklitckaia, S. Yastrebov, M. Chekulaev, J.A. Majewski
Uptake of Carbon Dioxide by Carbon Spiroids

38. A. Królicka, M. Michalska, A. Mirowska, M. Piersa, A. Materna
Impact of different conditions of technological process on thermoelectric properties of nano-grained n-type PbTe

39. J. Przybytek, J. Fink-Finowicki, G. Jung
Random Telegraph Noise in $La_{1-x}Ca_xMnO_3$ single crystals

40. M. Michalska, A. Królicka
Synthesis of thermoelectric Ca_2Co_2O5 nanocrystalline powder - structural and selected physical studies

41. B.S. Witkowski, V.Y. Ivanov, Ł. Wachnicki, S. Gierałtowska, M. Godlewski
Optical characterization of ZnO nanorods grown by the ultra-fast and low temperature hydrothermal process

42. M.A. Pietrzyk, E. Placzek-Popko, K. Paradowska, E. Zielony, A. Reszka, D. Jarosz, A. Kozanecki
Electro-optical characterization of ZnO/ZnMgO multiple quantum wells grown on Si (111) by MBE method

43. K. Strzałkowski, F. Firszt, A. Marasek
Lattice Disorder Effects on Thermal Properties of CdZnTe Crystals Grown by Vertical Bridgman Method

44. L. Ovsiannikova, G. Lashkarev, V. Kartuzov
Study of donor Al impurity by the help of fullerene like model

45. D. Jarosz, I. Gorczyca, A. Wierzbicka, P. Sybilski, J.M. Sajkowski, H. Teisseyre, A. Kozanecki
Structural and optical properties of Zn1-xMgxO layers grown by PA-MBE. Experiment vs. Theory

46. A. Wierzbicka, M.A. Pietrzyk, A. Reszka, E. Przeździecka, J. Dyczewski, A. Kozanecki
Spatial distribution of strain and Mg composition in $Mg_xZn_{1-x}O$ layers on a-plane sapphire examined by high-resolution x-ray diffraction

47. G. Tchutchulashvili, K. Klosek, K.P. Korona, M. Sobanska, Z.R. Zytkiewicz
Hybrid Organic/GaN Nanowire Structures for Solar Cell Applications

48. P. Materska, B.S. Witkowski, M. Godlewski
Influence of annealing on optical properties of ZnO nanorods obtained by the microwave-assisted hydrothermal process

49. A. Reszka, A. Wierzbicka, K. Sobczak, A.V. Kuchuk, J. Domagala, A. Pieniążek, M. Sobanska, K. Klosek, Z.R. Zytkiewicz, B.J. Kowalski
Spatially resolved strain analysis in GaN/$Al_xGa_{1-x}N$ nanowires — cathodoluminescence and X-ray diffraction studies

50. H. Turski, A. Feduniewicz-Żmuda, C. Cheze, M. Sawicka, F. Krzyżewski, M. Załuska-Kotur, M. Siekacz, G. Muzioł, K. Szkudlarek, C. Skierbiszewski
Step Flow Growth Mode of N-polar Ga(In)N Structures under N-rich conditions in Plasma-Assisted MBE

51. M. Siekacz, G. Staszczak, T. Suski, E. Grzanka, I. Gorczyca, H. Turski, T. Ernst, T. Schulz, M. Albrecht and C. Skierbiszewski
InN/GaN Short Period Superlattices grown by Plasma Assisted MBE

52. T.P. Surkova, V.I. Maksimov, E.N. Yushkova, B.S. Witkowski, M. Godlewski
Unhomogeneously Deformed Structure State of Highly-Doped ZnSe:V Crystals

53. W. Paśko, I. Tralle, P. Zięba, A. Çoruh
New Composite Gyrotropic Metamaterial

54. M. Kulczykowski, M. Matuszewski
Phase ordering kinetics of a nonequilibrium exciton-polariton condensate

55. D.V. Savchenko, V.N. Rodionov, A.A. Prokhorov, V.I. Uzhva, E.N. Kalabukhova
ESR and photoconductivity studies of n- and p-type polycrystalline 3C SiC

56. D.V. Savchenko, E.N. Kalabukhova, B.D. Shanina
ESR study of localized and delocalized electrons in nitrogen-doped 6H SiC crystals

57. *K. Kalbarczyk, M. Foltyn, M. Grzybowski, W. Stefanowicz, R. Adhikari, R. Kruszka, A. Piotrowska, A. Bonanni, T. Dietl and M. Sawicki*
Achieving electrical transport in GaN:Si/(Ga,Mn)N/GaN:Si structures

TUESDAY POSTER SESSION

1. K. Ptaszyński, B.R. Bułka
   Complementarity of the full counting statistics and waiting time distribution of the electron transport in two coupled quantum dots

2. A. Marek, K.I. Wysokiński
   Non-Equilibrium Transport Through a Single Level Quantum Dot

3. K.E. Öksüz, Ş. Şen, U. Şen
   Microstructural and Dielectric Properties of $Ba(Ti_{1-x}Zr_x)O_3$ Nano-ceramics

4. A. Opala, M. Pieczarka, G. Sęk
   One Dimensional Incoherently Pumped Polariton Condensate Flowing Against an Obstacle

5. P. Bugajny, L. Szulakowska, B. Jaworowski, P. Potasz, A. Wójs
   Analysis of symmetry in the graphene quantum dots and artificial graphene quantum dots

6. R. Kuna, S. Adamiak, S. Petit, P. Baroni, K. Gas, R. Minikayev, A. Szczerbakow, W. Szuszkiewicz
   Hardening of (Pb,Cd)Te Crystal Lattice with an Increasing CdTe Content in the Solid Solution

7. S. Adamiak, P. Adamski, K. Matracki, D. Ploch, E. Dynowska, P. Dziawa, A. Szczerbakow, B. Talashvili, M. Wiater, B. Witkowska, T. Wojtowicz, W. Szuszkiewicz
   Substantial Difference in Selected Mechanical Properties of CdTe and PbTe Crystals Grown by Equilibrium and Non-Equilibrium Growth Techniques

8. E. Dynowska, S. Adamiak, M. Wiater, B. Witkowska, T. Wojtowicz, W. Szuszkiewicz
   Is an Application of a Semiconductor in its Metastable Crystal Form a Danger for the Lifetime of Possible Device?

9. A. Maryński, M. Syperek, M. Pieczarka, J. Misiewicz, V. Liverini, M. Beck, J. Faist, G. Sęk
   Carrier dynamics of InAs/InP quantum dots ensemble embedded in various barrier layers

10. P.A. Dróżdż, K.P. Korona, M. Sarzyński, R. Czernecki, C. Skierbiszewski, G. Muzioł, T. Suski
    A model of radiative recombination from quantum well in potential fluctuations

11. G. Lashkarev, V. Kostylyov, V. Vlasiuk, V. Karpyna, I. Shtepliuk, D. Muzyka, M. Dranchuk, V. Popovich, P. Demydyuk, R. Pietruszka, M. Godlewski
    The properties of heterojunctions n+-ZnO:Al/n-Si and n+-ZnO/n-$ZnO_{1-x}S_x$/p-$CuIn_{0.8}Ga_{0.2}Se_2$

12. B. Szukiewicz, K.I. Wysokiński
    Three terminal efficient heat to electricity converter

13. P. Karwat, D.E. Reiter, T. Kuhn, P. Machnikowski, O. Hess
    Thermal phonon lasing in nanoscopic quantum systems

14. S. Stanionytė, V. Pačebutas, B. Čechavičius, A. Krotkus
    Optical And Structural Properties Of GaInAsBi/GaAs MQWs

15. M. Sarzyński, P.A. Dróżdż, K.P. Korona, S. Grzanka, R. Czernecki, E. Grzanka, J. Goss, T. Suski
    Two modes of luminescence energy control in polar and semipolar InGaN/GaN quantum wells

16. S. Ağan
    Magnetoresistance Measurements of Modulation Doped Si/Si0.8Ge0.2 Structure Grown by Molecular Beam Epitaxy (MBE) Technique

17. Z. Adamus, W. Kołkowski, M. Wiater, G. Karczewski, A. Kazakov, L. Rokhinson, T. Wojtowicz
    Quantum Hall Ferromagnet effect in CdMnTe

18. S. Głodzik, T. Domański
Interplay between the quantum interference and electron pairing in nanoscopic heterostructures

19. Y.H. Choi, S.H. Lee, J.S. Kim, S.J. Lee
Temperature dependent-photoreflectance of InAs/GaAs quantum dot

20. A. Kobiałka, T. Domański
Effect of the Majorana bound state on electron transport through the T-shape quantum dot

21. A. Socha, M. Szot, S. Chusnutdinow, K. Połczyńska, A.M. Witowski, L. Kowalczyk, K. Dybko, M. Wiater, T. Wojtowicz, T. Story, G. Karczewski
Photoluminescence studies of PbSe/CdSe heterostructures

22. K. Połczyńska, M. Szot, A. Socha, S. Chusnutdinow, A.M. Witowski, L. Kowalczyk, K. Dybko, M. Wiater, T. Wojtowicz, T. Story, G. Karczewski
Mid-infrared studies of PbTe/CdTe quantum dots in the regime of macro- and micro-photoluminescence

23. B.A. Orlowski, A. Pieniazek, M. Galicka, K. Goscinski
Minority Carriers Spectra in Photovoltaic Heterojunction

24. D. Jankowski, A. Kaminska, P. Strak, K.P. Korona, J. Borysiuk, E. Grzanka, M. Beeler, K. Sakowski, E. Monroy, S. Krukowski
Experimental and ab-initio study of electric field effects in GaN/AlN multi-quantum-wells at ambient and high hydrostatic pressure

25. M. Pieczarka, A. Opala, G. Sęk
Band Structure Modelling of GaAs-Based Quantum Dots Designed for Single Photon Sources at Telecommunication Wavelengths

26. M. Pieczarka, P. Podemski, G. Sęk
Influence of Piezoelectric Field on the Confined States in Low-strain and Asymmetric InGaAs Quantum Dots

27. M. Pieczarka, M. Syperek, D. Biegańska, C. Gilfert, V.I. Sichkovskyi, J.P. Reithmaier, G. Sęk, J. Misiewicz
Spatial Diffusion of Photogenerated Carriers in Coupled Quantum Well - Quantum Dot Structures

28. K. Koronski, A. Kaminska, D. Jankowski, P. Strak, M. Sobanska, A. Wierzbicka, K. Klosek, Z.R. Zytkiewicz, E. Grzanka, M. Beeler, J. Borysiuk, K. P. Korona, P. A. Drozdz, K. Sakowski, E. Monroy, S. Krukowski
Comparison of localization effects in AlGaN layers and GaN/AlN multi-quantum-wells

29. J. Kobak, T. Smoleński, M. Goryca, J.G. Rousset, W. Pacuski, A. Bogucki, K. Oreszczuk, P. Kossacki, M. Nawrocki, A. Golnik, J. Płachta, P. Wojnar, C. Kruse, D. Hommel, M. Potemski, T. Kazimierczuk
Magneto-optical properties of various excitonic complexes in CdTe and CdSe self-assembled quantum dots

30. A. Pieniążek, B.S. Witkowski, H. Teisseyre, D. Jarosz, J. Domagała, S. Kret, A. Reszka, M. Boćkowski, A. Kozanecki, M. Godlewski, B.J. Kowalski
Emission from the axial heterostructure on ZnO microrod observed by cathodoluminescence

31. P. Mrowiński, A. Somers, S. Höfling, J.P. Reithmaier, J. Misiewicz, G. Sęk
Towards a quantum emitter of linearly polarized or entangled photon pairs at telecommunication wavelengths utilizing InAs-InP based nanostructures

32. L. Bryja, J. Jadczak, K. Ryczko, M. Kubisa, J. Misiewicz, A. Wójs, F. Liu, D.R. Yakovlev, M. Bayer, C.A. Nicoll, I. .Farrer, D.A. Ritchie
The study of thermal dissociation of acceptor-bound positively charged excitons in $GaAs/Ga_{1-x}Al_xAs$ quantum wells

33. L. Owczarczyk, V.Yu. Ivanov, J. Debus, J.C. Schindler, M. Wiater, G. Karczewski, M. Godlewski
Energy transfer in the system of CdSe Quantum Dots embedded in quasi-bulk ZnSe layers.

34. T. Chwiej
Application of Picosecond Magnetic Pulses For Inducing An Electron Motion In Bi-Layer Nanowires

35. M. Świderski, M. Zieliński
Effect of substrate orientation and external electric field on the bright exciton splitting in nanowire quantum dot molecule

36. E. Wach, B. Szafran
Numerical simulations of the Coulomb blockade microscopy experiments: probing the local properties of the planar quantum dots using the scanning gate technique

37. M. Ściesiek, J. Suffczyński, W. Pacuski, M. Parlińska-Wojtan, T. Smoleński, P. Kossacki, A. Golnik
Individual Cd(Se,Te)/ZnSe Quantum Dots: Beyond the Crossroad of Se and Te Based Quantum Dot Systems

38. M. Sznajder, N. Hrushka, J.A. Majewski
Morphology and stability of the C/BN and SiC/GaN interfaces based on ab initio studies

39. E. Pozingytė, A. Rimkus, S. Paurazaitė, S. Tumėnas, R. Nedzinskas, L. Chang, M. M.C. Chou
Temperature-dependent Photoluminescence of Nonpolar ZnO/ZnMgO Quantum Wells

40. A. Wierzbicka, A. Kaminska, J. Borysiuk, D. Jankowski, K. Koronski, M. Sobanska, K. Klosek, Z.R. Zytkiewicz
Influence of superlattice period thickness on strain distribution in GaN/AlN multi-quantum-wells

41. M. Syperek, J. Andrzejewski, A. Maryński, W. Rudno-Rudziński, J. Misiewicz, S. Hein, S. Höfling, G. Sęk
A transition from 0D to Extended Ground State in InP-Substrate-Based Coupled Quantum Well - Quantum Dash System at 1.55 μm

42. M. Syperek, K. Ryczko, R. Weih, M. Dyksik, M. Kamp, S. Höfling, J. Misiewicz, G. Sęk
Room Temperature Carrier Dynamics in the W-type GaInSb/InAs/AlSb Quantum Well Structure Emitting in Mid-Infrared Spectral Range

43. E.M. Łacińska, P. Kaźmierczak, K.P. Korona, M. Sobańska, K. Kłosek, Z.R. Zytkiewicz, A. Wysmołek
Natural quantum dots formed in GaN nanowire-UV-LED

44. J. Mikulski, P. Wojnar, Ł. Kłopotowski, T. Smoleński, T. Kazimierczuk, B. Sikora, K. Fronc, J. Kossut
Single CdSe quantum dot containing a single copperion

45. K. Lekenta, R. Mirek, M. Król, J.-G. Rousset, M. Nawrocki, W. Pacuski, J. Szczytko, B. Piętka
Polariton lasing of semimagnetic exciton-polaritons

46. M. Deresz, D. Yavorskiy, K.J. Friedland, R. Hey, J. Łusakowski
Optically detected cyclotron resonance in a GaAs/GaAlAs heterostructure

47. C. Hopfmann, A. Carmele, A. Musiał, M. Strauß, C. Schneider, S. Höfling, M. Kamp, A. Knorr, S. Reitzenstein
Cavity quantum electrodynamics effects in resonantly excited strongly-coupled quantum dot – micropillar cavities

48. T. Smoleński, M. Goryca, T. Kazimierczuk, P. Wojnar, P. Kossacki
Mechanism and dynamics of biexciton formation from a long-lived dark exciton in a CdTe quantum dot

49. J. Sadowski, A. Siusys, T. Wojciechowski, M. Szot, A. Kaleta, A. Sanchez, S. Kret
GaAs-Ga(As,Bi) Core-Shell Nanowires – Structural and Optical Properties

50. P. Wojnar, J. Płachta, A. Kaleta, S. Kret, M. Szymura, R. Rudniewski, W. Zaleszczyk, L.T. Baczewski, G. Karczewski, T. Wojtowicz, J. Kossut
Growth of CdTe/(Cd,Mg)Te core/shell nanowires with high optical quality

51. E.N. Osika, B. Szafran
(1e,1h) states of carbon nanotube quantum dots

52. A. Mielnik-Pyszczorski, K. Gawarecki, P. Machnikowski
Charge and spin injection in a quantum well–quantum dot system

53. J. Krzywda, P. Szankowski, L. Cywinski
Protection of entangled states of N qubits with dynamical decoupling

54. M. Marchwiany, M. Popielska, M. Kruk, J.A. Majewski
Accuracy tests of EXX+RPA scheme in r-space implementation of KS-DFT

55. S.H. Lee, J.S. Kim, Y.H. Kim, C.B. Honsberg
The effect of localized electric field in the type-II InAs/GaAsSb quantum dot using photoreflectance spectroscopy

56. T.I. Mykytyuk, I.M. Fodchuk, V.V. Kulchynsky, O.L. Maslyanchuk, X. Mathew
Photoelectrical Properties of CdS/CdMgTe Heterostructure for Tandem Solar Cells

57. L.K. Preethi, T. Mathews
Phase Tuned TiO_2 Nanotubes for Enhanced Photocatalytic Hydrogen Generation: Anatase → Anatase-Rutile → Anatase-Rutile-Brookite

WEDNESDAY POSTER SESSION

1. Y. Yuan, M. Sawicki, R. Hübner, K. Potzger, E. Weschke, T. Dietl, M. Helm, S. Zhou
   1-D Fe-rich Konbu phase in InAs obtained by Fe ion implantation and pulsed laser melting
2. A. Kwiatkowski, M. Gryglas-Borysiewicz, P. Juszyński, J. Przybytek, M. Sawicki, J. Sadowski, D. Wasik, M. Baj
   Galvanomagnetic methods of Curie Temperature determination in low-TC (Ga,Mn)As samples.
3. A. Kwiatkowski, K. Puźniak, D. Wasik, K. Dybko, M. Szot, A. Szczerbakow, T. Story, P. Pfeffer, W. Zawadzki
   Hydrostatic pressure induced band inversion in $Pb_{1-x}Sn_xSe$ substitutional alloys
4. N. Czechowski, C. Backes, J.N. Coleman, P. Płochocka, Ł. Kłopotowski
   Plasmonic Enhancement of Photoluminescence Intensity in Liquid Exfoliated WS_2 – Silver Island Film Hybrid Structure
5. G. Lashkarev, V. Kladko, M. Radchenko, M. Bugayova, Y. Stelmakh, L. Krushinskaya, A. Baibara, A. Gudymenko, L. Petrosian, T. Osmanov, D. Fedorchenko
   Laplace pressure on Co nanopaticles distributed in alumina matrix (Co/Al_2O_3)
6. G. Lashkarev, M. Radchenko, M. Bugayova, Y. Stelmakh, L. Krushinskaya, A. Baibara, T. Story, W. Knoff, L. Petrosian, T. Osmanov, D. Fedorchenko
   Electrical and galvanomagnetic properties of ferromagnetic composites Co/Al_2O_3 in magnetic field
7. A.I. Dmitriev, M.V. Radchenko , M.E. Bugaiova, D.A. Fedorchenko, W. Knoff, T. Story, G.V. Lashkarev
   Comparative analysis of superparamagnetic and ferromagnetic resonances on Co/Al_2O_3 films
8. M. Tokarczyk, G. Kowalski, M. Gryglas-Borysiewicz, P. Ciepielewski, M. Możdżonek, W. Strupiński, J.M. Baranowski
   Structural Investigations of Graphene Layers Grown on 4H-SiC - Buffer Layer Engineering
9. J. Kutrowska-Girzycka, J. Jadczak, E. Zdanowicz, Y.S. Huang, L. Bryja
   Lattice dynamics and photoluminescence emission of the two-dimensional $Mo_{1-x}W_xS_2$ alloys
10. K. Norowski, K. Gołasa, M. Grzeszczyk, M. Król, K. Nogajewski, M. Potemski, B. Piętka, J. Szczytko
    Optical Properties of Defects in Exfoliated MoS_2 Measured by Reflectometry and Raman Scattering
11. K. Gołasa, M. Grzeszczyk, M. Zinkiewicz, K. Nogajewski, A. Wysmołek, M. Potemski, A. Babiński
    Resonant Raman spectra of suspended MoS_2
12. L.M. Szulakowska, P. Potasz, P. Hawrylak
    Magneto-optics of Massive Dirac Fermions in Strong Magnetic Fields.
13. M. Grzeszczyk, K. Gołasa, M. Zinkiewicz, K. Nogajewski, M.R. Molas, M. Potemski, A. Wysmołek, A. Babiński
    Anomalous effect of temperature on the Raman scattering in few-layer $MoTe_2$
14. T. Woźniak, J. Jadczak, P. Scharoch, A. Wójs
    Ab initio studies of dynamical properties of chosen group VI-B transition metal dichalcogenides systems
15. M. Król, R. Mirek, K. Lekenta, K. Nogajewski, A. Babiński, M. Potemski, J. Szczytko, B. Piętka
    WSe2 monolayers in dielectric cavities

16. J. Łysiak, P. Perkowska, A. Wysmołek, A. Reszka, M. Sobanska, K. Klosek, Z.R. Zytkiewicz
Strong interaction of GaN nanowires with bulk MoS_2: Raman and photoluminescence studies

17. M. Sadek, J.A. Majewski
Ab initio studies of graphene layers on insulating substrates

18. Ł. Bala, E.M. Łacińska, K. Nogajewski, A. Wysmołek, M. Potemski
Strong Photoluminescence Fluctuations In Laser-thinned Few-layer WS_2

19. M. Zinkiewicz, M. Grzeszczyk, K. Golasa, K. Nogajewski, A. Babinski
Temperature dependent studies of Raman modes in few-layers $MoSe_2$

20. Ł. Gelczuk, J. Kopaczek, T. Rockett, R.D. Richards, R. Kudrawiec
Deep-level defects in n-type $GaAs_{1-x}Bi_x$ with $0 < x < 2.3$ grown on GaAs by MBE

21. T. Tarkowski, J.A. Majewski, N. GonzalezSzwacki
Energy decomposition analysis of 2D boron crystals from first principles

22. I. Jendrzejewska, E. Maciążek, T. Groń, P. Zajdel, H. Duda, J. Kusz, A. Kita
Magnetic properties of singlecrystalline $Cd_xMn_yCr_zSe_4$ ($0.03 < y < 0.12$)

23. M. Gawełczyk, P. Machnikowski
Carrier spin dynamics in undoped double quantum dots

24. M. Krzykowski, M. Gawełczyk, K. Gawarecki, P. Machnikowski
Carrier spin dephasing in coupled quantum dots

25. K. Szałowski
Critical temperature of two-dimensional hydrogenated multilayer graphene-based diluted ferromagnet

26. J.J. Schindler, V.V. Belykh, D.R. Yakovlev, E.A. Zhukov, M.A. Semina, M. Yacob, J.P. Reithmaier, M. Benyoucef, M. Bayer
g-factor Properties of Electrons and Holes Confined in InAs Quantum Dots Emitting at Telecom Wavelengths

27. Z. Adamus, D. Sztenkiel, J. Wróbel, T. Wojtowicz
T-shaped spin-separator based on a magnetic two-dimensional electron gas

28. Y. Wang, Y. Liu, S. Gemming, M. Helm, S. Zhou
Defect induced magnetism in SiC

29. Z. Ogorzałek, K. Filipiuk, M. Gryglas-Borysiewicz, A. Kwiatkowski, J. Przybytek, A. Lemaitre, M. Sawicki, M. Baj, D. Wasik
Capacitance Studies of GaMnAs / GaAs Esaki diodes

30. K. Gas, G. Kunert, S. Figge, S. Stefanowicz, T. Baraniecki, P. Dłużewski, B. Kurowska, R. Jakieła, G. Mazur, D. Hommel, M. Sawicki
Impact of Mg Doped Cladding Layers on Ferromagnetism of (Ga,Mn)N Thin Films

31. A. Ciechan, J. Papierska, P. Bogusławski, M. Boshta, M.M. Goma, E. Chikoidze, Y. Dumont, A. Drabinska, H. Przybylinska, A. Gardias, J. Szczytko, A. Twardowski, M. Tokarczyk, G. Kowalski, B. Witkowski, K. Sawicki, W. Pacuski, M. Nawrocki, J. Suffczyński
Fe donor in ZnO: a Half-resonant Character Driven by Strong Intracenter Coulomb Coupling

32. K. Levchenko, T. Andrearczyk, E. Łusakowska, J. Sadowski, Z. Tkaczyk, J. Wróbel, T. Figielski, T. Wosiński
Magnetoresistive Effects in Nanostructures Tailored from (Ga,Mn)(Bi,As) Dilute Magnetic Semiconductor

33. D. Kwiatkowski, Ł. Cywiński
Decoherence of an NV center coupled to a bath of 13C nuclear spins

34. L.Yu. Beliaev
Measurements of longitudinal relaxation time of electrons in n-doped GaAs by means of spin noise spectroscopy

35. M. Popielska, M. Sznajder, J.A. Majewski
Electric and magnetic properties of Mn-dimers on zb-GaN/ zb-SiC(001)

36. H. Przybylińska, A. Grochot, G. Springholz, A. Ney, G. Bauer, W. Jantsch
Exchange bias induced suppression of ferroelectric domain switching in multiferroic GeMnTe

37. E. Kirstein, F. Heisterkamp, A. Greilich, E.A. Zhukov, T. Kazimierczuk, V.L. Korenev, I.A. Yugova, D.R. Yakovlev, A. Pawlis, M. Bayer
Inhomogeneous nuclear spin polarization induced by helicity-modulated optical excitation of fluorine-bound electron spins in ZnSe

38. O. Volnianska, P. Boguslawski
Electronic and magnetic properties of isolated Re(vs Mn) ion and Re-Re (vs Mn-Mn) complex in wurtzite - and zinc blende – ZnO in GGA +U approach

39. O. Volnianska, P. Boguslawski
Influence of spin polarization of p electrons of anions on a spin state of transition metal ion doped in ZnVI semiconductors. GGA+U calculations

40. H. Moldenhauer, C. Lüders, P. Waldkirch, D. Kudlacik, V. Sapega, J. Debus, A. Waag, D. Yakovlev, M. Bayer
Novel insights into the spin-flip Raman scattering of Mn 2+ ions

41. D.P. Zebrowski, B. Szafran, F.M. Peeters
The finite-flake graphene quantum dots in the presence of spin-orbit coupling

42. R. Mirek, M. Król, K. Lekenta, J.G. Rousset, M. Nawrocki, W. Pacuski, M. Matuszewski, J. Szczytko, B. Piętka
Condensation of semimagnetic exciton-polaritons in localised potential minima in magnetic field

43. G.P. Mazur, J. Sadowski, T. Dietl, M. Sawicki
Transport and magnetism at ferromagnetic-paramagnetic critical point in (Ga,Mn)As

44. P. Trocha, K. Wrzesniewski, I. Weymann
Cross-correlations in spin-dependent transport through a quantum dot Cooper pair splitter

45. P. Pfeffer, K. Dybko, M. Szot, A. Szczerbakow, A. Reszka, T. Story, W. Zawadzki
Nernst-Ettingshausen effect near zero energy gap in Pb_{1-x}Sn_xSe

46. B. Kuśmierz, A. Wójs
Analysis of orderings of partitions in the context of fractional quantum Hall effect

47. E. Bobko, D. Śnieżek, D. Płoch, M. Majewicz, M. Fołtyn, M. Wiater, T. Wojtowicz, J. Wróbel
Non-linear quantum transport in n- type CdMgTe/Cd(Mn)Te quasi-ballistic microstructure

48. P. Dziawa, B.M. Wojek, M.H. Berntsen, A. Forsman, B.J. Kowalski, A. Szczerbakow, C.M. Polley, M. Leandersson, T. Balasubramanian, J. Domagała, T. Wojciechowski, W. Knoff, O. Tjernberg, T. Story
Topological crystalline insulator transition and spin texture in (Pb,Sn,Mn)Se

49. B. Jaworowski, N. Rogers, M. Grabowski, P. Hawrylak
Synthetic Haldane phase of correlated electrons in a chain of semiconductor quantum dots embedded in a nanowire

50. G. Grabecki, K. Grasza, P. Skupiński, A. Avdonin, I. Yahniuk, E. Łusakowska, A. Reszka, M. Majewicz, T. Dietl
Three-Dimensional Dirac Semimetal–Insulator Transition in (Cd1-xZnx)3As2 Bulk Crystals

51. M. Brzezińska, P. Potasz, A. Wójs
Entanglement spectrum of topological band insulators on the Lieb lattice

52. W. Bardyszewski, S.P. Łepkowski
The effect of magnetic field on edge states in InN/GaN quantum wells

53. I. Yahniuk, G. Grabecki, M. Majewicz, J. Wróbel, T. Dietl, G. Cywiński, C. Skierbiszewski, S.S. Krishtopenko, S.A. Dvoretsky, N.N. Mikhailov, F. Teppe, W. Knap
Pressure studies of transition from topological insulator into Anderson topological insulator in HgTe quantum well

54. M. Bieniek, T. Woźniak, P. Potasz, A. Wójs
Electronic properties of bismuth and antimony thin films

55. M. Kupczynski, P. Potasz
Analysis of topological properties of Chern insulators

56. P. Kopyciński, S. Prucnal, K. Pyszniak, W. Grudziński, J. Żuk
Ion Implantation and Annealing Based Synthesizing of AIII-BV Nanostructures in SiO_2/Si Matrix

Magnetism: from molecules to materials

Stephen J. Blundell[1]

[1] *University of Oxford, Department of Physics, Clarendon Laboratory, Parks Road, Oxford OX1 3PU, United Kingdom*

In this tutorial lecture, the magnetic properties of atoms and molecules will be reviewed and it will be shown how these lead to the magnetic properties that arise in crystalline solids, including semiconductors (a useful background reading reference is [1]). Crystalline solids contain magnetic moments which can act together in a *cooperative* way and lead to behaviour that is quite different from what would be observed if all the magnetic moments were isolated from one another. This, coupled with the diversity of types of magnetic interactions that can be found, leads to a surprisingly rich variety of magnetic properties in real systems. Magnetic ions are particularly affected by their crystalline environment, and the concept of the *crystal field* is particularly important to the observed behaviour. I will also discuss how to build up a picture of magnetism in solids based on some basic, but counter-intuitive, principles of quantum mechanics that helps to explain the relationship between *entanglement*, *frustration* and *magnetic excitations*. The emphasis will be on focussing on the underlying physical principles and explaining the most important ideas that underpin this complex topic. I will also attempt to include plenty of examples of the application of these principles to real systems.

[1] S. J. Blundell, *Magnetism in Condensed Matter*, Oxford University Press (2001).

Electrical Transport in Topological Insulators

K. Dybko

Institute of Physics, Polish Academy of Sciences, 02-668 Warsaw, Poland

The revolutionary discovery of topological insulators has started new promises in manipulating spin and charge transport. Topological insulators can be viewed as new phases of quantum matter with topologically protected gapless boundary states. The topological protection is ensured either by time reversal symmetry or specific crystalline symmetry. The boundary topological states possess few intriguing characteristics like linear Dirac dispersion, spin polarization and spin-momentum locking. In consequence, they acquire π-Berry's phase in momentum space, which makes them immune to disorder backscattering.
In this talk I will give an overview of some of the manifestations of the above exotic properties in electrical transport experiments. Usually the observation of topological states in real experimental situation is very difficult task, as their conduction is very often hindered by highly conducting non-topological bulk states. In particular, I will discuss quantum correction to the conductivity in the form of antilocalization and quantum oscillatory phenomena like Shubnikov - de Haas effect, where topological states reveal almost directly.

Work supported by the Polish National Science Centre Grant No. DEC-012/07/B/ST3/03607.

Molecular Spintronics

Eugenio Coronado [1]

[1] *Instituto de Ciencia Molecular (ICMol), Univ. Valencia, Spain*

Spin-based electronics is one of the emerging branches in today's nanotechnology and the most active area within nanomagnetism. So far spintronics has been based on conventional materials like inorganic metals and semiconductors. A current trend in this area is that of incorporating molecules in the game. The resulting emergent field - namely molecular spintronics - is propelled by the possibility of preparing a second generation of spintronic devices based on molecular materials (organic spintronics), and by the possibility to manipulate the molecular spin individually (single-molecule nanospintronics).
In this talk these two trends will be illustrated with several examples taken from my own research: i) the use of single-molecule nanomagnets as spin qubits [1, 2]; ii) The electrical addressing of the spin in molecular nanoobjects [3]; iii) The use of single-molecule magnets based on rare-earths as components of new spin valves [4]; iv) the fabrication of spin-OLEDs (i.e., multifunctional molecular devices in which the light emission can be tuned through a magnetic field).

[1] J. M. Clemente-Juan, E. Coronado, A. Gaita-Ariño, *Chem. Soc. Rev.* **41**, 7464 (2012)
[2] M. Shiddiq et al., *Nature* **531**, 348 (2016)
[3] Dugay, J. et *al*. *Adv. Mater.* **27**, 1288 (2015).
[4] Bedoya-Pinto, A. et *al*. *Adv. Elect. Mater.* **1**, 1500065 (2015).

Sunday

Microscopic view on the ultrafast carrier dynamics in graphene

E. Malic[1], T. Winzer[2], F. Wendler[2], and A. Knorr[2]

[1] *Department of Physics, Chalmers University of Technology, Gothenburg, Sweden*
[2] *Institut für Theoretische Physik, Technische Universität Berlin, Germany*

Graphene is a unique structure to study the efficiency of carrier relaxation channels. Its linear and gapless band structure (Fig.1(a)) gives rise to distinct ultrafast phenomena, such as the technologically promising carrier multiplication (CM) and transient optical gain [1-3].

The talk gives a microscopic view on the carrier dynamics in graphene after optical excitation. The applied theoretical approach is based on Bloch equations providing access to time-, momentum-, and angle-resolved carrier-carrier and carrier-phonon relaxation channels [1]. This allows us to track the way of optically excited carriers towards the equilibrium distribution. Combining the theoretically predicted results with high-resolution pump-probe experiments, we obtain a fundamental understanding of the carrier dynamics in graphene.

In this talk, we focus on specific ultrafast phenomena characterizing the dynamics including: (i) main relaxation steps from optical excitation to carrier thermalization and carrier cooling, (ii) the appearance of a highly anisotropic carrier population and the efficiency of relaxation channels along and across the Dirac cone (Fig. 1 (b)-(d)), (iii) crucial role of Auger processes giving rise to a technologically promising multiplication of optically excited carriers, (iv) appearance of a phonon-induced transient population inversion in the strong excitation regime suggesting emission of coherent laser light, and (v) Coulomb- and phonon-induced carrier dynamics in Landau-quantized graphene in the presence of a magnetic field.

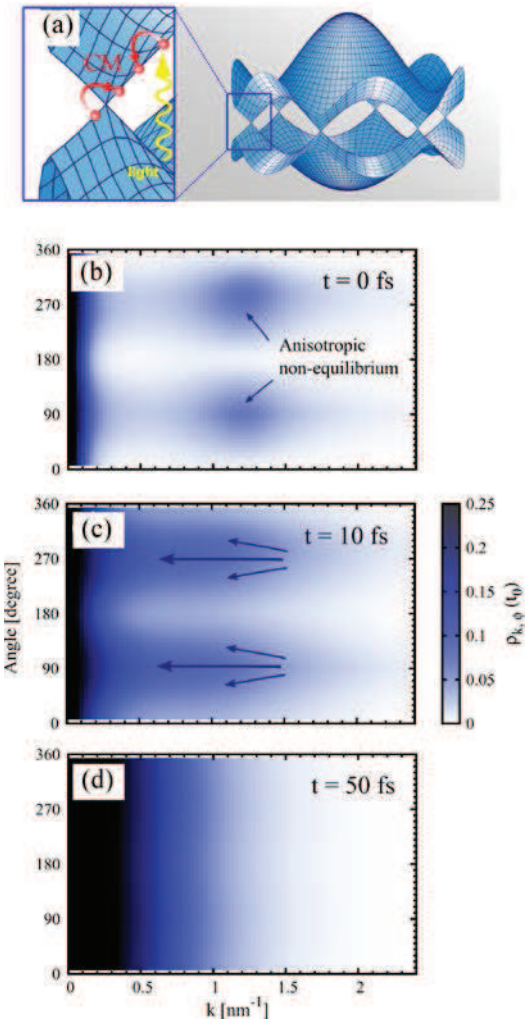

Fig. 1: (a) Electronic band structure of graphene. (b)-(d) Temporal evolution of the carrier occupation as a function of momentum and angle around the Dirac cone. Illustration of the ultrafast Coulomb- and phonon-induced relaxation channels leading to an isotropic equilibrium distribution already after 50 fs [1].

[1] E. Malic, A. Knorr, "Graphene and CNTs – Ultrafast relaxation dynamics and optics", VCH-Wiley, (2013).

[2] E. Malic, T. Winzer, F. Kadi, and A. Knorr, Microscopic view on ultrafast carrier dynamics in graphene, In R. Binder, Optical properties of graphene, World Scientific, Singapore (2016).

[3] F. Wendler, A. Knorr, and E. Malic, "Ultrafast carrier dynamics in Landau-quantized graphene", *Nanophotonics* **4** (review article), 224 (2015).

Thin-Film Alchemy: Using Strain and Dimensionality to Unleash the Hidden Properties of Oxides

Darrell G. Schlom
Department of Materials Science and Engineering and
Kavli Institute at Cornell for Nanoscale Science
Cornell University

Guided by theory, unparalleled properties—those of hidden ground states—are being unleashed by exploiting large strains in concert with the ability to precisely control dimensionality in epitaxial oxide heterostructures. For example, materials that are not ferroelectric or ferromagnetic in their unstrained state can be transmuted into ferroelectrics, ferromagnets, or materials that are both at the same time. Similarly, new tunable dielectrics with unparalleled performance have been created. Our studies reveal details about the microscopic growth mechanism of these phases, which are relevant to preparing multicomponent oxide heterostructures with atomic precision. A new era for multicomponent oxide materials for electronic applications is upon us: oxides by design.

Current induced switching of an antiferromagnet

P. Wadley, B. Howells, C. Andrews, M. Grzybowski, V. Hills, R. Campion, V. Novak, A. Rushforth, K. Edmonds, B. L. Gallagher, J.Zelezny, T. Jungwirth

School of Physics and Astronomy, The University of Nottingham, UK

The pioneer of the field of antiferromagnetism, Louis Neel, noted in his Nobel lecture that while abundant and interesting from the theoretical viewpoint, antiferromagnets did not seem to have any applications. Indeed, the alternating directions of magnetic moments on individual atoms and the resulting zero net magnetization make the moments in antiferromagnets hard to detect by common magnetic probes, and particularly hard to manipulate. Remarkably, in the same Nobel lecture, Neel pointed out the equivalence of antiferromagnets with ferromagnets in effects that are even in the magnetic moment. One such effect is anisotropic magnetoresistance (AMR). There have been several recent demonstrations of spintronic devices based on the anisotropic magnetoresistance (AMR) of antiferromagnetic materials (AF) [1, 2, 3,4]. In these devices either a coupled ferromagnet or cooling in an applied field is used to set the spin axis of the AF material, and only the reading is done electrically. Zelezny*et al* recently predicted a mechanism, by which an alternating field-like torque, termed a Neel order spin-orbit torque (NSOT), can be produced in crystals of specific symmetries [5] . In some AF materials these torques can coincide with the spin sub-lattices of the AF, and offer the tantalising prospect of current induced coherent rotation of the spin axis.

Here we report on the experimental demonstration of an all-electrically controlled antiferromagnetic memory device. In this device the NSOT is used to set the spin axis via a current pulse, and then the memory state is read electrically by measuring the AMR [6], and is also observed using photoemission electron microscopy (PEEM). All of this is performed at room temperature in the recently reported tetragonal AF CuMnAs [7].

[1] B. G. Park, et al., Nature materials 10, 347 (2011)
[2] X. Marti, et al., Nature materials 13, 367 (2014)
[3] I. Fina, et al., Nature communications 5, 4671 (2014).
[4] T. Jungwirth, P. Wadley et al., Nature Nanotech. 11, 231 (2016); Editorial, Nature Nanotech.11, 231 (2016).
[5] J. Zelezny, et al., Physical Review Letters 113, 157201 (2014).
[6] P. Wadley et al., Science 351, 587 (2016); C. Marrows (Editorial), Science 351, 558 (2016).
[7] P. Wadley, et al., Nature Communications 4, 2322 (2013).

Semiconductors with honeycomb nanogeometry: importance, synthesis, and opto-electronic properties

Daniel Vanmaekelbergh[1], C. Morais Smith[2] and C. Delerue[3]

[1]*Debye Institue for Nanomaterials Science, University of Utrecht, NL*
[2]*Institute for Theoretical Physics, University of Utrecht, NL*
[3]*ISEN-IEMN, University of Lille, Fr*

It has become clear recently that the bandstructure of 2-D semiconductors can be deeply changed by a superimposed nano-geometry. For instance, if 2-D semiconductors are molded in a honeycomb geometry, the valence- and conduction bands show a linear energy-wave vector dispersion relation, instead of a parabolic one; the other beneficial properties of the semiconductor become preserved. It is thus possible to design massless electron and hole excitations in conventional semiconductors by the action of geometry! The major question is how to fabricate these nanostructured systems. In the top-down route, lithography and etching is used to imprint the desired nanostructuring in the 2-D material. Secondly, the self-assembly and attachment of nanocrystals into atomically coherent 2-D semiconductors can be used.

Interfacial self-assembly and epitaxial attachment of colloidal Pb-chalcogenide semiconductors has resulted into two-dimensional *atomically coherent* PbX (X=S, Se, Te) semiconductors with remarkable geometry and strong electronic coupling between the nanocrystal sites. By Cd-for-Pb cation exchange, these honeycomb systems can be transformed into honeycomb semiconductors with a zinc blende CdX atomic lattice. Effective mass- and atomistic theory predict that 2-D semiconductors with honeycomb geometry have a bandgap similar to the 2-D quantum wells, however, with Dirac-type electronic conduction and valence bands. Due to strong spin-orbit coupling, the Dirac cone at the K-point can open, and host the quantum spin Hall effect.

I will discuss the theoretically predicted electronic band structure. I will show and discuss the first density-of-state measurements on honeycomb semiconductors and the transport characteristics of electrons and holes in these systems. Finally, the optical properties of freely suspended honeycomb semiconductors will be compared to those of simple quantum wells with the same thickness and same atomic lattice.

References
[1] Long-range orientation and atomic attachment of nanocrystals in 2D honeycomb superlattices
M. P. Boneschanscher, W. H. Evers, J. J. Geuchies, T. Altantzis, B. Goris, F. Rabouw, S. van Rossum, H. S. J. van der Zant, L. D. A. Siebbeles, G. Van Tendeloo, I. Swart, J. Hilhorst, A. V. Petukhov, Bals, and D. Vanmaekelbergh, Science 344, 1377 (2014).
[2] Dirac Cones, Topological Edge States, and Nontrivial Flat Bands in Two-Dimensional Semiconductors with a Honeycomb Nanogeometry. E. Kalesaki, C. Delerue, C. Morais Smith, W. Beugeling, G. Allan, and D. Vanmaekelbergh, Phys. Rev. X 4, 011010 (2014)
[3] Low-Dimensional Semiconductor Superlattices Formed by Geometric Control over Nanocrystal Attachment. W. H. Evers, B. Goris, S. Bals, M. Casavola, J. de Graaf, M. Dijkstra, D. Vanmaekelbergh, NanoLett. 13, 2317-2323 (2013)
[4] Topological states in multi-orbital HgTe honeycomb lattices. W. Beugeling et al. *Nature Communication s* 6, doi:10.1038/ncomms7316 (2015).

*E-mail: d.vanmaekelbergh@uu.nl

Topological materials doped with magnetic impurities

Tomasz Dietl

Institute of Physics, Polish Academy of Sciences, PL-02-668 Warszawa, Poland
Institute of Theoretical Physics, University of Warsaw, PL-02-093 Warszawa, Poland
WPI-Advanced Institute for Materials Research, Tohoku University, Sendai 980-8577, Japan

Since magnetic impurities break time reversal symmetry, their presence was initially regarded as a source of backscattering that can destroy topological protection and preclude the observation of signatures of topological matter such as the quantum spin Hall effect. Surprisingly, however, topological insulators doped with transition metals show a number of remarkable properties, the striking example being the quantum anomalous Hall effect, predicted theoretically [1] and then observed in macroscopic samples by several groups. The development of materials in which charge transport occurs entirely *via* a single edge chiral channel in the absence of an external magnetic field offers a number of novel spintronic capabilities.

In the talk, I will first discuss the role of relativistic effects in compounds of heavy elements and then survey the formal analogies between behavior of various type of fermions in vacuum--described by constrained Dirac equations--and properties of elementary excitations (Dirac electrons, Weyl fermions, and Majorana anyons) in particular families of topological materials. Particular attention will be paid to the role of exchange splitting of bands, which often changes the Chern numbers and hence the topological class of the system. I will then present the recent progress in the understanding of the nature of spin-spin interactions between magnetic ions in topological insulators, semimetals, and metals, *i.e.,* in bismuth/antimonite and lead/tin chalcogenides, mercury chalcogenides, and cadmium/zinc arsenide, respectively. In particular, I will discuss the physics and the relative importance of *ferromagnetic* Ruderman-Kittel-Kasuya-Yosida, Bloembergen-Rowland, and superexchange interactions, and their competition with *antiferromagnetic* superexchange, depending on the carrier concentration as well as on the location of magnetic impurities in the lattice and their charge state [2-4]. Finally, the role of topological boundary states in mediating exchange interactions between localized spins will be presented.

[1] Rui Yu, Wei Zhang, Hai-Jun Zhang, Shou-Cheng Zhang, Xi Dai, and Zhong Fang, *Science* **329**, 61 (2010).

[2] see, e.g., T. Dietl and H. Ohno, *Rev. Mod. Phys.* **86**, 187 (2014).

[3] see also, T. Dietl, K. Sato, T. Fukushima, A. Bonanni, M. Jamet, A. Barski, S. Kuroda, M. Tanaka, Phan Nam Hai, H. Katayama-Yoshida, *Rev. Mod. Phys.* **87**, 1311 (2015).

[4] C. Śliwa, J. A. Majewski, and T. Dietl, unpublished.

Imaging of Current-Induced Switching of an Antiferromagnet

Michał J. Grzybowski[1,2], Peter Wadley[1], Kevin W. Edmonds[1], Ryan Beardsley[1], Victoria Hills[1], Richard P. Campion[1], Francesco Maccherozzi[3], Sarnjeet S. Dhesi[3], Carl Andrews[1], Jas S. Chauhan[1], Vít Novák[4], Bryan L. Gallagher[1], Tomáš Jungwirth[1,4]

[1]*School of Physics and Astronomy, University of Nottingham, Nottingham NG7 2RD, UK*
[2]*Institute of Physics, Polish Academy of Sciences, al. Lotników 32/46, 02-668 Warsaw, Poland*
[3]*Diamond Light Source, Chilton, Didcot, Oxfordshire, OX11 0DE, UK*
[4]*Institute of Physics, Academy of Sciences of the Czech Republic, Cukrovarnická 10, 162 00 Praha 6, Czech Republic*

Antiferromagnetic materials are of increasing interest for potential applications in spintronics [1]. Their zero net magnetic moment, resulting from alternating directions of neighboring moments, makes them considerably insensitive to external magnetic field. However, magnetic order in antiferromagnets can be manipulated by staggered current-induced fields resulting from relativistic spin-orbit coupling in materials with local inversion asymmetry [2], which was shown for CuMnAs [3]. Here, we report a study of electrical switching of CuMnAs thin film devices with simultaneous electrical (anisotropic magnetoresistance – AMR) and photoemission electron microscopy (PEEM) measurements. Together, the applied techniques allow observation of the domain pattern of the material, identification of pronounced changes of the domains under the influence of current-induced torques, and determination of the dependence on current magnitude.

The PEEM images reveal a sub-micron scale magnetic domain structure (fig. 1) which is modified by successive current pulses applied along orthogonal axes. A clear correlation is observed between the domain images and the electrical signal recorded as part of the same pulse sequence (fig. 2). Reversible switching of some domain features and time relaxation effects were observed. The research conducted contributes to deeper insight into the current-induced switching of antiferromagnets and domain behavior in CuMnAs, necessary for potential application in spintronics and data storage.

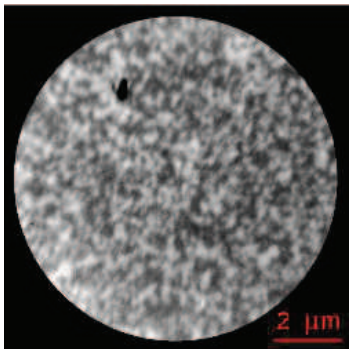

Fig.1 PEEM image of CuMnAs surface with domain structure visible.

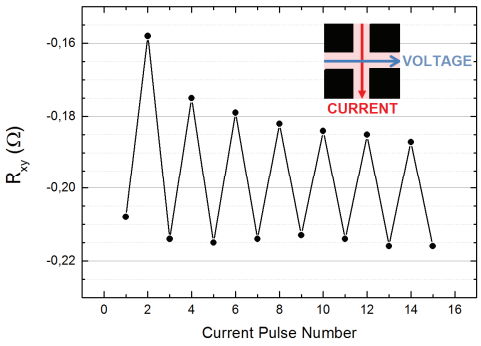

Fig.2 Electrical signals measured for CuMnAs switching.

[1] T. Jungwirth, X. Marti, P. Wadley, J. Wunderlich, *Nature Nanotechnology* **11**, 231 (2016).
[2] J. Železný, H. Gao, K. Výborný, J. Zemen, J. Mašek, A. Manchon, J. Wunderlich, J. Sinova, T. Jungwirth, *Physical Review Letters* **113**, 157201 (2014).
[3] P. Wadley, B. Howells, J. Železný, C. Andrews, V. Hills, R. P. Campion, V. Novák, K. Olejník, F. Maccherozzi, S. S. Dhesi, S. Y. Martin, T.Wagner, J. Wunderlich, F. Freimuth, Y. Mokrousov, J. Kuneš, J. S. Chauhan, M. J. Grzybowski, A. W. Rushforth, K.W. Edmonds, B. L. Gallagher, T. Jungwirth, *Science* **351**, 6273 (2016).

Individual CdSe/ZnSe quantum dots with a few Mn^{2+} ions.

K. Oreszczuk, M. Goryca, W. Pacuski, T. Smoleński, T. Kazimierczuk, M. Nawrocki, P. Kossacki

Institute of Experimental Physics, Faculty of Physics, University of Warsaw, ul. Pasteura 5, 02-093 Warsaw, Poland

Quantum dots (QDs) with magnetic ions are a useful tool in studies of ion-lattice interactions. Many interesting phenomena involving such dots have been investigated, such as an optical spin control of a single magnetic ion [1-2]. However, most of these studies were limited to CdTe and InAs QDs doped with Mn^{2+} ions, due to a common belief that photoluminescence is severely quenched in systems for which the exciton energy is higher than the intra-ionic transition energy. While this is true for highly doped materials [3,4], it was recently shown that exciton emission quenching is negligible in the case of single dopants in QDs [5]. In this work we investigate in detail the properties of individual CdSe QDs doped with single and a few Mn^{2+} ions, in order to understand all aspects of the photoluminescence quenching mechanism.

Sample used in our experiments contains MBE-grown, self-assembled CdSe/ZnSe QDs with a various manganese content. Using polarization-resolved photoluminescence measurements under non-resonant continuous-wave excitation in magnetic field of up to 10 T we are able to identify dots without magnetic ions, dots with single Mn^{2+} dopant, as well as those with a few manganese ions. With the use of time-resolved spectroscopy under pulsed excitation we analyze in detail the dynamics of exciton recombination in such dots. Although we can observe a slight decrease of the exciton lifetime in QDs under investigation, we conclude that presence of even a few magnetic dopants does not introduce an efficient non-radiative exciton recombination channel. In view of those results we discuss the role of the magnetic ions present in the barrier material in the photoluminescence quenching process, as well as possible importance of electron or hole Mn-assisted spin-flip, leading to creation of dark excitons in the QD.

[1] C. Le Gall, L. Besombes, H. Boukari, R. Kolodka, J. Cibert, and H. Mariette, *Phys. Rev. Lett.* **102**, 127402 (2009).
[2] M. Goryca, T. Kazimierczuk, M. Nawrocki, A. Golnik, J. A. Gaj, P. Kossacki, P. Wojnar, and G. Karczewski, *Phys. Rev. Lett.* **103**, 087401 (2009).
[3] W. Giriat and J. Stankiewicz, *Phys. Stat. Sol. (a)* **59**, K79-K80 (1980).
[4] S. Lee, M. Dobrowolska, and J. K. Furdyna, *Phys. Rev. B* **72**, 075320 (2005).
[5] J. Kobak, T. Smolenski, M. Goryca, M. Papaj, K. Gietka, A. Bogucki, M. Koperski, J.-G. Rousset, J. Suffczynski, E. Janik, M. Nawrocki, A. Golnik, P. Kossacki, and W. Pacuski, *Nat. Commun.* **5**, 3191 (2014).

Optical spin orientation of an individual Fe^{2+} ion in a quantum dot

T. Smoleński, T. Kazimierczuk, J. Kobak, M. Goryca, A. Golnik, P. Kossacki, W. Pacuski

Institute of Experimental Physics, Faculty of Physics, University of Warsaw, ul. Pasteura 5, 02-093 Warsaw, Poland

Processing and storing information using single dopants in semiconductors, major objectives of solotronics [1], require efficient optical pumping of an individual spin. For a single manganese ion it has been achieved by injection of spin polarized excitons into a quantum dot (QD) containing a single Mn^{2+} dopant with the use of circularly polarized optical excitation. Such an optical spin orientation was demonstrated using resonant excitation of CdTe QD pairs [2] and non-resonant excitation of CdSe QDs [3]. However, utilization of such an approach in other systems is not necessarily straightforward. In the case of recently presented system of nuclear spin-free Fe^{2+} ion in a CdSe QD [4], the zero-field splitting of the Fe^{2+} spin states may be considered as major obstacle in obtaining efficient spin orientation. In this work, however, we show that upon the application of even a small magnetic field it is possible to optically orient the spin of theFe^{2+} ion with a comparable efficiency to the one shown previously in similar systems.

The Fe^{2+} ion in bulk semiconductors exhibits a single non-degenerate ground state, which cannot be optically manipulated and used to store the quantum information. In an epitaxially strained nanostructure, however, reconfiguration of the Fe^{2+} energy spectrum leads to doubly degenerate ground state [4] split only by energy in the range of μeV. Since this splitting is much smaller than the strength of the *s,p-d* exchange interaction between the ion and the exciton, the optical orientation of the Fe^{2+} spin can be achieved in a similar way as in the case of Mn^{2+} ion, as long as the exciton is present in the QD. However, after the exciton recombination the Fe^{2+} spin undergoes fast oscillations between two spin-mixed eigenstates, which immediately cancels any exciton-induced orientation. This process can be suppressed by the application of a magnetic field as low as few tenths of Tesla. Under such conditions, the efficiency of the Fe^{2+} spin orientation becomes similar to the one obtained previously for the Mn^{2+} ion in the same QD material system (Fig. 1). Therefore the Fe^{2+} ion in a CdSe QD can be used as a robust, optically-controllable two-level system free of any nuclear spin fluctuations, thus a perfect candidate for quantum information processing.

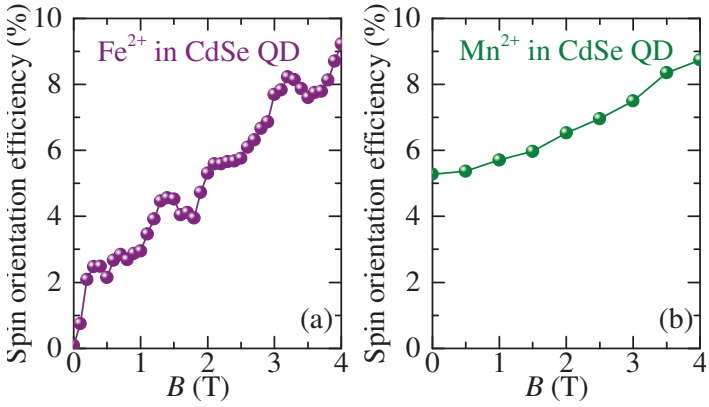

Fig. 1. Magnetic field dependence of optical spin orientation efficiency for an individual (a) Fe^{2+} and (b) Mn^{2+} ion in a CdSe QD.

[1] J. Kobak et al., *Nature Communications* **5**, 3191 (2014).
[2] M. Goryca et al., *Physical Review Letters* **103**, 087401 (2009)
[3] T. Smoleński et al., *Phys. Rev. B.* **91**, 045303 (2015).
[4] T. Smoleński et al., *Nature Communications* **7**, 10484 (2016).

Dynamics of nuclear spin polarization induced and detected by coherently precessing electron spins in fluorine-doped ZnSe

F. Heisterkamp[1], E. Kirstein[1], A. Greilich[1], E. A. Zhukov[1], T. Kazimierczuk[1,*],D. R. Yakovlev[1,2], A. Pawlis[3], and M. Bayer[1,2]

[1] *Experimentelle Physik 2, Technische Universität Dortmund, 44221 Dortmund, Germany*
[2] *Ioffe Institute, Russian Academy of Sciences, 194021 St. Petersburg, Russia*
[3] *Peter Grünberg Institute (PGI-9), Forschungszentrum Jülich, 52425 Jülich, Germany*

We study the dynamics of optically-induced nuclear spin polarization in a fluorine-doped ZnSe epilayer via time-resolved Kerr rotation (KR) [1]. The nuclear polarization in the vicinity of a fluorine donor is induced by interaction with coherently precessing electron spins in a magnetic field applied in the Voigt geometry. It is detected by nuclei-induced changes in the electron spin coherence signal. This all-optical technique (see Fig. 1) allows us to measure the longitudinal spin relaxation time T_1 of the ^{77}Se isotope in a magnetic field range from 10 to 130 mT under illumination. We combine the optical technique

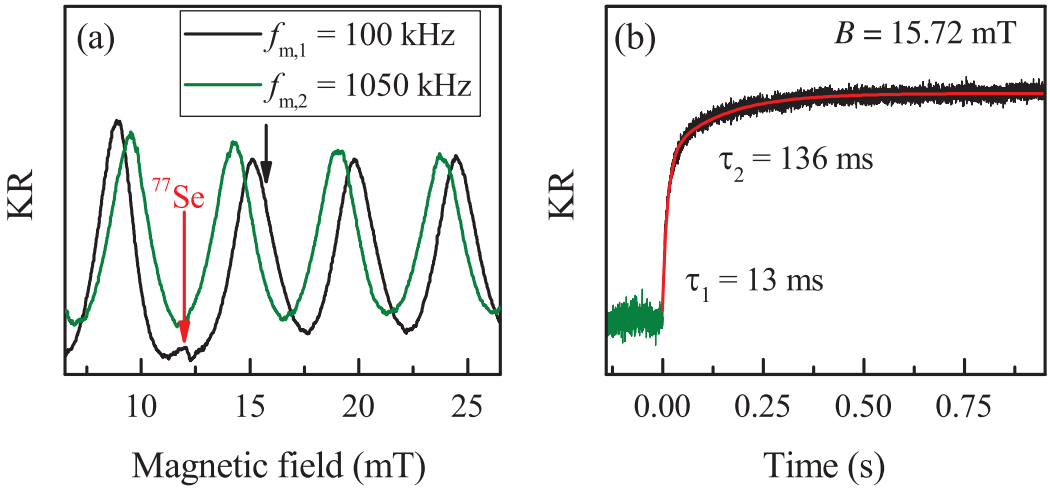

Figure 1: (a) Resonant spin amplification spectra measured at $f_{m,1} = 100$ kHz (black line) and $f_{m,2} = 1050$ kHz (green line). The red arrow marks the optically induced NMR of the ^{77}Se isotope at $f_{m,1} = 100$ kHz and the black arrow marks the magnetic field position ($B = 15.72$ mT) for the measurement shown in Fig. 1(b). (b) Change of KR amplitude at fixed magnetic field induced by switching from $f_{m,2}$ (green line) to $f_{m,1}$ (black line). Red line shows a double exponential fit to the data.

with radio frequency methods to address the coherent spin dynamics of the nuclei and measure Rabi oscillations, Ramsey fringes and the nuclear spin echo. The inhomogeneous spin dephasing time T_2^* and the spin coherence time T_2 of the ^{77}Se isotope are measured. While the T_1 time is on the order of several milliseconds, the T_2 time is several hundred microseconds. The experimentally determined condition $T_1 \gg T_2$ verifies the validity of the classical model of nuclear spin cooling for describing the optically-induced nuclear spin polarization.

[1]F. Heisterkamp, E. Kirstein, A. Greilich, E. A. Zhukov, T. Kazimierczuk, D. R. Yakovlev, A. Pawlis, and M. Bayer, *Phys. Rev. B* **93**, 081409(R)(2016).

*Present address: Institute of Experimental Physics, Faculty of Physics, University of Warsaw, 02-093 Warsaw, Poland.

Role of defects in alloy ordering of honeycomb graphene-like binary C-B, and C-N, and ternary C-N-B structures

Agnieszka Jamróz and Jacek A. Majewski

Faculty of Physics, University of Warsaw, ul. L. Pasteura 5, 02-093 Warszawa, Poland

Boron and Nitrogen doped graphene layers constitute very important class of materials, mostly because B and N constitute natural dopants for carbon systems (*p*- and *n*-type, respectively). At higher concentration of dopants, one should actually consider such systems as binary or ternary alloys. A fundamental issue for any alloy is the degree of ordering among its constituent atoms and to quantify the alloy position between its extreme phases (completely random alloy or perfectly ordered crystal). In our previous studies, it has been shown that binary B_xC_{1-x} and N_xC_{1-x} layered alloys constituting ideal honeycomb lattice exhibit for the dopant concentration x ranging from 0 to 0.5, and temperatures up to 1500 K rather pronounced short range order and deviate strongly from the random alloys.

In the present communication, we report the studies of B_xC_{1-x}, N_xC_{1-x}, and $B_xN_yC_{1-x-y}$ layered graphene based alloy structures containing typical for graphene internal defects, such as single and multiple vacancies, 5-7 Stone-Wales defects, and grain boundaries. We extent our studies also to the systems with reduced periodicity just considering the alloyed nano-ribbons and platelets. Through the studies of energetics of the system, we determine first the thermodynamic equilibrium morphology of the studied systems and then we analyze short-range and long-range ordering, as quantified by the Warren-Cowley short-range order and the Bragg-Williams long-range order parameter, respectively, employing the formalism successfully applied for nitride ternary and quaternary alloys [1]. This comprehensive analysis covers relevant range temperatures and is based on Monte Carlo (MC) calculations within the NVT ensemble employing Metropolis algorithm and Valence Force Field (VFF) approach to calculate the total energies of the of the system. We use Tersoff like potentials for C, N, and B atoms as parametrized by Matsunaga [2]. We perform also density functional theory based calculations (employing the *SIESTA* and sometimes *VASP* code) to test the predictions of VFF potential. We have also implemented into the computational algorithm the conjugate-gradient method to determine the equilibrium geometry. This turns out to be essential for systems containing edges and defects. To get reasonable statistics, we perform many Monte Carlo runs (with up to $2x10^5$ MC steps per run) and perform simulations for temperatures up to 1500 K.

The simulations are performed as follows. First, we choose a graphene ribbon or platelet and introduce randomly the required concentration of certain type intrinsic defects. We perform required number of MC steps to reach equilibrium at given temperature. Then we introduce the required concentration of dopant atoms by substituting carbon atoms by them according to the random distribution. Then we restart MC procedure and perform required number of MC steps till the equilibrium at given temperature is reached. Finally, we perform the analysis of the alloy ordering.

Generally, the simulations for defected structures confirm the existence of the short range order in alloys (at least up to 1500 K) and the finding that the mixed C-N and B-N bonds are favorable for all dopant concentrations up to 50%, whereas B-B and particularly N-N bonds are unfavorable. However, we observe also remarkable inhomogeneous distribution of B and N atoms around defects and edges in comparison to 'bulk' regions of alloys.

This research has been supported by the NCN grant *HARMONIA* (Contact No. UMO-2013/10/M/ST3/00793).

[1] M. Łopuszyński and J. A. Majewski, *Phys. Rev. B* **85**, 035211 (2012).
[2] N. Matsunaga *et al*., *Jpn. J. Appl. Phys.* **39**, 48 (2000).

Gate-induced Aharonov-Bohm interferometer in graphene nanoribbon

Alina Mreńca-Kolasińska[1], Stefan Heun[2], and Bartomiej Szafran[1]

[1] *AGH University of Science and Technology, Faculty of Physics and Applied Computer Science, al. Mickiewicza 30, 30-059 Krakw, Poland*
[2] *NEST, Istituto Nanoscienze-CNR and Scuola Normale Superiore, Piazza San Silvestro 12, 56127 Pisa, Italy*

In graphene it is possible to form regions of p- and n-type conductivity by electric gating [1], which allows for formation of n-p junctions that can be controlled by external voltages.

In the quantum Hall conditions the junction forms a waveguide [2] for the current due to the Lorentz force that in the adjacent n and p regions acts on the carriers in opposite directions.

We study an interference device, which exploits this effect, with a circular n-p region induced in a graphene ribbon by a tip of an atomic force microscope. We simulate the transport properties with the tight-binding Hamiltonian. The current along the junction forms localized states that enter into a Fano-type interference with the currents flowing along the edges of the ribbon. The interference induces conductance oscillations of the Aharonov-Bohm periodicity, and the voltage applied to the tip controls both the oscilation period and the lifetime of localized resonances.

We find that the states localized at the junction correspond to currents of the orientation which produces magnetic dipole moment opposite to the external magnetic field for which the snake orbits along the junction are stabilized by the Lorentz forces. Besides the periodic features of conductance, resonances with the currents constrained entirely under the tip are formed, with an opposite current circulation.

[1] A. H. Castro Neto et al. Rev. Mod. Phys. **81**, 109 (2009).

[2] T.K. Ghosh, et al. Phys. Rev. B 77 , 081404(R); (2008). A. Cresti, G. Grosso, and G. P. Parravicini, Phys. Rev. B **77**, 115408 (2008); Rickhaus et al. Nat. Comm. **6** , 6470 (2015).

Light Induced Modification of Graphene Oxide Layers on GaN

A.Łopion[1], L.Stobiński[2], K.Pakuła[1], R.Bożek[1], P.Kaźmierczak[1], A.Wysmołek[1] and R.Stępniewski[1]

[1] *Faculty of Physics,University of Warsaw, Pasteura 5, 02-093, Warsaw, Poland*
[2] *Faculty of Chemical and Process Engineering (Graphene Laboratory), Warsaw University of Technology, Waryńskiego 1, 00-645, Warsaw, Poland*

Graphene-based heterostructures are believed to make a vital contribution to future technological applications. One novel, perspective device is a high-electron-mobility transistor (HEMT) with a graphene gate, which could be chemically functionalised to perform various chemical or biological applications. An alternative material for such a gate is graphene oxide (GO), which in contrast to graphene, can be more easily functionalised.

Here, we report initial investigations of graphene oxide films, which could be employed in the proposed device. The samples were prepared by spin coating of graphene oxide suspension in various solvents on a substrate, which was GaN layer grown by metalorganic vapour phase epitaxy. Each sample was dried by heating to temperature below the boiling point of the applied solvent and then subjected to the process of liberation of bound water and/or oxygen-containing functional groups (reduction). Such samples were characterised by atomic force microscopy, Raman spectroscopy and resistivity measurements. We found that, graphene oxide was modified by high-temperature treatment, however a considerable modification was also observed as a result of laser light used to excite Raman scattering process. In the Raman spectrum two different contributions were observed: one called 'Raman' and the other, called 'Luminescence'. The second component gradually decreased after subsequent steps of light induced GO modification. It was confirmed by successive Raman spectra presented in Fig.1a.

To resolve these Raman-Luminescence combined spectra a very effective, procedure, based on the Hilbert space functional analysis, was developed. It allowed to separate both effects without any direct fitting. Example of such decomposition is shown in Fig. 1b. Such analysis allowed to discuss precisely an effect of GO modification by light, in particular upon the total light flux incident on the sample. Origin of different processes which are responsible for that behaviour and their kinetics will be discussed.

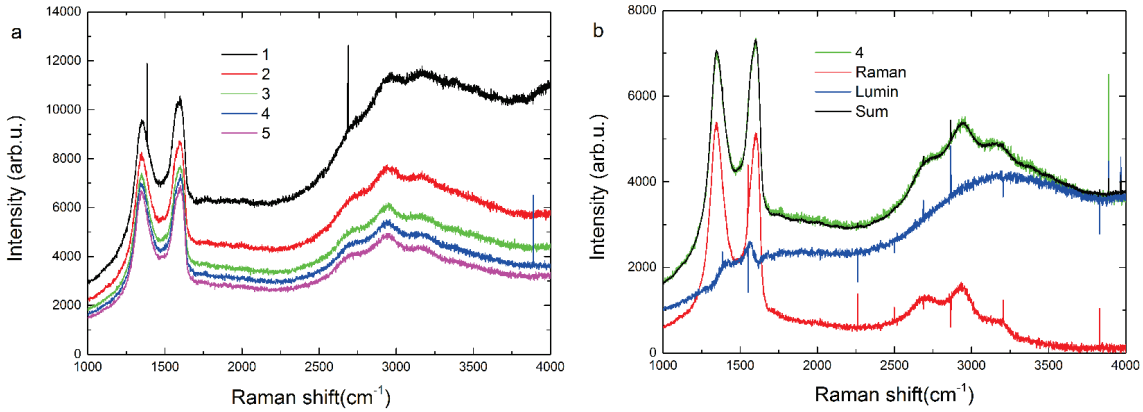

Figure 1: a) Successive Raman-luminescence spectra of graphene oxide on GaN. The disappearance of broadband luminescence is observed. b) Decomposition of exemplary 4th spectrum into Luminescence and Raman parts. It is seen that the measured spectrum is almost identical with a sum of two contributions.

Will borophene outperform graphene?

A. Dudek[1] and N. Gonzalez Szwacki[2]

[1] *Centre of New Technologies, University of Warsaw, Warsaw, Poland*

[2] *Institute of Theoretical Physics, Faculty of Physics, University of Warsaw, Warsaw, Poland*

Driven by a recent experimental evidence that single-atom layer boron sheets with hexagonal vacancies, called borophenes, can be produced on metallic substrates [1], we conducted a detailed computational analysis involving all the theoretically anticipated and experimentally obtained 2D boron structures.

Using first principles calculations, we established that the key mechanism that accounts for the stabilization of 2D boron structures (over 3D ones) on metallic substrates is the charge transfer from the substrate to the layer. In general, negative charge stabilizes 2D boron structures over 3D geometries, whereas positive charge makes bulk structures energetically more feasible. Moreover, the amount of the negative charge that is transferred may serve as a parameter that controls the type of structure that is formed on the substrate.

The second purpose of this work was to compare the properties of one specific form of borophene denoted as the β-sheet (see Fig. 1), that is predicted by theory but not yet obtained experimentally, with graphene. In the same way as benzene can be regarded as the origin of graphene, the β boron sheet has an aromatic building block called borozene [2]. From first principles calculations, we determined that the lattice constant of the β-sheet is about twice as large as that of graphene, however its density is more than two-times larger. The β-sheet is much softer (the 2D bulk modulus is 107 N/m) than graphene and therefore should be easier to wrap up into a nanotube. The electronic band structure of the β boron sheet (see Fig. 2) is quite similar to that of graphene with that main difference that the valence and conduction bands, instead of being in contact, overlap each other at the vicinity of the K point of the BZ. This and the newly-created sheets of boron atoms [1] could outperform even graphene as electrically-conductive material. The comparison of the β-sheet with other 2D and quasi 2D materials will be also given.

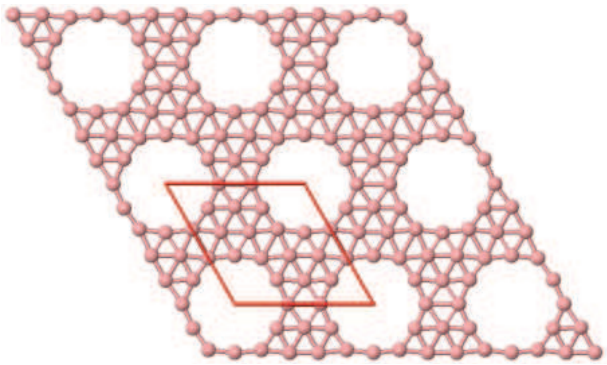

Figure 1: β boron sheet ($a = 4.963$ Å).

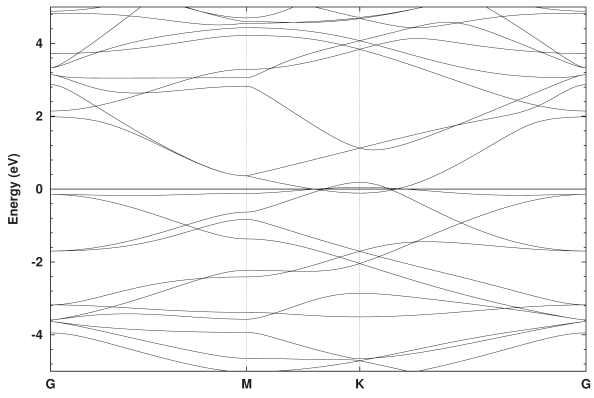

Figure 2: Electronic band structure.

[1] A. J. Mannix *et al.*, *Science* **350**, 1513 (2015).
[2] N. Gonzalez Szwacki, V. Weber, and C. J. Tymczak, *Nanoscale Res. Lett.* **4**, 1085 (2009).

Conductance of μm-long edge channels in HgTe/(Hg,Cd)Te 2D topological insulator

M. Majewicz[1], G. Grabecki[1,2] , P. Nowicki[1], Ł. Szyller[3] J. Wróbel[1,3], Ł. Cywiński[1], M. Zholudev[5], V. Gavrilenko[5], N. N. Mikhailov[6], S. A. Dvoretskii[6], W. Knap[4], F. Teppe[4] and T. Dietl[1,7,8]

[1]*Institute of Physics, Polish Academy of Sciences, al. Lotników 32/46, PL-02 668 Warszawa, Poland*

[2]*Department of Mathematics and Natural Sciences, College of Sciences, Cardinal Wyszyński University, ul. Wóycickiego 1/3, PL 01-938 Warszawa, Poland*

[3] *Faculty of Mathematics and Natural Sciences, Rzeszów University, al. Rejtana 16A, 35-959 Rzeszów, Poland*

[4]*Laboratoire Charles Coulomb (L2C), UMR CNRS 5221, University of Montpellier, 34095 Montpellier, France*

[5]*Institute for Physics of Microstructures, Russian Academy of Sciences, GSP-105, Nizhny Novgorod, 603950, Russia*

[6]*Institute of Semiconductor Physics, Siberian Branch, Russian Academy of Sciences, pr. Lavrentieva 13, Novosibirsk, 630090, Russia*

[7]*Institute of Theoretical Physics, Faculty of Physics, University of Warsaw, ul. Pasteura 5, PL-02-093 Warszawa, Poland*

[8]*WPI-Advanced Institute for Materials Research (WPI-AIMR), Tohoku University, 2-1-1 Katahira, Aoba-ku, Sendai 980-8577, Japan*

The origin of mechanism leading to topological protection breaking is an important challenge in the physics of two dimensional topological insulators [1, 2, 3], because it leads to a deviation from quantized conductance value [4] in devices with edge channels longer than several μm. In order to address this question we perform transport measurements on microstructures for which the length of edge channels is defined by the width of a top gate.

We present results of transport studies on microstructures of n-type 8-nm HgTe/(Hg,Cd)Te quantum well fabricated by employing processing at temperatures below 85°C [5]. Edge channels in the structure are defined by narrow top gate electrodes of the length from 1 to 8 μm. We have performed transport measurements as a function of the gate voltage, magnetic field up to 9 T, and at temperatures down to 1.6 K. When the gate voltage is swept to negative values and the quantum well under the electrode is depleted of electrons, we observe a saturation of conductance at non-zero value close to $0.92\,\frac{2e^2}{\hbar}$ (for 1 μm-width gate) indicating that charge transport occurs via the edge channels. This short-circuiting of conductance by edge channels persists even for large negative gate voltage, where the appearance of p-type conductance and the formation of highly resistive n-p-n diode is expected. This conclusion is supported by a strong nonlinearity of $I(V)$ characteristics in this regime. Moreover, in high magnetic field we observe a splitting of the resistance plateau, suggesting spin splitting of the edge channels.

The research was partially supported by National Center of Science in Poland (Decision No. 2015/17/N/ST3/02314), by grants RBFR "15-52-16017 NTSIL_a "and "15-52-16008 NTSIL_a "and by the CNRS through LIA TeraMIR project.

[1] M. König et al., Science **318**, 766 (2007); A. Roth et al., Science **325**, 294 (2009).
[2] G. M. Gusev et al., Phys. Rev. B **89**, 125305 (2014); Phys. Rev. Lett. **114**, 126802 (2015).
[3] G. Grabecki et al. Phys. Rev. B **88**, 165309 (2013).
[4] A. Bernevig et. al., Science **314**, 1757 (2006).
[5] M. Majewicz et al., Acta Phys. Pol. A **126**, 1174 (2014).

Rashba splitting in (111)-oriented PbSnTe:Bi topological crystalline insulators films

M. Galicka[1], V. Volobuev[2,3], P. Kacman[1], P. Mandal[4], J. O. Caha[5], J. Sanchez-Barriga[4], O. Rader[4], G. Bauer[2], G. Springholz[2] and R. Buczko[1]

[1] *Institute of Physics PAS, Al. Lotników 32/46, Warsaw, Poland*
[2] *Johannes Kepler Universität, Altenbergerstr. 69, A-4040 Linz, Austria*
[3] *National Technical University "Kharkiv Polytechnic Institute" , Frunze Str. 21, 61002 Kharkiv, Ukraine*
[4] *Helmholtz-Zentrum Berlin fuer Materialien und Energie, Elektronenspeicherring BESSY II, Albert-Einstein-Strasse 15, 12489 Berlin, Germany*
[5] *Masaryk University, Kotlarska 2, 61137 Brno, Czech Republic*

Exploiting the spin degree of freedom of the electrons is one of the primary goals in the rapidly growing field of spintronics. A promising candidate to achieve this goal is so-called Rashba effect observed in the inversion non-symmetric systems and with strong high spin-orbit interaction.

In the present work we show the results of theoretical modeling of Rashba splitting in (111)-oriented topological crystalline insulator PbSnTe films doped with Bi atoms which compared to experimentally obtained angle resolved photoemission spectra (ARPES) of epilayers grown by molecular beam epitaxy. The presence of Bi atoms affects the carrier concentration in the crystal and modifies the effective potential at the surface. The latter effect was simulated in the calculations by applying a potential described by Thomas-Fermi screening model. Using the tight-binding method we have calculated the surface spectral density of states in the normal and in topological crystalline insulator phases of the material. Sufficiently high surface potential leads to large Rashba splitting of states. Our theoretical results suggest however, that spin split surface states should be observed even without any additional potential due to the lack of the inversion symmetry at the surface. These states are much better visible in the case of anion terminated surface than in the case of the cation terminated one. The additional potential due to the Bi doping modifies the surface states increasing the Rashba splitting. By choice of appropriate band bending parameters a good agreement with the ARPES measurements of MBE grown PbSnTe:Bi films for various Sn content and temperatures is achieved.

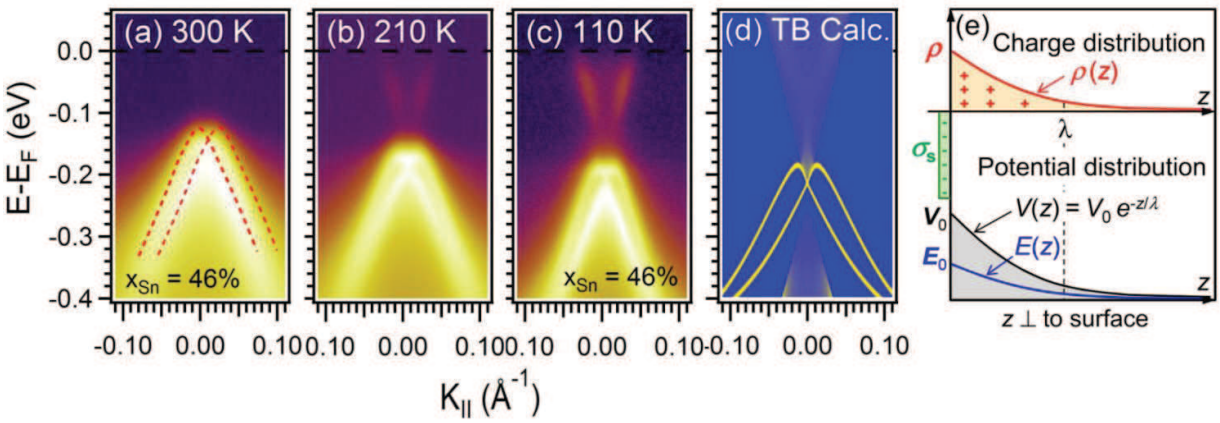

Figure 1: (a) - (c) Temperature dependent ARPES maps of a PbSnTe (111) epilayer with Bi doping of 0.25% at. measured with a photon energy of 18 eV around the Γ point of the surface Brillouin zone compared to tight binding calculations (d) performed for a surface band bending potential $V(z)=V_0e^{-z/\lambda}$ with V_0 = 0.3 V and λ = 2.5 nm. The corresponding charge, potential and electric field distribution is shown schematically in (e).

ARPES study of the interface states in normal/topological crystalline insulator heterostructures

C. Polley [1], A. Forsman [2], O. Tjernberg [2], R. Buczko [3], A. Szczerbakow [3], P. Dziawa [3], B.J. Kowalski [3], T. Story [3], and T. Balasubramanian [1]

[1] MAX IV Laboratory Lund University P.O. Box 118, SE-221 00 Lund, Sweden
[2] Materials Physics, KTH Royal Institute of Technology, 16440 Kista, Sweden
[3] Institute of Physics, Polish Academy of Sciences, 02-668 Warsaw, Poland

While some essential characteristics of topological interface states are dictated solely by considerations of symmetry and bulk band structure, small perturbations can still induce significant modifications. For example, the topological crystalline insulator (Pb,Sn)Se can be surface doped with rubidium atoms to achieve a rigid (i.e. $k_{||}$ independent) energy shift [1], whilst lattice distortions will open a gap [2] and changes in temperature or tin content can modify or eliminate the topological surface states [3].
A particularly interesting modification of the surface states can result from intervalley scattering. This effect requires a sharp confinement potential on a surface in which two or more inequivalent bulk valleys have the same in-plane momentum, and was heavily studied in silicon inversion layers. Among all of the currently known topological insulators, only the (100) face of (Pb,Sn)Se and (Pb,Sn)Te possess this property. The consequence is the existence of two sets of Dirac-like surface states at each $\bar{X}$ in the surface Brillouin zone, split in energy by the intervalley scattering [4].
Here we present an angle resolved photoemission study (ARPES) of the topological interface states in (100) oriented, in-situ grown PbSe/(Pb,Sn)Se heterostructures. We are able to observe the evolution of the topological surface states (TSS) as the TCI-normal interface is buried. With rising thickness of the capping layer the interevalley energy splitting of TSS oscillates and diminishes to zero for thick enough PbSe over-layer. For yet thicker cap TSS are completely buried and disappear in ARPES pictures. Instead, the oscillations of the density of states in the continuum energy regions start to be visible. Such oscillations, reported previously in the case of metallic thin films, appear due to the interference effect of electrons scattering at interface and surface of the system.
Most of the obtained effects have been qualitatively well described with the use of tight binding model. The calculated oscillatory effect, however has much lower amplitude. The similar oscillations with the width of the structure have been previously predicted in the case of electrons confined in quantum wells [5,6] but to date this has not been experimentally confirmed.

[1] I. Pletikosić, G. D. Gu, T. Valla, *Phys. Rev. Lett*. 112, 146403 (2014)
[2] B. M. Wojek, M. H. Berntsen, V. Jonsson, A. Szczerbakow, P. Dziawa, B. J. Kowalski, T. Story, O. Tjernberg, *Nature Comm*. **6**, 8463 (2015)
[3] B.M. Wojek, P. Dziawa, B.J. Kowalski, A. Szczerbakow, A. M. Black-Schaffer, M.H. Berntsen, T. Balasubramanian, T. Story, O. Tjernberg, *Phys. Rev. B* **90**, 161202(R) (2014)
[4] Junwei Liu, Wenhui Duan, Liang Fu, *Phys. Rev. B* **88**, 241303(R) (2013)
[5] D.Z.-Y. Ting, Yia-Chung Chang, *Phys. Rev. B* **38**, 3414 (1988)
[6] Timothy B. Boykin, Gerhard Klimeck, Mark Friesen, S. N. Coppersmith, Paul von Allmen, Fabiano Oyafuso, Seungwon Lee, *Phys. Rev. B* **70**, 165325 (2004)

Carrier Recombination Mechanisms in Multicolor InGaN/GaN Light Emitting Diode

Piotr A. Dróżdż[1,2], Marcin Sarzyński[2], Krzysztof P. Korona[1], Szymon Grzanka[2], Robert Czernecki[2], Ewa Grzanka[2], Jakub Goss[2], and Tadeusz Suski[2]

[1] *Faculty of Physics, University of Warsaw, Pasteura 5, 02-093 Warsaw, Poland*
[2]*Institute of High Pressure Physics "Unipress," Polish Academy of Sciences, Sokołowska 29/37, 01-142 Warsaw, Poland*

Miscut angle is one of the most important factors in epitaxial growth of every semiconductor structure. It governs kinetic processes on the growth front and influences structural, optical and electrical properties of quantum structures.

The ternary compound $In_xGa_{1-x}N$ bandgap and internal electric field are strongly dependent on indium composition, x. Wurtzite InGaN structures are usually grown along the polar c-direction. Although the main factor to determine indium composition is the growth temperature, it has been demonstrated that for c-plane substrate x significantly depends on the substrate miscut angle [1].

In our work, we developed a special patterning technique, which allowed us to locally tune the surface angle in relation to c-axis, and thus the indium content could be varied in different regions of one wafer.

We studied correlation of the wavelength of light emitted from quantum structures and devices prepared with this technique with the amount of indium and strength of the internal electric field. We measured temperature- and time- resolved photo-luminescence in MQW structure grown in substrate regions with different indium content. Based on these results we analyze radiative recombination mechanisms responsible for light emission in our structure. Finally, an electrically driven, multicolor LED device is demonstrated, with tuning range as large as 41 nm what means change from cyan to violet colors on one wafer. The recombination rate varies from 0.1 to 0.3 ns^{-1} decreasing with rising surface miscut angle.

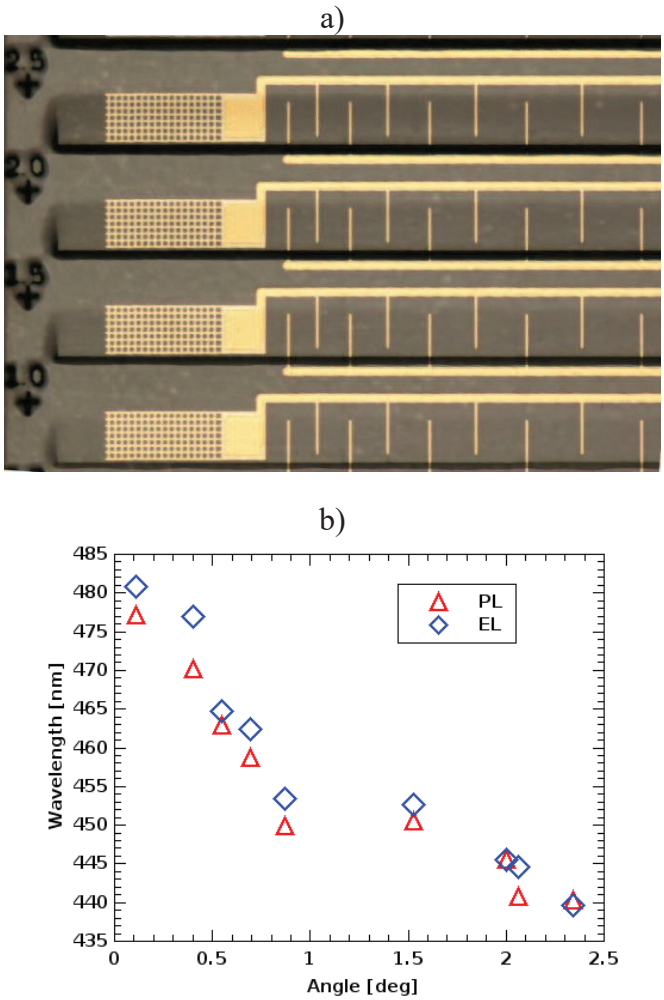

Fig. 1: a) Individual contacts made by photolithography. Regions tilted with respect to c wurzite plane can be seen. b) Electro – and photoluminescence wavelength dependences on miscut angle.

[1] M. Kryśko, G. Franssen, T. Suski, M. Albrecht, B. Łucznik, I. Grzegory, S. Krukowski, R. Czernecki, S. Grzanka, I. Makarowa, M. Leszczyński, and P. Perlin, *Appl. Phys. Lett.*, **91**, 21 (2007).

MnO_2 Nano-films for the Enhancement of Transparent Nanocoral ZnO-Based Supercapacitor Performance

M. A. Borysiewicz[1], M. Wzorek[1], M. Ekielski[1], M. Myśliwiec[1] and J. Kaczmarski[1]

[1] *Institute of Electron Technology, al. Lotników 32/46, 02-668 Warsaw, Poland*

We present thin MnO_2 films deposited by magnetron sputtering applied as capacitance-enhancing material to nanocoral ZnO-based transparent supercapacitors. The films were deposited using magnetron sputtering of a MnO_2 target in an Argon-oxygen mixture under 125 W RF power. The communication discusses the liaisons between the process parameters, MnO_2 structural properties and resulting device performance. Since very few literature works on the growth of MnO_2 by sputtering exist, a wide array of process parameters was studied. For the deposition, an argon flow of 10 sccm was used with the oxygen flow changing from 10 to 0 sccm in the experiment. Furthermore, total gas pressures ranging from 12 to 1.5 mtorr were applied. The growth rates of the MnO_2 were found to be very low, therefore the structural analysis was performed by electron diffraction in a transmission electron microscope for 10 nm thick samples, as scaled using X-ray reflectometry and deposited on TEM carbon grids.

We found that depending on the deposition parameters, the MnO_2 films can contain three MnO_2 crystalline phases: γ, β and λ. We selected the material containing each phase for tests in supercapacitor constructions. Symmetric supercapacitor electrodes were fabricated on fluorine-doped indium tin oxide covered glass. A 150 μm sealing tape was used as a separator and a LiCl/poly(vinyl alcohol) gel electrolyte was applied.

Supercapacitors were characterized in the range 0-1V using cyclic voltammetry, cyclic charge-discharge curves and electrochemical impedance spectroscopy. We show that only the λ-MnO_2 phase leads to capacitance enhancement as related to pure ZnO (30 μF/cm^2 v.s. 20 μF/cm^2). Furthermore, the device with λ-MnO_2 undergoes a chemical reaction in the first 100 cycles, increasing its capacitance to 80 μF/cm^2 and retaining it for the next 4900 charge-discharge cycles. It is put forward that a reaction from λ-MnO_2 to the isostructural $LiMn_2O_4$ spinel takes place, enabling more efficient Li ion intercalation leading to increased capacitance values. The device shows also a high optical transmission of 60% at 500 nm.

This research was supported by the National Centre for Research and Development in the frames of the Lider V Programme through the project 'Nanocoral zinc oxide-based supercapacitors for transparent electronics (NACZO)', contract: LIDER/030/615/L-5/NCBR/2014.

Dye Aggregation Influence on Dye Sensitized Solar Cell Performance in Nanocoral ZnO-Based Thin Film Cells Sensitized With N-719 and Rose Bengal Dyes

M. A. Borysiewicz [1], S. Chusnutdinow[2], M. Wzorek [1], T. Wojciechowski [2]

[1] *Institute of Electron Technology, al. Lotników 32/46, 02-668 Warsaw, Poland*
[2] *Institute of Physics, Polish Academy of Sciences, al. Lotników 32/46, 02-668 Warsaw, Poland*

Dye sensitized solar cells are regarded as a relevant class of photovoltaic devices offering significant efficiencies at a relatively low cost. One of the main challenges in the area lies in finding novel electrode materials and sensitizers. The goal of this work was to apply instead of the commonly used TiO_2 electrode a nanoporous ZnO material fabricated using the large throughput technique of sputtering and to evaluate its performance as a function of the material properties. Furthermore, a direct comparison of two dyes in one structure is performed leading to the assessment of a double-dye cell.

The electrodes were formed on fluorine-doped indium tin oxide (FTO) covered glass. The photoelectrode was fabricated through deposition of a nanocoral Zn film by magnetron sputtering with subsequent annealing in an oxygen flow at 400 °C for 5 minutes. To increase its conductivity, it was doped with hydrogen by annealing in an Ar/H_2 flow at 350 °C for 30 seconds. The photoelectrodes were sensitized by soaking in 0.25 mM ethanol solutions of the N-719 and RB dyes. A 0.5 mM solution was also prepared for the N-719 dye for comparison. The soaking times were in the range of 0.5 h to 100 hours. The counter electrode was a 5 nm thin Pt film on the FTO-covered glass. Holes were drilled for electrolyte filling in the counter electrode and the cell was assembled by gluing the two electrodes together using a 25 μm – thick adhesive gasket. Finally, the structure was filled with a iodide/tri-iodide acetonitrile-based electrolyte and sealed. Cell testing was performed using a solar simulator by measuring dark and illuminated J-V characteristics. A photodiode model was fitted to the data, yielding the series and shunt resistivities as well as diode ideality factors. Structural studies of the electrode material was performed by means of scanning (SEM) and transmission electron microscopy (TEM) with energy dispersive x-ray spectroscopy (EDX). The obtained data are discussed to relate the cell performance to the material structures.

We found that the optimum electrode sensitization time was 5 hours for N-719, yielding η = 1.37%. For longer times, an amorphous scale formed on top of the electrode film, deteriorating performance by blocking free electrolyte flow. By TEM imaging the structure and nanometer-scale thickness of these N-719 shells was determined. On the other hand, for the RB dye, sensitization times of the order of 100 hours are optimal but the efficiencies are significantly limited to fractions of the N-719 value. This dye covered the ZnO nanocrystals less effectively by forming a much thinner shell than the N-719 dye, which we believe to be the main reason for lowered efficiency.

This research was supported by the Ministry of Science and Higher Education in the frames of the Iuventus Plus programme through the project 'Studies on the Influence of Dye and Quantum Dot Aggregation on the Efficiency of Nanocoral ZnO-based Dye Sensitized Solar Cells', contract: 0038/IP2/2015/73.

Growth Mechanism Of Zn/ZnO Core-Shell Nanostructures Obtained By DC Reactive Magnetron Sputtering With Variable Absolute Gas Flow Values At A Set Ratio

M. Masłyk [1], M. A. Borysiewicz [1], M. Wzorek [1], T. Wojciechowski [2], M. Kwoka [3] and E. Kamińska [1]

[1] *Institute of Electron Technology, al. Lotników 32/46, 02-668 Warsaw, Poland*
[2] *Institute of Physics, Polish Academy of Sciences, al. Lotników 32/46, 02-668 Warsaw, Poland*
[3] *Institute of Electronics, Silesian University of Technology, ul. Akademicka 16, 44-100 Gliwice, Poland*

In reactive magnetron sputtering thin films growth is strongly determined by the properties of working gas in the vacuum chamber. The influence of the composition and flow, the type of reactive gas as well as the ratio of argon to reactive gas have been intensively studied, however there are no investigations on the effect of absolute gas flow values at a set ratio. In previous experiments we have proved that by changing the total pressure and the ratio of argon to oxygen in a DC magnetron sputtering of a Zn target it is possible to obtain either dense or porous films [1]. In this communication we show that changing the absolute gas flow value strongly influences the morphologies as well as the properties of nanostructures in a DC reactive magnetron sputtering under porous growth conditions.

In this experiment we consider the growth mechanism of Zn/ZnO nanostructured thin films obtained by room temperature reactive magnetron sputtering of a Zn target at 80 W DC power, low 3 mTorr total pressure and variable absolute $Ar+O_2$ flow values in sccm at a set 10:1 ratio as follows: 3:0.3, 6:0.6, 8:0.8, 10:1, 15:1.5, 20:2, 30:3. The properties of the deposited films were investigated by means of complementary structural (SEM, TEM, XRD), electrical (resistivity) and chemical (XPS, EDX) measurements. Plasma properties were also examined using Langmuir probe and optical emission spectroscopy.

SEM images proved strong dependence of film morphology on absolute gas flow values – from dendritic/nanopetal for low flow to dense porous for high flow with decreasing sizes of grains and progressive amorphization according to XRD measurements. TEM imaging, XPS and EDX delivered more detailed information about composition – the nanostructures have a Zn core with a ZnO shell resulting from surface oxidation of metallic films to 4 nm thick after exposure to atmospheric air. This shell causes an increase in resistivity, especially for more porous films. The growth mechanism of Zn/ZnO nanostructures can be explained based on structure zone model by Mahieu et al. [2] and about the effect of oxygen impurities existing during deposition process. We assumed that the structural evolution of these films is determined by the influence of oxygen incorporating into the film surface during growth and acting as an inhibitor – decreasing the sizes of crystallites and amorphizing the structure. We have also proved that plasma properties do not influence the discussed changes due to relatively constant parameters during all processes. Despite detailed investigations the growth of the observed ZnO nanopetals remains unclear and requires further studies.

[1] M.A. Borysiewicz et al., *Phys. Status Solidi A* 209, No. **12**, 2463–2469 (2012)
[2] S. Mahieu, P. Ghekiere, D. Depla and R. De Gryse, *Thin Solid Films* **515** (2006) 1229 – 1249

Identification of Recombination Centers in the CdTe-based Solar Cells by Means of PL-T and PL-V Techniques

E. Zielony[1], E. Płaczek-Popko[1], M. Morawski[1], J. Szatkowski[1], Z. Gumienny[1], K. Paradowska[1], S. Chusnutdinow[2] and G. Karczewski[2]

[1]Department of Quantum Technologies, Faculty of Fundamental Problems of Technology, Wroclaw University of Technology, Wybrzeże Wyspiańskiego 27, 50-370 Wroclaw, Poland
[2]Institute of Physics, Polish Academy of Sciences, al. Lotnikow 32/46, 02-668 Warsaw, Poland

It is well known that photoluminescence emission and nonradiative recombination through traps or recombination centers compete with current extraction and power production in a solar cell. Therefore for the improvement of a solar cell efficiency, it is crucial to identify the origin and parameters of recombination centers present in its absorber layer.

In this article the results of investigations of recombination centers in photovoltaic structures based on CdTe grown by the MBE technique have been presented. For the identification of recombination centers in the studied junctions the temperature- and bias-dependent photoluminescence (PL-T and PL-V) methods have been applied. In these experiments He-Ne (633 nm) laser was used. The PL-T measurements have been performed in the temperature range from 20 – 300 K, whereas the bias-dependent at a temperature of 12K.The analysis of photoluminescence experiments revealed the presence of recombination centers in the absorber layers of investigated samples. Two types of optical transitions were observed in the PL spectra, labeled as A and B (cf. Fig. 1). It has been found that their activation energies of ~ 6 and 11 meV correspond to the free excitons and donor-acceptor pair radiative recombination, respectively [1]. The PL-V measurements revealed the bias-evolution of both PL peaks. The analysis of the intensity vs voltage bias has been performed for the peak A of higher intensity. It was found that it decreases at a forward bias corresponding to the built-in voltage. This effect has been ascribed to the non-radiative recombination processes. The interpretation of the PL-V measurements has been given by means of the so called "dead layer" model [2] (cf. Fig. 2). Summarizing, the PL technique allowed for characterization of defects responsible for radiative recombination in the CdTe-based junctions.

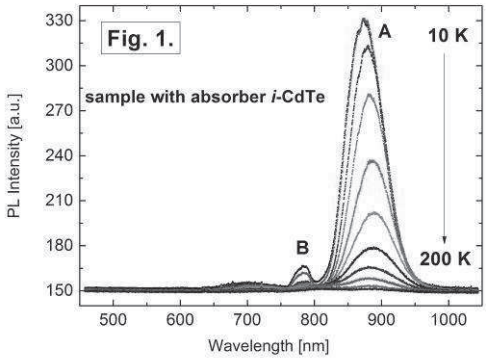

Fig. 1 PL spectra measured at different temperatures.

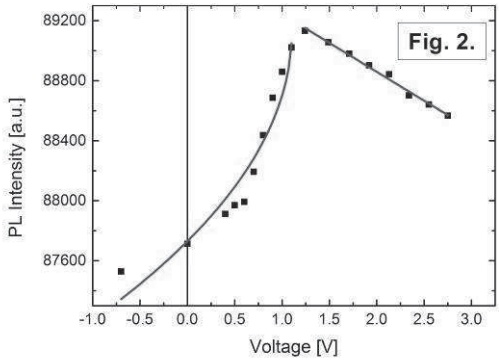

Fig. 2 PL intensity of peak A vs voltage bias. Solid lines – fitting to the experimental data, using the "dead layer" model.

[1] J. Lee, N. C. Giles, D. Rajavel, and C. J. Summers, *J. Appl. Phys.* **78**, 5669 (1995).
[2] D. Shvydka, V. G. Karpov, and A. D. Compaan, *Appl. Phys. Lett.* **80**, 3114 (2002).

Raman spectroscopy of epitaxial $Zn_xMg_{x-1}O$ layers doped with V-group elements grown by MBE

Karolina M. Paradowska[1], Ewa Przeździecka[2], Ewa Płaczek-Popko[1], Katarzyna Gwóźdź[1], Marcin Stachowicz[2], Jacek Sajkowski[2], Jan Dyczewski[2], Adrian Kozanecki[2]

[1] *Department of Quantum Technologies, Faculty of Fundamental Problems of Technology, Wroclaw University of Technology, Wybrzeze Wyspianskiego 27, 50-370 Wroclaw, Poland*
[2] *Institute of Physics, Polish Academy of Sciences, Al. Lotnikow 32/46, 02-668, Warsaw, Poland*

Zinc oxide has attracted more and more attention due to its interesting properties: it is a direct wide band-gap (3.37 eV) semiconductor with chemical and thermal stability in harsh environments. Possible applications of this material include short wavelength optoelectronic devices, mostly blue and white light emitting diodes [1], ultraviolet detectors [2] and more. However, technology meets large problems with fabrication of p-type ZnO, which is crucial for developing p-n junctions. The number of reports about stable p-type ZnO based materials is limited, yet some progress has been achieved. Among the proposed acceptor doping materials are, inter alia, Arsenic, Nitrogen and Antimony.

In our work, micro-Raman spectroscopy was applied to study structural properties of epitaxial $Zn_XMg_{X-1}O$ layers doped with V-group elements. The layers were grown on commercial GaN/Al_2O_3 substrates by plasma assisted Molecular Beam Epitaxy (PA - MBE). The substrates were chemically cleaned before growth and then out-gassed at 700°C in high vacuum. Knudsen cells were used as sources of arsenic, magnesium and zinc and an *rf* plasma cells as sources of oxygen and nitrogen. The power of the O_2 and N_2 *rf* sources were 350 W and 400 W, respectively. The growth temperature was about 450°C. Magnesium concentration was examined by low temperature luminescence as well as Rutherford backscattering spectrometry measurements. A reference GaN/Al2O3 sample was also studied for comparison.

Room temperature Raman spectra were measured from 300 cm^{-1} to 1200 cm^{-1} in the backscattering geometry, with an excitation of the 514 nm Ar+ laser line without polarization detection. Phonon modes A1(LO) and E1(LO) were observed and it was found that both were red shifted with respect to the phonon modes of bulk ZnO. Possible origin of the shift was discussed.

[1] A. Tsukazaki, A. Ohtomo, T. Onuma, M. Ohtani, T. Makino, M. Sumiya, K. Ohtani, S.F. Chichibu, S. Fuke, Y. Segawa, H. Ohno, H. Koinuma, M. Kawasaki, *Nat. Mater*. **4**, 42 (2005).
[2] E. Przeździecka, K. Gościński, M. Stachowicz, D. Dobosz, E. Zielony, J.M. Sajkowski, M.A. Pietrzyk, E. Płaczek-Popko, A. Kozanecki, *Sens. Actuators, A* **195**, 27 (2013).

Acknowledgements
This work has been partially supported by the statutory grant Wroclaw University of Technology, S50013, by the project of National Laboratory of Quantum Technologies (POIG. 02.02.00-00-003/08-00) and NCN project DEC- 013/11/B/ST7/01385. The Authors EP and MS was supported by the NCN project DEC-2013/09/D/ST3/03750.

Optoelectronic properties of PA-MBE ZnO-based heterojunctions

Karolina M. Paradowska [1], Ewa Płaczek-Popko [1], Mieczysław A. Pietrzyk[2], Adrian Kozanecki[2]

[1] *Department of Quantum Technologies, Faculty of Fundamental Problems of Technology, Wroclaw University of Technology, Wybrzeze Wyspianskiego 27, 50-370 Wroclaw, Poland*
[2] *Institute of Physics, Polish Academy of Sciences, al. Lotnikow 32/46, 02-668, Warsaw, Poland*

Recently, the branch of physics including ultraviolet light detectors has developed very fast due to technology progress and increasing number of possible applications of such devices. New materials and structures have been introduced, employing wide band gap semiconductors, which possess intrinsic "blindness" to visible light. One of the proposed materials is zinc oxide – a semiconductor with direct wide band gap of 3.3 eV, which can be further widen by adding magnesium oxide (7.8 eV) to the compound. This procedure is often used and allows to shift the wavelength cut-off edge to shorter wavelengths range.

During our work, two p-Si/n-ZnMgO structures were investigated in order to characterize their properties in terms of their applicability in ultraviolet detectors. Therefore a few experimental techniques have been applied: current-voltage (I-V) characteristics, photoluminescence (PL) and photoresponsivity measurements. I-V characteristics measurements were carried out at 310 K and provided information about basic parameters describing p-n junctions, which indicated rectifying properties of both structures. PL and photoresponsivity spectra were measured at room temperature. Beside the peaks corresponding to near-bandgap transitions, the emission bands associated with defects were noticed in one of the measured PL spectra. The photoresponse characteristics were thoroughly examined - both structures exhibit absorption of the UV light in the ZnMgO layer. However, the junctions possess some important disadvantages, which were presented together with possible solutions to appearing problems. Employing those results can lead to obtaining a well-working UV detectors.

Acknowledgements
This work has been partially supported by the statutory grant Wroclaw University of Technology, S50013, by the project of National Laboratory of Quantum Technologies (POIG. 02.02.00-00-003/08-00) and NCN project DEC- 013/11/B/ST7/01385. One author (M.A.P.) would like to acknowledge the support by the NCN project DEC-2013/09/D/ST5/03881.

Si, Ge and SiGe Nanocrystals for Memory Device and Solar Cell Applications

S. Ağan

University fo Kırıkkale, Department of Physics, 71450 Kırıkkale, Turkey

We have proposed to produced nano size materials which are promised for technological applications. In this aim, thin films have been grown using by Plasma Enhanced Chemical Vapor Deposition (PECVD). The grown films have been annealed to form nanocrystals inside the matrix for different temperature ranges. Due to annealing processes Si, Ge, SiGe nanocrystals in SiO_2 and Si_3N_4 thin films and size distributions have been investigated using by Transmission Electron Microscopy (TEM) and Raman Spectroscopy. SiO_2 and Si_3N_4 thin films have been grown with GeH_4, SiH_4 and N_2O gases at different flow rates using plasma chamber. The results show that nanocrystals sizes depend on annealing time, temperature and flow rates. Optical properties have been searched for these nanocrsytals using by Photoluminescence (PL) and FTIR Spectroscopy.

The Metal-Oxide-Semiconductor (MOS) Capacitors with Ge nanocrystals embeded in oxide have been fabricated to investigate the charge trapping effect Ge nanocrystals. The hysteresis phenomenon has also been observed in C-V measurements. The highest obtainable memory value with multilayer Ge nanocrystals was 0.52 V. Retention times were also checked for our devices. The Ge nanocrystals flash memory cells with this structure could be a promising candidate in future nonvolatile memory applications. On the other hand, our samples with Si nanocrystals formed in Si_3N_4 matrix showed good results to use for solar cells application to increase efficiency.

Transport characteristics of gated core-multishell nanowires: Self-consistent approach

T. Palutkiewicz, M. Wołoszyn, B.J. Spisak†

AGH University of Science and Technology,
Faculty of Physics and Applied Computer Science,
Al. A. Mickiewicza 30, 30-059 Kraków, Poland
e-mail: †bjs@agh.edu.pl

III-V semiconductor core-shell nanowires can be applicable in nanoelectronics, for example as transistors with characteristics controlled by electrostatic gates and operating in the coherent transport regime. Technologies developed in last few years allow manufacturing of smaller, more complex and more efficient devices than before [1, 2]. The earlier computational study [3] allowed determining the optimal design of such nanodevices, i.e., influence of the geometrical parameters of conduction and insulating layers on electric current was examined.

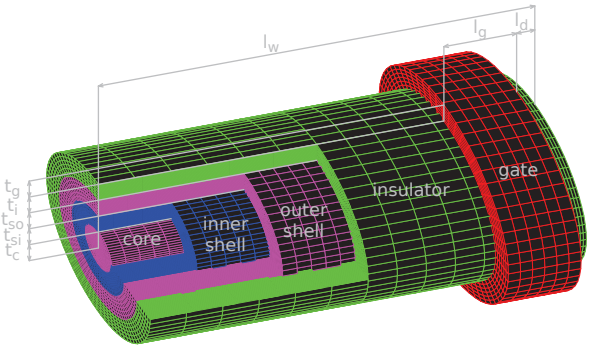

Figure 1: Schematic of core-multishell nanowire with the surrounding gate.

The influence of the applied gate voltage on the coherent propagation of the conduction electrons through the InGaAs/InP core-multishell nanowires with with varying dimensions of the core and shells and the surrounding gate is considered in this report.

The present calculations are based on the adiabatic and effective mass approximation of the three-dimensional Schrödinger equation [4]. The electrostatic potential distribution generated by the all-around gate placed in the vicinity of the drain electrode is determined using the self-consistent procedure applied to solve the Schrödinger-Poisson problem. Quantum transmission boundary method is used to calculate the transmission coefficient, and the transport properties of the considered nanosystem are obtained within the Landauer-Büttiker formalism.

T.P. is supported by the scholarship of Krakow Smoluchowski Scientific Consortium from the funding for National Leading Research Centre by Ministry of Science and Higher Education (Poland).

[1] Chen-Ming Lee, Bing-Yue Tsui, *IEEE Electron Device Letters* **31**, 7, 683 (2010).
[2] Xin Yan, Xia Zhang, Junshuai Li, Yao Wu, Jiangong Cuia, Xiaomin Rena, *Nanoscale* **7**, 1110 (2015).
[3] T. Palutkiewicz, M. Wołoszyn, J. Adamowski, P. Wójcik, B. J. Spisak, *A. Phys. Pol. A* **129**, 1A, A-111, (2016).
[4] M. Wołoszyn, J. Adamowski, P. Wójcik, B. J. Spisak, *J. Appl. Phys.* **114**, 164301 (2013).

Controlled Functionalization Of Graphene Based Solution Gated Field-Effect Transistors

J. Binder [1], R. Stępniewski [1], W. Strupiński [2] and A. Wysmołek [1]

[1] *Faculty of Physics, University of Warsaw, Pasteura 5, 02-093 Warsaw, Poland*
[2] *Institute of Electronic Materials Technology, Wólczyńska 133, 01-919 Warsaw, Poland*

Owing to its strictly two-dimensional character graphene is an intuitive candidate for sensing applications. Indeed it has been shown that graphene is very sensitive to its environment, a characteristic that is essential for application. On the other hand this sensitivity can cause undesired side-effects and can require the encapsulation of graphene to obtain a stable device operation. In order to make graphene sensitive to a given species it is therefore important to functionalize the surface.
Here, we report on the controlled functionalization of epitaxial graphene by electrochemical means. In order to obtain a well-controlled process it is indispensable to have the possibility to follow the functionalization *in-situ.* To this end we make use of a novel setup that allows to measure Raman spectroscopy while the actual functionalization is taking place [1].
Figure 1 shows the Raman response of an epitaxial graphene field-effect transistor (on a 4H-SiC(0001) substrate) in an aqueous NaCl solution to a gate voltage sweep. After a certain threshold voltage, new peaks appear in the spectrum that can be ascribed to CH vibrations (Fig. 1 (b)). The observation of CH peaks indicates the chemisorption of hydrogen on graphene. We show that this hydrogenation process can be reversed by a sweep in opposite direction [1]. The results hence show that we obtained an electrical switch to the functionalization of graphene, controlled by *in-situ* Raman spectroscopy. The chemisorbed hydrogen can be used as an anchor to graphene for more complex functionalization schemes, which opens up new possibilities for applications in life sciences.

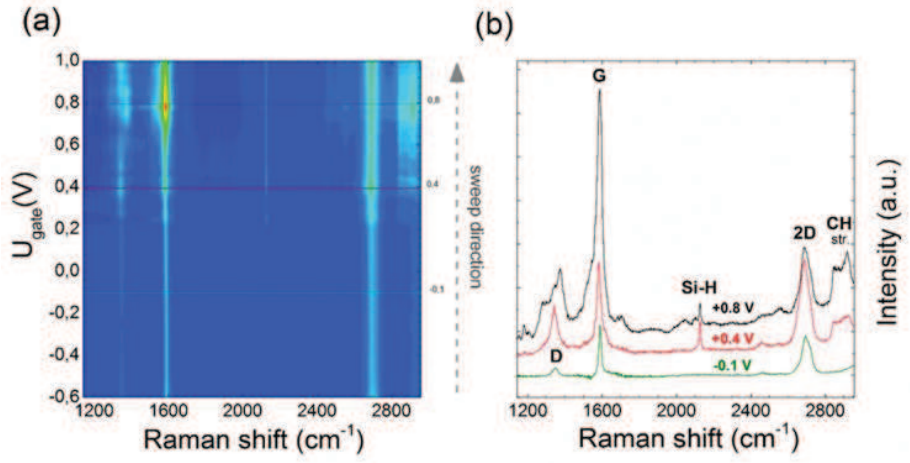

Fig. 1: (a) Raman false color map as a function of applied voltage. (b) Raman spectra for three different voltages.

[1] J. Binder et al. *Nanotechnology*, 27, 045704 (2016).

Acknowledgements:
This work was supported by the National Science Centre, Poland grant 2014/13/N/ST3/03772 and the European Union Seventh Framework Program under grant agreement n° 604391 Graphene Flagship.

Ultra-doped Ge: old material with new functionalities

S. Prucnal, Y. Berencen, W. Skorupa, S. Zhou

Institute of Ion Beam Physics and Materials Research, Helmholtz-Zentrum Dresden-Rossendorf, Germany

One of the main obstacles towards wide application of Ge in nanoelectronics is the lack of an efficient doping method for the fabrication of heavily doped Ge layers with well controlled junction depth. In fact, n-type doping of Ge is a key bottleneck in the realization of advanced negative-channel metal-oxide-semiconductor (NMOS) devices. Here we use ion implantation followed by flash-lamp (FLA) annealing for the fabrication of heavily doped Ge with comparably high mobility. In contrast to conventional annealing procedures, rear-side FLA leads to full recrystallization of Ge and dopant activation independently of pre-treatment. The maximum carrier concentration is well above 10^{20} cm^{-3} for n-type and above 10^{21} for p-type doping. The recrystallization mechanism and the dopant distribution during rear-side FLA are discussed in detail.

In this work, we report on the strong mid-IR plasmon absorption from heavily P-doped Ge thin films and superconductivity in Ga implanted Ge obtained by non-equilibrium thermal processing. Ultra-doped Ge layers were fabricated by ion implantation of P or Ga ions followed by rear-side flash lamp annealing in the millisecond range. This approach, in contrast to conventional annealing procedures, leads to full recrystallization of Ge films and high dopant activation. In this way single crystalline Ge thin films free of defects were obtained. The mid-IR plasmon spectral response at room temperature from those samples was characterized by means of Fourier transform infrared spectroscopy. It is proven that the position of the plasmonic resonance frequency signal can be tuned as a function of the P concentration.

Band gap engineering in Ge via non-equilibrium thermal processing and Sn doping

S. Prucnal, Y. Berencen, W. Skorupa and S. Zhou

Institute of Ion Beam Physics and Materials Research, Helmholtz-Zentrum Dresden-Rossendorf, Germany

The incorporation of different functional optoelectronic elements on a single chip enables performance progress which can overcome the downsizing limit in silicon technology. For example, the use of Ge instead of silicon as a basic material in nanoelectronics would enable faster chips containing smaller transistors. As was shown recently, Ge can be used not only for fast electronics but also for optical devices e.g. LEDs and detectors. In order to fully exploit and boost further its unique properties, the alloying of Ge with Sn and ultra-doping with P for n-type conductivity have to be explored. To this day, both Sn and P impurity are introduced into Ge mainly *in-situ* during the growth process (e.g. using molecular beam epitaxy (MBE) or chemical vapour deposition (CVD)).

In this work, we report on the band gap modification of Ge by Sn alloying and P co-doping. The doping of Ge was be performed using ion beam implantation of P and Sn with a concentration far exceeding the solid solubility limit of Sn in Ge (>> 0.2%). The implanted Sn was alloyed with Ge using rear-side flash lamp annealing. According to both XRD and HRTEM fabricated layer is single crystalline for the Sn doping up to 6 %. After P-implantation and annealing fabricated GeSn layers are n-type with active carrier concentration above 5×10^{19}cm^{-3}. The GeSn alloy made by presented method enable the integration of innovative Ge-based devices in the mainstream of Si CMOS technology which can be used for the fabrication of three-dimensional (3D) large-scale-integration devices with modulated optoelectronic properties.

Photoconversion of the Plasmonic Solar Cells Based on ZnO Nanorods and Silicon with Silver and Gold Nanoparticles

Katarzyna Gwóźdź[1], Ewa Płaczek-Popko[1], Eunika Zielony[1], Zbigniew Gumienny[1], Karolina Paradowska[1], Rafał Pietruszka[2], Bartłomiej S. Witkowski[2], Krzysztof Kopalko[2], Marek Godlewski[2,3], Witold Jacak[1], Liann-be Chang[4]

[1] *Department of Quantum Technologies, Faculty of Fundamental Problems of Technology, Wroclaw University of Technology, Wybrzeze Wyspiańskiego 27, 50-370, Wroclaw, Poland*
[2] *Institute of Physics, Polish Academy of Sciences, Al. Lotników 32/46, 02-668, Warsaw, Poland*
[3]*Department of Mathematics and Natural Sciences Collage of Sciences, Cardinal Stefan Wyszynski University, Dewajtis 5, 01-815, Warsaw, Poland*
[4]*Department of Electronic Engineering and Green Technology Research Center, Chang-Gung University, Taoyuan, Taiwan*

Quick development of new photovoltaic technologies encouraged the scientists to seek the new ways to improve their efficiency. One of the method frequently explored is plasmonics. The deposition of metal nanoparticles on top of a solar cell can cause the increase of the light absorption inside of the cell, which leads to higher photoconversion [1].

In our work we studied solar cells based on ZnO nanorods (NR), covered with silver nanoparticles (NPs) of diameters approximately 20 nm and gold of diameters approximately 10 nm, grown on the silicon substrate using the hydrothermal method. The nanorods were covered with ZnMgO and ZnO:Al layers using atomic layer deposition.

The sizes of the NPs were determined from the SEM images. Photovoltaic performance of the solar cells was analyzed using the spectral characteristics of the reflectance, sensitivity and external quantum efficiency. It was found that the sample with Ag NPs exhibits higher reflectance in the visible range than the reference sample without the NPs. Quantum efficiency is the highest for the sample with Au NPs in the whole measured spectrum of 300-1200 nm reaching 70%. The sample with Ag NPs exhibits lower quantum efficiency than the reference sample in the visible range of spectrum due to the increased reflectance. From the current-voltage characteristics under 1-Sun illumination the efficiency of the samples were obtained to be 4.45% for the reference sample, 4.6% for the sample with Ag NPs and 5.79% with Au NPs.

The gold nanoparticles of sizes approximately 10 nm are more promising in increasing the efficiency of the inorganic solar cells.

[1] W. Jacak, E. Popko, A. Henrykowski, E. Zielony, K. Gwozdz, G. Luka, R. Pietruszka, B. Witkowski, L. Wachnicki, M. Godlewski, L.-B. Chang, M.-J. Jeng, Solar Energy Materials and Solar Cells **147** (2016) 1-16.

Acknowledgments
This work has been partially supported by the Polish-Taiwanese/Taiwanese-Polish Joint Research Project DKO/PL-TW1/3/2013 and by the project of National Laboratory of Quantum Technologies (POIG. 02.02.00-00-003/08-00) and National Science Centre (Decision Nos. DEC-2012/06/A/ST7/00398 and DEC-2013/11/B/ST7/01385).

ZnO/GaAs heterojunction solar cells fabricated by ALD method

Piotr Caban[1], Rafał Pietruszka[1], Krzysztof Kopalko[1], Bartłomiej Witkowski[1], Marek Godlewski[1], Katarzyna Gwóźdź[2], Eunika Zielony[2], Ewa Płaczek-Popko[2]

[1]*Institute of Physics, Polish Academy of Sciences, al. Lotników 32/46, 02-668 Warsaw, Poland*
[2] *Wrocław University of Technology, ul. Wybrzeże Wyspiańskiego 27, 50-370 Wrocław, Poland*

In this work we tested the possibilities of application of an AZO electrode in GaAs based photovoltaic cells. For tests solar cells of a simple architecture were prepared.

ZnO/GaAs photovoltaic cells were fabricated by ALD (Atomic Layer Deposition) method. Thin layers of zinc oxide (ZnO) and aluminium doped zinc oxide (AZO) were deposited on p-type GaAs. We examined two types of solar cells architecture, differing in deposition sequence of the ALD layers and their function. In the first architecture, AZO was deposited on a ZnO layer. AZO plays role of a TCO (Transparent Conductive Oxide) electrode. In the second one, AZO layer was grown directly on the GaAs surface as TCO layer, but also as n-type partner in a heterojunction with a p-type GaAs. ALD processes were carried out in three different temperatures: 80, 160 and 250^0C on a lightly doped p-type GaAs with three different acceptor (Zn) concentrations.

Best efficiency (Eff. = 1.39%, with a fill factor of FF=0.39) was obtained for the AZO/ZnO/GaAs cell. This efficiency can be further improved after optimization of a top metal contact (point contact was used) and of thickness of AZO and ZnO layers. Their electrical properties should also be further optimized.

Acknowledgements

The research was partially supported by the Polish National Science Centre (NCN) (DEC-2012/06/A/ST7/00398)

Single Quantum Dot Spectroscopy in a Standard Macro-photoluminescence Setup

A. Bogucki , Ł. Zinkiewicz , P. Wasylczyk, W. Pacuski, P. Kossacki

Institute of Experimental Physics, Faculty of Physics, University of Warsaw, ul. Pasteura 5, 02-093, Warsaw, Poland

Solotronic [1,2] studies require access to single quantum emitters such as single defects or single quantum dots (QDs). The most common procedure is based on optical spectroscopy of a single emitters and application of micro-photoluminescence (μPL) setups. This can be technically realized either by microscopic objective placed outside the cryostat or miniature lens placed on piezo positioner in front of a sample. Above realizations are rather expensive and are not ideal in terms of photon extraction efficiency, stability and complexity.

In this work we present a new approach based on in-situ fabrication of micro-optic structures made of transparent resin placed on top of a semiconductor heterostructure. Micro-optic objects were produced with usage of three dimensional direct laser writing (3D-DLW) technique. The 3D-DLW is based on a two-photon absorption process which induces polymerization of a photoresist. In association with system that provides fast and accurate positioning of polymerization spot it allows printing arbitrary shaped 3D transparent structures. The great advantage of such polymer-micro optics is an ease of scaling up. Once printed structures can be used as a moulds for replication or masters for pattern transfer.

We demonstrate potential of proposed approach on self-assembled CdSe/ZnSe QDs. Placing spherical micro-lenses on a cylindrical support combined with an ordinary external lens fulfill imaging conditions for QDs placed 50 nm below surface of a sample. As a result presented "micro-bullet" structures allow studying PL of a single dot collected from the spot smaller than 1 μm but with standard macro PL setup.

We also demonstrate modifications of presented structures e.g. Fresnel lens geometry instead of spherical one or variation of a radius, and discuss photon extraction coefficient enhancement as well as combining 3D-DLW with single-color in-situ photolithography marking of an individual QD [3].

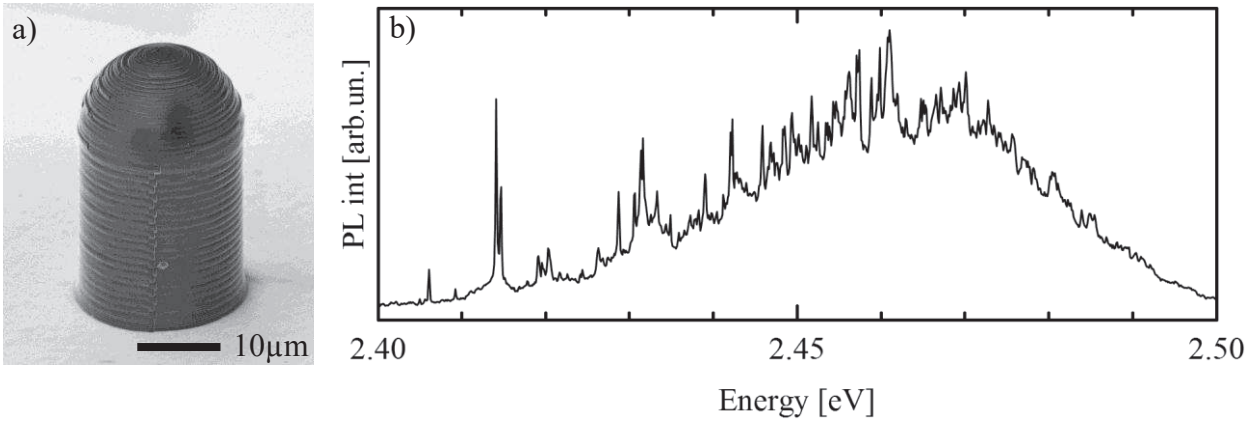

Fig. 1 a) Example SEM image of a "micro-bullet" structure fabricated by 3D-DLW technique, (b) corresponding spectrum of single QDs obtained in standard macro-PL setup.

[1] J. Kobak, *et al., Nat. Comm.,* **5**, 3191 (2014)
[2] T. Smoleński, *et al., Nat. Comm.,* **7**, 10484 (2016)
[3] K. Sawicki *et al*., *Appl. Phys. Lett.,* **106**, 012101 (2015)

Ab initio calculations for electronic structure engineering of Bi diluted III-V compounds and $Ge_{1-x}Sn_x$ alloy

Paweł Scharoch, Maciej Polak, Robert Kudrawiec

Faculty of Fundamental Problems of Technology
Wroclaw University of Science and Technology
Wybrzeże Wyspiańskiego 27,
50-370 Wrocław

Modern optoelectronics is stimulated to a large extent by the development of optical fiber telecommunication. E.g. transmitters or receivers are devices based on semiconductor nanostructures. Semiconductor alloys are materials of promising perspective in the field due the possibility of controlling technologically their structural and electronic properties. The knowledge of material properties is crucial at the stage of device design. Large scale *ab initio* calculations based on Density Functional Theory (DFT) offer an opportunity of predicting the properties. The main limitation of the research tool is the size of the system under investigation. However, valuable and helpful scientific information can be obtained from calculations for cell-periodic bulk, where, owing to translational symmetry, the system can be represented by a limited number of atoms. The presentation will focus on chosen aspects of *ab initio* modeling of the structural and electronic properties, on the example of III-V-Bi diluted systems and $Ge_{1-x}Sn_x$ alloy [1-5]. In particular such characteristics like composition dependent lattice parameters, band structures, band offsets, have been calculated and suitability of the systems for optoelectronic applications predicted. Moreover, in the case of $Ge_{1-x}Sn_x$ alloy the electronic properties have been studied in the full range of compositions, the effect of ion distribution discussed and a contribution of various physical processes to the band-gap bowing evaluated.

[1] M. P. Polak, P. Scharoch, R. Kudrawiec, *Semiconductor Science and Technology* **30**, 094001 (2015)
[2] K. Zelazna, M. P. Polak, P. Scharoch, J. Serafinczuk, M. Gladysiewicz, J. Misiewicz, J. Dekoster, and R. Kudrawiec, *Applied Physics Letters* **106** , 142102 (2015).
[3] J. Kopaczek, R. Kudrawiec, M. P. Polak, P. Scharoch , M. Birkett, T. D. Veal, K. Wang, Y. Gu., Q. Gong, S. Wang, *Applied Physics Letters*, **105** (22) (2014).
[4] M. P. Polak, P. Scharoch, R. Kudrawiec, J. Kopaczek, M. J. Winiarski, W. M. Linhart, M. K. Rajpalke, K. M.Yu, T. S. Jones, M. J. Ashwin, T. D.Veal, *Journal of Physics D*, **47** (35) (2014).
[5] R. Kudrawiec, J. Kopaczek, M. P. Polak, P. Scharoch, M. Gladysiewicz, J. Misiewicz, R. D. Richards, F. Bastiman, J. P. R. David, *Journal of Applied Physics*, **116** (23) (2014).

An influence of silicon substrate parameters on a responsivity of MOSFET-based THz detectors.

Krzysztof Kucharski [1], Przemysław Zagrajek [2], Daniel Tomaszewski [1],
Andrzej Panas [1], Grzegorz Głuszko [1], Jacek Marczewski [1]

[1] *Instytut Technologii Elektronowej, ul. Okulickiego 5E, 05-500 Piaseczno, Poland*
[2] *Military University of Technology, ul. Sylwestra Kaliskiego 2, 00-908 Warsaw, Poland*

Silicon field effect n-type MOSFETs have been recently used as terahertz (THz) radiation detectors. They are cheap, easy to integrate with silicon read-out and offer reasonable detectivity at room temperature. Their response, i.e. a DC voltage measured between the source and unbiased drain is proportional to a power of an incoming radiation. The response maximum is typically achieved at subthreshold range. The MOSFETs may be easily equipped with patch antennas fabricated on top of the circuit. It has been shown that an effective imaging with use of FETs can be achieved in atmospheric windows of 300 GHz and 600 GHz.

The effective coupling of the FET channel with the THz wave is strongly influenced by the fact that part of radiation is dissipated within the substrate. That may be minimized by thinning the substrate using a grinding technique or by fabricating the detectors on membranes using MEMS-related technologies. Highly resistive substrates may be also used especially if the detector backsides are exposed to radiation via dedicated glued lenses machined using highly resistive silicon. In this paper we examine several types of different substrates to make a suitable choice for a volume production of NMOSFET-based THz detectors.

The NMOSFETs with polysilicon gate and monolithically coupled antennas and with projected channel length of 3 μm have been used. They have been manufactured on the following substrate types: Silicon-On-Insulator (SOI) wafers, low resistivity Czochralski (Cz-Si) wafers, and high resistivity (HR) floating zone (FZ) wafers.

The substrates of the devices have been thinned down to 40 μm. In the case of SOI and Cz-Si wafers the membranes have been manufactured using a selective etching, while in the case of HR FZ wafers the grinding technique has been initially used. The selective etching in KOH solution could not have been applied in this case because of the wafer orientation (111). However, recently the detectors on (100) HR FZ wafers with membranes have been also processed.

The measurements of the MOSFET responsivity (DC voltage between drain and source) have been done. The largest response (100 μV) has been measured for MOSFETs on the SOI wafers with the local membranes. The response of 10÷20 μV has been achieved for MOSFETs on the thinned HR FZ wafers. The response of 1÷2 μV has been achieved for devices on membranes on the Cz-Si wafers. The recent measurements have revealed a high responsivity of the MOSFETs on membranes manufactured on HR FZ wafers, in some cases even higher (~500 μV) than for SOI wafers. This result is interesting not only from a research point of view, but also from manufacturing aspect - among others the HR FZ wafers are significantly cheaper than the SOI substrates. So the fabrication of the THz detectors on the HR FZ wafers becomes a promising option with respect to SOI-based technology.

Acknowledgment: The work has been supported by The National Centre for Research and Development under a grant PBS3/A3/18/2015

Thermal Emission of THz Radiation from Field Effect Transistors

Dmitriy Yavorskiy, Krzysztof Karpierz, Marcin Białek, Marian Grynberg, and Jerzy Łusakowski

Institute of Experimental Physics, Faculty of Physics, University of Warsaw, ul. Pasteura 5, 02-093 Warsaw, Poland

Properties of THz radiation, especially its non-invasive interaction with biological tissues and a low absorption in many materials stimulated a broad research- and applications-oriented activity. A steady progress in development of THz detectors resulted, e.g., in commercially available multipixel arrays operating at a video rate. However, most of current applications are based on non-resonant detectors because resonant ones, especially these working at room temperature, are still under development, in spite of a huge market and scientific demand. This shows an interesting path of investigations which could lead to fabrication of a resonant and tunable THz detector. On the other hand, modern THz applications need compact, efficient and cost-effective sources of radiation, possibly - spectrally selective ones. THz emitters available nowadays are typically large (like CO_2 - pumped lasers) and/or expensive (BWOs, frequency multipliers) so generation of THz radiation is even more perplexing than its detection.

We show results of spectrally sensitive measurements of a THz radiation emitted from FETs. A thin film of a high electron mobility InSb sample was used as a detector. Measurements were done at liquid helium temperatures in magnetic fields up to about 3 T with a modulated on/off biasing of the drain of a FET. A resulting emitted radiation was registered with the InSb detector placed in the magnetic field. An incident radiation causes transitions between Landau Levels in the conduction band of InSb (a cyclotron resonance transition) which leads to changes in the detector conductivity. Changing the magnetic field one gets a spectral tuneability of the detector.

The source of THz radiation was a commercially available GaAs/AlInAs FET. Additionally, as a reference source of radiation, a thermal source (a carbon resistor) was used. We compared thermal radiation spectra of the resistor with these of the FET (see Fig. 1). By applying an appropriate numerical treatment of the data, for the first time we show the spectrally resolved emission data. We show the FET emission is mainly of a thermal character. The differences between them are discussed.

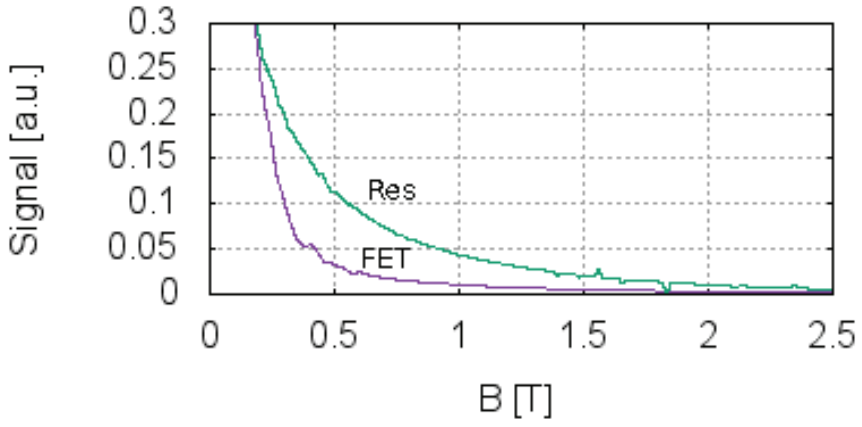

Fig. 1. Spectra of thermal emission originating from carbon resistor and FET. $T = 4.2$ K.

The study of glass transition temperature measured on P3HT:PCBM thin films using spectroscopic ellipsometry

B. Hajduk, B. Jarząbek, J. Jurusik

Centre of Polymer and Carbon Materials of the Polish Academy of Sciences,
34 Marie Curie-Skłodowska str, 41-819 Zabrze, Poland

Poly (3-hexylthiophene) P3HT (Fig.1a), as an organic semiconductor and (phenyl-C61-butyric acid methyl ester) PCBM (Fig.1b) as a fullerene derivative are the base for bulk organic solar cells with high efficiency. Typical efficiency of the P3HT:PCBM bulk solar cells, where P3HT is donor and PCBM is acceptor, is contained in the range 1-6%.

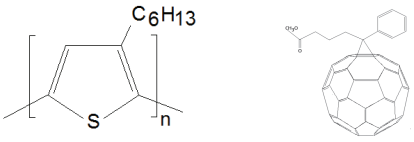

(a) (b)

Fig. 1 The chemical structures of P3HT (a) and PCBM (b)

Spectroscopic ellipsometry is a non-destructive method, commonly used to obtain the physical parameters, like optical and dielectrical constants, thickness, roughness etc. In this work the SENTECH SE 850E, the spectroscopic ellipsometer, working in the spectral range 240-2500 nm, with the thermal cell equipment was used. This thermal cell, connected with the temperature controller, gives us the opportunity to perform the measurements under low vacuum, during heating or cooling. The aim of this work is the study of influence of P3HT:PCBM thin films composition on its glass transition, using spectroscopic ellipsometry. The A.J. Person at al., in [1], have observed one or two glass transitions of the P3HT:PCBM blends. They showed the thickness dependence on temperature, where it is necessary to use of proper ellipsometric model with very low MSE (Mean Square Error). Additionally, the T.T. Ngo at al. [2] have showed the changes of glass transition temperature of the P3HT:PCBM in quenched state, basing on DSC technique. They have observed just one glass transition temperature for every sample. In this work we can observe the glass transition temperature, basing just on Psi and Delta measurements, where the physical model is not necessary for use. The P3HT:PCBM thin films were deposited on the glass substrates from the polymer-chlorobenzene solutions, using spin-coating method. The ratio of P3HT to PCBM weight concentrations in the solutions were changed from the pure P3HT to pure PCBM.

[1] A.J. Pearson, T. Wang, R.A.L.Jones, D.G. Lidzey, P.A. Staniec, P.E.Hopkins, A.M. Donald "Rationalizing Phase Transitions with Thermal Annealing Temperatures for P3HT:PCBM Organic Photovoltaic Devices", Macromolecules, 45 (2012) 1499-1508

[2] T.T. Ngo, D.N.Nguyen, V.T. Nguyen "Glass transition of PCBM, P3HT and their blends in quenched state", Advances in Natural Sciences: Nanoscience and Nanotechnology 3 (2012) 045001, 1-4

This work has been supported by the NCN grant (Poland) No. UMO-2013/09/B/ST8/01629

Investigation of Thermal and Plasmonic Emission from Grating-Gated GaN/AlGaN High Electron Mobility Transistors

Vytautas Janonis, Vytautas Jakštas, Ignas Grigelionis, Irmantas Kašalynas

[1] *Semiconductor Physics Institute of Center for Physical Sciences and Technology, Sauletekio al.3, Vilnius, Lithuania*

High frequency and high power electronics applications require material parameters, which are difficult to achieve with silicon technology. Gallium nitride (GaN) is one of the most promising materials, which would allow the fabrication of such devices. Preferable material parameters encouraged rapid development of GaN-based devices during recent years. A two dimensional electron gas (2DEG) formed at GaN/AlGaN heterojunction interface have been proposed to use for the development of field effect transistors (FETs) and antenna coupled terahertz (THz) detectors [1]. Moreover, the density and mobility of 2DEG can reach sufficiently high values at room temperature required for the development of an efficient THz emitter of the plasmonic GaN/AlGaN FET [2]. Radiative plasmonic oscillations at THz frequency originate in the transistor channel and couple out to free space via the grating electrodes which biasing can modulate the emission frequency via modulation of carrier density in the channel.

The aim of this work was to investigate THz emission spectra from the grating-gated AlGaN/GaN transistor structures at room and liquid nitrogen temperatures. The THz emitters with different geometry gratings were fabricated of the AlGaN/GaN structures grown on Al_2O_3 substrate [3].

The radiation power from dc-biased THz emitters was investigated at room environment using the two parabolic mirrors telescope and the pyroelectric THz detector and measuring the opto-mechanically modulated THz radiation with Lock-In technique. It was so called DC regime. In addition a supplied current was electrically modulated to realize an AC regime. A linear dependence between an electrical supplied power and an optical THz power was found. The THz emission power was slightly reduced upon sample cooling up to 80 K temperature. The decrease of the THz emission was attributed to the reduction of effective temperature of the 2DEG which was found depended on the supplied AC power.

In the next step, the radiation spectra of the sample in DC and AC regime were recorded using vacuumed Fourier spectrometer. Shape of the emission spectra in the DC regime was ascribed by thermal black body model without notable signatures of plasmonic radiation. Intensity of the thermal radiation in AC regime was reduced via an increase of ac-bias modulation frequency but without signature of emphasized plasmonic emission. It was found that thermal radiation from grating-gated GaN/AlGaN transistor dominated the spectrum. And the power of plausible plasmonic emission was at least ten times smaller than the thermal radiation power. Plasmonic THz power detection would require more sensitive He-cooled THz detectors with the response time faster than provided by used pyroelectic detectors. Recently it was demonstrated that the THz emitters would require more sophisticated electrical contacts [4] and better developed GaN/AlGaN heterojunction with electrons drift velocity higher by up to two orders of magnitude [5].

[1] Boppel, S. et al., IEEE Trans. Terahertz Science and Technology, **6**, no. 2, 348-350 (2016).
[2] Shur M., J. Phys.: Conf. Ser., **486**, 012025 (2014).
[3] Jakštas, V. et al., Lith. J. Phys. **54**, 227–232 (2014).
[4] Zheng Zhongxin et al., Journal of Semiconductors, **36**, No. 10, 104002 (2015).
[5] Sung-Min Hong, IEEE Trans. Electron Devices, **62**, Iss. 12, 4192 – 4198 (2015).

Photoelectrical properties of p-i-n diodes with PbSe quantum wells

S. Chusnutdinow, M. Szot, L. Kowalczyk, W. Zaleszczyk, V. Kolkovsky, M. Wiater, T. Wojtowicz and G. Karczewski

Institute of Physics, Polish Academy of Sciences, Warsaw, Poland

Lead selenide (PbSe) is a widely recognized material for infrared photodetectors which can be employed in infrared spectroscopy, gas and flame analysis, medical diagnostics etc. Due to favorable physical and chemical properties of PbSe, such as a narrow and direct band gap and a large Bohr radius, the PbSe-based detectors are very sensitive and can operate in the 1–5 μm spectral region. In addition, due to the large Bohr radius the quantum confinement effect in PbSe nanostructures is much stronger than in II-VI or III-V materials. On the other hand, PbSe exhibits a few drawbacks, such as high Auger recombination, high electrical permittivity, and very high thermal expansion coefficient. However, the rate of Auger recombination can be decreased by surrounding the PbSe structures by wide-gap material barriers. Introduction of PbSe nano-inclusions into wide-gap photodetectors would lead to an extension of the detection range toward lower energies, since the energy gap of PbSe is just 0.28 eV at 300 K. CdTe and PbSe has close value crystal lattice parameters, thus the lattice mismatch is ~ 5.5%. However, CdTe and PbSe crystallize in the zinc blend and rock salt, respectively. As a result of the difference in crystal structures these materials are almost immiscible. Limited miscibility allows creation of high-quality quantum size inclusions.

Here we report on photoelectrical investigations of p-CdZnTe/i-CdTe/n-CdTe thin-film diodes with PbSe nano-inclusions introduced into the intrinsic CdTe absorption layer. The thin-film heterojunctions were grown by molecular beam epitaxy (MBE) from elemental sources on monocrystalline, semi-insulating (100) GaAs substrates. The n-type CdTe films were produced by iodine doping. Depending of the growth parameters either PbSe quantum dots or PbSe quantum wells were formed in the intrinsic CdTe layer. The p-type CdZnTe layers were doped with nitrogen supplied from nitrogen-plasma source. The investigated structures exhibit very good diodes characteristics. The current-voltage characteristics of p-CdZnTe/i-CdTe/n-CdTe diodes were measured in darkness and under infrared illumination. The dark forward-to-reverse current ratio for this diode is equal to 1×10^4 at ±0.5V voltage bias and the diode ideality factor is about ~ 1.1 at 295 K. With the decreasing temperature the ideality factor increases to 44 at 13 K. This is probably due to the change in the carriers transport mechanism through the heterojunction. Electron Beam Induced Current (EBIC) measurements confirmed the formation of the junctions at the p-CdZnTe/i-CdTe interface. EBIC scan on cross-sectional indicated that the maximum of the EBIC current was occurring in the PbSe layer. The diffusion length and activation energy of charge carriers have been extracted from EBIC scan profiles.

The spectral response curves of the diodes reveal two peaks located at about 800 nm and 3000 nm. These peaks are related with absorption in CdTe and PbSe QW, respectively. Intensity of second peak very strongly depends on temperature and reaches maximum intensity at about temperature 200K. The investigated p-CdZnTe/i-CdTe/n-CdTe structures with PbSe nano-inclusions proved to be very promising for IR sensor applications.

This work was partially supported by the Foundation of Polish Sciences by the Master program № Mistrz5./2013

Electrical properties of $CuInVO_5$

T. Groń[1], M. Bosacka[2], E. Filipek[2], A. Pacześna[2], P. Urbanowicz[1], B. Sawicki[1] and H. Duda[1]

[1]*University of Silesia, Institute of Physics, ul. Uniwersytecka 4, 40-007 Katowice, Poland*
[2]*West Pomeranian University of Technology, Szczecin, Department of Inorganic and Analytical Chemistry, Al. Piastów 42, 71-065 Szczecin, Poland*

$CuInVO_5$ has been synthesised by heating the alloy of CuInV in pure oxygen atmosphere at 650°C for 48 hours. It crystallises in monoclinic system and its elementary cell parameters are: a = 0.8793 (2) nm, b = 0.61542(6) nm c = 1.5262(2) nm, β = 106.69(2)º, Z = 4 [1]. The structure of $CuInVO_5$ contains isolated Cu_4O_{18} – groups consisting of trans edge sharing CuO_6 – octahedral. Interconnection of the groups by $[In_4O_{16}]$ – ribbons running along [010] which are built of edge- and corner-sharing InO_6 – octahedral results in the formation of slabs perpendicular to the c-axis. VO_4^{3-} groups link the slabs to a three-dimensional framework. The structure may be derived from a cubic closet packing of the oxygen atoms with copper and indium atoms in the octahedral and vanadium atoms in the tetrahedral vacancies. In our study the compound $CuInVO_5$ as a pure phase has been obtained from the mixture of oxides V_2O_5, CuO and In_2O_3 used at the molar ratio 1 : 2 : 1 and from equimolar mixture of CuO and $InVO_4$ [2]. From IR spectroscopic studies it shows that $CuInVO_5$ is built with CuO_6, InO_6 octahedra and VO_4 tetrahedra [2].

The electrical conductivity $\sigma(T)$ and the *I-V* characteristics have been measured with the aid of the DC method in the temperature range 300–400 K using a KEITHLEY 6517B Electrometer/High Resistance Meter. The thermoelectric power *S(T)* was measured in the temperature range 300–600 K with the aid of a Seebeck Effect Measurement System (MMR Technologies, Inc., USA). Broadband dielectric spectroscopy measurements were carried out using pellet, polished and sputtered with (~80 nm) Ag electrodes in the frequency range from 5×10^2 to 1×10^6 Hz with a Novocontrol Alpha Impedance Analyser and in the temperature range 76–400 K. The sample electrode surface and thickness were 5 mm^2 and 1.0 mm, respectively. For measuring $\varepsilon_r = C/C_0$, where C_0 is the capacity of the empty capacitor and $\tan\delta = \varepsilon''/\varepsilon'$, where ε'' and ε' are imaginary and real part of complex dielectric permittivity, respectively.

The electrical conductivity of the Arrhenius-type characteristic for semiconductors with the activation energy E_A = 0.42 eV in the temperature range 300-400 K was observed. The temperature dependence of thermopower, *S(T)*, showed *n-p* transition at 465 K. The most interesting observation concerns the symmetric and linear characteristics *I-V* both at 300 and 400 K, showing a strong increase in electron emission and conductance by two orders of magnitude. A large carrier emission of the Arrhenius type observed in $CuInVO_5$ one can explain with the help of the Poole–Frenkel effect, because the electrons of copper ions on the unfilled 3*d* orbital are unscreened. For this reason, this compound can easily be polarized under the influence of an applied external electric field. The dielectric measurements showed non-linear and strong increase of the relative dielectric permittivity ε_r with increasing temperature above 200 K and its strong decrease with increasing frequency. Similar behavior has been observed for the loss tangent.

References

[1] P. Moser, V. Cirpus, W. Jung, *Z. anorg. allg. Chem.* **625**, 714 (1999).
[2] M. Bosacka, E. Filipek, A. Pacześna, *J. Therm. Anal. Cal.*, (2016), in press.

Electrical properties of $Sr_2InV_3O_{11}$

T. Groń[1], E. Filipek[2], A. Pacześna[2], P. Urbanowicz[1], B. Sawicki[1] and H. Duda[1]

[1]*University of Silesia, Institute of Physics, ul. Uniwersytecka 4, 40-007 Katowice, Poland*
[2]*West Pomeranian University of Technology, Szczecin, Department of Inorganic and Analytical Chemistry, Al. Piastów 42, 71-065 Szczecin, Poland*

The last few decades, intensification has been observed in the field of research on multicomponent oxide systems, which is frequently aimed at obtaining new materials of interesting electric, magnetic or catalytic properties. Investigations dealing with systems based on the oxides of divalent and trivalent metals have allowed among others to prove an existence of a series of compounds with the general formula $A_2BV_3O_{11}$ (where: A(II) and B(III)- metals), *e.g.* $Zn_2FeV_3O_{11}$, $Mg_2CrV_3O_{11}$, $Ni_2FeV_3O_{11}$ $Pb_2BiV_3O_{11}$, $Sr_2BiV_3O_{11}$. It can be concluded from bibliographic data that these compounds are likely to find an application for example as cathode materials in high-energy cells or as components of effective catalysts for the oxidation processes of light hydrocarbons.

The investigations of reactions occurring in the $SrO–V_2O_5–In_2O_3$ system have permitted a statement that also in this system a new compound on the formula $Sr_2InV_3O_{11}$ is formed [1–3]. Hitherto performed works have shown, that a synthesis of $Sr_2InV_3O_{11}$ can be conducted by heating the mixture of $SrCO_3$ /In_2O_3/V_2O_5 (in molar ratio 4:1:3) in the atmosphere of air in the temperature range 450-800°C [1,2]. The unit cell of such obtained $Sr_2InV_3O_{11}$ has been found to be monoclinic with the following parameters: a = 0.9671(3) nm, b = 1.9509(8) nm, c = 0.6570(2) nm, β = 96.60(3)°, V = 1.2313 nm^3. The experimental density of $Sr_2InV_3O_{11}$ is equal to 4.39 ± 0.05 g/cm^3 [3]. The energy gap calculated from the UV-vis measurements gave E_g = 3.5 eV.

The electrical conductivity $\sigma(T)$ and the *I-V* characteristics have been measured with the aid of the DC method in the temperature range 300–400 K using a KEITHLEY 6517B Electrometer/High Resistance Meter. The thermoelectric power $S(T)$ was measured in the temperature range 300–600 K with the aid of a Seebeck Effect Measurement System (MMR Technologies, Inc., USA). Broadband dielectric spectroscopy measurements were carried out using pellet, polished and sputtered with (~80 nm) Ag electrodes in the frequency range from 5×10^2 to 1×10^6 Hz with a Novocontrol Alpha Impedance Analyser and in the temperature range 76–400 K. The sample electrode surface and thickness were 5 mm^2 and 1.0 mm, respectively. For measuring $\varepsilon_r = C/C_0$, where C_0 is the capacity of the empty capacitor and $\tan\delta = \varepsilon''/\varepsilon'$, where ε'' and ε' are imaginary and real part of complex dielectric permittivity, respectively.

The *p*-type electrical conductivity below $\sigma = 3.4\cdot10^{-9}$ S/m in the temperature range 300-400 K was observed. Such small values of σ are typical for insulators and correlate well with the value of the energy gap Eg = 3.5 eV [3]. Moreover, in the temperature range 350-400 K a strong increase of σ with the activation energy E_A = 0.79 eV of the Arrhenius-type characteristic for semiconducting state appeared. Above 400 K only *n*-type thermoelectric power was observed.

[1] E. Filipek, A. Pacześna, Polish Patent No. P404202, Warsaw, 2015.
[2] A. Pacześna, E. Filipek, *2nd Central and Eastern European Conference on Thermal Analysis and Calorimetry*, 27-30 August, 2013, Lithuania, Book of Abstracts, Vilnius, p. 306.
[3] E. Filipek, A. Pacześna, M. Piz, *Ceram. Int.*, (2016), in press.

Influence of Cr-substitution on the magnetic properties of $Fe_{1-x}Cr_xSnSbO_6$

T. Groń[1], E. Filipek[2], G. Dąbrowska[2], H. Duda[1] and M. Oboz[1]

[1]*University of Silesia, Institute of Physics, ul. Uniwersytecka 4, 40-007 Katowice, Poland*
[2]*West Pomeranian University of Technology, Szczecin, Department of Inorganic and Analytical Chemistry, Al. Piastów 42, 71-065 Szczecin, Poland*

The oxides SnO_2, Fe_2O_3, Cr_2O_3 and Sb_2O_4 and known compounds formed with the participation of these oxides, due to their chemical, magnetic, electrical and catalytic properties are particularly attractive for basic research and for a large number of prospective applications. A new continuous substitution solid solution of a $Fe_{1-x}Cr_xSnSbO_6$ type is formed in the $FeSnSbO_6$–$CrSnSbO_6$ system and crystallize in the tetragonal system and they have the rutile-type structure [1,2]. The ultraviolet-visible and near-infrared measurements showed that the energy gap, E_g, in $Fe_{1-x}Cr_xSnSbO_6$ increases monotonically with increasing content x, *i.e.* E_g = 1.67, 1.88, 1.89, 1.96 and 2.01 eV for x = 0.0, 0.25, 0.5, 0.75 and 1.0, respectively [3]. Electrical measurements of $Fe_{1-x}Cr_xSnSbO_6$ solid solution showed semiconducting behaviour with the activation energy decreasing from E_A = 0.64 eV for x = 0.0 to E_A = 0.32 eV for x = 1.0 in the intrinsic conductivity temperature region as well as the *n*-type conduction at room temperature. The *I-V* characteristics and the conductance G at 300 and 400 K showed symmetrical and non-linear behavior in the voltage range (-100, 100 V) suggesting the electron emission over the potential barrier especially for the boundary compounds $FeSnSbO_6$ and $CrSnSbO_6$ [4].

Magnetization measurements were carried out using a Quantum Design System (MPMS XL). Static (dc) magnetic susceptibility was measured in the magnetic field H_{dc} = 1000 Oe and recorded both in zero-field-cooled (ZFC) and field-cooled (FC) mode. Dynamic (ac) magnetic susceptibility was measured at an internal oscillating magnetic field H_{ac} = 3.9 Oe with an internal frequency f = 300 Hz. Both dc and ac magnetic susceptibility were measured in the temperature range 2–300 K. Magnetization isotherms were measured in the temperature range 2-300 K in static (dc) magnetic fields up to 70 kOe.

Magnetic measurements showed that the $Fe_{1-x}Cr_xSnSbO_6$ solid solution is ferrimagnetic over the range of concentrations of chromium ions from x = 0.0 to x = 1.0. Only for x = 1.0 the long-range ferrimagnetic interaction with the Curie temperature T_C = 5 K is observed. In all samples, a short-range antiferromagnetic interaction occurred, seen in a negative paramagnetic Curie-Weiss temperature that varied from -41 K for x = 0.0 via -157 K for x = 0.5 to -190 K for x = 1.0. The effective magnetic moment increased from 3.585 μ_B/f.u. for x = 0.0 to 4.99 μ_B/f.u. for x = 1.0, suggesting the existence of both a mixed valence chromium and iron ions. The imaginary component of ac magnetic susceptibility showed the oscillating values close to zero, indicating a lack of the energy dissipation characteristic for the ferrimagnetic state and spin frustration. The most interesting observation was the appearance of the spin-glass-state with an increase in the content of chromium ions, for which the freezing temperature reached the highest value of 25 K for x = 1.0.

[1] J. Isasi, L. Veiga, C. Pico, *J. Mater. Sci. Lett.* **15**, 1022 (1996).
[2] V.A. Govorov, A.M. Abakumov, M.G. Rozova, A.G. Borzenko, S.Yu. Vassiliev, V.M. Mazin, M.I. Afanasov, P.B. Fabritchnyi, G.A. Tsirlina, E.V. Antipov, E.N. Morozova, A.A. Gippius, V.V. Ivanov, and G. Van Tendeloo, *Chem. Mater.* **17**, 3004 (2005).
[3] G. Dąbrowska, and E. Filipek, M. Piz, *Ceram. Int.* **41,** 12560 (2015).
[4] T. Groń, G. Dąbrowska, E. Filipek, H. Duda and B. Sawicki, *Acta Phys. Pol. A* **129**, 153 (2016).

Designing the active region of mode-locked interband cascade lasers

K. Ryczko[1], J. Misiewicz[1], M. Kamp[2], G. Sęk[1]

[1]*Laboratory for Optical Spectroscopy of Nanostructures, Department of Experimental Physics, Faculty of Fundamental Problems of Technology, Wrocław University of Technology, Wybrzeże Wyspiańskiego 27, 50-370 Wrocław, Poland*
[2]*Technische Physik, University of Würzburg & Wilhelm Conrad Röntgen Research Center for Complex Material Systems, Am Hubland, D−97074 Würzburg, Germany*

Interband cascade lasers (ICLs) have already been proven as a promising mid-infrared (MIR) source desirable for many applications in medical diagnostics, trace-gas analysis, pollution monitoring and molecular spectroscopy. Their application potential originates mostly from unique operational characteristics as, e.g., single mode, continuous-wave and high power operation at elevated temperatures in the range from below 3 to about 6 μm [1,2], broad spectral tunability [3,4], and low threshold currents and hence small electrical power consumption [5] when compared to the main competitor which are quantum cascade lasers.
A device that has not yet been realized is a mode-locked interband cascade laser. Such a source is of great interest for dual-comb spectroscopy, where two mode combs with a slightly different spacing are used to sample a wide spectral range [6]. While this is in principle possible with two Fabry-Perot lasers, the stable phase relation between the modes in a mode-locked device offers significant advantages for the practical implementation of dual comb spectroscopy. Passive mode-locking can be achieved by the insertion of a saturable absorber into the laser resonator. In semiconductor lasers, the saturable absorber can be realized by the application of reverse bias, which in case of ICL requires very careful band structure engineering since alignment of the levels in the minibands used to carrier transport depends on the polarity and the magnitude of the internal electric field. In addition to possible applications in mode-locked lasers, engineering of the active regions towards smaller oscillator strength is also beneficial for Q- or gain switched lasers.
In this work, we present results of theoretical modelling in the framework of eight-band k·p theory of the ICLs' band structure under external electric field performed in order to investigate the effect of the bias value and direcion, i.e. from normal lasing conditions as in the gain section to the reversed bias of the absorber part. We present several solutions of the respectively modified type-II QWs of InAs/(In,Ga)(As,Sb)/AlSb materials' system which allow obtaining the demanded lifetime (oscillator strength) ratio in the two parts of the mode-locked laser.

[1] J. Scheuermann, R. Weih, M. von Edlinger, L. Nähle, M. Fischer, J. Koeth, M. Kamp, S. Höfling, Appl. Phys. Lett. 106, 161103 (2015).
[2] M. Dallner, J. Scheuermann, L. Nähle, M. Fischer, J. Koeth, Sven Höfling, M. Kamp, Appl. Phys. Lett. 107, 181105 (2015).
[3] Y. Jiang, L. Li, Z. Tian, H. Ye, L. Zhao, R. Q. Yang, T. D. Mishima, M. B. Santos, M. B. Johnson, and K. Mansour, J. Appl. Phys. 115, 113101 (2014).
[4] M. von Edlinger, J. Scheuermann, R. Weih, L. Nähle, M. Fischer, S. Höfling, J. Koeth, M. Kamp, Proc. SPIE 9370, 9370A (2015).
[5] I. Vurgaftman, W. W. Bewley, C. L. Canedy, C. S. Kim, M. Kim, C. D. Merritt, J. Abell, J. R. Lindle, and J. R. Meyer, Nat. Commun. 2, 585 (2011).
[6] G. Villares, A. Hugi, S. Blaser and J. Faist, "Dual-comb spectroscopy based on quantum-cascade-laser frequency combs", Nature Communications 5, 5192 (2014).

The project has received funding from the European Union's Horizon 2020 research and innovation programme under grant agreement No 636930.

Dopant mapping in InP nanowires for solar cell applications

A. Rodil,[1] S. Kölling,[1] A. Cavalli,[1] E.P.A.M. Bakkers,[1, 2] and P.M. Koenraad [1]

[1] *Eindhoven University of Technology,* 5612 AZ, *Eindhoven, Netherlands*
[2] *Kavli Institute, Quantum Transport Group, Delft, 2628 CJ, Netherlands*

Nanowire solar cells are cheaper and consume less material than planar solar cells [1]. However, it is necessary to improve their performance in order to achieve competitive efficiencies. A nanowire solar cell is based on an array of nanowires doped as pn-junctions. At the pn-junction the electrical carriers (electrons and holes) created by light interacting with the nanowires are separated and thus electrical energy is generated.

Thus optimizing the pn-junction by controlling the dopant concentrations inside the nanowires is a crucial aspect to improve the performance of these nanowire solar cells. However, determining the dopant profile inside nanowires is challenging because of the small size of the nanowires. We use atom probe tomography (APT) to measure such concentration profiles [1]. APT enables us to map the atomic positions in a nanowire in three dimensions with sub-nm resolution [3].

We have examined Si (n-type) and Zn (p-type) doped InP nanowires using APT in order to extract the doping profiles from the nanowires with sensitivity down to the single digit ppm level. Here we present the sample preparation technique required to make these measurements, the doping profiles extracted from various nanowires and discuss the relations between nanowire shape and doping levels.

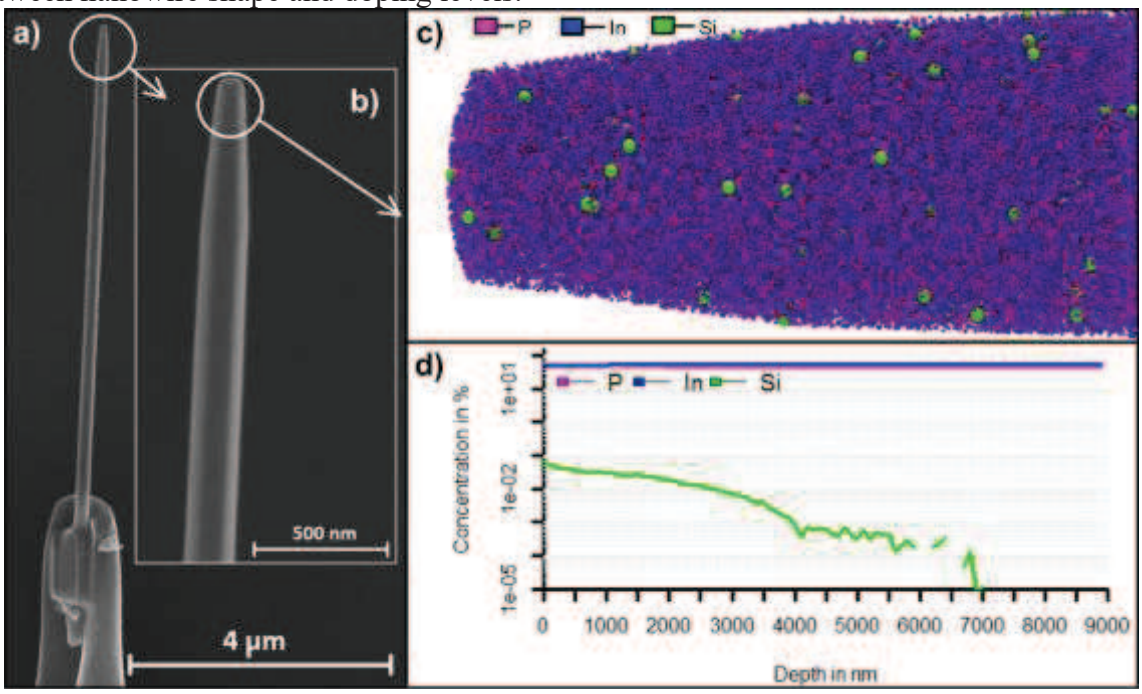

Figure 1: Si doped InP nanowire analysis results: a,b) SEM images, c) Atomic positions 3D reconstruction of 10% of the atoms, d) element concentration profiles

[1] Jesper Wallentin, Nicklas Anttu, Damir Asoli, "*InP Nanowire array solar cells achieving 13.8% efficiency by exceeding the ray optics limit"* Science **339**, 1057 (2013).
[2] M. K. Miller, A.Cerezo, M.G. Hetherington and G.D.W. Smith, *Atom Probe Field Ion Microscopy.* (1996), published by CLARENDON PRESS-OXFORD, *ISBN Q 19 851387 9.*
[3] P. Bas, A. Bostel, B. Deconihout, D. Blavette, "*A general protocol for the reconstruction of 3D atom probe data Applied Surface"* Science. **47-8**, 298 (1995).

Optical Functions of Rydberg Excitons

David Ziemkiewicz, Sylwia Zielińska-Raczyńska, and Gerard Czajkowski

UTP University of Science and Technology, Bydgoszcz,
Al. Prof. S. Kaliskiego 7, 85-789 Bydgoszcz, Poland

Recently Rydberg Excitons have attracted more attention [1-3]. After their detection in a natural crystal of copper oxide found at the Tsumeb mine in Namibia [1] an intensive research, both theoretical and experimental, have started. Due to the fact that the optical properties of Rydberg excitons have been experimentally examined, there is a need for theoretical description and interpretation of their unusual features. We show how to compute the optical functions (reflectivity, transmissivity, and absorption) of semiconductor crystals when Rydberg excitons exist, taking into account the effect of the coherence between the electron-hole pair and the electromagnetic field. Our method which based on the so-called real density matrix approach [3]. Having in mind the experimental results, we focus the attention on the optical spectra of Cu_2O. As it follows by the analysis of crystal symmetry, the lines related to odd angular momentum exciton number $\ell = 1, 3, ..$ are observed [2]. The dominant role play the P-excitons (the so-called yellow series), but also excitonic states with higher than $\ell = 1$ angular momentum (for example, the F-excitons with $\ell = 3$ and H- excitons with $\ell = 5$) were observed in one-photon absorption spectra of high-quality cuprous oxide. The method we developed, described in details in ref. [3], allows one to computed not only the energy eigenvalues, but also the line shapes of the optical functions. The presented theory explains many peculiar characteristics of Rydberg excitons such as deviations from n^{-3} law of oscillator strengths or derivation from n^{-2} law for the excitonic energies, gives the polariton dispersion relation. Using anisotropic effective masses, we show the energy splitting of the P, F, and H excitons. Our numerical results are in almost perfect agreement with experimental results obtained by Kazimierczuk *et al.* [1] and Thewes *et al.* [2].

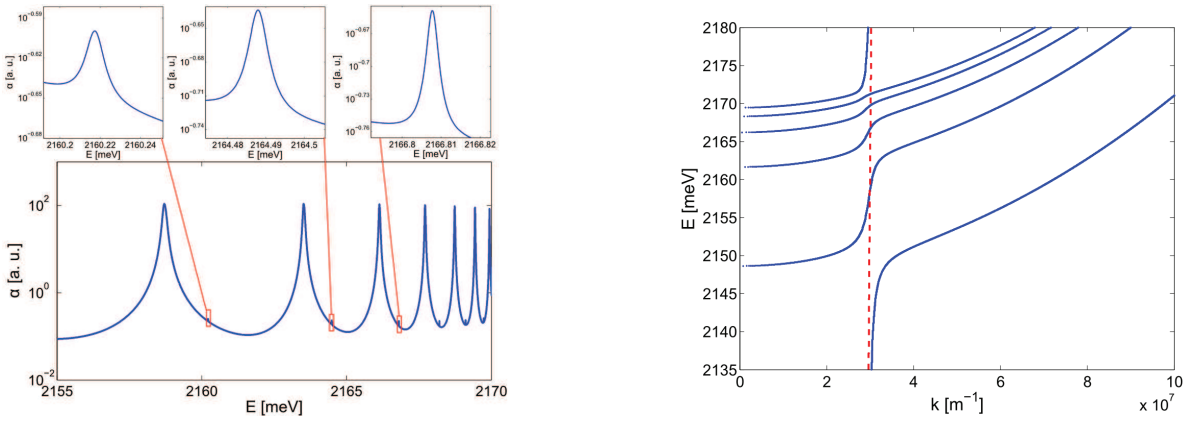

Figure 1: a) The absorption spectra including the effect of P and F excitons. b) The polariton dispersion for a Cu_2O crystal for 5 lowest excitonic states.

[1] T. Kazimierczuk, D. Fröhlich, S. Scheel, H. Stolz, M. Bayer, *Nature* **514**, 344 (2014).
[2] J. Thewes, J. Heckötter, T. Kazimierczuk, M. Aßmann, D. Fröhlich, M. Bayer, M. A. Semina, and M. M. Glazov, *Phys. Rev. Lett.* **115**, 027402 (2015).
[3] S. Zielińska-Raczyńska, G. Czajkowski, and D. Ziemkiewicz, *Phys. Rev. B* **93**, 075206 (2016).

The influence of PEDOT to PSS ratio on the optical properties of PEDOT:PSS thin solid films-insight from spectroscopic ellipsometry

H. Bednarski, B. Hajduk, J. Jurusik, M. Domański, B. Jarząbek, K. Łaba and M. Łapkowski

Centre of Polymer and Carbon Materials, Polish Academy of Sciences, ul. M. Curie-Skłodowskiej 34., 41-819 Zabrze, Poland

The low band gap organic semiconductor poly(3,4-ethylenedioxythiophene) (PEDOT) doped with poly(4-styrenesulfonate) (PSS) found many different practical applications in organic optoelectronics [1]. Success of this material reflects also its wide commercial availability in the form of water colloidal dispersion with different PEDOT to PSS ratios. It is well known, that electrical conductivity of PEDOT:PSS thin solid films depend primary on the content of conductive PEDOT. Whereas, PSS acts as doping agent and enables hydration in the form of colloidal dispersion, but simultaneously significantly lowers electrical conductivity of the PEDOT:PSS system. It has been demonstrated, see e.g. Ref. [2], that the spectroscopic ellipsometric characterization of the optical properties of PEDOT:PSS thin films is consistent with the electrical conductivity values. This feature makes ellipsometry especially useful as nondestructive experimental technic in studies on PEDOT:PSS thin layers.

The uniaxial optical anisotropy in thin solid films of PEDOT:PSS has been identified by Pettersson et al. using multi sample and variable angle spectroscopic ellipsometric data analysis [3]. The authors used wavelength-by-wavelength fit procedure in order to determine reflection indexes and extinction coefficients. Recently, the isotropic Drude-Lorentz optical model was applied in description of ellipsometric data of PEDOT:PSS films [2,4]. In this work, we study details of the influence of the PEDOT to PSS ratio on the optical properties of PEDOT:PSS thin solid films using spectroscopic ellipsometry. Samples were prepared from commercially available aqueous dispersions with different PEDOT to PSS ratio by the spin coating technic. The emphasis is put on studies of the relation between the content of PEDOT and optical anisotropy of PEDOT:PSS films. For this reason, the limiting cases i.e. thin solid films of pure PEDOT and pure PSS are also studied. In our ellipsometric data analysis, we developed a consisted description based on the effective medium approximation in order to accounts for PSS contribution within the Tauc-Lonentz optical model and for PEDOT part within the Drude-Lorentz model. It appears, that the birefringence in studied PEDOT:PSS thin solid films is positive. For long wavelengths a systematic decrease of the real part of the ordinary component of dielectric function is observed for increasing content of PEDOT.

[1] A.M. Nardes, et. al., *Organic Electronics* **9,** 727 (2008).
[2] J. Gąsiorowski, et al., *Thin Solid Films* **536,** 211 (2013).
[3] L.A.A. Pettersson, S. Ghosh and O. Inganäs, *Organic Electronics* **3**, 143 (2002).
[4] S. H. Chang, et al., *IEEE Photonics Journal* **6**, 8400307 (2014).

Work supported by the NCN grant (Poland) No. DEC-2013/09/B/ST8/01629.

The influence of morphology on the optical properties of PEDOT:PSS thin solid films - insight from spectroscopic ellipsometry studies

H. Bednarski, B. Hajduk, J. Jurusik, M. Domański, K. Łaba and M. Łapkowski

Centre of Polymer and Carbon Materials, Polish Academy of Sciences, ul. M. Curie-Skłodowskiej 34., 41-819 Zabrze, Poland

It became well known that microstructure, particular molecular conformations, or more generally, morphology of the active organic layers formed of conjugated polymers influence strongly their optoelectronic properties [1]. PEDOT (poly(3,4-ethylenedioxythiophene)) is one of important members of this family of conjugated polymers known for its good electrical conductivity. However, PEDOT as poorly soluble polymer is difficult in application for optoelectronic devices fabrication. For this reasons, aqueous dispersion of PEDOT with the polyelectrolyte poly(4-styrenesulfonate) (PSS) has been evolved. For example, thin solid films of PEDOT:PSS are commonly used as auxiliary layers or even as transparent electrode in optoelectronic devices, especially in organic photovoltaic cells. As follows from literature, morphology of PEDOT:PSS thin films prepared from solutions can be modified by deposition technics [2], applying diverse chemical additives to the dispersion [3], as well as, by applying diverse post-deposition physical processes [4].

It has been demonstrated that spectroscopic ellipsometry is an accurate and sensitive tool to study influence of morphology on the optical properties of thin polymer films. Importantly, such characterization of the optical properties of PEDOT:PSS thin films is consistent with the conductivity values determined from electrical measurements [5]. In this work, we report results from spectroscopic ellipsometry studies on series of PEDOT:PSS thin films undergo to the morphology modification. Our main purpose is to analyze consequently the results within the uniaxial anisotropic optical model of PEDOT:PSS. For this reason, we developed a consisted description based on the effective medium approximation in order to accounts for PSS contribution within the Tauc-Lonentz optical model and for PEDOT part within the Drude-Lorentz model. Generally, in our description the samples with improved electrical conductivity are characterized by the increased relaxation time of the free carriers.

[1] Ioan Botiz and Natalie Stingelin, *Materials* **7**, 2273 (2014).
[2] Stergios Logothetidis, et al., *Solar Energy Materials & Solar Cells* **112**, 144 (2013).
[3] O.P. Dimitriev, Synthetic Metals **159**, 2237 (2009).
[4]S.A. Rutledge and A.S. Helmy, *Journal of Applied Physics* **114**, 133708 (2013).
[5] J. Gąsiorowski, et al., *Thin Solid Films* **536,** 211 (2013).

Work supported by the NCN grant (Poland) No. DEC-2013/09/B/ST8/01629.

Studies on the influence of temperature on the optical properties and electrical conductivity changes of PEDOT:PSS thin solid films

H. Bednarski, B. Hajduk, J. Jurusik, M. Domański, H. Janeczek and M. Łapkowski

Centre of Polymer and Carbon Materials, Polish Academy of Sciences, ul. M. Curie-Skłodowskiej 34., 41-819 Zabrze, Poland

Poly(3,4-ethylenedioxythiophene) (PEDOT), a low band gap organic semiconductor, belongs to the family of conjugated polymers and is known for its good electrical conductivity and good thermal stability. Practical applications in organic optoelectronics of PEDOT are strongly limited by its poor solubility in organic solvents. An alternative, free of this deficiency, gives poly(4-styrenesulfonate) (PSS) doped PEDOT system. Conductive thin solid films of Poly(3,4-ethylenedioxythiophene):poly(4-styrenesulfonate) (PEDOT:PSS) can be easily prepared from commercially available aqueous colloidal dispersion of these polymers blend. Electrical conductivity of PEDOT:PSS films depend primary on the content of conductive PEDOT. Whereas, highly hygroscopic PSS acts as doping agent which enables preparation of aqueous dispersion of the whole system. For this reason, the solid films of PEDOT:PSS are also highly hygroscopic.

In this work we study the influence of temperature on optical properties and electrical conductivity changes of PEDOT:PSS thin solid films at temperatures from 290 K to 490 K. The optical properties are studied within spectroscopic ellipsometry equipped with the heated sample support. Whereas, electrical conductivity changes are measured using Keithley electrometer. The ellipsometric results are interpreted consistently within our uniaxial optical model of PEDOT:PSS, which base on the effective medium approximation in order to accounts for PSS contribution within the Tauc-Lonentz optical model and for PEDOT part within the Drude-Lorentz model. Correlations between electrically and optically determined conductivity are analyzed in details. As expected, dominating thermal effect, at temperatures from 290 to 370 K, is pronounced change in the sample thicknesses connected with loss of water in the heating cycle and uptake of water in the cooling cycle. This effect has been additionally confirmed by the differential scanning calorimetry (DSC) and the gravimetric measurements. At higher temperatures week influence on optical and electrical properties is observed.

Work supported by the NCN grant (Poland) No. DEC-2013/09/B/ST8/01629.

Fast response HOT (111) HgCdTe MWIR detectors

K.Grodecki[1], P. Martyniuk[1], W. Pusz[2],A. Kowalewski[1] D. Stępień[1,2], A. Kębłowski[2], J. Piotrowski[2], D. Stanaszek[2,] W. Gawron[2] and A. Rogalski[1]

[1]Institute of Applied Physics, Military University of Technology, 2 Kaliskiego Str., 00-908 Warsaw, Poland
[2]Vigo System S.A., 129/133 Poznanska Str., 05-850 Ożarów Mazowiecki, Poland

Higher operation temperature (HOT) condition of the middle-wave (4.1μm) photodetectors is one of the most important research areas in infrared technology. The development of the new detector architectures ($N^+pP^+n^+$) has been driven by applications requiring fast response operation. This requirement stays in contradiction with reaching high detectivity in terms of detector optimization.

Typically, the response time is determined by drift and diffusion of photogenerated charge carriers to the contact region for higher voltage condition, while for weak reverse bias recombination decay plays dominant role. Assuming that, the depletion region occupies only small part of active region and absorption occurs in neutral region of absorber, the response time is conditioned by recombination decay and diffusion of photogenerated carriers to the contacts. For absorber thickness comparable or larger than diffusion length, the response time is limited by the recombination time.

The device presented in this work was fabricated in the joint laboratory run by VIGO Systems S.A. and Military University of Technology (MUT). The (111) HgCdTe layers were grown on 2"in., epiready, semi-insulating (100) GaAs substrates in a horizontal MOCVD AIX 200 reactor. The time response was measured with optical parametric oscillator (OPO) producing 25 ps pulses of tunable wavelengths in range of 1.55–16μm.

The time response of the MWIR HgCdTe detector with 50% cut-off wavelength of $\lambda c \approx 4{,}1\mu m$ at T = 230 K was estimated at the level of τ <1 ns for V >500 mV.

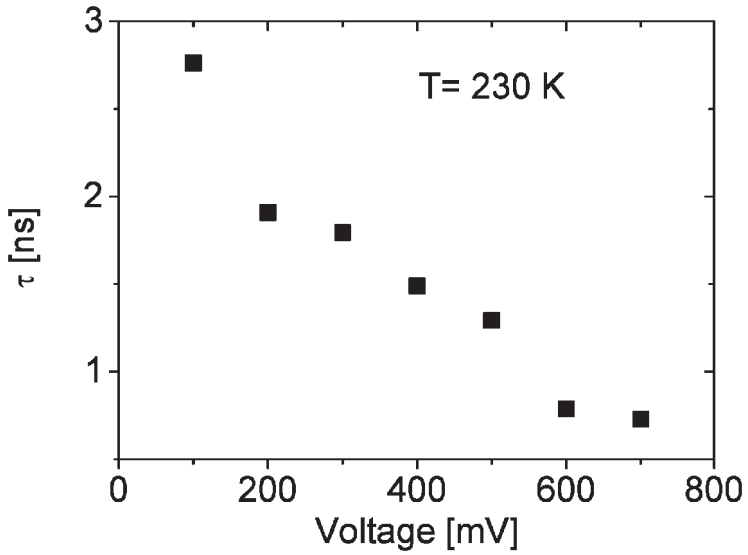

The effect of synthesis pressure on properties of Eu-doped ZnO nanopowders prepared by microwave hydrothermal method.

J. Rosowska[1], J. Kaszewski[1], B. Witkowski[1], Ł. Wachnicki[1], M. Godlewski[1,2]

[1]Institute of Physics, Polish Acad. of Sciences, Al. Lotników 32/46, 02-668 Warsaw, Poland
[2]Dept. of Mathematics and Natural Sciences College of Science, Cardinal S. Wyszyński University, Dewajtis 5, 01-815 Warsaw, Poland

Nowadays, rare-earth doped II-VI semiconductors attract a lot of attention due to their wide potential applications in biology and medicine, including biological labels, biosensors or drug delivery systems. One of the most popular and suitable host material for doping is zinc oxide ZnO. This semiconductor has a wide band gap (3.37 eV) and high exciton binding energy (60 meV). Last but not least, ZnO is nontoxic and biocompatible material. Among rare earth, Eu^{3+} ions have been investigated especially in view of their strong, sharp emission lines in red region.

In this work, the effects of synthesis pressure on the morphologies, crystal structures and optical properties of Eu-doped ZnO were analyzed by Scanning Electron Microscopy (SEM), X-ray diffraction (XRD), cathodo- (CL) and photoluminescence (PL).

ZnO nanopowders doped with 5 mol % of Eu were prepared by a microwave hydrothermal method using $(NO_3)_2$ Zn · $6H_2O$ and $Eu(NO_3)_3$ · $5H_2O$. The solutions were alkalized with aqueous ammonia solution (25%, Carl Roth) to pH=10. Hydrothermal process was conducted at 20, 40, 60, 80 and 100 bar by 20 min. The samples were dried overnight. All Eu-doped ZnO nanopowders were prepared with the same procedure to study the pressure dependence on properties of obtained samples.

First of all, the results revealed improvement in crystal structure with increasing synthesis pressure. From XRD patterns, most of the diffraction peaks could be indexed to wurtzite type ZnO structure (according to JCPDS card no. 36-1451), so majority of Eu^{3+} ions were doped into ZnO lattice. However, diffraction peaks from impurities were detected in samples obtained at pressures: 20, 40 and 100 bar. This fact corresponds with the results of PL investigations. PL spectrum for λ_{exc}=466nm indicates that in case of samples obtained at 60 and 80 bar, trivalent europium ions are doped into ZnO and located at a symmetry site C_{3V}. In the remaining samples (obtained at pressures 20, 40 and 100 bar), Eu^{3+} ions have taken a lot of different crystallographic sites. In addition, the near band edge (NBE) in PL spectrum of ZnO is absent in the sample prepared at 20 bar, suggesting the lowest crystallographic quality. The SEM images of Eu-doped ZnO nanopowders indicate that samples prepared at different pressures vary in shape and size.

Experimental and theoretical analysis of room temperature thermoelectric and thermal properties of PbTe-CdTe solid solution

M. Szot, K. Dybko, P. Pfeffer, A. Szczerbakow, L. Kowalczyk, P. Dziawa, T. Zayarnyuk, K. Piotrowski, M. U. Gutowska, A. Szewczyk, W. Zawadzki, T. Story

Institute of Physics, Polish Academy of Sciences, Al. Lotników 32/46, 02-668 Warsaw, Poland

The relentless focus on the investigation of PbTe-CdTe semiconductor system originates from the expectation, that addition of Cd can improve widely known good thermoelectric properties of PbTe. Moreover, limited mutual solubility of both semiconductors favors this system in realization of the idea of phonon-glass electron-crystal material for thermoelectric applications in the form of PbTe-CdTe nanocomposite [1]. So far only polycrystalline $Pb_{1-x}Cd_xTe$ bulk samples with low Cd content $x\approx0.01$ were studied [2]. In this paper we present the results of experimental and theoretical studies of thermoelectric properties of $Pb_{1-x}Cd_xTe$ crystals grown by self-selecting vapour growth method [3]. This growth technique allows to obtain the high quality monocrystalline $Pb_{1-x}Cd_xTe$ ternary semiconductor with Cd content up to $x\approx0.11$. The investigated samples exhibit *p*-type conductivity for all Cd content studied, with the room temperature carriers concentration changing in the range from $p\approx4\times10^{18}$ cm^{-3} to $p\approx2\times10^{18}cm^{-3}$ with x increasing from 0.01 to 0.11. Increase of Cd content leads to an enhancement of *Seebeck* coefficient from $S \approx 220$ μV/K for $x \approx 0.01$ to 500 μV/K for $x \approx 0.1$. and for samples with high x observed thermopower is considerably improved with respect to the reference p-PbTe crystals (*Pisarenko* plot). This important experimental finding we analyze theoretically within the two-band ***k·p*** model, in which the increase of effective mass of light holes, resulting from experimentally confirmed increase of energy gap in $Pb_{1-x}Cd_xTe$ crystals, was taken into account. Further, the total thermal conductivity κ of investigated samples decreases from 2 $Wm^{-1}K^{-1}$ for reference PbTe to 0.9 $Wm^{-1}K^{-1}$ for x= 0.09 crystal. Since the electronic part of the thermal conductivity in the case of $Pb_{1-x}Cd_xTe$ is limited by relatively low conductivity, the observed decrease of κ is attributed to the enhanced phonon scattering on disorder within the unit cell of $Pb_{1-x}Cd_xTe$ crystal arising from the substitution of Pb ions by Cd. The observed thermal conductivity behavior of $Pb_{1-x}Cd_xTe$ crystal with increasing Cd content is well described based on Callaway approximation [4].

This work was supported by the European Union within the European Regional Development Fund, through the Innovative Economy grant (POIG.01.01.02-00-108/09).

[1] M. Szot et al., *Cryst. Growth Des*., **11**, 4794 (2011)
[2] K. Ahn, et al., *J. Am. Chem. Soc*. **132** (14), 5227 (2010)
[3] A. Szczerbakow, K. Durose, *Prog. Cryst. Growth Charact. Mater.* **51**, 81 (2005)
[4] J. Callaway, H.C. von Baeyer, *Phys. Rev*. **120**, 1149 (1960)

MBE Growth, Magnetic and Structural Properties of $Sn_{1-x}Mn_xTe$ Layers

M. Zięba, B. Taliashvili, P. Dziawa, W. Knoff, W. Wołkanowicz, K. Dybko, R. Minikayev, E. Łusakowska, A. Reszka, T. Story

Institute of Physics, Polish Academy of Sciences, al.Lotników 32/46, 02-668 Warsaw, Poland

$Sn_{1-x}Mn_xTe$ is a IV-VI diluted magnetic (semimagnetic) semiconductor exhibiting ferromagnetic, spin glass or paramagnetic properties depending on conducting hole concentration and Mn content [1]. In bulk crystals grown by the Brigdman method the thermodynamic solubility limit of Mn in rock-salt SnTe crystals is x=0.12. The corresponding ferromagnetic Curie temperatureisabout 20 K for optimal hole doping [1]. In the early studies of thin $Sn_{1-x}Mn_xTe$ layers grown by molecular beam epitaxy (MBE) the single crystal rock-salt phase was observed only for quite low Mn content $x \leq 0.04$[2].Recent renewal of interest in SnTe-based semiconductor alloys is related to the discovery of topological crystalline insulator states at (001) and (111) surfaces of bulk SnTe crystals [3], with a variety of new theoretical proposals concerning ultrathin SnTe layers and SnTe-based materials with nonzero magnetization [4]. In this work, we study the growth of $Sn_{1-x}Mn_xTe$ layers by MBE under various stoichiometry regimes known to determine carrier (hole) concentration and magnetic properties.

$Sn_{1-x}Mn_xTe$ monocrystalline layers of the thickness of about 0.7 micron were grown by MBE on cleaved BaF_2 (111) substrate using SnTe, Mn and Te effusion cells to vary both Mn content (x=0, 0.015, 0.03, 0.05, 0.09) and crystal stoichiometry controlled by additional Te flux. The X-ray diffraction analysis of the layers ($x \leq 0.05$) revealed the expected (111) growth direction and the rock-salt crystal structure with the lattice parameter following the Vegard law. For the layer with the highest Mn content (x=0.09) additional diffraction peaks were found and assigned to inclusion of $Sn_{1-x}Mn_xTe$ with (001) crystal orientation and inclusions of antiferromagnetic MnTe. Magnetic properties of the layers were examined by electron paramagnetic resonance (EPR) studies carried out over temperature region T=3-300 K. The layers grown under close to stoichiometry regime revealed Curie-Weiss paramagnetic properties with the EPR angular dependence indicating only a weak dipolar anisotropy effects. For $Sn_{1-x}Mn_xTe$ layers grown under excess tellurium regime a ferromagnetic transition was observed at helium temperatures.

[1] P.J.T. Eggenkamp, H.J.M.Swagten, T. Story et al., Phys. Rev. B **51**, 15250 (1995).
[2] A. Nadolny, J. Sadowski, B. Taliashvili et al., J. Magn.Magn. Mat. **248**, 134 (2002).
[3] Y. Tanaka, Z. Ren, T. Sato at al., Nat. Phys. **8**, 800 (2012).
[4] J. Liu, T.H. Hsieh, P. Wei, et al., Nat. Mat.**13**, 178 (2014).
[5] S. Safaei, M. Galicka, P. Kacman, R. Buczko, New J. Phys. **17**, 063041 (2015).

Design and optical properties of micropillars with two vertically coupled ZnTe microcavities

M. Ściesiek[1], W. Pacuski[1], J.-G. Rousset[1], M. Parlińska-Wojtan[2], A. Golnik[1], and J. Suffczyński[1]

[1] *Institute of Experimental Physics, Faculty of Physics, University of Warsaw, Pasteura 5 St., 02-093 Warsaw, Poland*
[2] *Institute of Nuclear Physics, Polish Academy of Sciences, Radzikowskiego 152 St., 31-342 Kraków, Poland*

Coupled photonic structures attract recently an increasing attention, mainly due to perspective of their implementations in quantum information and laser technologies. Previously, horizontally coupled microcavities in double micropillar structures were studied. Here, we present design and optical properties of innovatively designed micropillars containing two vertically coupled ZnTe microcavities. The single micropillar geometry should enable advanced experiments like coupling of quantum emitters through a delocalized cavity mode with a high collection efficiency.

Epitaxially grown samples comprising two vertically coupled planar microcavities are designed through Transfer Matrix Method calculations, grown by Molecular Beam Epitaxy, and characterized by scanning transmission electron microscopy. The whole structure is lattice matched to ZnTe, with Distributed Bragg Reflectors (DBR) made of alternating ZnTe and MgSe/ZnTe/MgTe/ZnTe superlattice layers. Mutually perpendicular gradient of cavities thickness enables continuous change of the cavities coupling by adjustment of the position on a sample. Photoluminescence (E_{exc} = 2.33 eV or 3.06 eV) and reflectivity at T = 10 K and T = 300 K mapping measurements are performed with spatial resolution down to 0.05 mm over a whole surface of a 2-inch wafer.

The optical spectra reveal two optical modes. Linewidths of the modes determined in momentum space measurements are equal to 0.95 meV, what points toward quality factor of the cavities Q = 2000. Energies of the modes are determined as a function of the position on the sample. As predicted by the simulations, in the region, where cavity modes are at resonance, the spatial mapping reveals a clear anticrossing of the modes (energy splitting of 45 meV or 17 meV for 6 DBR or 12 DBR pairs separating the microcavities, respectively). Modes intensity and linewidth are equal at the resonance.

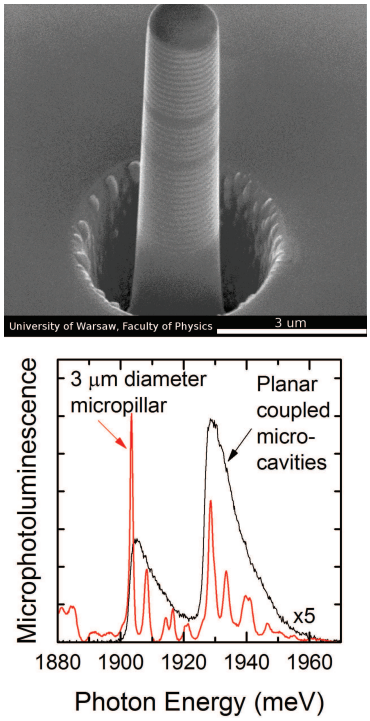

Figure 1: (upper) A micropillar with two coupled ZnTe microcavities. (lower) Micro-PL spectra: unstructurized sample and 3 μm micropillar.

Micropillars with a diameter from 3 μm down to 0.7 μm, are etched out of the coupled planar microcavities using Focused Ion Beam in the regions where the microcavities are maximally coupled (see Fig. 1). The microstructuralization results in a quantization of the cavity mode into a set of discrete submodes (see Fig. 1). With the decreasing pillar diameter, that is with an increasing photon confinement, the submodes energies and distances between the consecutive submodes increase. This indicates the perspective for control of coupling strength between the coupled modes.

Inelastic X-ray Scattering Studies of the Phonon Dispersion in PbTe and (Pb,Cd)Te Solid Solution

R. Kuna [1], R. Minikayev [1], M. Trzyna [2], A. Szczerbakow [1], K. Gas [3,1], J. Łażewski [4], A. Bosak [5], and W. Szuszkiewicz [2,1]

[1] *Institute of Physics, Polish Academy of Sciences, Al. Lotników 32/46, 02-668 Warsaw, Poland. E-mail: kuna@ifpan.edu.pl*
[2] *Faculty of Mathematics and Natural Sciences, University of Rzeszów, ul. S. Pigonia 1, 35-310 Rzeszów, Poland*
[3] *Institute of Experimental Physics, Faculty of Physics and Astronomy, University of Wrocław, pl. M. Borna 9, 50-204 Wrocław, Poland*
[4] *Institute of Nuclear Physics, Polish Academy of Sciences, ul. Radzikowskiego 152, 31-342 Kraków, Poland*
[5] *ESRF - The European Synchrotron 71, Avenue des Martyrs Grenoble, France*

Thermoelectric materials are of great interest for energy applications transforming heat into electricity. Lead telluride PbTe is a well known thermoelectric semiconductor (SC) with rock salt structure, while cadmium telluride CdTe is of sphalerite structure. The difference in the PbTe and CdTe crystal structure types strongly limits the composition range of the (Pb,Cd)Te solid solution. Investigation and interpretation of the lattice dynamics is essential in order to understand heat and electron transport in SCs. Primary parameters describing collective atom motion in the lattice are momentum transfer (Q) and energy (E), that could be measured by neutron spectroscopy (inelastic neutron scattering - INS). In the 70's an idea has emerged to investigate lattice dynamics using inelastic X-ray scattering (IXS). Recent successful growth of relatively big (~1 cm^3), metastable (Pb,Cd)Te single crystals with the rock salt structure obtained by self-selecting vapour growth (SSVG) method at the Institute of Physics PAS [1,2] made it possible to investigate their lattice dynamics by the INS technique. In the present work bulk crystals of pure PbTe, as well as of (Pb,Cd)Te solid solution with 2% of CdTe, were used to determine the phonon dispersion by the IXS and to check our selected results obtained by the INS method.

The ID28 beamline in ESRF used for the measurements reported here is equipped with a typical IXS spectrometer for studying phonon dispersion in the condensed matter. High energy of interacting photons (E = 18 keV) leads to the possibility of investigating phonons for every momentum in the Brillouin zone (BZ), and an extremely high energy resolution ($\Delta E/E = 10^{-7}$) of scattered photons was achieved. Almost complete phonon dispersion for PbTe and (Pb,Cd)Te solid solution was determined in the BZ along Γ-X ([100]) direction, we have also observed phonon dispersion for two branches (TO, TA) along Γ-K ([110]) direction in both PbTe and (Pb,Cd)Te as well. The IXS results confirm our INS data and show, e.g., an increase of the FWHM value for TO phonon mode close to the BZ center along Γ-X and Γ-K directions. However, some of our results do not agree with selected findings reported previously in [3].

This work was partially supported by the research grant (UMO-2014/13/B/ST3/04393) from National Science Centre (Poland) and by the European Synchrotron Radiation Facility (ESRF), Grenoble, France.

[1] A. Szczerbakow and K. Durose, *Prog. Cryst. Growth Charact. Mater.* **61**, 81 (2005).
[2] M. Szot et al., *Acta Phys. Pol.* A **116**, 959 (2009).
[3] O. Delaire et al., *Nat. Mater.* **10**, 614 (2011).

Uptake of Carbon Dioxide by Carbon Spiroids

A. Siklitckaia[1*], S. Yastrebov[2], M. Chekulaev [2], and J. A. Majewski [1]

[1]Faculty of Physics, University of Warsaw, L. Pasteura 5, 02-093 Warszawa, Poland
[2] A. F. Ioffe Physical-Technical Institute, 26 Polytekhnicheskaya,
194021 St. Petersburg, Russia

Spiral carbon nanoparticles (spiroids) are relatively new types of nanoclusters [1-4] with the unique geometry that might be very prospective for possible applications ranging from hydrogen storage, transport and related energy applications, drug delivery for biochemistry and medicine, up to new types of nanocapacitors [4]. Further understanding of the carbon dioxide adsorption mechanisms might be useful for the novel technologies meant to deal with the global warming process through the reduction of the CO_2 atmospheric concentration by sequestration. Therefore, the adsorption of the CO_2 to various carbon compounds has been earlier research topic. In particular, we have previously studied adsorption mechanisms of carbon dioxide to graphene layers [5].

In the present studies, we use *ab initio* Car-Parrinello molecular dynamics [6] method in the framework of the density functional theory (DFT) with the energy functional containing van der Waals (vdW) correction to analyze the capability of carbon dioxide to be adsorbed by spiroids in a comparison with carbon spheroids. The goal of the study is to demonstrate whether the maximum concentration of absorbed carbon dioxide might be obviously achieved for the case of carbon spiroidal particle in comparison with spheroidal one, containing the same number of atoms. The stability and dynamics of the spiral carbon nanoonion- adsorbed carbon dioxide is studied in the temperature range 4.2 to 2000 K.

This work has been supported by the SHALESEQ project within the Polish-Norwegian Research Program (EEA Grant PL12-0109)

[1] M. Ozawa, E. Osawa, and H. Goto, Proc. Amer. Inst. Phys. **590**, 517 (2001).
[2] S. Yastrebov, R. Smith, and A. Siklitskaya, *Mon. Not. R. Astron. Soc.* **409**, 1577 (2010).
[3] A. Siklitskaya, S. Yastrebov, and R. Smith, *Diamond Relat. Mater.* **32**, 32 (2013).
[4] P. Ganesh, P. R. C. Kent, and V. Mochalin, *J. Appl. Phys.* **110**, 073506–1 (2011).
[5] M. Wlazlo and J. A. Majewski, *Acta Physica Polonica A* **129**, A-142 (2016); DOI: 10.12693/APhysPolA.129.A-142 .
[6] CPMD, http://www.cpmd.org/, Copyright IBM Corp 1990-2008, Copyright MPI fur Festkörperforschung, Stuttgart 1997-2001.

* E-mail address: aleksandra.siklitckaia@fuw.edu.pl

Impact of different conditions of technological process on thermoelectric properties of nano-grained n-type PbTe

A. Królicka, M. Michalska, A. Mirowska, M. Piersa, A. Materna

Institute of Electronic Materials Technology, 133 Wólczyńska Str. Warsaw, Poland

Almost all world's electrical power is produced by heat engines. Up to two-thirds of this is lost as waste heat and not converted into electricity [1]. Thus, there is strong need for searching materials that can directly convert heat to electrical energy. Lead chalcogenides, which contain lead telluride compounds have this peculiar future.

PbTe compounds exhibit variety of interesting properties especially in the field of thermoelectrics. However, detailed understanding their structure is crucial for appropriate designing all stages of technological process.

The aim of this work is intentional structuring of the material so as to give opportunity to analyze the combined influence of alloying, nanoscale precipitates and different-sized grain boundaries on thermoelectric parameters. As reported in the literature [2] and on the basis of our experiments, such procedure results in obtaining high quality thermoelectric material.

In order to achieve this goal PbTe ingot doped with Cr and I was obtained by the Bridgman method. Subsequently ball milling was conducted at different milling times (5, 15 and 25 h), which was followed by pressing and sintering.

In order to estimate crystallites diameters x-ray diffraction (XRD) was applied. The average diameters of crystallites after different milling times, using Scherrer formula, were 21, 16 and 13 nm (for milling times 5, 15 and 25 h respectively). The influence of different milling times on eventual grain sizes is analyzed. Studies of electrical and thermoelectric (TE) properties of materials versus grain sizes are performed and compared. In order to analyze the morphology and reveal presence of precipitates scanning electron microscopy (SEM) and energy-dispersive X-ray spectroscopy (EDX) were performed. EDX analysis revealed presence of Cr-Te precipitates.

The mean values of κ for materials with 21 and 16 nm grains is 0,6 W/mK and 0,45 W/mK respectively at 673 K. The measured maximum values of the absolute Seebeck coefficient for 30 and 40 nm specimens were 220 μV/K and 240 μV/K respectively at 540 K.

[1] https://www.iop.org/resources/energy/
[2] K. Biswas, J. He, I.D. Blum, C.I. Wu, T.P. Hogan, D.N. Seidman, V.P. Dravid, M.G. Kanatzidis, *Nature* **489**, 414 (2012).

Random Telegraph Noise in $La_{1-x}Ca_xMnO_3$ single crystals

Jacek Przybytek[1], Jan Fink-Finowicki[2], and Grzegorz Jung[2,3]

[1] *Institute of Experimental Physics, Faculty of Physics, University of Warsaw, 02-093 Warsaw, Poland*
[2] *Institute of Physics, Polish Academy of Sciences, 02-668 Warsaw, Poland*
[3] *Department of Physics, Ben Gurion University of the Negev, 84105 Beer Sheva, Israel*

Electric noise measurement in many different materials are usually aimed at the evaluation of the intrinsic noise level important for the performance of electronic devices made of these materials. However, noise measurements are also effective tool to provide insight into fundamental charge transport mechanisms in these materials (see eg. [1]). $La_{0.86}Ca_{0.14}MnO_3$ is mixed-valence oxide material which due to its rich variety of crystallographic, electronic and magnetic phases and abundance of interesting physical phenomena remains a training area for fundamental research [2]. The ferromagnetic insulating state appears at temperatures below Curie temperature (T_C) which in these materials coincides with the temperature of the metal-insulator transition.

We report on the robust Random Telegraph Noise (RTN) of the conductivity of $La_{0.86}Ca_{0.14}MnO_3$ manganite at low temperatures. At room temperatures, the spectra of the conductivity fluctuations are featureless and follow the $1/f$ shape in the entire investigated frequency and current bias range. However, at low temperature, slightly above T_C, a clear Lorentzian excess noise appears and eventually dominates the spectral behavior. The cutoff frequency of the excess noise is bias and magnetic field independent but is clearly thermally activated with an activation energy of 300 meV. In time domain the responsible fluctuator appears as a pronounced two level random telegraph noise which persisted and could have been monitored in exceptionally wide temperature range of more than 50 K. At all temperatures where it could have been observed, the amplitude of RTN decreases exponentially with increasing bias current in exactly the same manner as the sample resistance increases with the current, pointing out to a nontrivial physical origin of these fluctuations. It has to be emphasized that, surprisingly, the responsible two-level fluctuator has a macroscopic character and affects the resistance of the entire sample. We propose the model for such behavior based on our previous investigations of the metastable resistivity states in the ferromagnetic insulating manganite [3]. We tentatively associate the robust macroscopic RTN with the transitions of a critical cluster along the percolation path between the stable high resistivity states and metastable low resistivity one.

[1] C. Barone, C. Aruta, A. Galdi, P. Orgiani, O. Quaranta, L. Maritato and S. Pagano, *J. Phys. D: Appl. Phys.* **43**, 245001 (2010).
[2] J. M. D. Coey, M. Viret and S. von Molnár, *Advances in Physics*, 1999, Vol. **48**, No. 2, 167 - 293.
[3] J. Przybytek, J. Fink-Finowicki, R. Puźniak, V. Markovich, and G. Jung, *J. Appl. Phys.* **118**, 043903 (2015).

Synthesis of thermoelectric $Ca_2Co_2O_5$ nanocrystalline powder – structural and selected physical studies

M. Michalska[1], **A. Królicka**[1]

[1]*Institute of Electronic Materials Technology, Wólczyńska 133 street, 01-919 Warsaw, Poland*
Email: monika.michalska83@gmail.com

Recently the growing interest in the development of new renewable energy sources is observed. Large expectations are put, among others, on thermoelectric materials, as potential source of renewable energy. This is largely related with development of methods and techniques of manufacturing nanocrystalline structures observed nowadays. This development was found to be very beneficial for thermoelectric materials properties.

Oxide materials have large potential for applications in thermoelectricity, especially when high temperatures are concerned. They have a lot of advantages among heavy metallic alloys: they are environmentally friendly, non-toxic, their natural resources are high. The aim of this work is to compare two different methods of obtaining thermoelectric $Ca_2Co_2O_5$ nanocrystalline powders and analyze their structural, morphological and electrical parameters.

$Ca_2Co_2O_5$ single-phase materials were obtained using: a) solid state synthesis – mechanosynthesis („*top down*") and b) modified sol-gel method („*bottom up*"). During the Conference we will present the effects of our experiments, impact of these two different methods on the structural parameters using XRD analysis (crystallite sizes, lattice parameters and volume cells), morphologies by SEM (size and distribution of grains), and electrical properties.

Optical characterization of ZnO nanorods grown by the ultra-fast and low temperature hydrothermal process

B.S. Witkowski[1], V.Y. Ivanov[1], Ł. Wachnicki[1], S. Gierałtowska[1], M. Godlewski[1,2]

[1]Institute of Physics, Polish Acad. of Sciences, Al. Lotników 32/46, 02-668 Warsaw, Poland
[2]Dept. of Mathematics and Natural Sciences College of Science
Cardinal S. Wyszyński University, Dewajtis 5, 01-815 Warsaw, Poland

Zinc oxide is a II-VI semiconductor material that focused a growing interest in various fields such as biology, medicine or electronics. It has a direct energy gap of about 3,37eV at room temperature and high transparency in a visible light spectral region. This semiconductor reveals very special physical and chemical properties, which imply many applications including a active layer or transparent electrode in solar cells or LED diodes. ZnO is also tested for applications in new generations of electronic devices as an active part of transparent transistors and cross-bar memories. For sensor and photovoltaic applications developed surface morphology is very important, so the nanorods form is very desirable.

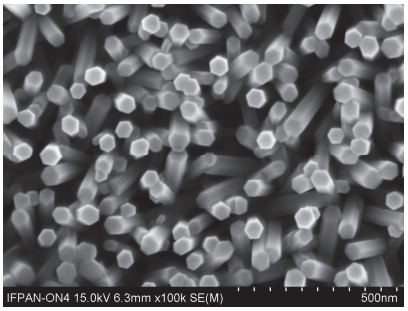

In this work we present advanced optical characterization of ZnO nanorods obtained by the extremely fast and efficient variation of the microwave-assisted hydrothermal method [1]. This environment friendly and fully reproducible method allows growth of nanorods in few minutes time on various substrates, without any catalyst or complexing agent. Growth temperature does not exceed 50ºC and growth can be performed at atmospheric pressure. Moreover the method is also very safe, it requires organic, non-toxic and low-price precursors. The growth can be performed on almost any type of substrate through the homo-nucleation as well as hetero-nucleation. The received nanorods are characterized by a very high quality - they are monocrystalline as confirmed by transmission electron microscopy.

We also present results of photoluminescence (PL) and cathodoluminescence (CL) investigations. An inter-link between samples microstructure and emission properties is investigated. We also present comparison of optical properties between ZnO nanorods and ZnO layers grown by Atomic Layer Deposition. These investigations allow estimation of relaxation process observed along the growth direction. We also study shifts of excitonic emission bands, which are associated by us with the localization effects and stress in the layers. Importantly oxygen vacancies are not found in the PL measurements. In addition, the CL intensity collected from single isolated nanorod is orders of magnitude lower than for one excited nanorod inside nanorods array. Detail information about experiments will be presented.

This work was partly supported by the Polish National Science Centre (NCN) grant no. DEC-2012/06/A/ST7/00398.

[1] B. S. Witkowski, et al., *Ultra-fast growth of the monocrystalline zinc oxide nanorods from the aqueous solution*, Int. J. Nanotechnol., Vol. 11, Nos. 9/10/11, 2014

Electro-optical characterization of ZnO/ZnMgO multiple quantum wells grown on Si (111) by MBE method

M.A. Pietrzyk[1], E. Placzek-Popko[2], K. Paradowska[2], E. Zielony[2], A. Reszka[1], D, Jarosz[1], A. Kozanecki[1]

[1] *Institute of Physics Polish Academy of Sciences, Al. Lotnikow 32/46 02-668 Warsaw, Poland*

[2] *Institute of Physics, Wroclaw University of Technology, Wybrzeze Wyspianskiego 27,50-370 Wroclaw, Poland*

The object of our investigations were 10-period ZnO/ZnMgO multiple quantum wells (MQWs) that have been fabricated on (111) Si by molecular beam epitaxy (MBE) at very high temperatures [1]. The thickness of barriers was kept constant to 2 and 15 nm, whereas the well thicknesses was varied from 1.7 to 3.0 nm. Complex characterization of the obtained samples has been performed using various measurement methods. The optical properties were analyzed by photoluminescence (PL) and cathodoluminescence (CL) techniques. Based on the grown structures, diodes were processed and their electrical properties have been checked by means of current-voltage (I-V) and capacitance – voltage (C-V) measurements. To study the origin of defects in the junctions a deep level transient spectroscopy (DLTS) has been also applied.

CL analysis revealed that the MQWs show excitonic near-band edge emission at room temperature. Panchromatic and monochromatic spectra of CL show the emission from the ZnMgO barrier at 3.341 eV and from the MQWs at 3.373 eV. PL results measured as a function of temperature yield the MQWs peak shift. Namely, we observe the exciton localization effect which may induce red-blue-red shift of the peak energy with increasing temperature. The latter indicates inhomogeneity due to interface fluctuation and the band tail states originating from the high density of defects. The presence of the defects was confirmed by the electrical measurements.

The studied diodes exhibit rectifying properties, however the obtained ideality factor value is greater than unity suggesting that possible mechanisms of current transport in the junction can be e.g.: generation-recombination, tunneling or carrier trapping by the surface states or impurities etc. The double logarithmic forward bias dark I–V plots indicate that the charge transport mechanism is governed by the space charge limited current with the participation of deep traps which are exponentially distributed in the band gap. From the temperature dependence of saturation current the activation energies of the traps present in the studied junctions were calculated and their possible origin has been ascribed. The C-V characteristics that exhibit the so called plateau due to the charge accumulation at quantum wells. The DLTS spectra reveal three deep traps of activation energies equal to 0.017 eV, 0.07 eV and 0.18 eV. Their possible origin has been discussed. DLTS signal analysis let us assume that the defects are located either with the Si or ZnO side of the junction or they can be related also to the heterointerface – most probably the interface ZnMgO-Si.

[1] M.A. Pietrzyk, M. Stachowicz, A. Wierzbicka, P. Dluzewski, D. Jarosz, E. Przezdziecka and A. Kozanecki, *J. Cryst. Growth* **408,** 102-106 2014

Acknowledgements The project was supported by the Polish National Science Centre (NCN) based on the decision No: DEC-2013/09/D/ST5/03881

Lattice Disorder Effects on Thermal Properties of CdZnTe Crystals Grown by Vertical Bridgman Method

K. Strzałkowski, F. Firszt and A. Marasek

Institute of Physics, Faculty of Physics, Astronomy and Informatics, Nicolaus Copernicus University, Grudziadzka 5,87-100 Toruń, Poland.

Investigated in this work mixed $Cd_{1-x}Zn_xTe$ compounds are interested materials for modern electronics and materials science. CdTe based crystals are promising materials as x-ray and gamma-ray detectors [1] but also substrate for infrared sensors (HgCdTe) [2]. The variation in composition allows tuning of their fundamental parameters like energy band-gap and lattice constant, what is very important from application point of view.

The phenomenon of the transport of the heat in semiconductor materials is a complex matter, particularly in the case of mixed ternary and quaternary crystals. It depends on the composition, structural characteristics and the preparation process. From application point of view the most important parameters characterizing usable materials, in particular materials used in electronics, are the thermal conductivity and diffusivity. The knowledge about them is required in the design and construction of semiconductor devices. Determination of thermal parameters of completely new materials is therefore very important.

Photothermal methods are widely used in studying thermal properties of solid samples [3]. Among them, photopyroelectric technique is fast, simple, high sensitivity and non-destructive experimental method [4]. Photopyroelectric (PPE) calorimetry in the back (BPPE) and front (FPPE) configuration will be applied for thermal investigation of solid samples. The thermal diffusivity and effusivity of investigated crystals will be derived from the experimental data. Since dynamic thermal parameters are connected with each other, thermal conductivity of the specimens can be calculated from theoretical dependencies between them.

The aim of this work is to characterize the thermal properties (effusivity, diffusivity and conductivity) of $Cd_{1-x}Zn_xTe$ mixed crystals as a function of the composition and to investigate disorder effect in given materials. The results will be analyzed, among others, in the model proposed by Sadao Adachi [5] for mixed semiconducting crystals.

[1] T.E. Schlesinger, J.E. Toney, H. Yoon, E.Y. Lee, B. A. Brunett, L. Franks, R. B. James, *Mater. Sci. Eng. R* **32**, 103 (2001).
[2] S. Sen, C. S. Liang, D. R. Rhiger, J. E. Stannard, H. F. Arlinghaus, *J. Electron. Mater.* **25**, 1188 (1996).
[3] A. Mandelis and M. M. Zver, *J. Appl. Phys.* **57**, 4421 (1985).
[4] D. Dadarlat, M.N. Pop, M. Streza, S. Longuemart, M. Depriester, A. Hadj Sahraoui and V. Simon, *Int. J. Thermophys.* **31**, 2275 (2010).
[5] S. Adachi, *J. Appl. Phys.* **102**, 063502 (2007).

Study of donor Al impurity by the help of fullerene like model

L. Ovsiannikova, G. Lashkarev, V. Kartuzov

Frantsevich Institute for Problems of Material Science, NASU, 03680, Kiev-142, Ukraine,
Phone +38 044 4240102, avilon57@ukr.net

Fullerene like model (FLM) was used successfully by us earlier for a solution of band engineering problems in $Zn_{1-x}Cd_xO$ alloys and precipitation of CdO phase in this matrix [1-4].

For technology of growing and control of properties for film materials based on ZnO doped by Al and their applications in photovoltaic and optoelectronic devices the minimization of self-compensation of donor impurity by intrinsic acceptor defects (V_{Zn}, O_i etc.) is required. Exponential dependence of defect concentration on their formation energy shows, that in any crystal the only almost defects with minimal energy are present. For determination of dominating defects we started the series of computational experiments.

The basic model of isolated FL $Zn_{32}Al_4O_{36}$ cluster was formed. In this cluster four three-valent Al atoms substitute two-valent Zn in its cation sublattice. This cluster has zero charge. Its electronic structure was investigated. The computation of optimized geometry, full energy and the value of forbidden zone was fulfilled in the frames of functional B3LYP electronic density method with basis set 6-31G(d). Energy gap between Al level and the conduction band was evaluated as 80 meV. This ionization energy agrees satisfactorily with experimental value calculated from the temperature dependence of Hall coefficient (60 meV) [5].

Thus FLM provided again its capable of living, what allows to use it in future for investigation the electroactivity of donor impurities of the third group due to their compensation by intrinsic acceptor defects of ZnO crystal lattice.

.

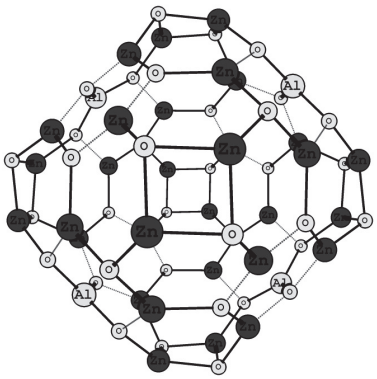

Fig.1. Optimized geometry of the $Zn_{32}Al_4O_{36}$ cluster.

[1] L.I. Ovsiannikova, *Acta Physica Polonica A* **122**, 1062 (2012)..
[2] L.I. Ovsiannikova, *Acta Physica Polonica A* **126**, 1090 (2014)..
[3] L. Ovsiannikova, V. Kartuzov, I. Shtepliuk,G. Lashkarev, *Acta Physica Polonica A* **129**, A-41 (2016)..
[4] I.I. Shtepliuk, V. Khranovskyy , G. Lashkarev, et al., *Solid-State Electronics,* **81**, 72-77 (2013)
[5] H.V. Wenckstern et al., Adv. in Solid State Phys **45**, 263 (2005)

Structural and optical properties of $Zn_{1-x}Mg_xO$ layers grown by PA-MBE. Experiment vs. Theory

D. Jarosz [1], **I. Gorczyca**[2], **A. Wierzbicka**[1], **P. Sybilski**[1] **J.M. Sajkowski**[1], **H. Teisseyre**[1,2], **A. Kozanecki** [1]

[1] *Institute of Physics, Polish Academy of Sciences, Al. Lotników 32/34,02-668 Warsaw, Poland*

[2] *Institute of High Pressure Physics, Polish Academy of Sciences, Sokołowska 29/37,01-142 Warsaw Poland*

Wurtzite $Zn_{1-x}Mg_xO$ and $Zn_{1-x}Cd_xO$ have been studied for over a decade. However, it should be emphasized that there is still a lack of detailed knowledge of many physical parameters for these materials. Knowledge of these properties is important in modeling and designing future devices. Nevertheless, the main parameters of the wurtzite MgO and CdO are not exactly known, as they are not stable in wurtzite structure.

The aim of our work was to determine experimentally basic properties of wurtzite $Zn_{1-x}Mg_xO$ layers and compare with the calculated values.

Our samples were grown by plasma-assisted molecular beam epitaxy on **a**-plane sapphire. The system was equipped with RF plasma cell as a source of gas and standard effusion cells for the group II elements. The growth was performed around 460ºC under nearly-stoichiometric conditions. The in-situ growth rate measured during epitaxy from optical reflectometry was at the level of 0.36 μm/h. A streaky pattern from the sample surface was revealed during and after sample growth by reflection high-energy electron diffraction (RHEED). Our samples were characterized by using various methods like atomic-force microscopy, absorption, photoluminescence, and X-ray diffraction. We also use different techniques (like X-ray diffraction and Rutherford backscattering spectrometry) to estimate the composition of Mg in $Zn_{1-x}Mg_xO$ layers.

Band structures of $Zn_{1-x}Mg_xO$ alloys were obtained by self-consistent ab-initio calculations based on the Local Density Approximation (LDA) to density functional theory. The relaxed atomic positions were determined by minimization of the Hellman-Feynman forces using pseudopotentials as implemented in the Vienna Ab-initio Simulation Package (VASP). Subsequently, in a second step of the calculations, the band structures were obtained by the Linear-Muffin-Tin-Orbital (LMTO) method in a full-potential (FP) version. A semi-empirical correction (LDA+C) for the deficiency of LDA in predicting semiconductor gaps was applied.

Experimentally obtained band gaps of $Zn_{1-x}Mg_xO$ for different magnesium concentrations, *x*, are in good agreement with the calculated values.

Spatial distribution of strain and Mg composition in $Mg_xZn_{1-x}O$ layers on *a*-plane sapphire examined by high-resolution x-ray diffraction

A. Wierzbicka, M.A. Pietrzyk, A. Reszka, E. Przezdziecka, J. Dyczewski, A. Kozanecki

Institute of Physics, Polish Academy of Sciences, Al. Lotnikow 32/46, 02-668 Warsaw, Poland

We have studied the influence of the magnesium doping on strain distribution in the $Mg_xZn_{1-x}O$ layers on *a*-plane sapphire substrate grown by molecular beam epitaxy. The main technique to examine this effect was high-resolution x-ray diffraction (HR-XRD). The estimation of Mg concentration in $Mg_xZn_{1-x}O$ layers on *a*-plane sapphire substrate is not obvious. We assume the linear dependence of Mg level for lattice parameters. The calculation of Mg concentration is difficult because of no existence of wurzite-MgO. To accurate determination of relaxed lattice parameters of $Mg_xZn_{1-x}O$ layers we need to know the lattice parameters and Poisson ratio of wurzite-MgO. Therefore we use the results of Mg composition from energy dispersive X-ray spectroscopy and Rutherford backscattering spectrometry. For the small amount of Mg content ($0 < x \leq 0.1$) the results obtained from these three techniques are in agreement. The optimization of wurzite-MgO lattice parameters is crucial for determination of $Mg_xZn_{1-x}O$ structural behavior. Taking into account the information obtained for the above considerations, we can investigate the strain distribution in $Mg_xZn_{1-x}O$ layers on *a*-plane sapphire substrate. We observe the gradual gain of strain with the increase of Mg content in $Mg_xZn_{1-x}O$ layer. The examination of lattice parameters shows that the $Mg_xZn_{1-x}O$ layers are biaxially strained on a-plane sapphire. The values of lateral coherence length obtain from HR-XRD is the smallest for sample with the highest content.

Acknowledgements: The project was supported by the Polish National Science Centre (NCN) based on the decision No: DEC-2013/09/D/ST5/03881.

Hybrid Organic/GaN Nanowire Structures for Solar Cell Applications

Giorgi Tchutchulashvili[1], Kamil Klosek[1], Krzysztof P. Korona[2], Marta Sobanska[1], Zbigniew R. Zytkiewicz[1]

[1]*Institute of Physics, Polish Academy of Sciences, Al. Lotników 32/46, 02-668 Warsaw, Poland*
[2]*Faculty of Physics, University of Warsaw, Pasteura 5, 02-093 Warsaw, Poland*

Organic semiconductors are the type of material which recently found application in consumer electronics. Conductive polymers with conjugated π-bonds in molecular chain are extensively studied as a p-type material for inexpensive solar cells. Good light-absorbing properties of π-conjugated polymers led to an idea to combine organic and inorganic semiconductors into one photovoltaic device [1]. In this work we present our results on fabrication and characterization of hybrid solar cell combining π-conjugated polymer with GaN nanowires grown on conductive nucleation layer. Such nucleation layer enables to grow self-assembled nanowires on virtually any substrate. Moreover, it serves as buried electrical contact to nanowires. Superior electrical properties of nanowires enhance conductivity of light-absorbing layer, which in case of organic photovoltaics is limited by low charge carrier mobility.

Hybrid structures of poly(3-hexylthiophene-2,5-diyl) (P3HT) [2] and GaN nanowires were fabricated and characterized for this study. Self-assembled GaN nanowires were grown on conductive nucleation layer deposited on top of non-conductive crystalline silicon substrate using Plasma-Assisted Molecular Beam Epitaxy technique. Bottom contact to GaN nanowires was provided through nucleation layer which is an amorphous material of metallic electrical conductivity deposited on silicon substrate. P3HT solution was put on the array of nanowires by spin-coating resulting in a layer of p-type polymer with embedded n-type nanowires. The layer was covered by PEDOT:PSS electron blocking layer. Top contacts to a solar device were made using transparent conductive Indium Tin Oxide (ITO) layer or by depositing thin metal pattern on the surface of the device.

Morphology studies show that the space orientation of nanowires remains close to perpendicular to the substrate surface independently from nucleation layer thickness, which is consisted with reported results for growth of self-assembled nanowires on different amorphous substrates [3]. Quantum yield spectroscopy measurements were made in closed circuit mode. The results (see fig. 1.) show that structure exhibits photogenerated current maxima at 1.9 eV and 3.4 eV energy light which correspond to bandgap edge of P3HT and GaN respectively. This means that light generates electron-hole pairs in both materials and that there is efficient transfer between the materials. The observed direction of photocurrent confirms that GaN works as n-type layer and P3HT is a p-type layer in this heterostructure.

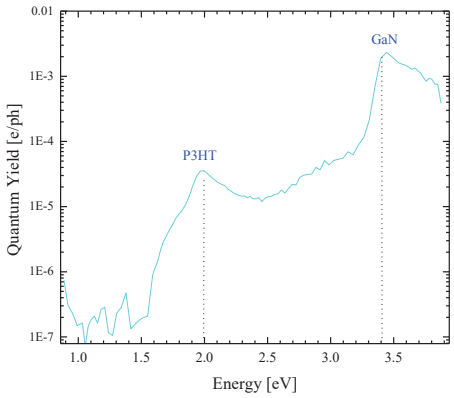

Fig. 1 Photocurrent spectrum

Electrical characteristics of nucleation layer-GaN interface were measured showing good ohmic contact between the components. Dependence of structures charge carrying properties on GaN doping is shown as well as electrical characteristics of polymer-GaN interface.

Finally, future possible improvements to the proposed design are discussed.

Ref:
1. Feng Qian et al., Chin. Phys. B Vol. 23, No. 2, 028802 (2014).
2. Ge, Weihao, Solid State Physics II, (2009).
3. M. Sobanska et al., J. Appl. Phys. 115, 043517 (2014).

Influence of annealing on optical properties of ZnO nanorods obtained by the microwave-assisted hydrothermal process

P. Materska[1,2], B.S. Witkowski[1,2] and M. Godlewski[1,2]

[1]Dept. of Mathematics and Natural Sciences College of Science
Cardinal S. Wyszyński University, Dewajtis 5, 01-815 Warsaw, Poland
[2]Institute of Physics, Polish Acad. of Sciences, Al. Lotników 32/46, 02-668 Warsaw, Poland

Zinc oxide is extensively studied II-VI semiconductor with a direct energy gap of about 3.37 eV at room temperature and possible defect-related emission in visible light spectral region. Due to these properties, ZnO is an attractive material for applications in photovoltaic, electronic and optoelectronic devices. ZnO nanorods, due to a well-developed surface, have potential of applications in sensor technology. Disoriented nanorods can also be applied in photovoltaic as anti-reflective layer.

In this work we present a new inexpensive method of the ultra-fast growth of ZnO nanorods from the aqueous solution. This environment friendly and fully reproducible method allows growth of nanorods in few minutes time on various substrates, without any catalyst or complexing agent. Growth temperature does not exceed 50ºC and growth can be performed at atmospheric pressure. Moreover the method is also very safe, it requires organic, non-toxic and low-price precursors [1]. ZnO nanorods were obtained on silicon and gallium nitride substrates. As nucleation layer we used ZnO nanoseeds obtained by the ALD (Atomic Layer Deposition) method. Received nanorods take the hexagonal form, which is characteristic for the structure of wurtzite. The nanorods form mixture with pH=8 have smaller sizes than those formed from pH=7.5 in the case of the silicon substrate. For GaN-based nanorods all crystallographic directions overlap.

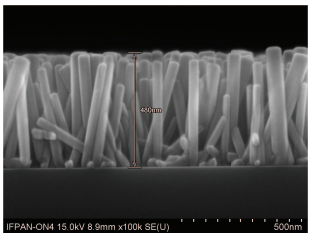

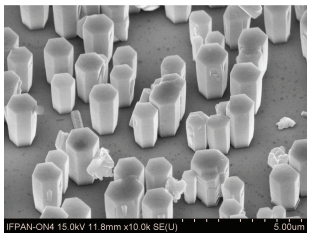

Picture on the left presents nanorods made on silicon substrate. Picture on the right shows nanorods on GaN substrate.

Prepared samples were annealed in different temperatures: 200ºC, 400ºC and 800ºC in the presence of two types of gases: oxygen and nitrogen. The process was carried out in a RTP oven. On the GaN substrate, when nanorods are heated in nitrogen, red light is received, when in oxygen, there appears UV luminescence. It is also possible to obtain mixed light. On silicon substrate luminescence of nanorods consists only from UV range, suggesting that in this case the nanorods are not as highly defected as those on the GaN substrate. On a silicon base there are no defects such as oxygen vacancies or the formation of zinc interstitial. It is possible to control the light intensity, but there is no influence on a range of emission. The higher the pH of the reaction mixture is, the greater light intensity is received. Detailed information about experiments will be presented.

This work was partly supported by the Polish National Science Centre (NCN) grant no. DEC-2012/06/A/ST7/00398.

1. B. S. Witkowski, et al., *Ultra-fast growth of the monocrystalline zinc oxide nanorods from the aqueous solution*, Int. J. Nanotechnol., Vol. 11, Nos. 9/10/11, 2014

Spatially resolved strain analysis in GaN/$Al_xGa_{1-x}N$ nanowires — cathodoluminescence and X-ray diffraction studies

A. Reszka[1], A. Wierzbicka[1], K. Sobczak[1], A. V. Kuchuk[2,3], J. Domagala[1], A. Pieniążek[1], M. Sobanska[1], K. Klosek[1], Z. R. Zytkiewicz[1] and B. J. Kowalski[1]

[1]Institute of Physics PAS, Al. Lotników 32/46, 02-668 Warsaw, Poland
[2] Institute for Nanoscience and Engineering, University of Arkansas, West Dickson 731, Fayetteville, Arkansas 72701, United States
[3]V. Lashkaryov Institute of Semiconductor Physics, National Academy of Sciences of Ukraine, Pr. Nauky 41, 03680 Kyiv, Ukraine

Near-band-gap excitonic emission shift can be used as a strain probe in semiconductors. Spatially and spectrally resolved cathodoluminescence (CL) spectroscopy and imaging allows us to observe and analyse the strain state and its distribution in the heterostructure nanowires (NWs). The X-ray Diffraction (XRD) studies and calculations of c- and a-lattice parameters provide an information about the out- and in-plane strain values, respectively. The results from both techniques enable detailed analysis of the strain in the nanoscale.

GaN nanowires with $Al_xGa_{1-x}N$ segments (x = 0.2, 0.5, 1) and accompanying Al-rich shell surrounding the lower part of the NW were grown on in-situ nitridated Si(111) substrates without any catalyst by plasma-assisted molecular-beam epitaxy. NWs were characterised with the use of scanning and transmission electron microscopy. Luminescent properties of individual NWs were studied by low-temperature CL spectroscopy and imaging. High resolution XRD technique was used to determine accurate values of lattice parameters of the NW heterostructures.

CL maps and line-scans taken along the individual NWs have shown a strong localised luminescence in the core-shell region. The blue-shifted near-band-gap emission of GaN core, compressively strained by Al-rich shell, with a value of 3.50-3.57 eV (depending on Al content in the $Al_xGa_{1-x}N$ segment and shell) was observed. The calculations of the out-of-plane strain (responsible for blue-shift of CL energy) from XRD studies revealed presence of the compressive strain in the GaN core on the level of 1.1 to almost 2 GPa. Comparison of the average values of CL energy and XRD results, allowed us to find the relationship between the blue-shift of CL luminescence and the compressive out-of-plane strain in GaN core.

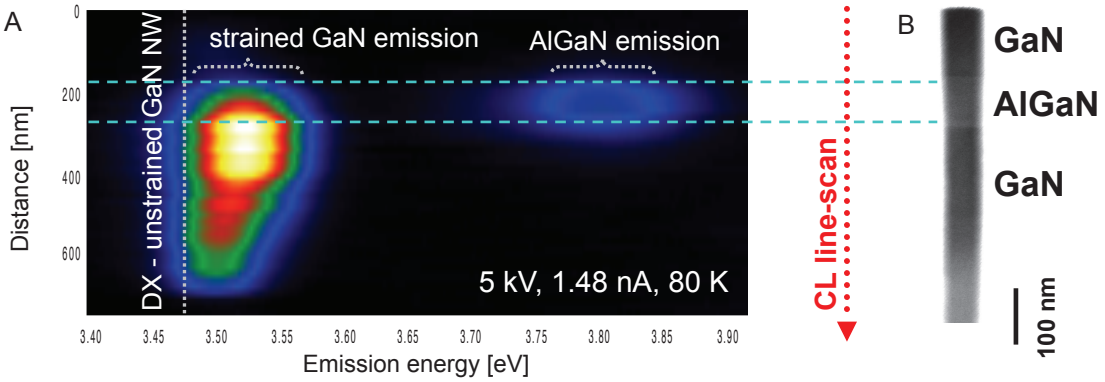

Fig. 1. A. CL spectra series (line-scan) taken along individual GaN/$Al_{0.2}Ga_{0.8}N$ NW with strong blue-shifted GaN core emission visible, B. SEM-TE image of the NW.

This work was partly supported by the Polish National Science Centre (NCN) Grant No. DEC-2012/07/B/ST5/02484

Step Flow Growth Mode of N-polar Ga(In)N Structures under N-rich conditions in Plasma-Assisted MBE

H. Turski,[1] A. Feduniewicz-Żmuda,[1] C. Cheze,[3] M. Sawicka,[1,2] F. Krzyżewski,[4] M. Załuska-Kotur,[4] M. Siekacz,[1,2] G. Muzioł,[1] K. Szkudlarek,[1] C. Skierbiszewski[1,2]

[1] *Institute of High Pressure Physics, Polish Academy of Sciences, Sokolowska 29/37, 01-142 Warsaw, Poland*

[2] *Top-GaN Ltd., Sokolowska 29/37, 01-142 Warsaw, Poland*

[3] *Paul-Drude-Institut für Festkörperelektronik, Hausvogteiplatz 5-7, 10117 Berlin, Germany*

[4] *Institute of Physics, Polish Academy of Sciences, Al. Lotników 32/46, 02-668 Warsaw, Poland*

Growth of GaN layers on bulk GaN $(000\bar{1})$ substrates by plasma-assisted molecular beam epitaxy (PAMBE) was studied. Influence of growth parameters: III/V ratio and substrate offcut on the morphology of GaN and InGaN layers grown at 650-750°C was investigated.

We found that for the growth under nitrogen excess the growth mode was changed from 3D growth (Fig. 1(a)) to layer-by-layer growth (Fig. 1(b)) on $(000\bar{1})$ orientation by using increased nitrogen flux and offcut angle of the substrates. The same conditions for growth of GaN on (0001) GaN surface orientation resulted always in 3D morphology. This difference can be attributed to higher gallium adatoms mobility on $(000\bar{1})$ than on (0001) nitrogen terminated surfaces [1].

We investigated also the PAMBE nitrogen – rich growth of $(000\bar{1})$ InGaN/GaN quantum wells. The role of the growth temperature on the PL emission intensity was studied. High growth temperature promotes increase of the PL intensity which can be explained by lower unintentional oxygen incorporation [2].

Optimal growth conditions for GaN and InGaN layers will be presented. Experimentally observed crystal morphologies will be compared with Monte Carlo simulations.

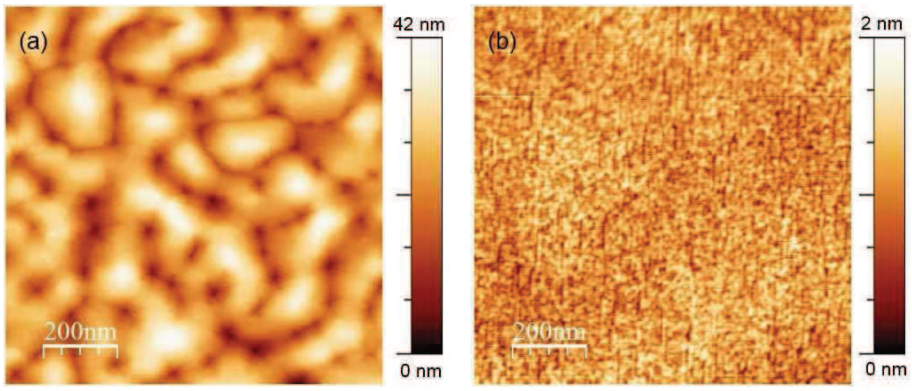

Fig. 1.
Morphology of GaN layer grown on bulk $(000\bar{1})$ GaN substrates using (a) nitrogen flux of $3.6 \cdot 10^{14}\ \frac{atoms}{cm^2}$, offcut angle of 1 deg, and (b) nitrogen flux $1.1 \cdot 10^{15}\ \frac{atoms}{cm^2}$, offcut angle 4 deg.

[1] T. Zywietz et al., Appl. Phys. Lett., **73** (1998) 487,
[2] T. Zywietz et al., Appl. Phys. Lett., **74**, (1999) 22.

Acknowledgements: *This work was supported partially by the Polish National Centre for Research and Development Grant PBS3/A3/23/2015, the project LIDER/287/L-6/14/NCBR/2015 and National Science Centre (grant decision No. DEC-2013/11/N/ST7/02788).*

InN/GaN Short Period Superlattices grown by Plasma Assisted MBE

M. Siekacz[1,2], G. Staszczak[1], T. Suski[1], E. Grzanka[1,2], I. Gorczyca[1], H. Turski[1], T. Ernst[2], T. Schulz[3], M. Albrecht[3] and C. Skierbiszewski[1,2]

[1] Institute of High Pressure Physics, PAS, Sokolowska 29/37, 01-142 Warszawa, Poland
[2] TopGaN Ltd, Sokolowska 29/37, 01-142 Warszawa, Poland
[3] Leibniz-Institute for Crystal Growth, Max-Born-Str. 2 12489 Berlin, Germany

Ultra thin InN/GaN short-period superlattices (SPSL) consisting of single or few atomic monolayers (ML) of InN and GaN are interesting for growth of high In content digital alloys. They may become an alternative for InGaN/GaN quantum structure used for light emitting diodes (LEDs) and laser diodes (LDs) in a vast spectral range where large lattice mismatch between InN and GaN makes the growth of high In content InGaN layers very challenging. InN/GaN SPSL grown by Plasma Assisted Molecular Beam Epitaxy (PAMBE) permits gap engineering in the blue-green range of the light spectrum. Also it can be useful for effective manipulation of the internal polarization fields in InGaN QWs, high efficiency multi-junction solar cell applications and topological insulators [1]. Yoshikava et al. [2] claimed to achieve growth of such SPSL with 1 ML of InN at high temperatures (e.g. 650°C) at which thicker InN layers are decomposing. However, intriguing work was done recently by Suski et al. [3], where careful TEM studies of InN/GaN SPSL grown at such conditions showed that SPSL contain not 1 ML of InN, but 1 ML of InGaN with 33% of In. Also Duff et al. [4] suggests that for pseudomorphic growth on GaN substrates, thin InN layer is intrinsically unstable due to lower In and Ga chemical potentials. They have theoretically predicted a window for growth of InN which appears for substrates of higher lattice parameters. An $In_{0.25}Ga_{0.75}N$ substrate would meet these criteria.

In this work we investigate InN/GaN short period superlattices (SPSL) grown by PAMBE at temperature range 650°C - 580°C on two types of substrates. Directly on (0001) MOVPE GaN/sapphire and special substrates having relaxed $In_{0.2}Ga_{0.8}N$ buffers on top of (0001) GaN/sapphire where the lattice constant "a" is higher than for GaN. The properties of InN/GaN SPSL grown on such substrates are compared using low temperature PL and XRD method. For the SPSL grown coherently to GaN substrate XRD and HRTEM analysis show that instead of 1 ML of InN we have 1 ML of InGaN with In content of 11-22%. On the other hand for the growth of SPSL on relaxed InGaN buffers it was possible to achieve 1 ML of pure InN as it is confirmed by XRD data. Moreover, we observed a strong photoluminescence shift to longer wavelengths for SPSL grown on substrates with higher relaxation which supports the XRD results. We discuss the impact of substrate a-lattice constant and growth temperature for growth of 1 ML containing more than 30% of In and identify the mechanisms which allows to achieve 1ML of InN. We compare experimental results with theoretical simulations of SPSL variation with the well and the barrier thicknesses using band structure calculation in the Local Density Approximation with a semiempirical correction for the gap error.

[1] M. S. Miao et al. *PRL* **109**, 186803 (2012)
[2] A. Yoshikawa et al. *APL* **90**, 073101 (2007).
[3] T. Suski et al. *APL* **104**, 182103 (2014).
[4] A. I. Duff et al. *PRB* **89**, 085307 (2014).

Acknowledgements. *This work was supported partially by the National Centre for Research and Development Grant PBS3/A3/23/2015 and EU SPRING Marie Curie Grant Agreement No 642574.*

Unhomogeneously Deformed Structure State of Highly-Doped ZnSe:V Crystals

Tatiana P. Surkova[1], Veniamin I. Maksimov[1], Elena N. Yushkova[1], Bartlomiej S. Witkowski[2] and Marek Godlewski[2]

[1] *Institute of Metal Physics UB RAS, 620990 S. Kovalevskaya street 18, Ekaterinburg, Russia*
[2] *Institute of Physics PAS, 02-668 Al. Lotnikow 32/46, Warsaw, Poland*

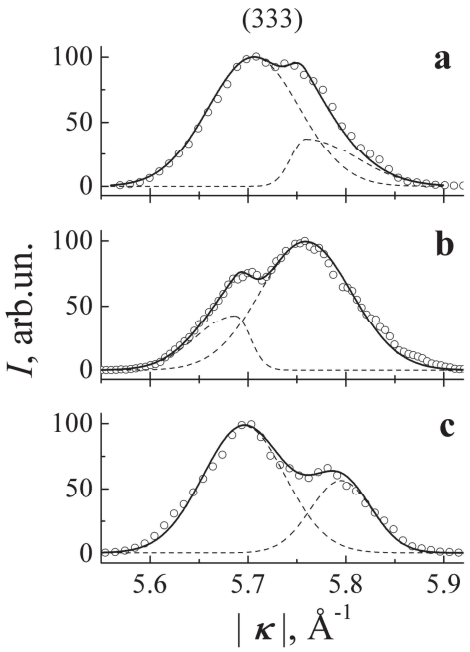

Fig. 1. Neutron diffraction scans of (333) reflections measured along [111] direction of $Zn_{1-x}V_xSe$ single crystals: a) x=0.01, b) x=0.05, c) x=0.10. T=300K. ○ – experimental results; dash lines denote fitting of components; solid lines – resulting curves represented by sum of components.

Properties of $A^{II}B^{VI}$:V alloys belonging to diluted magnetic semiconductors (DMSs) are interesting by their alterations introduced by doped impurity [1]. The presented work is devoted to results of neutronographic structure research carried out on $Zn_{1-x}V_xSe$ single crystals possessing heightened content of foreign Vanadium ions: x=0.01, 0.05, 0.10. The crystals were grown by vapor transport. It is checked by neutronographic attestation, the main structure motif of crystal phase of doped crystals should assume sphalerite.

Manifestation of additional "radial" components of neutron scattering depicting the main structure knots (fig.1) of ZnSe:V samples seems to be caused by structure deformed state. Such neutronographic results, in their totality, obtained from the crystals contained high but different content of Vanadium characterize variances of resulting non-uniform deformation field based on local atomic displacements. Rough estimations of "diffraction" deformation characteristics were made by fitting of structure peaks by separation their components along radial directions. Taking into account visible diffuse neutron scattering along tangential directions in the vicinity of strong Braggs, reasons of complicated scattering effects like those demonstrated by fig.1 are discussed. Conclusion about substantial fluctuations from homogeneous volume distribution of foreign Vanadium ions is argued for all studied compositions. With appearance of small peaks corresponded by (1/3 1/3 1/3) $2\pi/a_c$ (a_c – the cubic lattice parameter) knots being in character for II-VI DMSs based on high content of 3*d*-ions [2], some extra observations are presented to shed light on fcc↔hcp pre-transition state detected on investigated ZnSe:V crystals.

The work was done at IVV-2M Neutron Material Science Complex within IMP Program "Potok" № 01201463334 with partial support of the Program "Basic problems of material science and electrophysics" of the Ural Division of the RAS (project № 15-17-2-32).

[1] M. Herbich, W Mac, A. Twardowski, and M. Demianiuk, *Phys. Rev. B* **59**, 2726 (1999).
[2] V. I. Maksimov, S. F. Dubinin, and T. P. Surkova, *Crystallogr. Reports* **61**, 111 (2016).

New Composite Gyrotropic Metamaterial

W. Paśko[1], I. Tralle[1], P. Zięba[2], A. Çoruh[3,4]

[1] *Faculty of Mathematics and Natural Sciences, Theoretical Physics Department, University of Rzeszów, Pigonia 1, 35-310 Rzeszów, Poland*
[2] *Faculty of Mathematics and Natural Sciences, Chair of Computer Science, University of Rzeszów, Pigonia 1, 35-310 Rzeszów, Poland*
[3] *Faculty of Science and Dialogue, Department of Physics, Sakarya University, Sakarya, Turkey*
[4] *Faculty of Science, Department of Physics, H. Ahmet Yasevi Kazak – Turk University, Turkistan - Kazakstan*

In recent years, one can observe the rapid growth of research activities devoted to the materials, which exhibit the negative value of refractive index. These materials are commonly called *metamaterials*. In this work we propose a relatively simple way to produce metamaterial using the mixture of three ingredients, where one of them (single-domain ferromagnetic nanoparticles) is responsible for the negativity of real part of mixture's permeability $\mathrm{Re}[\mu(\omega)]$ and the other two (silver and $Hg_{1-x}Cd_xTe$ or $Pb_{1-x}Sn_xTe$) are responsible for the negative value of real part of mixture's effective permittivity $\mathrm{Re}[\varepsilon(\omega)]$. We have shown by computer simulations that by the proper fitting of model parameters (e.g. the radius of nanoparticles, their magnetic moments, the relative concentration of ingredients) it is possible to obtain the metamaterial with negative refraction index in a relatively broad range of temperatures and external magnetic fields, both for the $Hg_{1-x}Cd_xTe$ [1] and $Pb_{1-x}Sn_xTe$ compounds.

[1] I. Tralle, P. Zięba, and W. Paśko, *J. Appl. Phys.* **115**, 233509 (2014).

Phase ordering kinetics of a nonequilibrium exciton-polariton condensate

Michał Kulczykowski[1] **and Michał Matuszewski**[1]

[1] *Instytut Fizyki Polskiej Akademii Nauk, Aleja Lotników 32/46, 02-668 Warsaw, Poland*

We investigate the process of coarsening via annihilation of vortex-antivortex pairs, following the quench to the condensate phase in a nonresonantly pumped polariton system. We analyze in detail two distinct cases, corresponding to shorter and longer polariton lifetime. In the case of a short polariton lifetime, we find that the late-time dynamics is a clean example of universal phase ordering kinetics, characterized by scaling of correlation functions in time. The evolution of the characteristic length scale $L(t)$ is the same as for the two-dimensional XY model, described by a power law with the dynamical exponent $z \approx 2$ and a logarithmic correction. In contrast, in the case of a long polariton lifetime, we obtain the exponent $z \approx 1$, which agrees with previous studies of conservative superfluids.

ESR and photoconductivity studies of n- and p-type polycrystalline 3C SiC

Dariya V. Savchenko[1,2], Vladimir N. Rodionov[1], Andrey A. Prokhorov[2], Valeriy I. Uzhva[1], Ekaterina N. Kalabukhova[3]

[1] *National Technical University of Ukraine "Kyiv Polytechnic Institute", pr. Peremohy 37, 03056, Kyiv, Ukraine*
[2] *Institute of Physics of the Czech Academy of Sciences, Na Slovance 2, 182 21, Prague, Czech Republic*
[3] *V.E. Lashkaryov Institute of Semiconductor Physics, NAS of Ukraine, pr. Nauky 41, 03028, Kyiv, Ukraine*

The bulk pc-SiC samples of 3C polytype were obtained by thermal decomposition of CH_3SiCl_3 vapor in a hydrogen atmosphere. Two series of the 3C pc-SiC samples were studied. The first set of the samples was initial n-type 3C pc-SiC with $(N_D - N_A) \approx 5 \cdot 10^{16}$-$2\ 10^{18}$ cm^{-3} with specific resistance 10^{-1}-10^{1} Ω·cm. The second set of the samples was p-type pc-3C SiC doped with boron during the growth process with specific resistance 10^{2}-10^{4} Ω·cm. The structural analysis has shown that the obtained samples are single phase stoichiometric SiC. The temperature dependence of photocurrent was measured at T = 80-600 K, while the time-resolved photoresponse decay was recorded after an excitation by square pulse at 77 K. The ESR measurements were performed on X-band (9.4 GHz) Bruker ELEXYS E580 spectrometer at T = 6-297 K.

It was found that in the n-type 3C pc-SiC samples the intensity ratio between impurity and intrinsic photoconductivity (PC) signals is higher than those observed in n-type 3C SiC monocrystals. The relaxation processes in n-type pc-3C SiC turned out to be more inertial than those observed in n-type 3C SiC monocrystals and the value of the residual PC was found to be higher in the pc 3C SiC. After the boron doping the properties of 3C pc-SiC were changed significantly. In p-type 3C pc-SiC the intensity of impurity PC signal increases in comparison to those measured in n-type 3C pc-SiC. At the same time the impurity PC in p-type p3C pc-SiC is higher than the intrinsic one. The photocurrent decay curves in p-type 3C pc-SiC turned out to be shorter than those in n-type 3C pc-SiC. The observed differences in the behavior of the PC in n-type 3C pc-SiC pc and SiC monocrystals as well as the distinction in the photocurrent decay for n- and p-type 3C pc-SiC can be explained by the presence of the intrinsic defects and different degree of their compensation in n- and p-type 3C pc-SiC.

The ESR spectra measured in 3C pc-SiC of n- and p- type at T = 297 K consist of three overlapping signals with isotropic g-factors (g_{iso}) and different linewidth (H_{pp}). These signals are typically observed in 3C epitaxial layers and films. As a result, we may attribute the first signal with g_{iso} = 2.0029(3), H_{pp} = 0.2 mT to the carbon dangling bonds (CDB). The second signal with g_{iso} = 2.0042(3), H_{pp} = 0.22 mT was assigned to silicon dangling bonds (SiDB). And the third signal with g_{iso} = 2.0040(3), H_{pp}=0.5-0.6 mT can be attributed to the D-center (a Si excess defect, (·Si≡Si_3)). With the temperature decrease the intensity of SiDB ESR line in n-type 3C pc-SiC dramatically increase exhibiting the typical behavior for this type of the paramagnetic center. The absence of the nitrogen ESR spectrum in n-type 3C pc-SiC (in contrast to the n-type 6H SiC micropowders) can be explained by the compensation of nitrogen donors by deep level defects. At T < 100 K the quartet hyperfine lines were observed in p-type 3C pc-SiC due to the boron acceptor substituting cubic site (B_k) in 3C SiC. The spin concentration of the CDB, SiDB and D-center was significantly lower in p-type 3C pc-SiC than that in n-type samples that can be explained by their compensation by boron acceptors.

The work was supported by Ministry of Education and Science of Ukraine (Project F2904), MEYS SAFMAT LM2015088 and LO1409 projects.

ESR study of localized and delocalized electrons in nitrogen-doped 6H SiC crystals

Dariya V. Savchenko[1,2], Ekaterina N. Kalabukhova[3] and Bela D. Shanina[3]

[1] *Institute of Physics of the Czech Academy of Sciences, Na Slovance 2, 182 21, Prague, Czech Republic*
[2] *National Technical University of Ukraine "Kyiv Polytechnic Institute", pr. Peremohy 37, 03056, Kyiv, Ukraine*
[3] *V.E. Lashkaryov Institute of Semiconductor Physics, NAS of Ukraine, pr. Nauky 41, 03028, Kyiv, Ukraine*

We have studied the temperature behavior of the electron spin resonance (ESR) spectra of nitrogen (N) donors in n-type 6H polytype of silicon carbide (SiC) crystals grown by Lely and sublimation sandwich methods (SSM) with a donor concentration of about $(N_D - N_A) \approx 10^{17}$ cm^{-3} at $T = 60$-150 K. The broad ESR signal with Lorentzian lineshape and $g_{\|} = 2.0043(3)$, $g_{\perp} = 2.0030(3)$ appeared in the ESR spectrum at $T > 80$ K was reassigned. This line was observed previously in [1, 2] and was attributed to N in the thermally excited antisymmetric 1s(E) state. Based on the analysis of the ESR lineshape, linewidth and *g*-tensor of the observed single broad line, we have attributed it to the conduction electrons (CE) appeared in the ESR spectrum of the n-type 6H SiC at high temperatures due to the ionization of the electrons from ground 1s(A_1) and excited 1s(E) state of the N donors to the conduction band.

We have found that the temperature dependence of CE ESR linewidth is described by the exponential law (Orbach process) in the temperature range from 80 K to 150 K with the activation energy corresponding to the energy separation between 1s(A_1) and 1s(E) energy levels for N donors at quasi-cubic "k1" and "k2" sites ($N_{k1,k2}$). The exponential increase of the CE ESR linewidth with the temperature is explained by coupling of the CE with the spin system of localized electrons.

The observed reduction of the hyperfine (hf) splitting for the $N_{k1,k2}$ donors at $T > 75$ K with the temperature increase has been explained by electron jumping over the donor states, resulting in the fluctuation of local field (averaging of the hf interaction) determined by the temperature-dependent correlation time of fluctuations.

The electrical characteristics of both n-type 6H SiC samples were studied by the contact-free MW conductivity method. From the theoretical analysis of the temperature variation of the ESR cavity *Q*-factor loaded with n-type 6H SiC samples we have found that the ionization of free electrons in the conduction band occurs from the $N_{k1,k2}$ energy levels in Lely grown sample and from N_h energy level in 6H SiC sample grown by SSM. The ionization of free electrons from the different energy levels in two samples can be explained by the different position of the Fermi level and amounts of the distant donor pairs formed between N atoms residing at quasi-cubic and hexagonal sites in two samples. A small amount of the distant pairs in 6H SiC grown by SSM gives rise to the significantly higher concentration of the shallow N donors substituting hexagonal ("h") position (N_h) in the isolated electrically active state and as a result leads to the ionization of the free electrons from N_h energy level to the conduction band.

The work was supported by GA ČR 13-06697P, SAFMAT CZ.2.16/3.1.00/22132 projects and Ministry of Education, Youth and Sports of Czech Republic Project No. LO1409.

[1] S. Greulich-Weber, *phys. stat. sol. (a)* **162**, 95 (1997).
[2] E. N. Kalabukhova and S. N. Lukin, *Mat. Sci. Forum* **338-342**, 791 (2000).

Achieving electrical transport in GaN:Si/(Ga,Mn)N/GaN:Si structures

K. Kalbarczyk[1], M. Foltyn[1], M. Grzybowski[1], W. Stefanowicz[1], R. Adhikari[2], R. Kruszka[3], A. Piotrowska[3], A. Bonanni[2], T. Dietl[1,5,6], and M. Sawicki[1]

[1]*Institute of Physics, Polish Academy of Sciences, Warszawa, Poland*
[2]*Institut für Halbleiter - und Festkörperphysik, Johannes Kepler University, Linz, Austria*
[3]*Institute of Electron Technology, Warszawa, Poland*
[4]*Institute of Experimental Physics, University of Wrocław, Wrocław, Poland*
[5]*Institute of Theoretical Physics, University of Warsaw, Warszawa, Poland*
[6]*WPI-Advanced Institute for Materials Research, Tohoku University, Sendai, Japan*

The rise of semiconductor spintronics both creates new opportunities for novel electronic devices but at the same time it poses new requirements on spin manipulation in semiconducting materials [1]. While the search for a technology-viable magnetic semiconductor at room temperature is still the subject of active research a great deal of knowledge on the underlying physical processes can be gained from investigation of other system at their relevant temperatures. Our material of choice is (Ga,Mn)N – an emerging ferromagnetic insulator whose long range ferromagnetic ordering has been confirmed at the low end of cryogenic temperatures [2]. On the other hand, the mid-gap position of the $Mn^{2+/3+}$ level assures an insulating character, what in turn makes this material well suited for spin filtering and (magnetic) resonant tunneling devices [3]. In this study we report on separate 2- and 4- probe electrical measurements of in GaN:Si/(Ga,Mn)N/GaN:Si spin filter structures with two different magnetic layer thickness: 5 and 7.5 nm. The material has been grown by MOVPE technique on c-plane sapphire substrates and structured for vertical transport configuration by means of e-beam aided mask deposition and reactive ion etching. Electrical contacts of Ti/Al/Au were evaporated and annealed at about 750 ^{o}C for 30 sec in nitrogen atmosphere. The transport measurements revealed a strong non-ohmic behavior at helium temperatures accompanied with a sizable magnetoresistance at millikelvin temperatures in 2-probe configuration. On the contrary, in the 4-probe configuration an ohmic behavior is registered. The results are analyzed in view of a possible contribution of the contact metal/semiconductor barrier to the overall resistance of the GaN-based structure.

This work has been supported in parts by the National Science Centre (Poland) through grant OPUS (DEC-2013/09/B/ST3/04175) and by the EU 7th Framework Programme "EAgLE" (REGPOT-CT-2013-316014).

[1] T. Jungwirth et al., Rev. Mod. Phys. 86, 855 (2014).
[2] M. Sawicki et al., Phys. Rev. B 85, 205204 (2012); G. Kunert et al., Appl. Phys. Lett. 101, 022413 (2012).
[3] T. S. Santos and J. S. Moodera, Phys. Rev. B 69, 241203 (2004); A. Slobodskyy et al., Phys. Rev. Lett. 90, 246601 (2003).

Laser cooling of II-VI semiconductor nanostructures: Towards all solid state semiconductor optical cooler

Qihua Xiong[1,2,3,*]

[1] *School of Physical and Mathematical Sciences, Nanyang Technological University, Singapore 637371*
[2] *NOVITAS, Nanoelectronics Centre of Excellence, School of Electrical and Electronic Engineering, Nanyang Technological University, Singapore, 639798*
[3] *MajuLab, CNRS-UNS-NUS-NTU International Joint Research Unit, UMI 3654, Singapore*
*(*Email Address: Qihua@ntu.edu.sg)*

Optical irradiation accompanied by spontaneous anti-Stokes emission can lead to cooling of matter, a phenomenon known as laser cooling or optical refrigeration proposed in 1929 by Peter Pringsheim. In solid state materials, the cooling is achieved by annihilation of lattice vibrations (*i.e.*, phonons). Since the first experimental demonstration in rare-earth doped glasses, considerable progress has been made particularly in ytterbium-doped glasses or crystals with a recent record of ~110 K cooling from ambient, surpassing the thermoelectric Peltier cooler. On the other hand, attempts of laser cooling of semiconductors based on III-V quantum wells have led to very minimum progress. In this talk, I will present the background of laser cooling of solids, and our recent breakthrough of 40 Kelvin laser cooling of semiconductors in II-VI semiconductors in nanoribbon morphology. The laser cooling is achieved by longitudinal optical phonon assisted photoluminescence upconversion. Recent results on semiconductor bulk crystals and organic-inorganic perovskite thin films for laser cooling towards the next generation optical refrigeration applications will also be discussed, which exhibit great promises in the field of cryogenics with the advantage of compactness, vibration- and cryogen-free, high reliability and direct integrability into nanoscale electronic and photonic devices.

References:
1. S.T. Ha, C. Shen, J. Zhang and Q.H. Xiong*, "Laser Cooling of Organic-inorganic Lead Halide Perovskites", ***Nature Photonics*** **10**, 115–121 (2016)
2. D.H. Li, J. Zhang, X.J. Wang, B.L. Huang and Q.H. Xiong*, "Solid-State Semiconductor Optical Cryocooler Based on CdS Nanobelts", ***Nano Lett***. **14**, 4724–4728 (2014)
3. D.H. Li, J. Zhang and Q.H. Xiong*, "Laser cooling of CdS nanobelts: Thickness matters", ***Opt. Express*** **21**, 19302-19310 (2013)
4. J. Zhang, D.H. Li, R.J. Chen and Q.H. Xiong*, "Laser cooling of a semiconductor by 40 Kelvin", ***Nature*** **493**, 504-508 (2013) (Cover Highlight, highlighted by Nature Photonics in its April and May issues)

Recent Advancement of Growth of InN and In-rich InGaN by RF-MBE

Yasushi Nanishi[1], Tomohiro Yamaguchi[2] and Tsutomu Araki[1]

[1]*Ritsumeikan University, 1-1-1 Noji-Higashi, Kusatsu, Japan*
[2]*Kogakuin University , 2665-1 Nakano-machi , Hachiouji, Japan*

Finding much narrower bang gap of InN in 2002 gave great impact and drew much attentions on new and exciting expectations to expand application fields of group III nitrides from UV to IR wavelength range. Further studies on material properties of InN revealed much higher mobility and smaller effective mass than we have ever believed, which again brought much attention on application of InN to high frequency devices. As this material system covers almost all spectrum range of solar energy, extending application field to highly effective solar cell also attracted much attention.

Research and development on these devices, however, have not made big progress during the last 14 years, due to difficulty in obtaining high quality material of InN and In-rich InGaN. Low dissociation temperature coupled with low growth temperature, large lattice miss-match between InN and GaN and inherent immiscible nature of InGaN are the main causes of poor quality of this material system.

We have developed a new RF-MBE growth method called DERI (Droplet Elimination by Radical Beam Irradiation) for the purpose to grow high quality InN reproducibly. This growth method is consisted of the two series of growth steps with In-rich growth step (MRGP: Metal Rich Growth Process) and consecutive nitrogen radical beam irradiation step (DEP: Droplet Elimination Process). In this growth method, InN is gown under the condition very similar to atomic level liquid phase epitaxy, which makes it possible to grow InN under almost thermal equilibrium condition.

We have applied this DERI method to InGaN alloy growth, where we have observed strong phase separation, with preferable capture of Ga to growing crystal from In-Ga metal coverage layer on the surface and In is swept out. Using this phase separation phenomenon positively, we have successfully grown InN/ InGaN and InGaN/InGaN MQW layers. This growth technology has a potential for fabrication of IR and green wavelength light emitting devices based on group III nitride semiconductors.

This material system tends to make strong phase separation. This implies essential difficulty to obtain uniform InGaN alloys throughout entire compositional range. We have found new method to obtain uniform and thick InGaN in full compositional range by DERI method through controlling Ga flux while maintaining growth surface covered by more than two mono-layers of In. This technology offers very useful method for application of InGaN both to solar cell and to relaxed template for longer wavelength LEDs. Trial to passivate misfit dislocations induced by large lattice mismatch between InN and GaN is underway using phase separation positively growing wider bandgap alloy surrounding dislocation cores.

This work is supported by MEXT through grant-in-Aids for Scientific Research, "Hoga"#26600090 and "B" # 15H03559

Current Fluctuations in Mesoscopic Systems

Kensuke Kobayashi [1]

[1] *Graduate School of Science, Osaka University, Toyonaka, Osaka 560-0043, Japan*

By virtue of nanofabrication technique we are able to investigate fascinating behaviors of "mesoscopic systems", namely, electronic devices that work in quantum regime. Since 1980's they have been serving as ideal test-beds to demonstrate various quantum effects in a controllable and thus transparent way, as the electron transport through a single quantum site can be precisely probed and tuned. Especially, the Landauer-Büttiker formalism embodies this advantage of mesoscopic physics as has been successfully applied to many mesoscopic conductors (e.g. Aharonov-Bohm ring, quantum dot etc.), through which mesoscopic physics has been established [1].

So far, researchers in this field have mostly focused on the electric current, which is the average number of electrons that pass through the system for a finite time. These days, however, fluctuation (or "noise") in electric current, namely the fluctuation of the number of electrons passing through the system, is invoking great interest [2].

In this Lecture, I would like to discuss what we can learn from noise in mesoscopic systems. After introducing mesoscopic transport and noise, I will discuss non-equilibrium behavior of the many body state formed at a quantum dot where the Kondo effect occurs [3]. This topic clearly tells the significance to study noise.

The Kondo effect is a typical many body effect associated with spin, and therefore, its realization in a quantum dot (QD) in 1998 [4] has made it possible to test various theoretical predictions for Kondo physics. As shown in Figure 1, a single Kondo state can be formed in a quantum dot coupled to the leads. By tuning several parameters such as the number of spins in the dot, the temperature, the magnetic field, and the source-drain voltage, we can precisely address the behavior of the Kondo state from equilibrium to far-from-equilibrium. Especially, the non-equilibrium aspects of Kondo physics are recently attracting great interest. To understand how many-body states behave in the non-equilibrium still remains a big challenge in modern physics.

Recently, we have experimentally tuned a single-carbon-nanotube quantum dot in an ideal Kondo state and have successfully established non-equilibrium universal properties of the Kondo state. We detected an enhancement of the current fluctuations, which is perfectly explained by an effective charge for quasi-particles induced by residual interaction. Our achievement will pave a new road toward fully controlling quantum many body states [3].

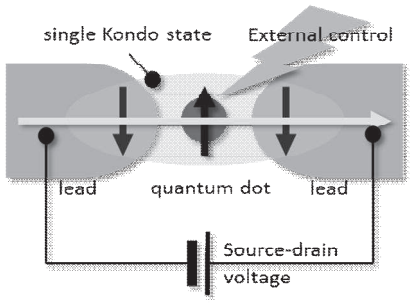

Figure 1: Kondo state formed in a quantum dot.

[1] S. Datta, *Electronic Transport in Mesoscopic Systems* (Cambridge University Press, Cambridge, England, 1997).
[2] Ya. M. Blanter and M. Büttiker, *Phys. Rep.* **336,** 1 (2000).
[3] M. Ferrier, T. Arakawa, T. Hata, R. Fujiwara, R. Delagrange, R. Weil, R. Deblock, R. Sakano, A. Oguri, K. Kobayashi, *Nature Physics* **12,** 230 (2016).
[4] D. Goldhaber-Gordon *et al., Nature* **391,** 156 (1998); S. M. Cronenwett, T. H. Oosterkamp, and L. P. Kouwenhoven, *Science* **281,** 540 (1998); J. Schmid, J. Weis, K. Eberl, and K.v. Klitzing, *Physica B* **256-258,** 182 (1998).

Magneto-optical studies of Methylammonium and Formamidinium based organo-lead halide perovskite semiconductors

Krzysztof Galkowski[1,2], Anatolie Mitioglu[1], Atsuhiko Miyata[1], Paulina Plochocka[1], Oliver Portugall[1], Jacob Tse-Wei Wang[3], Thomas Stergiopoulos[3], Samuel D. Stranks[3], Henry J. Snaith[3] and Robin J. Nicholas[3]

[1]*Laboratoire National des Champs Magnetiques Intenses, CNRS-UJF-UPS-INSA, 31400 Toulouse, France.*
[2]*Institute of Experimental Physics, University of Warsaw, 02-093 Warsaw, Poland.*
[3]*University of Oxford, Clarendon Laboratory, Oxford, OX1 3PU, United Kingdom.*
krzysztof.galkowski@lncmi.cnrs.fr

The family of organo-lead halide perovskite materials has generated tremendous interest in the field of photovoltaics due to their high conversion efficiencies. Despite the intensive development of perovskite based solar cells, there is still considerable controversy over their fundamental electronic properties. Two of the most important parameters are the binding energy of the exciton (R*) and its reduced effective mass (m*). In 2015, Miyata *et al*. [1] have shown that high field magneto-spectroscopy provides a direct way to measure both R* (16meV) and m* (0.104m_e) in $MAPbI_3$.

Here we present magneto-optical studies of Bromide and Iodide perovskite materials based on the archetypal Methylammonium (MA) and recently introduced Formamidinium (FA) organic cations. We fit the excitonic states as a hydrogenic atom in magnetic field and also observe Landau levels for free carriers to give R* and m*. Both parameters increase slowly with the material band gap and even for the large gap Bromides the value of R* (24-33 meV) remains relatively small [2].

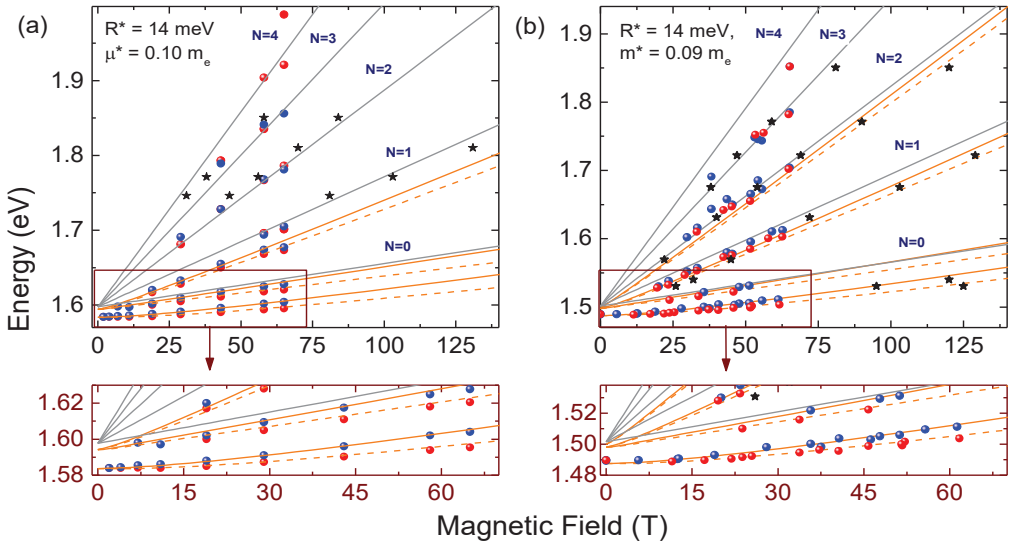

Figure 1. (a),(b) transition energies at $T = 2$ K obtained from the experimental data and results of the fit to the data for $MAPbCl_xI1_{3-x}$ and $FAPbI_3$, respectively. The red and blue points correspond to the polarization resolved minima in the absorption for σ^+ and σ^- respectively. The stars are the data obtained during the short pulsed measurements, where polarization was not used. The results of the theoretical fit are presented by grey and orange lines.

[1] A. Miyata *et al., Nature Physics* **11**, 582–587 (2015)

[2] K. Gałkowski *et al.*, *Energy & Environmental Science* **9**, 962-970 (2016)

Geometrically confined magnetoplasmons in a 2DEG

M. Białek,[1] D. Śnieżek,[2] J. Wróbel,[2,3] V. Umansky,[4] and J. Łusakowski[1]

[1] *Faculty of Physics, University of Warsaw, ul. Pasteura 5, 02-093 Warszawa, Poland*
[2] *Institute of Physics, PAS, al. Lotników 32/46, 02-668 Warsaw, Poland*
[3] *Rzeszów University, al. Rejtana 16A, 35-959 Rzeszów, Poland*
[4] *Weizmann Institute of Science, Rehovot 76100, Israel*

We report on the investigation of magnetoplasmons excited with a THz radiation in a two-dimensional electron gas (2DEG) of finite dimensions. Since the work of Dyakonov and Shur [1], the research on THz detectors based on field-effect transistors (FETs) has led to development of commercially available multipixel cameras [2]. These devices use a non-resonant signal generated in FETs. However, THz detectors with tunable resonant frequency are required. This has brought us to examine plasma resonances at low temperatures and at magnetic fields. Our previous research has shown that magnetoplasmons are excited resonantly with a wave vector related to a sample width [3]. In the case of samples with a thin gate metallization (15 nm), the wave vector of an n-th magnetoplasmon is given by $k_n = (4n-1)\pi/W$, where W is the width of a sample.

Basing on this result, we have fabricated new samples of different channel widths (8 μm, 14 μm and 20 μm) covered with a 15 nm-thick Au/Ti gate. The length of all samples was 400 μm. We have used electron beam lithography with a wet etching method. Experiments were performed with an electronic monochromatic THz source in the frequency range of 630–660 GHz and at the temperature of 4 K. We have measured a photovoltage generated by the incoming radiation between source and drain contacts of samples as a function of the magnetic field. Results show a maximum which appears at magnetic fields corresponding to theoretically predicted positions. Observed positions depend on the samples' widths and confirms our previous conclusion that the first magnetoplasmon mode wave vector is $k_1 = 3\pi/W$.

We also managed to reduce an amplitude of higher order modes ($n > 1$) by etching 100 μm-wide trenches at sides of samples. On the other hand, we also observed a large amplitude non-resonant signal, which we attribute to interferences of the incoming THz radiation. Such interferences make the non-resonant signal strongly dependent on small geometrical distortions of the THz beam geometry. The non-resonant signal is challenging when considering our devices as resonant THz detectors, because in some situations its amplitude might be comparable to the amplitude of the actual resonant signal, which could limit the usability of our devices.

In summary, presented results provide a yet unexplored resonant THz detector based on a 2DEG strip of a finite width and covered with a thin gate. The plasma resonant frequency is determined by the width of the 2DEG strip. By etching wide trenches around a strip an amplitude of high order plasmon modes can be limited. However, suppressing a non-resonant signal remains a challenge for the proposed resonant detector. This work was partially supported by a Polish National Science Centre Grant No. DEC-2011/03/B/ST7/03062.

[1] M. Dyakonov et al., *IEEE Trans. Electron Devices* **43**, 380 (1996).
[2] R. Al Hadi et al., *IEEE Journal of Solid-State Circuits* **47**, 2999 (2012)
[3] M. Białek et al., *Appl. Phys. Lett.* **104**, 263514 (2014).

Photo-induced Charge Transfer in Third Generation Solar Cells

Sylwia Grankowska Ciechanowicz[1], Krzysztof P. Korona[1], Agnieszka Wołoś[1,2], Aneta Drabińska[1], Agnieszka Iwan[3], Bartosz Boharewicz[3], Igor Tazbir[3], Jacek Wojtkiewicz[1] and Maria Kamińska[1]

[1]Faculty of Physics, University of Warsaw, Paustera 5, 02-093 Warsaw, Poland,
[2]Institute of Physics Polish Academy of Sciences, al. Lotnikow 32/46, 02-668 Warsaw, Poland
[3]Electrotechnical Institute, Division of Electrotechnology and Materials Science, M. Skłodowskiej-Curie 55/61, 50-369 Wroclaw, Poland

The third generation solar cells (TGSCs) are considered as promising, cost-effective way to harness solar energy. They are built of semiconducting organic macromolecules, inorganic nanoparticles or hybrids.
We will present results of our studies of two sub categories of TGSCs, one based on polymeric donor and fullerene derivative acceptor, and the second one built from recently discovered hybrid perovskites.
In TGSCs the most important process deciding on efficient performance of solar cell is charge transfer (CT) occurring at the interfaces of TGSC components, after sun-light induced creation of excitons and their diffusion. An exciton dissociation is possible only with energy gain larger than the exciton binding energy. In the simplest picture, when neglecting Coulomb and exchange interactions within exciton pair and relaxation of atoms within molecules, the CT process is possible if HOMO (the highest occupied molecular orbital) and LUMO (the lowest unoccupied molecular orbital) levels have lower energies for an acceptor constituent than the respective energies for a donor constituent.
Two experimental techniques applied by us enabled observation of the CT process, namely Time-Resolved Photoluminescence (TRPL) and Light-Induced Electron Spin Resonance (LESR) Spectroscopies. In the case of effective photo-induced CT, luminescence quenching of donor-acceptor blend is observed as compared to the luminescence of separate components. On the other hand, the photo-induced CT generates free charges – holes and electrons, which appear in a LESR spectrum as two lines, one from positive polaron on a donor site, and the other one from negative polaron on an acceptor site.
Photo-induced CT process was studied in mixtures made of strong electron acceptor - [6,6]-phenyl C_{61} butyric acid methyl ester (PCBM) and polymers from polyazomethine group. As reference, we used results obtained by us for poly(3-heksylotiophene):PCBM blend, typically applied as donor-acceptor in bulk heterojunction polymer solar cells. Moreover, we studied CT process in $CH_3NH_3PbI_{3-x}Cl_x$ perovskite. For all the respective solar cells I-V characteristics were made, and also external quantum efficiency spectra were obtained.
From the TRPL and LESR experiments we determined polymer-fullerene blends having efficient CT and the ones, which performed not well. These observations were consistent with the respective solar cell efficiencies.
The experimental results were supported by our theoretical calculations of HOMO and LUMO energy levels, using the density functional theory method. These calculations allowed to determine what chemical modification of polyazomethines leads to change of their HOMO/LUMO energy levels and energy gap.
The full coherent picture of the studied solar cells consisting of (i) component material properties, (ii) corresponding solar cell efficiencies, and (iii) HOMO/LUMO model, will be presented.

Revisiting Ru-Si-O as a nanocrystalline Schottky electrode for oxide semiconductors

Jakub Kaczmarski[1], Michał A. Borysiewicz[1], Andrzej Taube[1,2], Torben Boll[3], Marcin Myśliwiec[1,2], Krzysztof Piskorski[1], Marek Wzorek[1], Krystyna Stiller[3], and Eliana Kamińska[1]

[1] *Institute of Electron Technology, Al. Lotników 32/46, 02-668, Warsaw, Poland*
[2] *Institute of Microlelectronics and Optoelectronics, Warsaw University of Technology, Koszykowa 75, 00-662 Warsaw, Poland*
[3] *Department of Physics, Chalmers University of Technology, Fysikgränd 3, SE-412 96 Gothenburg, Sweden*

Ruthenium has been regarded as a promising gate electrode for wide bandgap devices due to its high work function, high conductivity, as well as chemical and thermal stability. However, due to its high chemical affinity to O_2, the deposition of a single metal on the surface of an oxide semiconductor leads to the drainage of oxygen from the subsurface region. This alters the charge distribution and the formation of accumulation region in the vicinity of metal/semiconductor interface, deteriorating Schottky barrier properties. The possible solution is a mictamic alloy being a mixture of two immiscible binary oxides with different crystalline structures, leading to crystalline frustration, and thus enhancing an amorphization of microstructure.

In this work we performed in-depth study of nanostructure, chemical composition, and transport properties of Ru-Si-O thin films fabricated by sputter-deposition under variable oxygen content in the deposition plasma. According to X-ray diffraction, all deposited films are amorphous. However, high resolution transmission electron microscopy revealed randomly oriented nanocrystalline inclusions embedded in an amorphous matrix. With the increase in $\%O_2$ one can observe an expansion of the amorphous matrix. The density recorded for the sample deposited without oxygen is 7.3 g/cm^3 and the final density is 2.42 g/cm^3, close to the density of amorphous SiO_2 (2.19 g/cm^3). Atom probe tomography studies enabled to identify nanoparticle as pure ruthenium with a Ru-O shell and the amorphous matrix as SiO_2. The resistivity increases from 6.2×10^{-4} Ω·cm for oxygen-free films up to 3.6×10^{4} Ω·cm for layers deposited at 100% of O_2. Values of work function extracted from internal photoemission spectroscopy changed from 5.65 to 5.85 eV for 0% and 30% O_2, respectively. The understanding of Ru-Si-O process-property relationship allowed us to introduce this mictamic alloy as a Schottky barrier and gate electrode of such IGZO-based devices as Schottky diodes and metal-semiconductor field-effect transistors (MESFET).

Ru-Si-O films deposited at $\%O_2$ equal to 20%, 30%, and 50% form Schottky contacts to amorphous IGZO with rectification ratios of 1×10^5, 3×10^5, and 9×10^2 respectively. Schottky barrier heights and ideality factors (n), evaluated by fitting exact solutions of the Schottky diode equation based on the thermionic emission model to experimental I-V curves for Ru-Si-O deposited at $\%O_2$ = 20%, 30% and 50% were Φ_B = 0.91 eV, n = 1.76 Φ_B = 0.93 eV, n = 1.59, and Φ_B = 0.69 eV, n = 3.57, respectively. As a proof of concept, we designed and fabricated MESFETs on flexible PET and paper substrates with field-effect mobility exceeding 9 cm^2/Vs, on-to-off current ratio above 10^5, and subthreshold swing as low as 210 mV/dec.

This work was partially funded by the European Union within European Regional Development Fund, through grant Innovative Economy (POIG.01.03.01-00-159/08, "InTechFun"), and from the Polish National Science Centre as part of PhD scholarship ETIUDA3, decision UMO-2015/16/T/ST7/00179 and from the ITE fund, as part of PhD scholarship, decision 53.03.003.

Polarization in Nitrides Determination by Direct Slab Calculations - *ab initio* Results and Experimental Verification

P. Strak[1], P. Kempisty[1], K. Sakowski[1], A. Kaminska[2,3], D. Jankowski[2], K. Korona[4], J. Borysiuk[2,4] M. Beeler[5,6], E. Grzanka[1,7], E. Monroy[5,6] and S. Krukowski[1]

[1]*Institute of High Pressure Physics, Polish Academy of Sciences, Sokolowska 29/37, 01-142 Warsaw, Poland*

[2]*Institute of Physics Polish Academy of Sciences, Al. Lotników 32/46, 01-142 Warsaw, Poland*

[3]*Cardinal Stefan Wyszynski University, College of Science, Department of Mathematics and Natural Sciences, Dewajtis 5, 01-815 Warsaw, Poland*

[4]*Faculty of Physics, University of Warsaw, Pasteura 5, 02-093 Warsaw, Poland*

[5]*Université Grenoble-Alpes, 38000 Grenoble, France*

[6]*CEA Grenoble, INAC-PHELIQS, 17 av. des Martyrs, 38000 Grenoble, France*

[7]*TopGaN Ltd. Sokolowska 29/37, 01-142 Warsaw, Poland*

Polarization in the infinite solid system is critically analyzed. It is demonstrated that Berry phase polarization corresponds to an unphysical state which may be used for determination of spontaneous polarization by appropriate addition of polarization induced electric fields. These fields are obtained by the use of continuity of the electric displacement field across the whole system in the absence of free charge. The obtained spontaneous polarization is much smaller than Berry phase polarization obtained from geometric phase formalism. The electric fields in III-nitride superlattices (SL) are consistent with those obtained by Bernardini et al. [1] provided that the appropriate rescaling of polarization is made. The spontaneous polarization and polarization related electric fields in bulk AlN, GaN and InN were determined using *ab initio* slab calculations. The obtained spontaneous polarization values are: $8.69 \cdot 10^{-3}$ C/m^2, $1.88 \cdot 10^{-3}$ C/m^2, and $1.96 \cdot 10^{-3}$ C/m^2 for AlN, GaN and InN, respectively. The related Berry phase polarization values are $8.69 \cdot 10^{-2}$ C/m^2, $1.92 \cdot 10^{-2}$ C/m^2, and $2.86 \cdot 10^{-2}$ C/m^2, for these three compounds. These values are in good agreement with the earlier derived values. The GaN/AlN multi-quantum well (MQWs) were also simulated using *ab initio* calculations. The obtained electric fields in structures are in good agreement with the fields derived from bulk values. GaN/AlN MQWs structures, obtained by plasma assisted molecular beam epitaxial (PA - MBE) growth, were characterized by transmission electron microscopy (TEM) and X-ray measurements. Time dependent photoluminescence (PL) measurements were used to determine optical transition energies in these structures. The PL obtained energies are in good agreement with *ab initio* data confirming overall agreement between model and experimental data. It was found that decay rates decreases four order of magnitude with increase of the SL period what confirms existence of high electric field. The electric field caused by spontaneous polarization reshapes waves in valence and conductions bands in such a way that it reduces recombination probability.

[1] F. Bernardini, V. Fiorentini, and D. Vanderbilt, "Spontaneous Polarization and Piezoelectric Constants in III-V Nitrides", Phys. Rev. B **56**, R10024, 1997.

Justification of different approaches including Van der Waals interaction on the example of graphene-like-structures on metallic and insulating substrates.

M. Popielska[1], M. Marchwiany[1,2], M. Kruk[1], A. Gąsiorowski[1] and J. A. Majewski[1]

[1]Faculty of Physics, University of Warsaw, ul. Pasteura 5, 02-093 Warszawa, Poland
[2]Interdisciplinary Centre for Mathematical and Computational Modelling (ICM), University of Warsaw, Pawinskiego 5a, 02-106 Warsaw, Poland

It is well known that for the standard exchange-correlation functionals (such as LDA or GGA) of the KS-DFT method, there is a lack of the proper description for long-range Van der Waals Interactions. These interactions are of particular importance for graphene-like structures grown and/or placed onto metallic and insulating substrates. In the recent years variety of correction schemes have been developed that attempt at most to fix this shortcoming [1, 2, 3, 5].

In this communication, we report extensive *ab initio* calculations in the framework of the DFT with the Van der Waals interactions included. These studies can be categorized according to different approaches: (i) force-field corrections known as a family of DFT-D [1] methods (DFT-D2, DFT-D3, DFT-D3-Becke-Jonson, DFT-Tkachenko-Scheffler); (ii) constructions of the semi-empirical functionals known as vdW-DF [2] (vdw-DF2, opt-PBE-vdW, opt-B88-vdW, opt-B86b-vdW); and (iii) the adiabatic-connection fluctuation-dissipation theorem (AC-FDT) in the random phase approximation (RPA) [3]. All of these approaches are implemented in the *VASP* package [4].

We have examined the interactions between graphene and the metallic surfaces in a top-fcc configuration (Ni(111), Ag(111), Cu(111),) as well as insulating substrates (h-BN, and MoS_2). Our studies reveal that the opt-B88-vdW [5] or DFT-D2 approach can be much cheaper computationally than the very accurate RPA approach (in particular for metallic surfaces) and typically give similar or better results for binding energies. In the case of graphene monolayer on the Ni(111) surface, the computed distance between the carbon and nickel atom is in the range of 2.08 Å – 2.23 Å (the best agreement with experimental value is for DFT-D3-Becke-Jonson approach), depending on Van der Waals approach used in our calculations. Moreover, the magnetic moments of the Ni atoms at the interface layer are smaller in comparison to the bulk values (0.48 – 0.53μ_B at the interface and 0.6 - 0.62μ_B, and bulk region). Simultaneously, we observe that the small spin magnetic moments on carbon atoms belonging to A and B sublattices of graphene have been induced (-0.019 – -0.011μ_B and 0.025-0.03μ_B for atoms from A and B sublattices, respectively).

In case of the fluorinated and hydrogenated graphene layers on Ni(111) surface, different picture of magnetism emerges. There are no local magnetic moments induced for graphene layer and the atoms attached, however, the spin magnetic moment on the Ni atoms at the interface largely decreases (even to -0.21 – 0.19μ_B per Ni atom). Moreover, the mixed covalent/ionic binding between the graphene and attached molecule has been predicted. The equilibrium distance between the carbon and hydrogen atom is in the range of 1.49 - 1.6 Å and 1.14 - 1.19 Å for carbon and fluor atoms, respectively. Additionally, the role of the substrate and its influence on structural, electronic and magnetic properties of graphene layer has been also examined.

The research was supported in part by PL-GRID Infrastructure, and computing facilities of the Interdisciplinary Centre of Modelling of the University of Warsaw within the project No. G36-15. The work has been funded by the NCN grant *HARMONIA* (no. UMO2013/10/M/ST3/ 00793).

[1] S. Grimme, *J. Comp. Chem.* **27**, 1787 (2006).
[2] M. Dion, *et al*., *Phys. Rev. Lett*. **92**, 246401 (2004).
[3] J. Harl and G. Kresse, *Phys. Rev. Lett*. **103**, 056401 (2009).
[4] G. Kresse and J. Hafner, *Phys. Rev. B* **47**, 558 (1993).
[5] J. Klimeš, D. R. Bowler, and A. Michaelides, *J. Phys.: Cond. Matt.* **22**, 022201 (2010).

Light-Emitting Tunneling Van Der Waals Heterostructures In Magnetic Fields

J. Binder [1], F. Withers [2], M. R. Molas [1], K. Nogajewski [1], C. Faugeras [1], K. S. Novoselov [2] and M. Potemski [1]

[1] *Laboratoire National des Champs Magnétiques Intenses, CNRS-UJF-UPS-INSA, 25 Rue des Martyrs, 38042 Grenoble, France*
[2] *School of Physics and Astronomy, University of Manchester, Oxford Road, Manchester M13 9PL, UK*

The toolbox of available two-dimensional (2D) crystals comprises a variety of materials with different electronic properties (metallic, semiconducting and insulating). By vertically stacking different types of 2D crystals one can create more complex systems, which are referred to as *van der Waals heterostructures* (vdWs) [1]. Lately, vdWs were fabricated using ultrathin layers of graphene, hexagonal boron nitride (hBN) and transition metal dichalcogenides. The first successful demonstration of devices like field-effect tunneling transistors [2] or light-emitting tunneling diodes [3] highlight the great versatility of the approach.

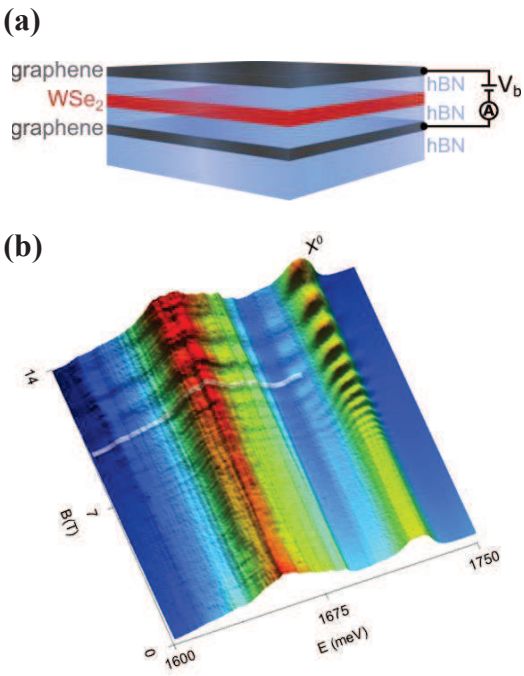

Fig.1: (a) sample structure, (b) 3D false color plot of the EL of the vdW as a function of magnetic field

Here, we report on magneto-optoelectronic measurements of a light-emitting tunneling structure based on a WSe_2 monolayer (ML) as the active emission material. The actual stacking sequence for the samples was hBN / graphene / hBN / WSe_2 / hBN / graphene (Fig. 1 (a)). Remarkably pronounced magneto-oscillations were observed for the electroluminescence (EL) of the free exciton emission line (X^0) of the WSe_2 ML (Fig.1 (b)). The results can be interpreted in terms of a modulation of the tunneling injection processes into the WSe_2 caused by the Landau quantization of the graphene electrodes. These oscillations can be used to deduce an effective valence band offset for the graphene / WSe_2 / hBN system.

Surprisingly, the EL signal was registered even at sub-bandgap voltages, which can be explained by taking into account tunneling into exciton states, which are situated well (~ 0.4 eV) below the bandgap of the WSe_2 ML. These findings indicate the great potential of vdWs for optoelectronic applications. The sheer number of materials and combinations for vdWs should allow to tailor many more device schemes suitable for a plethora of applications.

[1] A. K. Geim et al. *Nature* **499**, 419 (2013).
[2] L. Britnell et al. *Science* **335**, 947 (2012).
[3] F. Withers et al. *Nature materials* **14**, 301 (2015).

Acknowledgements:
This work was supported by the EC Graphene Flagship project (no. 604391)

Tuning valley polarization in a WSe_2 monolayer with a tiny magnetic field

T. Smoleński[1], M. Goryca[1], M. Koperski[1,2], C. Faugeras[2], T. Kazimierczuk[1], A. Bogucki[1], K. Nogajewski[2], P. Kossacki[1] and M. Potemski[2]

[1] *Institute of Experimental Physics, Faculty of Physics, University of Warsaw, ul. Pasteura 5, 02-093 Warsaw, Poland*
[2] *Laboratoire National des Champs Magnétiques Intenses, CNRS-UGA-UPS-INSA-EMFL, 25 Rue des Martyrs, Grenoble 38042, France*

In monolayers of semiconducting transition metal dichalcogenides (S-TMDs), the light helicity ($\sigma^{\pm}$) is coupled to the valley degree of freedom ($\pm K$), leading to the possibility of optical initialization of distinct valley populations [1]. Unfortunately, an extremely rapid valley pseudospin relaxation (at the time scale of picoseconds) occurring for optically bright (electric-dipole active) excitons [2] imposes severe limitations on the development of opto-valleytronics. The character of the ground exciton states in S-TMDs monolayers can be, however, very different, depending on the actual order of spin-orbit split bands in the conduction band. Whereas the ground state of the exciton appears to be optically active in monolayers of molybdenum dichalcogenides, in tungsten dichalcogenides (such as WSe_2) it is, to the first approximation, electric-dipole forbidden (optically dark).

Here we show that the inter-valley scattering is suppressed by two orders of magnitude for the dark excitons in a WSe_2 monolayer as compared to previously studied bright excitons. Moreover, we demonstrate that this inter-valley scattering can be completely switched off by a tiny magnetic field < 100 mT [3]. These findings are evidenced by our optical orientation experiments. The photoluminescence (PL) spectra measured under circularly-polarized excitation (Fig. 1) clearly demonstrate the effect of the enhancement of the PL polarization upon application of the magnetic field in the Faraday geometry, which appears in the low energy range corresponding to the *localized excitons* (LEs). Crucially, the critical field $B_0 \approx 20$ mT needed to enhance the polarization is found to be the same for all LEs evidencing their common origin. Based on the long valley pseudospin depolarization time deduced from the small value of B_0 we conclude that the effect occurs at the intermediate state being the dark ground state of the neutral exciton. Such an attribution explains the low efficiency of the pseudospin relaxation, since dark excitons in S-TMDs monolayers are rather weakly affected by depolarization effects arising due to the electron-hole exchange interaction [2]. Our interpretation is finally confirmed by the time-resolved experiments, which reveal the pseudospin dynamics to be a two-step relaxation process. An initial decay of the pseudospin occurs at the level of dark excitons on a time scale of 100 ps, which is tunable with a magnetic field. This decay is followed by even longer decay (> 1 ns), once the dark excitons form the LEs allowing for their radiative recombination. Our findings of slow valley pseudospin relaxation easily manipulated by the magnetic field open new prospects for engineering the dynamics of the valley pseudospin in monolayers of S-TMDs.

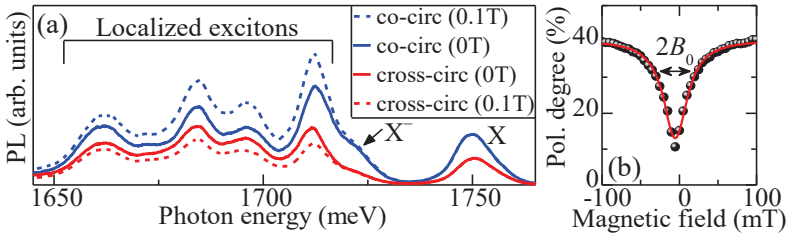

Fig 1. (a) PL spectra of the WSe_2 monolayer detected in opposite circular polarizations under σ^- polarized excitation (at two values of the magnetic field, as indicated). (b) The circular polarization degree of the LEs emission as a function of the magnetic field.

[1] T. Cao *et al*, *Nature Commun.* **3**, 887 (2012).
[2] M. M. Glazov *et al.*, *Phys. Rev. B* **89**, 201302(R) (2014).
[3] T. Smoleński *et al.*, arXiv:1512.00839 (2015).

Inter-valley exciton relaxation in strongly excited monolayer WSe_2

Ł. Kłopotowski[1], A. Mitioglu[2,3], G. Deligeorgis[4], L. Kulyuk[3], D. K. Maude[2], and P. Plochocka[2]

[1] *Institute of Physics, Polish Academy of Sciences, Warsaw, Poland*
[2] *LNCMI, CNRS-UJF-UPS-INSA, Grenoble and Toulouse, France*
[3] *Institute of Applied Physics, Chisinau, Republic of Moldova*
[4] *FORTH-IESL, Microelectronics Research Group, Heraklion, Crete, Greece*

In this work, we investigate polarization-resolved, low temperature photoluminescence (PL) of monolayer WSe_2 and show that scattering of excitons between the $+K$ and $-K$ valleys accelerates with increasing excitation power. We discuss this result within the framework of the current theory of intervalley relaxation in monolayer transition metal dichalcogenides (TMDs) — the one invoking electron-hole exchange interaction as the source of mixing of different valley states. We argue that increased excitation results in higher occupation of high kinetic energy states, giving rise to a faster inter-valley scattering.

Monolayer WSe_2 flakes were obtained by mechanical cleavage from a bulk sample grown by chemical vapor transport. The PL signal was excited by a frequency doubled output of an optical parametric oscillator (OPO) providing pulses of 300 fs duration. Time-integrated PL was detected with a nitrogen-cooled CCD camera coupled with a monochromator. Time-resolved PL was measured with a synchroscan streak camera with an overall resolution of about 5 ps. The dynamics of valley polarization is monitored via measurement of the circular polarization degree P of the PL [$P = (I^+ - I^-)/(I^+ + I^-)$, where $I^\pm$ denote PL intensities in $\sigma^\pm$ polarizations].

The PL spectrum of monolayer WSe_2 consists of peaks due to the recombination of the neutral exciton (X), charged exciton (trion, T), and emission related to localized states (L). As the excitation power is increased, the L peak saturates whereas the X intensity remains in linear regime up to highest excitation powers where heating sets in. This shows that in our experimental conditions non-linear processes such as biexciton formation or X-X annihilation are absent although at highest excitation densities average X-X distances are comparable to the X Bohr radius. PL temporal profiles for the X and T transitions both exhibit a double exponential decay. We attribute the short decay occurring with a characteristic time of $\simeq$ 10 ps to radiative recombination, while the long one with a characteristic time of $\simeq$ 50 ps to reactivation of excitons trapped on dark states. The decay times do not exhibit any excitation power dependence. Crucially, excitation with σ^+ polarized OPO beam results in $P > 0$, showing that the valley polarization survives the processes of energy relaxation, exciton formation, and recombination. Moreover, the decay time of P depends on the excitation power: decreasing from about 30 ps to 7 ps in the investigated power range. As argued in several papers, intervalley scattering occurs as a result of electron-hole exchange interaction, which acts onto the valley pseudospin as an effective in-plane magnetic field. The magnitude of this field was shown to increase with exciton kinetic energy. Thus, we attribute the increased intervalley scattering rate to increased occupation of excitonic states out of the radiative cone, where the valley states are more strongly mixed. This fraction of the exciton population undergoes a faster intervalley scattering giving rise to an increased decay of P. Our results highlight the potential of TMDs for novel valley-based devices and constitute an important contribution to the ongoing investigations of exciton dynamics in these materials.

Robust trion emission in two-dimensional $Mo(S_xSe_{1-x})_2$ alloys

J. Jadczak [1], L. Bryja [1], P. Kapuściński [1], P. Sitarek [1], A. Wójs [2], Y. S. Huang [3]

[1] *Department of Experimental Physics, Wrocław University of Technology, Wrocław, Poland*
[2] *Department of Theoretical Physics, Wrocław University of Technology, Wrocław, Poland*
[3] *Department of Electronic Engineering, NTUS&T, Taipei, Taiwan*

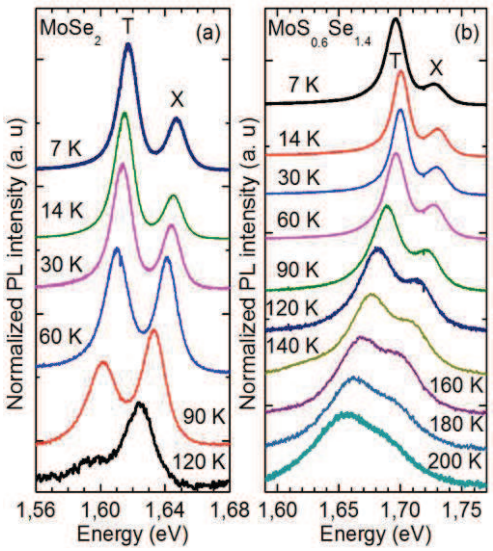

Fig. 1 The temperature evolution of the PL spectra of (a) $MoSe_2$ and (b) $MoS_{0.6}Se_{1.4}$.

Transition metal dichalcogenides (TMDCs) have attracted significant attention due to the discovery of the indirect-to-direct bandgap transition and the coupling of the spin and valley degrees of freedom when reducing thickness to one monolayer. Due to the strong confinement to single layer, the TMDC excitons have very high binding energies of a few hundreds of meV. In optical spectra of $MoSe_2$ and WSe_2 well-resolved exciton and charged exciton (trion) transitions were detected. The strong spin-orbit coupling in these materials leads to the spin splitting of A-exciton between the dark and bright states, approximately equal to the splitting of the conduction band Δ^{cb}_{so}. As predicted in theoretical calculations, Δ^{cb}_{so} for WSe_2 is negative, whereas for $MoSe_2$ it is positive. This mainly results in the contrasting lowest energy exciton sub-bands: dark in WSe_2 and bright in $MoSe_2$. Despite the same value of trion binding energy in both diselenides, there is a significant difference in the temperature evolution of the trion emission intensity. In $MoSe_2$, trion PL intensity strongly decreases with the increase of temperature and is negligible in the spectra at temperatures above $T > 100$ K, whereas in WSe_2 trion emission is prominent even up to $T \approx 200$ K. In both materials, the neutral exciton PL intensity increases with the increasing temperature compared to trion and finally exceeds it at the highest temperatures.

Here, we employ temperature-dependent micro-photoluminescence (μ-PL) spectroscopy to probe variation in the relative intensity ratio between the neutral and charged excitons in $Mo(S_xSe_{1-x})_2$ for the small sulfur content x ($0.1<x<0.3$). We have found that in contrast to $MoSe_2$ and WSe_2, for all samples with sulfur admixture, the trion emission intensity exceeds exciton intensity in the entire temperature range from $T = 7$ K to 200 K. We also present the complementary μ-Raman scattering measurements performed at $T = 300$ K in backscattering geometry. As the composition x slightly increases, we observe the characteristic splitting of the out-of plane vibration A'_1 into two phonon branches. They evolve in different manner as a function of the composition x, and they are likely related to the different distribution of the chalcogenide atoms within the $Mo(S_xSe_{1-x})_2$ layers (Se-Se and Se-S pairs). Interestingly, the trion binding energy, determined from PL spectra, takes the value accurately from the middle of the frequency range definite by corresponding phonon branches. This leads to distinctive resonant condition that makes these 2D semiconductors an excellent platform to study exiton-phonon interaction. We interpret the robust thermal trion emission in $Mo(S_xSe_{1-x})_2$ alloys to strong increase of trion-exciton coupling mediated by optical phonon.

Optical study of monolayer, few-layer and bulk tungsten disulfide

M. R. Molas, K. Nogajewski, J. Binder, and M. Potemski

Laboratoire National des Champs Magnétiques Intenses,
CNRS-UGA-UPS-INSA-EMFL, 25 rue des Martyrs, 38042 Grenoble, France.

Semiconducting transition metal dichalcogenides (TMDCs) such as MoS_2, $MoSe_2$, WS_2, or WSe_2 have recently attracted a lot of attention due to their unique electronic structures and optical properties. When thinned down to a monolayer, TMDCs transform from indirect- to direct-bandgap semiconductors and exhibit a number of intriguing optical phenomena such as valley-selective circular dichroism, doping-dependent charged excitons, or strong photocurrent response.

Here, we report a comprehensive study of the optical properties of thin films of WS_2 with thicknesses ranging from monolayer (1 ML) to octalayer (8 MLs) and of a bulk flake, carried out in a wide temperature range (5-300 K) using micro-photoluminescence (μ-PL) and micro-reflectance contrast (μ-RC) spectroscopy techniques.

The indirect- to direct-bandgap transformation is observed in the μ-PL experiment at liquid helium temperature as the layer thickness is being reduced down to an 1 ML. In terms of quantity, the emission intensity increases by 4 orders of magnitude when the flake thickness is being decreased from 8 MLs to 1 ML. The μ-PL spectrum of the 1 ML emerges at about 2.0 eV and displays several well-resolved emission peaks with the broadenings on the order of ∼10 meV, which are associated with the recombination of direct excitons (neutral, charged and localized/bound) formed at the K point of the Brillouin zone. Moreover, at low excitation power (∼1 μW) the μ-PL from the 1 ML is dominated by a broad emission band extending from about 1.65 eV to the main signal occurring at ∼2.0 eV. We tentatively ascribe this emission to the donor-acceptor pair recombination. The indirect-related emission shifts to lower energy with increasing the flake thickness, from ∼1.7 eV for the 2 ML flake to ∼1.4 eV for the 8 ML flake, which is a consequence of a simultaneous reduction of the fundamental bandgap. Due to opposite types of temperature behaviour (redshift and blueshift), we claim that the indirect recombination processes involve two different valleys in the conduction band, K and Λ, and the same valley in the valence band, Γ. For 2 MLs and 3 MLs, we demonstrate that a thermally-driven crossover from indirect to direct transitions that occurs when a sample is heated up from 5 K to 300 K.

We also study the effect of thickness on the excitonic resonances with the aim of μ-RC measurements. Our results display three main features, which we associate with the absorption of light by A, B, and C excitons. The features related to A and B excitons display only a weak sensitivity to the number of layers, while the energy of the C resonance quickly decreases with increasing the film thickness. Moreover, in the case of the 1 ML, apart from typically observed the neutral and charged exciton-related resonances within the A exciton, we show a new feature which is attributed to the absorption light by a localised/bound exciton. For flakes thicker than 1 ML, we demonstrate that the A exciton resonance exhibits a double structure, which has not been reported so far.

Complementarity of the full counting statistics and waiting time distribution of the electron transport in two coupled quantum dots

Krzysztof Ptaszyński, Bogdan R. Bułka

Institute of Molecular Physics, Polish Academy of Sciences, ul. M. Smoluchowskiego 17, 60-179 Poznań, Poland

Current fluctuations can give useful information about the underlying mechanism of the mesoscopic transport. There are two approaches to the study of these fluctuations. Full counting statistics (FCS) analyses the number of transferred particles in the given time interval. In an alternative approach, distribution of time delays between subsequent physical events, known as waiting dime distribution (WTD), is studied [1].

In this work we study the current fluctuations in the system of two capacitively coupled quantum dots in the regime of sequential tunneling with strong Coulomb blockade using a Markovian master equation. We show, that FCS and WTD give complementary information about the dynamics of the system. In example, when tunneling rates in one quantum dot depends on the occupation of the other quantum dot, Fano factor and randomness parameter, characterizing respectively the FCS and WTD, becomes unequal, in contrast to the transport in an independent quantum dot. Difference of these coefficients depends on the relative difference of timescales of the quantum dots dynamics – when the dynamics of the second dot is much slower or faster than of the first, it respectively becomes especially significant or vanishes.

Furthermore, we study correlations of subsequent waiting times. These correlations were studied previously for coherent transport in a quantum point contact [2], but not in systems described by a Markovian master equation. We show, that when the transport in one quantum dot is influenced by the other, the dynamics of the part of the system becomes effectively non-Markovian, which leads to non-zero correlations. Magnitude and sign of these correlations provide information about the relative change of tunneling rates due to the interaction with the second dot.

Finally, we show that complementary use of aforementioned quantities for characterizing the current fluctuations in one quantum dot can be used for the analysis of the dynamics of the whole system, including determination of individual tunneling rates. Complementarity of FCS and WTD enables us to achieve this goal without the use of higher cumulants, which can be difficult to measure.

We believe that our results can be relevant to the study of systems of coupled quantum dots, which had been realized experimentally [3], as well as other types of bipartite stochastic systems [4].

[1] T. Brandes, *Ann. Phys. (Berlin)* **17**, 477 (2008).
[2] D. Dasenbrook, P. P. Hofer, and C. Flindt, *Phys. Rev. B* **91**, 195420 (2015).
[3] D. T. McClure, L. DiCarlo, Y. Zhang, H.-A. Engel, C. M. Marcus, M. P. Hanson, and A. C. Gossard, *Phys. Rev. Lett.* **98**, 056801 (2007).
[4] J. M. Horowitz and M. Esposito, *Phys. Rev. X* **4**, 031015 (2014).

Non-Equilibrium Transport Through a Single Level Quantum Dot

A. Marek [1,2], **K. I. Wysokiński** [1]

[1] *Institute of Physics, M. Curie-Skłodowska University, ul. Radziszewskiego 10A, 20-031 Lublin, Poland*
[2] *Off-Campus Faculty of Law and Social Sciences in Stalowa Wola, Institute of Environmental Engineering, John Paul II Catholic University of Lublin, ul. Kwiatkowskiego 3A, 37-450 Stalowa Wola, Poland*

A single level interacting quantum dot coupled to two normal electrodes characterised by different temperatures and chemical potentials have been studied. The resulting strongly non-equilibrium situation is analysed by means of the equation of motion technique for the Green functions as developed recently by. M. Lavagna [1]. The method uses the famous Lacroix approximation, but takes the higher order renormalisations approximately into account. We apply the technique to study linear transport coefficients in the whole temperature range. At lowest temperatures the method describes formation of the Kondo cloud and results in the appearance of additional transport channel, the so called Abrikosov-Suhl resonance. We calculate conductance and the Seebeck coefficient of the system. The results of the calculations have been compared with other works using different techniques.

(The work has been partially supported by the grant DEC-2014/13/B/ST3/04451)

[1] M. Lavagna, Journal of Physics: Conference Series **592** 012141 (2015).

Microstructural and Dielectric Properties of $Ba(Ti_{1-x}Zr_x)O_3$ Nano-ceramics

Kerim Emre Öksüz[1], Şaduman Şen[2] and Uğur Şen[2]

[1]*Cumhuriyet University, Department of Metallurgical & Materials Engineering, 58140, Sivas, Turkey*
[2] *Sakarya University, Department of Metallurgical & Materials Engineering, 54187, Sakarya, Turkey*

$Ba(Ti_{1-x}Zr_x)O_3$, (x=0, 0-0.3) lead-free nano-ceramics were synthesized using the solid-state reaction method by adopting the ball milling technique. The influence of the substitution content on crystallographic structure, phase transition, microstructure and dielectrical behavior of BT (Barium Titanate) and BZT (Barium Zirconium Titanate) ceramics were investigated. XRD analysis at room temperature revealed a structural transformation from tetragonal to rhombohedral with enhancement of the ZrO_2 content in the barium titanate matrix. The scanning electron microscope (SEM) and energy-dispersive x-ray spectroscopy (EDS) were used to investigate the microstructure and surface morphology of the sintered samples. Dielectric characteristics of Zr doped barium titanate were studied using a Hioki 3532-50 LCR meter in the frequency range of 1 kHz-1 MHz. It is found that dielectric permittivity (ε_r) decreases and loss tanδ decreases with increase in zirconium oxide percentage. Zr^{+2} ions occupy the atomic spaces took place in the ZrO_2 added $BaTiO_3$ ceramics, and so caused to high dielectric constant values than that of the $BaTiO_3$ ceramics.

One Dimensional Incoherently Pumped Polariton Condensate Flowing Against an Obstacle

A. Opala, M. Pieczarka, G. Sęk

Laboratory for Optical Spectroscopy of Nanostructures, Division of Experimental Physics, Faculty of Fundamental Problems of Technology, Wrocław University of Science and Technology, Wrocław, Poland

Exciton-polaritons, are bosonic quasiparticles that arise from strong coupling between exciton and photon modes in a semiconductor microcavity. Polaritons form condensates similar to atomic Bose-Einstein condensates, which can be described in the mean-field theory by a modified open-dissipative Gross-Pitaevskii equation [1]. The dissipative nature of exciton-polariton condensate comes from their intrinsic short lifetime of the order of ps, which is caused by the escape rate of photons outside the microcavity. Additionally, semiconductor microcavities are always under influence of some level of disorder naturally present in the sample. For this reason, exciton polaritons are a great platform to investigate bosonic condensation in random disorder potentials in analogy to atomic Bose-Einstein condensates in randomly generated optical potentials. Additionally, special attention is paid to condensates of lowered dimensionality, where the influence of disorder is enhanced.

In polariton systems dimensionality can be reduced by spatial patterning of the sample, creating quasi-one-dimensional microwires. Here we present theoretical investigations of a one-dimensional polariton condensate, created with nonresonant pumping and flowing against a localized obstacle. We employ an open-dissipative Gross-Pitaevskii equation, coupled to a reservoir rate equation, which captures the full reservoir-condensate dynamics, contrary to single-equation description [1],[2]. We investigate different wave patterns induced by an obstacle and demonstrate features controlling the flow velocity of the condensate and the system parameters, exploring the phase diagram of stability of a exciton-polariton condensate. Additionally, linear Bogoliubov-de Gennes analysis is performed to check stability conditions of the polariton condensate flow.

[1] N. Bobrovska, M. Matuszewski, Phys. Rev. B 92, 035311 (2015)

[2] P.-É. Larré, N. Pavloff, and A. M. Kamchatnov Phys. Rev. B 86, 165304 (2012)

Analysis of symmetry in the graphene quantum dots and artificial graphene quantum dots

P. Bugajny[1], L. Szulakowska[2], J. Jaworowski[1] P. Potasz[1], A. Wójs[1]

[1] *Wrocław University of Technology,Wybrzeże Wyspiańskiego 27, Wrocław, Poland*
[2] *University of Ottawa, 75 Laurier Ave E, Ottawa, Canada*

We investigate the optical properties of symmetric graphene quantum dots (GQD) [1] and artificial graphene quantum dots (AGQD) using the theory of representation of point groups. We classify symmetry of electronic states in the energy spectra obtained within tight-binding model (TB) of GQD (AGQD) with different sizes and edge termination. This enables us to determine allowed optical transitions. Next, we analyze the influence of edge effects on optical properties by studying structures with similar sizes, and zigzag and armchair edges. Optical transitions between edge-type and bulk-type states are investigated and compared with two types AGQD. A comparison between analytical and numerical results is presented. Absorption spectra for symmetric GQD (AGQD) for different sizes and edges are shown.

[1] Z.Z. Zhang, K. Chang, F.M. Peeters, *Phys. Rev. B*, **77** (2008) 235411.
[2] T. Yamamoto, T. Noguchi, K. Watanabe, *Phys. Rev. B*, **74** (2006) 121409.
[3] A. D. Guclu, P. Potasz, P. Hawrylak, *Phys. Rev. B*, **82** (2010) 155445.
[4] M. Ezawa, *Phys. Rev. B* **76** (2007) 245415.
[5] J. Fernandez-Rossier, J. J. Palacios, *Phys. Rev. Lett.*, **99** (2007) 177204.
[6] J. Akola, H. P. Heiskanen, M. Manninen,*Phys. Rev. B*, **77** (2008) 193410.
[7] W. L. Wang, O. V. Yazyev, S. Meng, E. Kaxiras, *Phys. Rev. Lett.*, **102** (2009) 157201.
[8] P. Potasz, A. D. Guclu, P. Hawrylak,*Phys. Rev. B* **81** (2010) 033403.
[9] D. Subramaniam, F. Libisch, Y. Li, C. Pauly, V. Geringer, R. Reiter, T. Mashoff, M. Liebmann, J. Burgdorfer, C. Busse, T. Michely, R. Mazzarello, M. Pratzer, M. Morgenstern, *Phys. Rev. Lett.* **108** (2012) 046801.
[10] S.K. Hamalainen, Z. Sun, M. P. Boneschanscher, A. Uppstu, M. Ijas, A. Harju, D. Vanmaekelbergh, P. Liljeroth, *Phys. Rev. Lett.*, **107** (2011) 236803.

Hardening of (Pb,Cd)Te Crystal Lattice with an Increasing CdTe Content in the Solid Solution

Rafał Kuna [1], Stanisław Adamiak [2], Sylvain Petit [3], Patrick Baroni [3], Katarzyna Gas [4,1], Roman Minikayev [1], Andrzej Szczerbakow [1], and Wojciech Szuszkiewicz [2,1]

[1] *Institute of Physics, Polish Academy of Sciences, al. Lotników 32/46,02-668 Warsaw, Poland. E-mail: kuna@ifpan.edu.pl*
[2] *Faculty of Mathematics and Natural Sciences, University of Rzeszów, ul. S. Pigonia 1, 35-310 Rzeszów, Poland*
[3] *Laboratoire Léon Brillouin, CEA-CNRS, CEA Saclay, 91191 Gif-sur-Yvette Cedex, France*
[4] *Institute of Experimental Physics, Faculty of Physics and Astronomy, University of Wrocław, pl. M. Borna 9, 50-204 Wrocław, Poland*

Lead telluride PbTe is among the chalcogenides the one, that has found much usefulness in the field of thermoelectricity and infrared detection. In a single PbTe bulk crystal grown by the Bridgman method, the microhardness maintains almost constant value of ~ 30 HV for various carrier concentrations [1]. Due to the relatively low microhardness value a layer of PbTe is so soft that it can be scratched easily. As a consequence, some devices consisting of PbTe layers are not robust enough to withstand damages possible in standard fabrication processing [2]. In order to avoid this problem, more robust materials are chosen typically as the outermost layers. However, there is another possibility by replacement of the PbTe by its solid solution containing another compound, e.g., GeTe [2].

The aim of present studies is to demonstrate the crystal lattice hardening resulting from noticeable CdTe content in the (Pb,Cd)Te solid solution. All single (Pb,Cd)Te crystals containing from 0 to 9% of the CdTe were grown at the Institute of Physics PAS by the self-selecting vapor growth (SSVG) method [3]. The room temperature data about microhardness and Young's modulus were determined by the nanoindentation method using an Ultra nano-hardness tester CSM UNHT/AFM and the Berkovich indenter tip. The maximum load equal to 1 mN was applied during 30 s, both the increase of the load during application and the removal of the load were performed in a linear manner with the same upload and download rate 0.033 mN. The average values and standard deviations of the hardness and Young's modulus were extracted from the determined load-displacement results. The composition-dependent modification of ultrasound velocity was estimated for the same set of solid solutions using the LA phonon dispersion data, obtained by inelastic neutron scattering (INS) measurements. Correlation between the composition of investigated crystals and their selected mechanical properties is given and discussed in comparison with available relevant data for (Pb,Ge)Te solid solution.

This work was supported in part by National Science Centre (Poland) through grant UMO-2014/13/B/ST3/04393.

[1] A. J. Crocker and M. Wilson, *J. Mate. Sci.* **13**, 833 (1970).
[2] B. Li, P. Xie, Zhang, and D. Liu, *J. Mater. Sci.* **46**, 4000 (2011).
[3] A. Szczerbakow and K. Durose, *Prog. Cryst. Growth Charact. Mater.* **61**, 81 (2005).

Substantial Difference in Selected Mechanical Properties of CdTe and PbTe Crystals Grown by Equilibrium and Non-Equilibrium Growth Techniques

Stanisław Adamiak [1], Piotr Adamski [1], Krzysztof Matracki [1], Dariusz Płoch [1], Elżbieta Dynowska [2], Piotr Dziawa [2], Andrzej Szczerbakow [2], Badri Talashvili [2], Maciej Wiater [2], Barbara Witkowska [2], Tomasz Wojtowicz [2], and Wojciech Szuszkiewicz [1,2]

[1] *Faculty of Mathematics and Natural Sciences, University of Rzeszów, ul. S. Pigonia 1, 35-310 Rzeszów, Poland*
[2] *Institute of Physics, Polish Academy of Sciences, al. Lotników 32/46, 02-668 Warsaw, Poland*

A range of physical properties of CdTe and PbTe, which can be found in many textbooks and databases, have been obtained long time ago with the use of bulk single crystals, i.e. materials grown by the equilibrium growth techniques. Due to development of non-equilibrium growth techniques, utilized for these group of semiconductors at least for the last 30 years the interest of the solid state physics shifted from 3D materials to low-dimensional objects such, as heterostructures, superlattices, nanowires or quantum dots. The same tendency is observed in the area of applications. The planar technology is today the basis of modern electronic industry, and the numerous semiconductor devices contain low-dimensional structures obtained by MBE or ALD. Under these circumstances the question arises: are the mechanical properties of these structures the same as those determined long time ago for the bulk materials or not? The small FWHM values of rocking curves determined by the X-ray diffraction measurements in MBE-grown layers, which demonstrate a much better crystal quality in comparison to that of corresponding bulk materials, suggests a negative answer to this question. To our knowledge, however, a difference in selected mechanical properties of the MBE-grown layer and the same material in the bulk form was not a subject of numerous, separated studies dedicated to this particular problem.

The aim of present studies is to compare the vales of mechanical properties of two types of crystals: bulk materials grown using the equilibrium growth technique and obtained by non-eqilibrium growth method – MBE. The cadmium telluride and the lead telluride, well known for a long time and widely investigated, typical semiconducting compounds of II-VI and IV-VI type, respectively, were chosen for this purpose. The investigated CdTe bulk crystal was grown by the Bridgman method, the bulk PbTe was obtained by the self-selecting vapor growth (SSVG) technique [1]. The 8 μm thick CdTe layer deposited onto GaAs substrate and 6 μm thick PbTe layer grown on BaF_2 were selected for the comparison. The room temperature data about microhardness and Young's modulus were determined for all samples by the nanoindentation method [2]. The parameters of the applied load were as follows: maximum load 1 mN, linear change of the load during application and removal of the load 0.033 mN, application time of the maximum load 30 s. The average values and standard deviations of the hardness and Young's modulus were extracted from the determined load-displacement results. Possible origins of observed, substantial difference in relevant values determined in MBE-grown layers and bulk materials are given and discussed.

This work was supported in part by National Science Centre (Poland) through grant UMO-2014/13/B/ST3/04393.

[1] A. Szczerbakow and K. Durose, *Prog. Cryst. Growth Charact. Mater.* **61**, 81 (2005).
[2] A.J. Crocker and M. Wilson, *J. Mater. Sci.* **13**, 833 (1970).

Is an Application of a Semiconductor in its Metastable Crystal Form a Danger for the Lifetime of Possible Device?

Elżbieta Dynowska [1], Stanisław Adamiak [2], Maciej Wiater [1], Barbara Witkowska [1], Tomasz Wojtowicz [1], and Wojciech Szuszkiewicz [2,1]

[1] *Institute of Physics, Polish Academy of Sciences, al. Lotników 32/46, 02-668 Warsaw, Poland*
[2] *Faculty of Mathematics and Natural Sciences, University of Rzeszów, ul. S. Pigonia 1, 35-310 Rzeszów, Poland*

The idea of possible semiconductor superlattice growth and the prediction of particular physical properties of new, low-dimensional structures have been presented for the first time at the ICPS in Warsaw in 1972. Since this conference an enormous development of the non-equilibrium techniques like, e.g., the molecular beam epitaxy (MBE) serving for the growth of low-dimensional objects, is observed in the solid state physics. From one side there exists an interest in the growth and characterization of low-dimensional semiconductor in the same crystal phase, as that of its bulk equivalent. On the other side an application of MBE technique makes it possible to create thin layers of material with quite a new crystal structure, which does not exist in nature. The materials obtained in such a manner often exhibit new, required physical properties, corresponding to particular needs of given device or application. The success of non-equilibrium growth technology results from well selected crystal symmetry and lattice parameter values of the substrate. The proper choice of the substrate material due to a presence of a compressive or tensile strain introduced in the grown layer stabilize its structure. For some particular purposes like, e.g., the space applications like the space missions etc. the long lifetime of electronic elements and other devices is a crucial problem. Up to our knowledge up to now the stability of 'metastable' form of semiconductor compounds were out of the interest. We have selected this problem as a topic of our present studies.

One from the best known semiconducting compounds widely investigated in its metastable crystal structure, obtained for the first time in [1], is the MnTe in the zinc blende structure (the stable MnTe crystal phase exhibits a hexagonal structure of NiAs type). Due to its particular magnetic order of AF III type the zinc blende MnTe was intensively studied since 1989 first in the form of thin layers (see, e.g., [1-4]) and next as a constituent of superlattices and other low-dimensional quantum structures. In the present work several few μm thick MnTe layers with the zinc blende structure grown onto GaAs substrate by MBE during different periods were investigated by the SEM, AFM, XRD, and nanoindentation methods. A partial decomposition of the oldest investigated layers was demonstrated. The selected structure properties of single metastable MnTe layers were compared with those of superlattices containing this crystal phase as well as with those corresponding to the bulk MnTe crystal in its stable form.

This work was supported in part by National Science Centre (Poland) through grant UMO-2014/13/B/ST3/04393.

[1] S.M. Durbin, J. Han, O. Sungki, et al., *Appl. Phys. Lett.* **55**, 2087 (1989).
[2] T.M. Giebultowicz, P. Klosowski, N. Samarth, et al., *Phys. Rev.* B **48**, 12817 (1993).
[3] E. Janik, E. Dynowska, J. Bąk-Misiuk, et al., *Thin Solid Films* **267**, 74 (1995).
[4] B. Hennion, W. Szuszkiewicz, E. Dynowska, et al., *Phys. Rev.* B **66**, 224426 (2002).

Carrier dynamics of InAs/InP quantum dots ensemble embedded in various barrier layers.

A. Maryński[1], M. Syperek[1], M. Pieczarka[1], J. Misiewicz[1], V. Liverini[2,*], M. Beck[2], J. Faist[2], G. Sęk[1]

[1] *Laboratory for Optical Spectroscopy of Nanostructures, Division of Experimental Physics, Wrocław University of Science and Technology, Wrocław, Poland*
[2] *Institute of Quantum Electronics, ETH Zürich, Zürich, Switzerland*
[*] *currently at: Albis Optoelectronics AG, Rüschlikon, Switzerland*

In certain realization of photonic devices based on quantum dots (QDs) e.g. photon detectors, one need to assure lateral electronic coupling between ground states among ensemble of confined states. However, such coupling must be avoided in other type of devices e.g. lasers or amplifiers and can lead to deteriorate strongly their efficiency. In the following work we have focused on self-assembled QDs with their ground state emission centered around 1.55 mm. These dots can be well suited for optoelectronic devices (lasers, amplifiers, or detectors) operating in the C-band window of silica fibers. As we demonstrate, properties of a ground state of an entire system can be efficiently tuned by manipulating the chemical composition of the barrier and thus influencing the overall electron-hole confinement conditions.

We consider two kinds of QDs made of InAs submerged into different barriers lattice matched to InP: (i) InAlAs, and (ii) InGaAlAs. While in the former case one to expect a strong e-h confinement condition, in the latter case the confinement is slightly weaker (for electrons/or holes?). Both structure where examined in temperature-dependent photoluminescence (PL) and time-resolved photoluminescence (TRPL) experiments at T=5K where structure are excited in quasi-resonant conditions (Laser = 0.855eV).

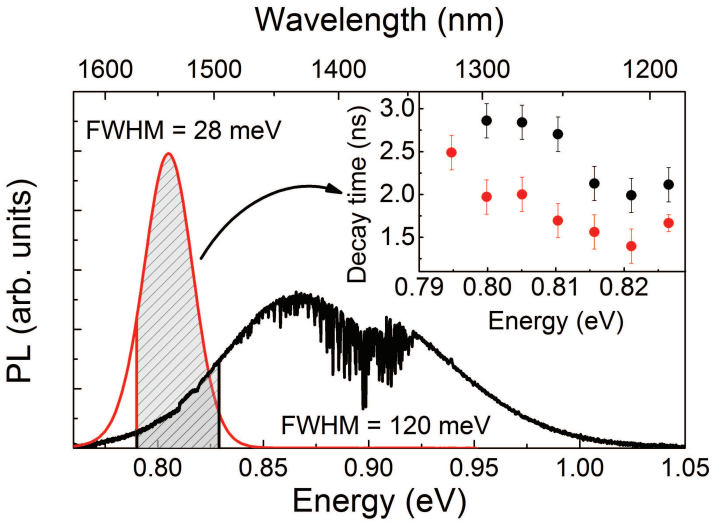

Figure 1 Photoluminescence at 5K. Red line corresponds to InGaAlAs sample, black one corresponds to InAlAs sample. Inset shows decay times for the up mentioned samples.

First, a strong difference between both structures is observed as considering the PL quench that is much slower for the InAs/InAlAs QDs structure than for the InAs/InAlGaAs one. In the latter case, the PL quench starts just above T = 5K. As far as we assume that the barrier is fully relaxed without any defect states, and the wetting layer density of states is not extended down to the QD ground state thus the PL quench process can be related to the in-plain coupling among QDs ensemble. This property can be additionally confirmed in the TRPL experiment. While for the QD structure with a strong e-h confinement the PL decay time lies in the range of ~2-2.8 ns, for the structure with lower confinement the PL decay time is 0.4-0.6 ns shorter that suggests existence of e-h transfer process between adjacent QDs influencing the overall PL decay.

A model of radiative recombination from quantum well in potential fluctuations

Piotr A. Dróżdż[1,2], Krzysztof P. Korona[1], Marcin Sarzyński[2], Robert Czernecki[2], Czesław Skierbiszewski[2], Grzegorz Muziol[2] and Tadeusz Suski[2]

[1] *Faculty of Physics, University of Warsaw, Pasteura 5, 02-093 Warsaw, Poland*
[2]*Institute of High Pressure Physics "Unipress", Polish Academy of Sciences, Sokołowska 29/37, 01-142 Warsaw, Poland*

Anomaly behavior of photoluminescence energy dependence on temperature is very often observed in InGaN/GaN quantum wells. The energy first decrease in low temperatures, than increase while the temperature grows up, and decrease again at high temperatures which gives so called S – shape. Such behavior is explained by existence of potential fluctuations caused by inhomogenities of indium content in quantum wells.

In last 15 years, several attempts were made to describe the PL energy dependence on temperature. The first approach, in which Gaussian density of states in potential minima was assumed, was done by Eliseev *et al.* [1]. The PL dependence on temperature was obtained by using Boltzmann distribution, however, this theory does not fit to experimental data in range of low temperatures. Theory of Eliseev was later improved by Li *et al.* [2]. Li and collaborators showed that the PL energy dependence on temperature can be described properly by using Fermi-like distribution, however, they assume radiative recombination time to be independent on energy and temperature.

Since experimental evidence points to significant thermal dependence of lifetime, we propose an improved approach to problem of fluctuation-induced S – shape. Our model is next development step of theories presented by Eliseev *et al.* and Li *et al.* Gaussian density of states in potential minima and continuos delocalization of carriers are assumed. Radiative recombination time dependence on temperature and energy is taken into account and formula describing luminescence decay time is proposed. In this model, it is also assumed that the effective temperature of exciton gas is changing with the temperature of crystal lattice. From this assumptions, formula to describe S – shape is obtained, that fits to experimental data in range from helium temperature (4 K) to room temperature as can be seen in Fig. 1.

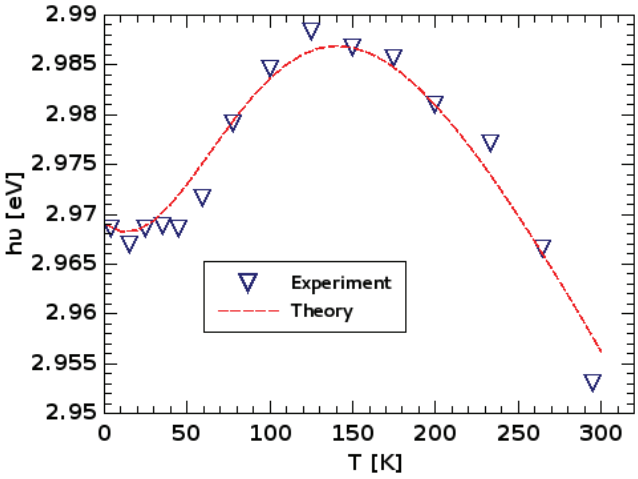

Fig. 1: PL energy dependence on temperature for the sample with 10 nm GaN alloy sandwiched between AlGaN and AlInGaN layers. Experimental data are marked by triangles, whereas dashed red line corresponds to presented theory.

[1] P. G. Eliseev, *J. Appl. Phys.* **93**, 5404, (2003).
[2] Q. Li, S. J. Xu, W. C. Cheng, M. H. Xie, S. Y. Tong, C. M. Che, and H. Yang, *Appl. Phys. Lett.* **79**, 1810 (2001).

The properties of heterojunctions n+-ZnO:Al/n-Si and n+-ZnO/n-$ZnO_{1-x}S_x$/p-$CuIn_{0.8}Ga_{0.2}Se_2$

G. Lashkarev[1], V. Kostylyov[2], V. Vlasiuk[2], V. Karpyna[1], I. Shtepliuk[1], D. Muzyka[1], M. Dranchuk[1], V. Popovich[1], P.Demydyuk, R. Pietruszka[3] and M. Godlewski[3]

[1]Institute for Problems of Material Science, NASU, Krzhizhanovskogo 3, Kyiv, Ukraine
[2]Institute of Semiconductor Physics, NASU, prosp. Nauky 45, Kyiv, Ukraine
[3]Institute of Physics, PAN, al. Lotnikow 32/46, Warsaw, Poland

For investigation of the compatibility of transparent electrodes based on highly doped ZnO:Al films with Si they were deposited on n-type Si substrates (isotype heterojunction). The n+-ZnO films were deposited by ALD technology using diethylzinc and water vapour as zinc and oxygen precursors. The growth temperature was 200 ^{0}C. Ellipsometric measurements at 633 nm wavelength were used in order to determine the thickness of films which was within 260-420 nm.

Spectral dependences of external quantum efficiency (EQE) were investigated in the spectral range 400-1200 nm in the regime of constant quantity for incidence photons on the sample. These dependences were oscillating ones due to interference in the n+-ZnO layer (optical film thickness was 550-840 nm). The short wavelength fall of inner quantum efficiency (IQE) was calculated by the equation $IQE(\lambda)= EQE(\lambda)/T(\lambda)$ and had the magnitude about 10-20 %. The last testifies to low rate of surface recombination and therefore to the high enough quality of interface n+-ZnO/n-Si. Transparency spectrum of the n+-ZnO film $T(\lambda)$ was obtained by elipsometric measurements of thickness and refractive index in a supposing that ZnO films do not absorb light in the studied spectral interval.

Obtained results jointly with literature data allowed to construct band diagram of the heterojunction n+-ZnO/n-Si. The calculated widths of the space charge area for prepared structures are different ones for different samples and are about ~230 nm (99,9 % of this area is situated in Si). Contact potential difference which was not less than 181-268 mV was determined out of the open circuit voltage in the conditions of irradiance intensity of illumination of 1000 W/m^2. As a result the near surface zone bend essentially decreased what allowed us to evaluate the low boundary of n+-ZnO work function which appeared about 2.45± 0.1 eV for different samples.

Thus we were able to determine the important characteristics of transparent electrode n+-ZnO:Al which are necessary for further investigations and for optimization of characteristics for photovoltaic devices using ZnO:Al.

Solar cells prototypes with efficiency of 8-13% based on $ZnO_{1-x}S_x$ solid solution and CIGS with the use of transparent ZnO:Al electrodes were processed. Uniform single phase $ZnO_{1-x}S_x$ solid solutions are characterized by linear dependence of lattice period (Vegard law) and unusual (parabolic) dependence of E_g on sulfur content that makes these films of better choice for photovoltaic applications compared to ZnCdO where phase separation and spinodal decomposition were observed. Developed solar cells heterojunctions with structure n+-ZnO/n-$ZnO_{1-x}S_x$/p-$CuIn_{0.8}Ga_{0.2}Se_2$ demonstrated similar photovoltaic characteristics as CdS/CIGS heterojunctions and are perspective for development cadmium-free solar cells.

This work was partially supported by the National Science Center (decision No.DEC-2012/06/A/ST7/00398).

Three terminal efficient heat to electricity converter

Barbara Szukiewicz and Karol I. Wysokiński

Institute of Physics, M. Curie-Skłodowska University, ul. Radziszewskiego 10, 20-031 Lublin

Thermoelectric properties of the efficient heat to electricity converter have been studied. The system consisting of two independently controlled quantum dots connected to three terminals has been modeled by the Anderson Hamiltonian. In the configuration with one hot and two cold electrodes, the electric current flows in the direction effectively perpendicular to the heat current. We have calculated linear transport coefficients and the resulting efficiency. Interestingly the power factor obtained from the knowledge of the linear electrical conductance and the thermopower surprisingly well compares to the exactly calculated (in the strongly nonlinear regime) value of optimal power of the device. The roles of asymmetry in the couplings and temperature difference between two cold electrodes have been explored in order to further optimise the performance of the system.

This work has been partially supported by the National Science Centre under the grant no. DEC-2014/13/B/ST3/04451

Thermal phonon lasing in nanoscopic quantum systems

P. Karwat[1,2], D. E. Reiter[2], T. Kuhn[2], P. Machnikowski[1], O. Hess[3]

[1] *Department of Theoretical Physics, Wrocław University of Technology, Wybrzeże Wyspiańskiego 27, 50-370 Wrocław, Poland*
[2] *Institut für Festkörpertheorie, Westfälische Wilhelms-Universität Münster, Wilhelm-Klemm-Strasse 10, 48149 Münster, Germany*
[3] *The Blackett Laboratory, Department of Physics, Imperial College London, South Kensington Campus, SW7 2AZ, United Kingdom*

With the rapid progress in miniaturization many types of devices have reached the nanoscale where quantum effects become more prevalent, e.g., quantum lasers. On properly designed nanoscopic quantum systems a heat gradient can lead to inversion in parts of it, that could be utilized e.g. for the generation of coherent light or phonons.

We study a theoretical concept of a nanoscopic quantum system representing the active medium of a thermal laser. Our model consists of a central three-level system interacting with a two-level subunit at each side. Each two-level system is coupled to a heat bath. The different temperatures of the baths impose a heat gradient. The heat gradient leads to a flow of excitation from the hotter to the colder bath. At the central unit the flow is accompanied by the emission of a photon or phonon. For certain parameters, this transition can generate lasing. Our description of the system kinetics is based on the Lindblad form of a Quantum Master Equation and the coupling to the lasing electromagnetic or lattice displacement field is described via a semiclassical equation.

In this presentation, we show that a positive inversion within the upper two levels of the central system takes place, which is a requirement to enable lasing. We also discuss how to turn the above concept into reality. We suggest as envisioned nanoscopic quantum system three semiconductor quantum dots stacked upon each other.

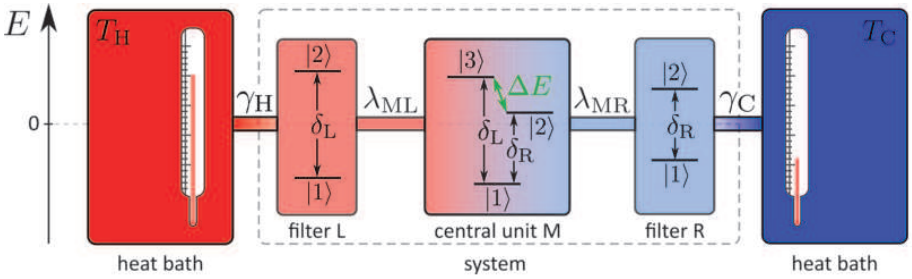

Figure 1: The model system.

Optical And Structural Properties Of GaInAsBi/GaAs MQWs

S. Stanionytė [1], V. Pačebutas [1], B. Čechavičius[1] and A. Krotkus[1].

[1] *State research institute Center for Physical Sciences and Technology*
Savanorių ave. 231, LT-02300 Vilnius, Lithuania

III-V group compounds attract scientists because of their wide use in optoelectronic devices. GaInAs layers for quite a long time are used for diodes and photodetectors in the near infrared spectral range. Incorporation of bismuth into this alloy has several advantages such as weaker energy bandgap temperature dependence and fast reduction of the bandgap even with small percentage of Bi. The aim of this work was to grow and investigate GaInAsBi multiple quantum wells (MQWs).

GaInAsBi/GaAs MQWs were grown by molecular beam epitaxy (MBE) on GaAs (100) substrates. The substrate temperature was varied in the range of 240–300 °C. QW thicknesses were ~7.5 nm and the barriers were ~9.5 nm thick. MQWs were characterized by high resolution X-ray diffraction (HR-XRD) and photoluminescence (PL). The strongest PL signals and, according to the HR-XRD results, the best crystalline structure was achieved for MQWs grown at 270 °C. To investigate the indium influence on bismuth incorporation and to determine exact In and Bi concentrations GaInAs/GaAs and GaAsBi/GaAs MQWs were grown additionally. Growth temperatures were kept the same as for GaInAsBi/GaAs MQWs. Bismuth and indium fluxes were fixed in order to calculate the composition of quaternary GaInAsBi quantum well. HR-XRD rocking curves (Fig. 1) showed that indium does not have significant influence for incorporation of bismuth into GaInAs. HR-XRD results measured on different experimental structures correlate with the PL data.

GaInAsBi/GaAs MQWs with different bismuth content were grown. From XRD results these layers compositions are ~8% of In and 0,9–4,2 % bismuth. The higher bismuth concentration shifts PL peak to smaller peak energies.

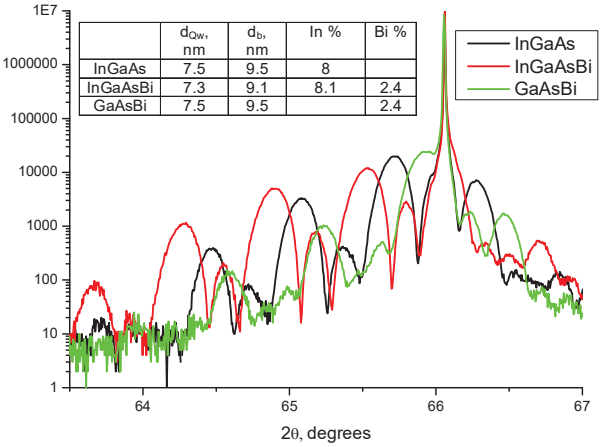

	d_{Qw}, nm	d_b, nm	In %	Bi %
InGaAs	7.5	9.5	8	
InGaAsBi	7.3	9.1	8.1	2.4
GaAsBi	7.5	9.5		2.4

Figure 1. HR-XRD rocking curves of InGaAs, InGaAsBi and GaAsBi MQWs.

In conclusion, the GaInAsBi/GaAs MQWs were grown on GaAs substrates. The influence of the substrate temperature and the Bi flux was investigated. It has been found that the best PL results were obtained from layers grown at 270 °C temperature. Such MQWs could be used as active regions of the light emitting or laser diodes.

Two modes of luminescence energy control in polar and semipolar InGaN/GaN quantum wells

Marcin Sarzyński[1,2], Piotr A. Dróżdż[1,3], Krzysztof P. Korona[3], Szymon Grzanka[1,2], Robert Czernecki[1,2], Ewa Grzanka[1,2], Jakub Goss[1], and Tadeusz Suski[1]

[1] *Institute of High Pressure Physics PAS, Sokolowska 29/37, 01-142 Warszawa, Poland*
[2] *TopGaN Ltd., Sokolowska 29/37, 01-142 Warszawa, Poland*
[3] *Faculty of Physics, University of Warsaw, Pasteura 5, 02-093 Warszawa, Poland*

The majority of InGaN quantum structures are grown on c-plane polar substrate orientation in the step-flow growth mode. In such case indium composition (and so the bandgap) is determined mostly by the growth temperature and directly influences the energy of emitted light. However, it was shown that indium content also depends on the substrate miscut angle (with respect to the c polar plane). We have investigated structural and optical properties of such structures as a function of miscut and the main observations are as follows: i) indium content decreases and bandgap increases for higher miscut angle, ii) photoluminescence decay time decreases for higher miscut, which is due to both lower indium content and weaker quantum confined Stark effect.

In this work we focused on similar research for InGaN structures grown on semipolar (20-21) plane, for which internal field is strongly reduced. In contrast to growth on the polar plane, it turned out that indium content did not depend on the substrate miscut, what was confirmed by XRD. However, in contrary to the expectations the following results were achieved: both emission energy and luminescence decay time were sensitive to the miscut angle. We show that these effects can be attributed solely to the variation in built-in electric field.

According to calculations performed by Wernicke and coworkers [1] the internal field magnitude should depend on the semipolar substrate miscut angle and has spontaneous (along the c-axis) and piezoelectric (due to strain in the growth plane) components.

We will also discuss results for polar and semipolar structures, in terms of the growth mode and carrier recombination mechanisms.

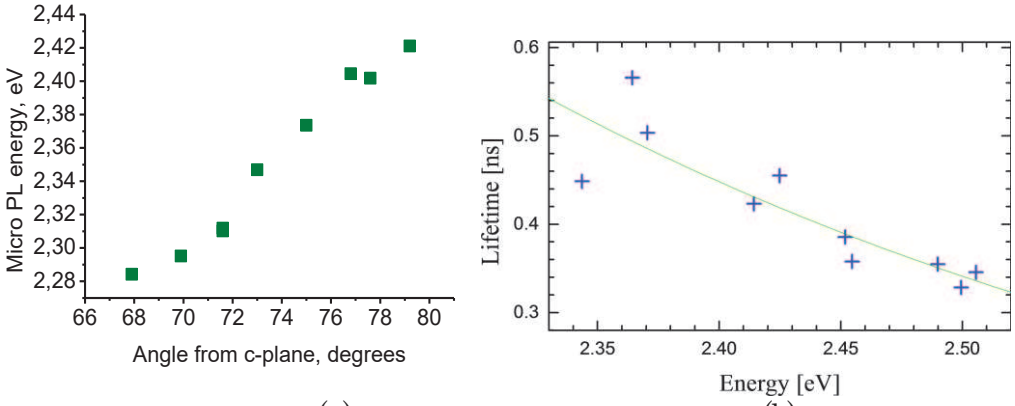

(a) (b)

Fig. 1. a) Luminescence energy as a function of substrate miscut angle for 5QW structure grown on (20-21) plane GaN. b) Luminescence decay time as a function of energy for the same sample.

[1] T. Wernicke et al., Semicond. Sci. Technol. **27**, 024014 (2012).

Magnetoresistance Measurements of Modulation Doped $Si/Si_{0.8}Ge_{0.2}$ Structure Grown by Molecular Beam Epitaxy (MBE) Technique

S. Ağan

University fo Kırıkkale, Department of Physics, 71450 Kırıkkale, Turkey

Magnetoresistance oscillations are obtained in the inverted modulation doped molecular beam epitaxy (MBE) grown $Si/Si_{0.8}Ge_{0.2}$ sample. The variation of the longitudinal resistivity ρ_{xx} (at B=0) and sheet conductivity σ_{xx} with temperature has been found. The 2D hole denstiy per well has been calculated from the plots of the reciprocal magnetic field (1/B). In these structures a quasi-two dimensional hole gas (2DHG) was formed in the $Si_{0.8}Ge_{0.2}$ quantum wells with 4.2 K sheet carrier denstiy measured in the range (2.5 x 6.5) x 10^{11} cm^{-2}.

Magnetotransport measurements of the longitudinal sheet resistivity ρ_{xx} and Hall resistance ρ_{xy} were made in the range B = -0.5 – 12 T and T = 0.330 – 1.5 K. At 0.3 K, Hall mobility is 4070 $cm^2V^{-1}s^{-1}$. From SdH (Shubnikov-de Haas oscillations) low temperature magnetotransport measurements in the temperature range 332 mK - 2.5 K, the role effective mass $m^* = (0.26 \pm 0.01)\ m_0$ was extracted for the corresponding carrier density of n_s = 3.8 x 10^{11} cm^{-2}.

The experimental thermopower and thermal conductivity measurements have been carried in the temperature range 1.4 – 300 K. The thermoelectric power is found to be dominated by the phonon drag contribution in the range 1.4 – 20 K. A fit to phonon drag thermopower theory for $Si_{0.8}Ge_{0.2}/Si$ heterostructures yields a value of 4.5 eV for the acoustic phonon deformation potential. The phonon mean free paths of the structures have been calculated from the thermal conductivity measurements.

Quantum Hall Ferromagnet effect in CdMnTe

Zbigniew Adamus[1], Walery Kołkowski[1], Maciej Wiater[1], Grzegorz Karczewski[1], Aleksandr Kazakov[2], Leonid Rokhinson[2] and Tomasz Wojtowicz[1]

[1] *Institute of Physics PAS, 02-668 Warsaw, al. Lotników 32/46, Poland*

[2] *Department of Physics, Purdue University, West Lafayette, IN 47907 31, USA*

The presence of magnetic ions in two-dimensional electron gas (2DEG) leads to correlation effects, which modulate Landau levels (LLs) splitting. In particular, LLs corresponding to opposite spin orientations may overlap at the Fermi level. As a consequence spin order is expected in the 2DEG system and such state is called the quantum Hall ferromagnet (QHFM). One of the manifestation of QHFM is the abrupt increase of longitudinal megnetoresistance ($R_{xx}(B)$) at certain B_c[1]. The idea of our experiment came from the opportunity of the manipulation of the 2DEG concentration in wide range (from $3 \times 10^{11}\text{cm}^{-2}$ to $6.4 \times 10^{11}\text{cm}^{-2}$).

We investigated structures with Mn ions uniformly incorporated in the modulation-doped CdTe quantum well. $R_{xx}(B)$ and $R_{xy}(B)$ were measured in magnetic field up to B=8.5 T at temperature T=1.5 K. Sample was illuminated gradually by the green light emitting diode (λ=530 nm). The illumination changed 2DEG concentration and hence position of the Fermi level. Therefore, we observed evolution of the $R_{xx}(B_c)$ cusp related to QHFM: changes of the cusp amplitude and shift of the cusp position. Moreover, we noticed a peculiar behavior of $R_{xy}(B)$: sudden increase or decrease of $R_{xy}(B_c)$ in respect of the filling factor. Deviation from discrete value $R_{xy}(B) = h/ie^2$ were already predicted and observed in Ref.[2,3,4]. However, presented results are the first systematic studies of $R_{xy}(B)$ in CdMnTe with different 2DEG concentration.

We identified that experimental results can not be interpreted as "overshooting". $R_{xx}(B)$ and $R_{xy}(B)$ were analyzed with the proposed model of the moving Fermi level crossing the broadened LLs. Electron-electron interaction and coupling to Mn ions are possible explanations of the observed phenomena.

The research was partially supported by National Science Centre (Poland) grant DEC-2012/06/A/ST3/00247 and by the ONR grant N000141410339.

[1] J. Jaroszyski *et al.*, *Phys.Rev.Lett* **89**, 266802 (2002).
[2] H.J.P Freire *et al.*, *Phys.Rev.Lett* **99**, 026801 (2007).
[3] I. Shlimak *et al.*, *Phys.Rev.B* **73**, 205324 (2006).
[4] E.M. Kendirlk *et al.*, *Scientifiv Raports* **3**, 3133 (2013).

Interplay between the quantum interference and electron pairing in nanoscopic heterostructures

S. Głodzik and T. Domański

Institute of Physics, M. Curie-Skłodowska university, 20-031 Lublin, Poland

When nanoscopic objects (such as atoms, molecules, or nanowires) are brought in contact with the superconducting electrodes they absorb electron pairing and become superconducting nano-grains. Besides the usual balistic tunnelling the charge transport can be provided via such entities as the anomalous Andreev mechanism, in which electrons are converted into holes and simultaneously the Copper pairs are injected to the superconducting reservoir. We study the multi-dot configuration and confront such mechanism with the hopping processes, responsible for the strong quantum interference effects [1]. We show that their interplay causes a substantial transfer of the quasiparticle spectral weights [2], analogous to the Dicke effect known in quantum optics [3]. We discusss experimental methods for detecting these features in the subgap Andreev [4] or the Josephson [5] spectroscopies.

[1] I. Weymann, B.R. Bułka, & J. Barnaś, Phys. Rev. B **83**, 195302 (2011).
[2] P. Trocha & J. Barnaś, Phys. Rev. B **78**, 075424 (2008).
[3] A. Sitek & A. Manolescu, Phys. Rev. A **88**, 043807 (2013).
[4] J. Barański & T. Domański, J. Phys.: Condens. Matter **25**, 435305 (2013).
[5] G.-Y. Yi, X.-Q. Wang, H.-N. Wu, & W.-J. Gong, Physica E **81**, 26 (2016).

Temperature dependent-photoreflectance of InAs/GaAs quantum dot

Y. H. Choi [1], S. H. Lee[1], J. S. Kim[1*] and S. J. Lee [2]
[1] *Department of Physics, Yeungnam University, Gyeongsan 712-749, South Korea*
[2] *Division of Convergence Technology, Korea Research Institute of Standards and Science, Daejeon 305-340, South Korea*
E-mail: jongsukim@ynu.ac.kr

We performed temperature dependent-photoreflectance (TDPR) of InAs/GaAs quantum dot (QD) structure with above- and below-pump source, which are 633 nm He-Ne laser and 975 nm laser diode (LD), respectively. Above-pump source can excite energy states of GaAs bulk and InAs while below-pump source excites only InAs QD regions. Using both of two different pump sources, Temperature behavior of InAs/GaAs quantum dot was studied in this work.

Fig. 1 (a) and (b) exhibit the TDPR spectra with various temperatures. A 900 nm short pass filter (SPF) was used to reduce photoluminescence (PL) signal. We observed GaAs band edge transition and Franz-Keldysh oscillation (FKO). GaAs related signals follow general blue-shifted with decreasing temperature. In addition, FKO periods changes with decreasing temperature because the junction electric field (F) is closely related to FKO period [1]. We evaluated the strength of F by using fast Fourier transform (FFT) methods.

Fig.1 (c) shows the evaluated F as a function of temperature. For below pump, a peculiar temperature behavior was revealed. There are two regions: (i) T ~ 150 K, (ii) 150 ~ 300 K. In the region of (i), photo-excited carriers by below-pump are redistributed between InAs dots. Generally, for dots embedded in a GaAs matrix, the temperature dependent-line width of the dot photoluminescence (PL) goes to a minimum value while PL intensity moves into a maximum value at T ~150 K in agreement with earlier work on similar samples [2]. Hence, carrier confinement effect is a dominant process resulting in enhanced photovoltaic (PV) effect from 100 K to 0 K and correspondingly, in diminished PV effect from 150 to 100 K. In the region of (ii), the temperature behavior has a general dynamics caused by PV effect [3]. For above-pump, the number of photo-excited carriers in GaAs region is much larger than that in InAs QD region. Therefore, the overall temperature behavior of above-pump leads to that of GaAs bulk.

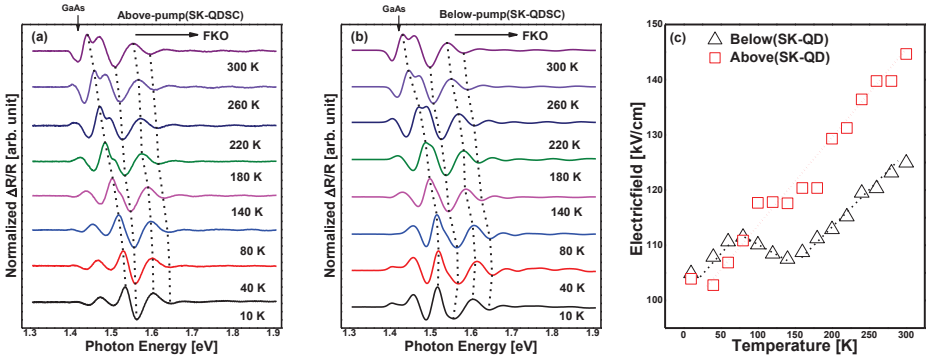

Figure 1. TDPR spectra of InAs/GaAs QD with (a) above- and (b) below-pump source, and (c) junction electric fields evaluated from PR spectra as function of temperature.

[1] C. Van Hoof, K. Deneffe, J. De Boeck, J. D. Arent and G. Borghs, *Appl. Phys. Lett*. 54, **608** (1989).
[2] H. Lee, W. Yang, and P. C. Sercel, *Phys. Rev. B.* **54**, 11528 (1996).
[3] T. M. Hsu, W. C. Lee, J. R. Wu and J.-I. Chyi, *Phys. Rev. B.* **51**, 17215 (1995).

Effect of the Majorana bound state on electron transport through the T-shape quantum dot

A. Kobiałka and T. Domański

Institute of Physics, M. Curie-Skłodowska university, 20-031 Lublin, Poland

We study the electronic transport through the quantum impurity (dot) laterally coupled to the external reservoirs and additionally side-coupled to the quantum wire [1], hosting at its edges the Majorana type quasiparticles. Due to hybridization between these nanoscopic objects the Majorana end-state *leaks* into the quantum dot [2], affecting its electronic spectrum and the transport properties of the device [3,4]. We discuss experimental signatures of this effect, manifested in the differential conductance [1], the thermopower [5] and the shot-noise [6]. We also provide hints for similar features appearing in the Andreev transport when one of the external reservoirs is superconducting.

[1] W.-J. Gong *et al*, Phys. Rev. B **89**, 245413 (2014).
[2] D.A. Ruiz-Tijerina *et al*, Phys. Rev. B **91**, 115435 (2015).
[3] C. Jiang, G. Lu, & W.-J. Gong, J. Appl. Phys. **116**, 103704 (2014).
[4] P. Stefański, Acta Phys. Polon. A **127**, 198 (2015).
[5] S. Valentini, R. Fazio, V. Giovannetti, & F. Taddei, Phys. Rev. B **91**, 045430 (2015).
[6] D.E. Liu, M. Cheng, & R.M. Lutchyn, Phys. Rev. B **91**, 081405(R) (2015).

Photoluminescence studies of PbSe/CdSe heterostructures

A. Socha[1], M. Szot[2], S. Chusnutdinow[2], K. Połczyńska[1], A.M. Witowski[1], L. Kowalczyk[2], K. Dybko[2], M. Wiater[2], T. Wojtowicz[2], T. Story[2], G. Karczewski[2]

[1] Faculty of Physics, University of Warsaw, Pasteura 5, 02-093 Warsaw, Poland
[2]Institute of Physics, Polish Academy of Sciences, Lotników 32/46, 02-668 Warsaw, Poland

PbSe is a narrow band gap IV-VI semiconductor known for applications in mid-infrared detectors and lasers but also from investigations of epitaxial PbSe quantum dots [1] and colloidal core/shell dots, like PbSe/CdX (X = S, Se, Te) [2]. The recent discovery of topological insulators gave new impulse for studies of PbSe-based heterostructures as this semiconductor with proper addition of Sn constitutes new class of topological materials, namely topological crystalline insulators [3]. In this paper we concentrate on optical investigations of quantum wells of rock-salt PbSe with wide gap barriers of sphalerite CdSe grown on GaAs (001) substrate. The preparation of PbSe/CdSe heterostructure in the form of quantum well shifts the region of optical activity of PbSe (Eg≈150 meV at 4K) to the higher energies due to the quantum size effect. It can be crucial in the case of future photoluminescence measurements of topological $Pb_{1-x}Sn_xSe$ material as the increase of tin content decreases the energy gap to the region in which the non-radiative recombination processes dominate.

The samples were grown by molecular beam epitaxy technique with use of separate effusion cells for Pb, Se, and Cd. The growth temperatures were 365 °C for CdSe and 263 °C for PbSe material. First, samples containing thin CdSe buffer and 300 nm thick PbSe layer were prepared for different Se/Pb flux ratio η varying from 1 to 2.2. The best photoluminescence efficiency was obtained for samples with $\eta \approx 1.6$. For such samples we observe band-to-band transitions with maximum shifting from 165 meV at 15 K up to 275 meV at room temperature. The 15 meV shift observed at low temperatures as compared to bulk PbSe is due to stress resulting from difference in temperature expansion coefficient for PbSe and GaAs substrate and CdSe buffer. It is also worth to notice, that the 30 min annealing (in nitrogen atmosphere) of the samples grown for η significantly different from 1.6 can considerably increase their photoluminescence activity. Such behavior is a result of improved crystal quality by reduced number of intrinsic defects (like Pb vacancies and Se interstitials) during annealing process.

Further, three samples containing single CdSe/PbSe/CdSe quantum well with thicknesses of 100 nm, 80 nm and 50 nm respectively were grown. For 100 nm PbSe QW samples we observe the blue-shifted photoluminescence emission up to 225 meV at 50 K due to quantum size effect. Increase of temperature in the case of this sample causes further shift of the luminescence peak to 275 meV at 230 K. Surprisingly, for samples with thinner PbSe QWs the photoluminescence signal is observed only at higher temperatures starting from 130 K and 150 K for 80 nm and 50 nm QW respectively, and is much weaker as compared to the 100 nm sample. This unexpected temperature behavior of photoluminescence will be discussed within the model taking into account quasi-type II band alignment expected in the case of PbSe/CdSe heterostructures [2]. In this localization regime the electrons are delocalized while the holes remain localized within the region of PbSe material. It makes the investigated structures very sensitive to the temperature induced change of the conduction band offset.

[1] G. Springholz, *et al., Science* **282**, 734 (1998)
[2] De Geyter *et al., ACS Nano* **5**, 58-66 (2011)
[3] P. Dziawa *et al*., *Nature Materials* **11**, 1023 (2012)

Mid-infrared studies of PbTe/CdTe quantum dots in the regime of macro- and micro-photoluminescence

K. Połczyńska[1], M. Szot[2], A. Socha[1], S. Chusnutdinow[2], A. M. Witowski[1], L. Kowalczyk[2], K. Dybko[2], M. Wiater[2], T. Wojtowicz[2], T. Story[2], G. Karczewski[2]

[1] Faculty of Physics, University of Warsaw, Pasteura 5, 02-093 Warsaw, Poland
[2]Institute of Physics, Polish Academy of Sciences, Lotników 32/46, 02-668 Warsaw, Poland

The progress in understanding of optical properties of quantum objects like quantum dots (QD) or nanowires (NW) was achieved as a consequence of developing of micro-photoluminescence and scanning microscope cathodo-luminescence techniques. Both techniques give the opportunity to study individual quantum objects or verify the local properties of extended two-dimensional systems. Unfortunately, the transmission of standard optical elements - even in the case of advanced glass microscopic objectives - is limited to the visible or near infrared region i.e. up to light wavelength ≈ 2μm. Thus, in experimental practice only the QD based on wide gap semiconductors are investigated by these methods. In this paper we compare the experimental results obtained in the regime of macro- and micro-photoluminescence (μ-PL) for narrow gap PbTe quantum dots with CdTe barriers. Here the mirror microscope objective with spectral range from 0.5 to 20 μm was used for light collection in the case of μ-PL measurements. Since the energy band gap of PbTe is 190 meV at 4 K, the PbTe/CdTe quantum dots are optically active in the mid infrared region 3÷5μm [1]. Moreover, because of the small effective mass ($m^*_c \approx 0.04$) and large dielectric constant ($\varepsilon_0 \approx 1000$) the quantum effects can be observed even for relatively big PbTe dots as compared to wide gap ones. Typical photoluminescence experiment (PL exited and collected from the top of the sample, laser spot diameter ≈300 μm) performed at 50 K on the sample containing PbTe quantum dots with average diameter ≈80 nm reveals the strong, ground state emission blue-shifted by about 60 meV as compared to the bulk PbTe due to quantum confinement. This emission exhibits wide, asymmetrical shape typical for the ensemble of QDs with distribution of spatial sizes. Moreover, in strong excitation conditions, we observe additional line with lower amplitude shifted ≈15 meV further in energy, which we attribute to the first exited state transitions in PbTe QDs [2]. When the photoluminescence is collected from the edge of the sample, internal structure of the ground state line becomes visible. It results from significant decrease of the number of quantum dots covered by the laser spot, as the thickness of the layer with quantum dots is of the order of 1 μm. Further limitation of the amount of excited dots was achieved using mirror microscope objective for photoluminescence measurements. In this case we clearly observe the separation of the PL signal into several sharp lines (see Figure). Such behavior is typical for the emission from individual quantum dots in wide gap III-V or II-VI semiconductors in the regime of μ-PL. This result opens the way for investigation of single nano-objects of narrow gap semiconductors.

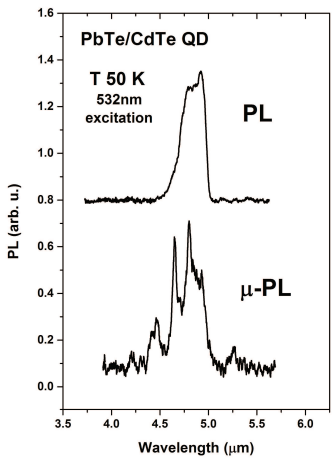

[1] Karczewski G. et al., Nanotechnology. **26**, 135601 (2015)
[2] Xu T. N. et. al., Phys. Rev. B 76, 155328 (2007).

Tuesday

Minority Carriers Spectra in Photovoltaic Heterojunction

B.A. Orlowski, A. Pieniazek, M. Galicka, K. Goscinski

Institute of Physics, PAS, Al. Lotnikow 32/48, 02-668 Warsaw, Poland

The paper describes model of photovoltage generation in semiconductors photovoltaic heterojunction [1,2]. This is based on the fundamental effects, how the carriers chaotic movement energy can create ordered photovoltaic effect. This effect of carriers entropy decrease is caused due to different relative change of semiconductors minority and majority carriers density obtained under proper heterojunction illumination. The correlations between the changes of basic parameters: minority and majority carriers concentration, Quasi Fermi levels, and corresponding to it change of photovoltage are presented. In photovoltaic effect the change of carriers concentration leads to corresponding change of quasi Fermi levels and it leads to the change of measured photovoltage value. The changes of carriers quasi Fermi levels at the opposite side of heterostructure are different for the same carriers electrons or for the holes. These differences of the quasi Fermi levels contribute to the value of generated photovoltage [2]. Proper choice of energy hν of illumination allows to generate carriers n = p in semiconductor of only one side of heterojunction and it allows to create different relative change of the density of states for minority and majority carriers. It allows as well to estimate contribution of both side of heterojunction to the measured photovoltage. The illumination intensity spectra of photovoltage are obtained as a continuous curves, due to continuous scan of quasi Fermi levels of minority carriers in related band gaps. The defect states of the band gaps disturb continuous scan of minority carriers quasi Fermi level. The photovoltaic intensity spectra allow to estimate energy position of the defect states related to the minority carriers. This will help to recognize and exclude parasitic defects of heterojunction. For general theoretical description the main set of equations [3] can be used.

The work was supported by the Polish National Centre for Research and Development (NCBiR) through the project PBS2/A5/34/2013 and by the
Polish National Science Centre (NCN) Grant No. DEC-2012/07/B/ST5/02484.

[1]. S.M. Sze, Semiconductor Devices, Physics and Technology, Second edition, John Wiley and Sons Inc., 2001.
[2]. B.A. Orlowski, A. Pieniazek, K. Goscinski, K. Kopalko, Acta Phys.Pol, 129, (2016) A-100.
[3]. L. Sosnowski, B. Orlowski, phys.stat.sol. (a) 3, 117 (1970).

Experimental and *ab-initio* study of electric field effects in GaN/AlN multi-quantum-wells at ambient and high hydrostatic pressure

D. Jankowski[1], A. Kaminska[1,2], P. Strak[3], K. P. Korona[4], J. Borysiuk[1,4], E. Grzanka[3], M. Beeler[5,6], K. Sakowski[3], E. Monroy[5,6], and S. Krukowski[3]

[1] *Institute of Physics, Polish Academy of Sciences, Al. Lotników 32/46, 01-142 Warsaw, Poland*
[2] *Cardinal Stefan Wyszynski University, College of Science, Department of Mathematics and Natural Sciences, Dewajtis 5, 01-815 Warsaw, Poland*
[3] *Institute of High Pressure Physics, Polish Academy of Sciences, Sokolowska 29/37, 01-142 Warsaw, Poland*
[4] *University of Warsaw, Faculty of Physics, Pasteura 5, 02-093 Warsaw, Poland*
[5] *Université Grenoble-Alpes, 38000 Grenoble, France*
[6] *CEA-Grenoble, INAC-PHELIQS, 17 av. des Martyrs, 38000 Grenoble, France*

The emission properties of nitride quantum heterostructures are strongly related to built-in electric fields caused by the spontaneous and piezoelectric polarizations characteristic for wurtzite structure. In this work we report on the correlation of ambient and high-pressure photoluminescence (PL) study of GaN/AlN multi-quantum-wells (MQWs) with *ab initio* calculations of their electronic (band structure, density of states) and optical properties (emission energies and their pressure derivatives, oscillator strength). The study was performed on GaN/AlN MQWs with various well thicknesses synthesized by plasma-assisted molecular-beam epitaxy on AlN-on-sapphire substrates. The quality of the structures was validated by X-ray diffraction (XRD) and transmission electron microscopy (TEM). PL measurements as a function of the hydrostatic pressure were conducted in a diamond anvil cell. The optical properties of the MQWs were strongly affected by the quantum confined Stark effect stemming from the polarization-induced internal electric fields. Therefore, the ambient pressure PL peak energies decreased by over 1 eV with QW thicknesses increasing from 1 nm up to 6 nm [1]. Furthermore, the respective PL decay times increased from about 1 ns up to 10^4 ns, exhibiting changes of dynamics characteristic of strong built-in electric field. The pressure coefficients of the PL energy were significantly reduced in the MQWs as compared to bulk AlN and GaN crystals, and they strongly depended on geometric factors such as the thickness of the wells and barriers.

The transition energies, their pressure dependences and oscillator strengths were modelled for tetragonally strained structures of the same geometry using a full tensorial representation of the strain in the MQWs under external pressure. The same MQWs were also simulated directly using density functional theory (DFT) calculations [2]. The good agreement between these two approaches and the experimental results indicates that the nonlinear effects induced by the tetragonal strain related to the lattice mismatch between the substrate and the MQWs are responsible for the drastic decrease of the pressure coefficients observed experimentally.

Acknowledgements: The authors acknowledge support of the Polish National Science Centre by grant No. DEC-2012/05/B/ST3/03113.

[1] A. Kaminska, P. Strak, J. Borysiuk, K. Sobczak, J. Z. Domagala, M. Beeler, E. Grzanka, K. Sakowski, S. Krukowski, and E. Monroy, *J. Appl. Phys.* **119**, 015703 (2016).
[2] P. Strak, K. Sakowski, A. Kaminska, and S. Krukowski, *J. Phys. Chem. Solids* **93**, 100 (2016).

Band Structure Modelling of GaAs-Based Quantum Dots Designed for Single Photon Sources at Telecommunication Wavelengths

Maciej Pieczarka, Andrzej Opala, Grzegorz Sęk

Laboratory for Optical Spectroscopy of Nanostructures, Division of Experimental Physics, Faculty of Fundamental Problems of Technology, Wrocław University of Science and Technology, Wrocław, Poland

Semiconductor quantum dots (QDs) have been demonstrated as ideal candidates for sources of single and entangled photons for quantum computation and quantum information processing. However, simple implementation of this kind of device as a QD embedded in a semiconductor matrix suffers from a poor extraction efficiency of the emitted photons. Therefore, additional structure modifications enhancing the photon extraction efficiency have been developed. Recently, a deterministic etching of GaAs microlenses on top of a chosen QD has been demonstrated as an approach of controlled and high yield of the obtained devices [1] However, the emission wavelength of these structures was below 1 μm, i.e. far of 1.3 or 1.55 μm required in fiber-based secure communication schemes. As for the long wavelength quantum communications the InAs-InP material system is explored and seems to be the most promising, the short to mid distance transmission systems could operate employing the GaAs-based quantum-dot single photon sources, in which the high extraction efficiency architecture is combined with the properly designed emitter.

In this work we model In(Ga)As/GaAs QDs designed for telecommunication wavelengths, to achieve the desired active region for microlens single photon source to be used in fiber-based technologies. We employ multi-band **k·p** modeling of a the three-dimensional QD structure, taking into account strain and piezoelectric fields. We explore different approaches to shift the QD emission to longer wavelengths, such as enlarged InAs dots on GaAs [2],InGaAs strain-reducing layer [3] or dot-in-a-well design [4]. We calculate the single particle states and analyse strain piezoelectric field profiles to find the most suitable design of such QDs. Additionally, we determine the optical transitions as well as the s-p shell splitting (in order to maximize the latter for the necessary good thermal stability of such sources), i.e. parameters crucial with respect to the exploitation in the microlens single photon source fabricated within the GaAs mature technology.

[1] Gschrey, M. et al. , *Nat. Commun.* **6**, 7662 (2015)
[2] Alloing, B. et al., *J. Appl. Phys*. **101**, 024918 (2007)
[3] Paul, M. et al., *Appl. Phys. Lett.* **106**, 122105 (2015)
[4] Kong, L. *J. Appl. Phys.* **101**, 126101 (2007)

Influence of Piezoelectric Field on the Confined States in Low-strain and Asymmetric InGaAs Quantum Dots

Maciej Pieczarka, Paweł Podemski, Grzegorz Sęk

Laboratory for Optical Spectroscopy of Nanostructures, Division of Experimental Physics, Faculty of Fundamental Problems of Technology, Wrocław University of Science and Technology, Wrocław, Poland

Low-indium content $In_{0.3}Ga_{0.7}As$/GaAs self-assembled quantum dots (QDs) are an unique kind of quasi-zero-dimensional nanostructures with large volume and in-plane shape asymmetry in comparison to well-studied epitaxial self-assembled InAs/GaAs QDs. They have been demonstrated to show atypical properties like ultra-small fine structure splitting and low degree of linear polarization of photons emitted from the surface (despite the distinct nanostructure in-plane asymmetry – lateral aspect ratio exceeding 2) [1]. Additionally, influence of quasi-zero-dimensional density of states within the wetting layer has been shown to have influence on the energy transfer in the structure [2].

Hereby, we present theoretical studies of the confined states in low-strain In(Ga)As quantum dots (QDs) of that type. The 8-band **k·p** model together with the continuum elasticity theory and piezoelectric fields were employed to calculate the confinement potential and the confined electron and hole eigenstates. It has been found that the piezoelectric potential affects the total confinement potential to such an extent that the hole eigenstates can get the spatial in-plane orientation orthogonal to the main axis of dot elongation. This influences both, qualitatively and quantitatively, many of the electronic and optical properties. We have obtained that due to the low-strain regime of these dots the second-order piezoelectric field does not change the field distribution significantly, whereas the linear piezoelectric field provides an additional confinement in the perpendicular direction to the elongation axis. This causes unusual polarization of photons emitted from the structure, where the linear polarization axis of light is perpendicular to the elongation direction of the QD, which is contradictory to the case of pure InAs QD case. Eventually, importance of the degree of the shape asymmetry or the dots' size, and differences between the low-strain (low-In-content) QDs and pure InAs dots formed in high strain conditions are discussed [3].

[1] A. Musiał et al., *Phys. Rev. B* **90**, 045430 (2015)
[2] P. Podemski, M. Pieczarka et al., to appear in *Superlattices and Microstructures* (2016)
[3] M. Pieczarka, G. Sęk, to appear in *Physica B: Condensed Matter* (2016)

*Financial support from the National Science Centre, Poland, grant 2014/15/D/ST3/00813 is acknowledged

Spatial Diffusion of Photogenerated Carriers in Coupled Quantum Well - Quantum Dot Structures

M. Pieczarka[1], M. Syperek[1], D. Biegańska[1], C. Gilfert[2], V. I. Sichkovskyi[2] J. P. Reithmaier[2], G. Sęk[1], and J. Misiewicz[1]

[1]Laboratory for Optical Spectroscopy of Nanostructures, Division of Experimental Physics, Faculty of Fundamental Problems of Technology, Wrocław University of Science and Technology, Wrocław, Poland
[2]Institute of Nanostructure Technologies and Analytics, Technische Physik, CINSaT, Universitaet Kassel, Germany

A semiconductor quantum well (QW) separated from a sheet of quantum dots (QDs) by a thin potential barrier can act as a large reservoir and transport channel of carriers that subsequently populate QDs' states. As it has been proposed previously, such a tunnelling scheme can be beneficial for high modulation rate QD-based semiconductor lasers [1] or memory devices [2], however, the carrier diffusion in this complex structure has not been investigated so far. In this approach one has to take into account not only a classical physical phenomenon related to spatial distribution of carriers, their concentration's gradient and mobility but also quantum mechanical processes accounted for tunnelling of carriers through a thin potential barrier and additional energy relaxation processes.

In this work we investigate spatial diffusion of photogenerated carriers in a system of coupled QW-QDs layers for a set of structures consisted of a 7-nm-wide or 15-nm-wide $In_xGa_{1-x}As$ QW separated from $In_{0.6}Ga_{0.4}As$ QDs by a 2-nm-wide barrier made of GaAs. The electronic coupling between QW and QDs is tailored by changes in indium content in the QW. [3]. In the experiment, the initial population of carriers is created locally by irradiating the structure with a laser beam, and a subsequent carriers' diffusion process at 5 K is monitored by spatially-resolved micro-photoluminescence technique with 2D imaging. The diffusion is considered in different regimes: varying the excitation density as well as the excitation wavelength, tuning it to the resonance with characteristic energies of the QW or the QD ensemble. Carrier diffusion coefficients are determined from analysis of spatially-resolved photoluminescence intensity profiles. The results show that (i) the diffusion process in the structure with QDs only and weakly-coupled QW-QDs system is quite similar pointing to a typical carrier redistribution process within 2D electronic states, and (ii) with increasing of the coupling strength between the QW and QDs the diffusion is slowing down. This latter effect can be related to (a) elongation of the carriers' transfer time between QW and QDs' states in respect to the interband relaxation time, (b) selectivity of the transfer process due to electronic coupling, and (c) effective trapping of carriers by QDs after the transfer process.

[1] T. Chung, G. Walter, and N. Holonyak Jr., *Appl. Phys. Lett.* **79**, 4500 (2001).

[2] A. Marent, T. Nowozin, M. Geller, and D. Bimberg, *Semicond. Sci. Technol.* **26**, 014026 (2011).

[3] M. Syperek, J. Andrzejewski, W. Rudno-Rudziński, G. Sęk, J. Misiewicz, E. M. Pavelescu, C. Gilfert, and J. P. Reithmaier, *Phys. Rev. B* **85**, 125311 (2012).

The work has been performed within grant No. 2013/10/M/ST3/00636 of the National Science Centre in Poland and the QuCoS project of Deutsche Forschungsgemeinschaft in Germany.

Comparison of localization effects in AlGaN layers and GaN/AlN multi-quantum-wells

K. Koronski[1], A. Kaminska[1,2], D. Jankowski[1], P. Strak[3], M. Sobanska[1], A. Wierzbicka[1], K. Klosek[1], Z. R. Zytkiewicz[1], E. Grzanka[3], M. Beeler[4,5], J. Borysiuk[1,6], K. P. Korona[6], P. A. Drozdz[3,6], K. Sakowski[3], E. Monroy[4,5], and S. Krukowski[3]

[1] *Institute of Physics, Polish Academy of Sciences, Al. Lotników 32/46, 01-142 Warsaw, Poland*
[2] *Cardinal Stefan Wyszynski University, College of Science, Department of Mathematics and Natural Sciences, Dewajtis 5, 01-815 Warsaw, Poland*
[3] *Institute of High Pressure Physics, Polish Academy of Sciences, Sokolowska 29/37, 01-142 Warsaw, Poland*
[4] *Université Grenoble-Alpes, 38000 Grenoble, France*
[5] *CEA-Grenoble, INAC-PHELIQS, 17 av. des Martyrs, 38000 Grenoble, France*
[6] *University of Warsaw, Faculty of Physics, Pasteura 5, 02-093 Warsaw, Poland*

A series of $Al_xGa_{1-x}N$ layers with $0.12 \leq x \leq 0.24$ and GaN/AlN multi-quantum-wells (MQWs) with QWs thicknesses between 1 and 6 nm was grown by molecular beam epitaxy. The samples were characterised by X-ray diffraction and transmission electron microscopy techniques.

Continuous wave spectra of the photoluminescence (PL) of these structures were measured at temperatures ranging from 15 to 300 K, and temperature behaviour of PL peak emission energies was analysed. It exhibited in general an S-shape behaviour characteristic for disordered systems, however some differences were observed between AlGaN layers and GaN/AlN QWs. In the AlGaN layers typical S-shape dependence was observed, reported also in other alloy systems including InGaN, which can be analysed within a model of potential fluctuations caused by alloy disorder [1]. In GaN/AlN MQWs systems the quantum well width fluctuations seem to constitute the main contribution to potential fluctuations, however the creation of AlGaN on GaN QWs and AlN quantum barriers interfaces has to be taken also into account. Additionally, the Quantum Confined Stark Effect (QCSE) influences emission properties of QWs. As a result the much more varied temperature behaviour of QWs PL peaks is observed. These conclusions are confirmed by theoretical analysis of the experimental data.

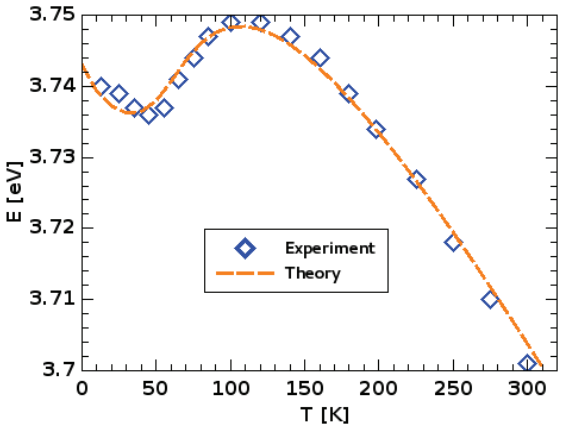

Fig. 1. PL energy dependence of $Al_{0.12}Ga_{0.88}N$ layer on temperature. Experimental data are marked with blue diamonds, whereas dashed line represents theoretical model of potential fluctuations.

Acknowledgements: The authors acknowledge support of the Polish National Science Centre by grant No. DEC-2012/05/B/ST3/03113.

[1] P. A. Dróżdż, K. P. Korona, M. Sarzyński, T. Suski, R. Czernecki, and D. Wasik, *Phys. Status Solidi B*, **253**, 284–291 (2016).

Magneto-optical properties of various excitonic complexes in CdTe and CdSe self-assembled quantum dots

J. Kobak [1], T. Smoleński [1], M. Goryca [1], J.-G. Rousset [1], W. Pacuski [1], A. Bogucki [1], K. Oreszczuk [1], P. Kossacki [1], M. Nawrocki [1], A. Golnik [1], J. Płachta [2], P. Wojnar [2], C. Kruse [3], D. Hommel [3], M. Potemski [4], and T. Kazimierczuk [1]

[1] *Institute of Experimental Physics, Faculty of Physics, University of Warsaw, Pasteura 5, 00-093 Warsaw, Poland*
[2] *Institute of Physics, Polish Academy of Sciences, al. Lotników 32/64, 02-688 Warsaw, Poland*
[3] *Institute of Solid State Physics, Semiconductor Epitaxy, University of Bremen, PO Box 330 440, D-28334 Bremen, Germany*
[3] *Laboratoire National des Champs Magnétiques Intenses CNRS-UGA-UPS-INSA-EMFL, 30942 Grenoble, France*

In this work we present systematic comparison of two systems of self-organized quantum dots (QDs): CdTe/ZnTe and CdSe/ZnSe.

To reduce the influence of the effects related to the specific growth technique and sample, we examined 7 structures fabricated in 3 molecular beam epitaxy laboratories. In order to determine statistically significant data and determine typical QDs properties we have investigated over 160 individual dots (Fig 1.). Based on such systematic, statistical approach we obtained various parameters describing magneto-optical properties of the excitonic complexes in CdTe/ZnTe and CdSe/ZnSe QDs.

In particular, we focused on difference between transition energy of neutral exciton (X) and biexciton (XX), fine-structure splitting, g-factor and diamagnetic shift. Studied quantities have been already measured for single QDs, but here we analyze experimental results in terms of average values taking into account variation across the large QD population (Fig. 1).

As a result we found statistically important correlations between key parameters describing internal structure of excitonic complexes.

[1] J. Kobak, *arXiv:submit/1486068* (2016).

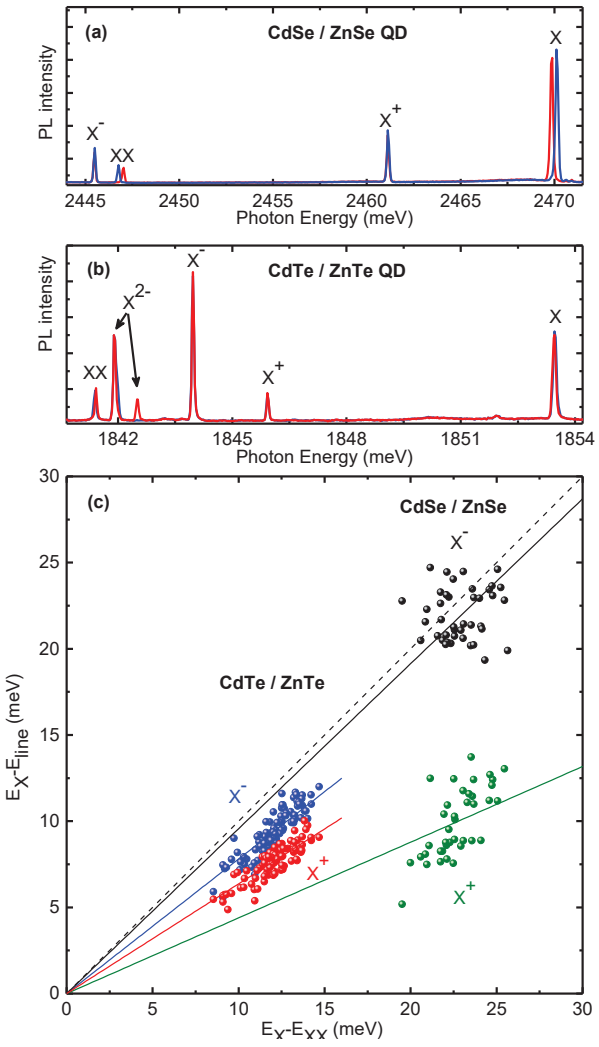

Fig. 1. Typical spectra of individual CdSe (a) and CdTe (b) QD contain several emission lines that form a characteristic pattern. Energy difference between the neutral exciton line and the charged exciton lines plotted versus the energy difference between the neutral exciton line and the biexciton line for CdTe/ZnTe (red and blue symbols) and CdSe/ZnSe (black and green symbols) QDs (c).

Tuesday

Emission from the axial heterostructure on ZnO microrod observed by cathodoluminescence

Agnieszka Pieniążek[1], Bartłomiej S. Witkowski[1], Henryk Teisseyre[1,2], Dawid Jarosz[1], Jarosław Domagała[1], Sławomir Kret[1], Anna Reszka[1], Michał Boćkowski[2], Adrian Kozanecki[1], Marek Godlewski[1,3] and Bogdan J. Kowalski[1]

[1]Institute of Physics, Polish Academy of Science, Al. Lotników 32/46, 02-668 Warsaw, Poland
[2] Institute of High Pressure Physics, Polish Academy of Sciences, Sokołowska 29/37, 01-142 Warsaw, Poland
[3]Cardinal S. Wyszyński University, ul. Dewajtis 5, 01-815 Warsaw, Poland

Optical properties of individual ZnO microrods (MRs) grown by hydrothermal method with axial $Zn_{1-x}Mg_xO/ZnO/Zn_{1-x}Mg_xO$ heterostructure grown (on top of the ZnO microrod) by plasma-assisted molecular beam epitaxy have been studied by spatially resolved cathodoluminescence (CL) spectroscopy and imaging. The CL spectroscopy has been combined with other techniques: X-ray diffraction and transmission electron microscopy, in order to get insight into the lattice parameters and local stress in ZnO-based heterostructures.

The CL depth profiling (as a function of the electron beam energy – accelerating voltage (AV)) has provided the data for analysis of the behavior of excitonic emission from ZnO MR, ZnO buffer, a single quantum well (QW) and $Zn_{1-x}Mg_xO$ barriers. The spectrum measured at AV=4 kV (Fig. 1a) contains a sharp peak located at 3.38 eV. It is related to recombination of excitons in the 4 nm ZnO single QW. The line at 3.35 eV is assigned to donor-bound excitons (DX) emission in ZnO MR. At the high-energy part of the spectrum a peak with maximum at 3.60 eV occurs, which originates from recombination in $Zn_{1-x}Mg_xO$ barrier. CL emission energy enables us to determine the Mg concentration x in the $Zn_{1-x}Mg_xO$ barrier as x=0.16.

We have also performed cross-sectional mapping of CL. An example of the results obtained by this method is shown in Fig. 1b. It clearly indicates the difference between CL emission from the ZnO MR, ZnO QW and $Zn_{0.84}Mg_{0.16}O$ barriers.

Our studies clearly confirmed the presence of axial heterostructure grown on ZnO MRs and enabled determination of its basic parameters: QW thickness and Mg concentration in the barrier from the CL transition energy.

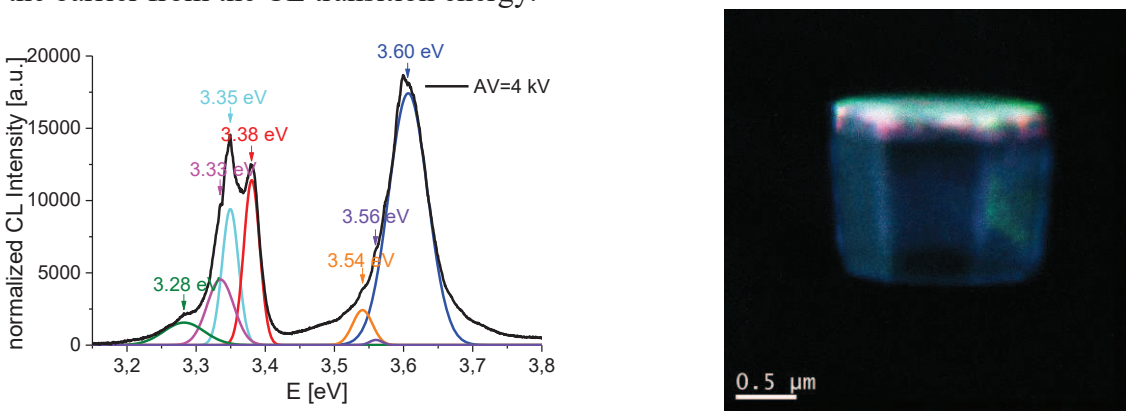

Fig. 1. a) CL spectrum taken at AV=4 kV, b) False colour CL image of ZnO MR with axial heterostructure: 3.60 eV – green, 3.38 eV – red, 3.35 eV – blue.

This work was partly supported by the Polish National Science Centre (NCN) Grant No. DEC-2012/07/B/ST5/02484 and No. 2014/13/B/St7/01773

Towards a quantum emitter of linearly polarized or entangled photon pairs at telecommunication wavelengths utilizing InAs-InP based nanostructures

P. Mrowiński [1], A. Somers[3], S. Höfling[3,4], J. P. Reithmaier[5], J. Misiewicz[1], G. Sęk[1]

[1] Laboratory for Optical Spectroscopy of Nanostructures, Division of Experimental Physics, Faculty of Fundamental Problems of Technology, Wrocław University of Science Technology, Wrocław, Poland
[3] Technische Physik & W. C. Röntgen-Center for Complex Material Systems, Universität Würzburg, Germany
[4] SUPA, School of Physics and Astronomy, University of St. Andrews, North Haugh, KY16 9SS St. Andrews, United Kingdom
[5] Institute of Nanostructure Technologies and Analytics, Technische Physik, Universität Kassel, Germany

Linearly polarized single photon source and entangled photon pair generation are both relevant elements for quantum communication protocols of secure data transmission (BB84, Ekert92). In this context, a deterministic quantum emitter based on a semiconductor platform and operating at telecommunication wavelengths of fiber-based transmission systems is strongly desired.

In that context, there have been investigated InAs/InGaAlAs/InP quantum dashes (QDashes) that emission wavelength overlaps with the 2nd and 3rd low-loss windows of silica fibers. Their application potential as non-classical emitters operated on both charged and neutral exciton and as a source of classically correlated photons from biexciton-exciton cascade has been demonstrated recently [1,2].

Optical properties of such nanostructures have been studied systematically showing their intrinsic properties like significant degree of linear polarization (DOLP) of emission and fine structure splitting (FSS) depending on the structures' morphology. The asymmetric confinement potential of QDashes involves both the valence band mixing and strong exchange interactions which give rise to well separated linearly polarized exciton transitions of unequal intensities. Further enhancement of DOLP up to 80% can be realized by a post-growth modification of the dielectric environment by forming asymmetric mesa structures. On the other hand, the exciton FSS tuning is feasible by the in-plane magnetic field in a range of ~300 μeV using 5 Tesla, reducing the zero-field value as large as ~220 μeV. Thus, the exciton bright-state crossing has been achieved in a range of 2-4 Tesla. Such tuning knob has a potential for obtaining a polarization entangled photons, as it was shown for inverted InAs/GaAs quantum dots [3]. The experimental data on high DOLP and reduced FSS has been collected for number of QDashes in a broad spectral range from below 1.3 to above 1.55 μm, and appeared to be a typical property of such nanostructures. Therefore, the single InAs QDashes might be considered as an active element of the future non-classical emission nanophotonic devices.

[1] Ł. Dusanowski, M. Syperek, P. Mrowiński, W. Rudno-Rudziński, J. Misiewicz, A. Somers, S. Höfling, M. Kamp, J. P. Reithmaier, and G. Sęk, Appl. Phys. Lett., 105, 021909 (2014);
[2] Ł. Dusanowski, M. Syperek, W. Rudno-Rudziński, P. Mrowiński, G. Sęk, J. Misiewicz, A. Somers, J. P. Reithmaier, S. Höfling, A. Forchel, Appl. Phys. Lett., 103, 253113 (2013)
[3] A. J. Hudson, R. M. Stevenson, A. J. Bennett, R. J. Young, C. A. Nicoll, P. Atkinson, K. Cooper, D. A. Ritchie, and A. J. Shields Phys. Rev. Lett. 993, 266802 (2007)

The study of thermal dissociation of acceptor-bound positively charged excitons in GaAs/$Ga_{1-x}Al_xAs$ quantum wells

L. Bryja [1], J. Jadczak [1], , K. Ryczko [1], M. Kubisa [1], J. Misiewicz [1], A. Wójs [2], F. Liu [3,4], D. R. Yakovlev [3,4], M. Bayer [3,4], C. A. Nicoll [5], I. Farrer [5], D. A. Ritchie [5]

[1] *Department of Experimental Physics, Wrocław University of Technology, Wrocław, Poland*
[2] *Department of Theoretical Physics, Wrocław University of Technology, Wrocław, Poland*
[3] *Experimentelle Physik 2, Technische Universität Dortmund, Dortmund, Germany*
[4] *Ioffe Physical-Technical Institute, Russian Academy of Sciences, St. Petersburg, Russia*
[5] *Cavendish Laboratory, University of Cambridge, Madingley Road, Cambridge, UK*

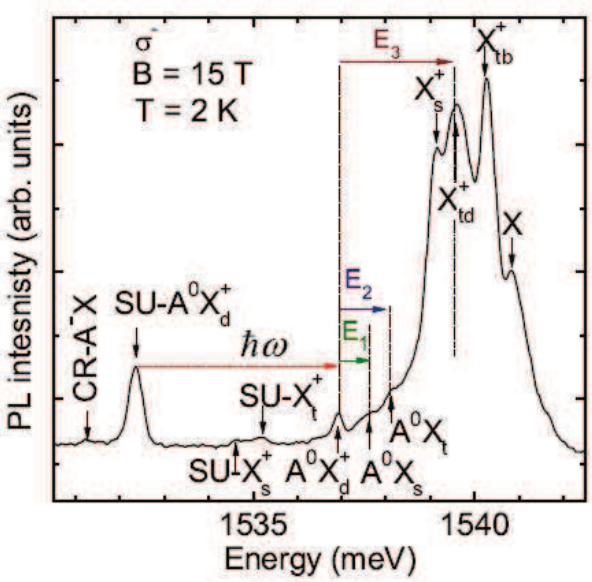

Fig. 1. Comparison of activation energies of dissociation processes with PL spectra.

The three-particle system of fermions, bound by Coulomb interaction are fundamental problem in nuclear, atomic and solid-state physics. Negative and positive trions (X^-=2e+h or X^+=2h+e), analogs of the negative hydrogen ion (H^-) and the positive hydrogen molecule (H^+_2), have been successfully detected in the two dimensional (2D) structures. All investigations of 2D trions were performed at low temperatures, mainly due to their small binding energy. However, temperature dependent emission investigations of trions, free or bound on impurities, may provide valuable information on trion physical properties.

Here, we study the thermal dissociation of free and acceptor-bound positive trions by measurements of temperature dependence of the integrated emission in high magnetic fields up to 17 T in superior quality GaAs quantum wells with 2D hole gas. Three dissociation processes are observed for the well-resolved hole cyclotron replicas ("shake-up") of positive trions bound to neutral acceptors in the hole spin-doublet state (SU-$A^0X^+_d$). To proof that the hole involved in the shake-up process is not bound by the Coulomb interaction to the charged A^0X^+ complex, we have performed numerical calculations of the valence band Landau levels in the Luttinger model beyond the axial approximation. The calculated value of the hole cyclotron energy agrees well with the experimental value of the energy separation of the AX^+ and SU-AX^+ lines determined from the PL spectra. At low temperatures, below 6 K, the dominant dissociation results in a free hole and the exciton bound to the neutral acceptor in the hole spin-singlet or -triplet state ($A^0X^+_d \rightarrow A^0X_s$+h or A^0X_t+h). At higher temperatures, above 9 K, the dissociation into the free positive trion and the neutral acceptor ($A^0X^+_d \rightarrow A^0+X^+$) predominates. From the temperature evolution of the integrated emission of free trion lines (X^+) we evaluated transition energy between two triplet trion states: dark (X^+_{td}) and bright (X^+_{tb}). The ionization energies of all detected dissociation processes are compared with the spectral positions of relevant radiative recombination lines and an excellent quantitative agreement was achieved.

Tuesday

Energy transfer in the system of CdSe Quantum Dots embedded in quasi-bulk ZnSe layers.

Łukasz Owczarczyk[1], Vitalii Yu.Ivanov[1], Joerg Debus[2], Janina C.Schindler[2], Maciej Wiatr, Grzegorz Karczewski and Marek Godlewski [1,3]

[1]*Institute of Physics Polish Acad. Sci., 02-668 Warsaw, Al. Lotników 32/46, Poland*
[2]*Experimentelle Physik 2, TU Dortmund, 44221 Dortmund, Germany*
[3]*Dept. Mathematics and Natural Sciences College of Science, Cardinal S. Wyszyński University, Warsaw, Poland*

Semiconductors planar nanostructures based on self-assembled Quantum Dots (QDs) exhibits an essential potential in application in novel photonics devices, for example, in integral optical circuits as emitters, amplifiers, ultrafast switchers etc. Development of technology of such devices requires a comprehensive study of electronic and optical properties of these nanostructures and of main mechanisms of energy and charge transfer processes between ensembles of QDs and the matrix material.

Ultrathin layers of CdSe have been deposited by ALE-MBE technique on the 1,5 μm thick (001) ZnSe/GaAs substrate and covered by a 400 nm thick ZnSe cap layer. Stress relaxation of in this material system leads to the formation of CdSe QDs with an average thickness about 2,6 nm. The lateral dimensions of the QDs are in the order of 30 nm. These nanostructures show high quantum efficiency of exciton emission in the green-yellow spectral region even at room temperature. Micro-PL measurements show intensive, very narrow emission lines characteristic for single QD (Fig.1).

One of the most remarkable property of the studied structures is a very effective transfer of optical excitation from the electronic states in the bulk ZnSe to the CdSe QDs. The effectiveness of emission from CdSe QDs exceeds the PL emission from the ZnSe bulk by three orders of magnitude. This fact indicates a strong coupling of the electronic states of the QDs with electronic states of the ZnSe matrix. PLE spectra of CdSe QD reveal two excitation mechanisms: excitation via ZnSe exciton states and direct excitation of excitons in QDs. In the first case the mechanism of energy transfer due to auto-ionization of excitons states in QDs, interacted with excitons in ZnSe matrix, seems to be possible. In detailed study of CdSe/ZnSe QD PLE spectra we observed characteristic features of the Fano resonance.

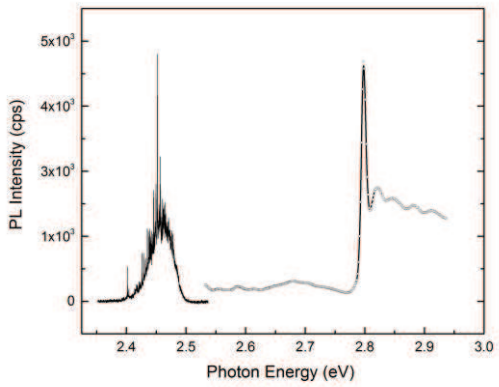

Fig.1. μ-PL and PLE spectra of QD CdSe/ZnSe at T=10K.

This work was supported in the part by Polish National Science Center by "Harmonia" Grant and by EAgLE EU Project FP7-REGPOT-2012-2013-1 (Project Number: 316014)

Application of Picosecond Magnetic Pulses For Inducing An Electron Motion In Bi-Layer Nanowires.

Tomasz Chwiej

AGH University of Science and Technology, al. Mickiewicza 30, 30-198 Carcow, Poland

We consider an interaction of single electron confined in a piece of nanowire with a short magnetic pulse of time duration between a few up to a few tens of picoseconds [1]. If the external confinement of considered nanowire is prepared as a double inverted heterojunction based on e.g. InAs/InGaAs or AlGaAs/GaAs materials and its width in growth direction is quite large (30 nm) then due to unequally doping of the $\delta -$ layers placed below and above the well, two tunnel coupled transport layers are formed inside. For such specific confinement, the vertical components of an electron's wave functions can be easily hybridized in magnetic field. If static magnetic field is directed perpendicularily to both, the wire axis and to the transport layers, such hybridization transforms single minima in the lowest energy subbands E(k) into two deep lateral minima what introduces negative dispersion relation into E(k) and can be experimentally detected in standard conductance measurements [2]. We have found another interesting regime the effect of magnetic hybridization in the bi-layer nanowire can be used for, namely, to change the electron's motion energy in short period of time [3]. This results directly from the Faraday law $\partial\vec{B}/\partial t = -\nabla \times \vec{E}$ which predicts the formation of temporary electric field with opposite directions in both the upper and lower layers when the magnetic pulse pierces the nanostructre. Based on the results of computer simulations we have found that for a symmetric confinement in vertical (growth) direction, both parts of a single electron wavepacket move in nanowire in opposite directions according to local electric field. However, if the confinement is nonsymmetric, the majority of the electron density is accelerated into arbitrarily chosen direction dragging simultaneously the minority against the local electric field in second layer what results in a coherent motion of both parts of an electron wavepacket. In our work we present a simple theoretical model taking into account the magnetic hybridization effect and show how its magnitude depends on three factors: i) the degree of the confinement asymmetry, ii) efective mass of an electron and, iii) the time duration of the magnetic pulse. We also show how this new effect combined with the Coulomb Blockade mechanism can be utilized as a buliding block of the magnetically driven current valve.

[1] C. Vicario, C. Ruchert, F. Ardana-Lamas, P. M. Derlet, B. Tudu, C. P. Hauri, *Nat. Photon.* **7**, 720 (2013).
[2] T. Chwiej, *Physica E* **77**, 169 (2016).
[3] T. Chwiej, *arXiv:1601.03880* (2016).

Effect of substrate orientation and external electric field on the bright exciton splitting in nanowire quantum dot molecule

M. Świderski [1] and M. Zieliński [1]

[1] *Institute of Physics, Nicolaus Copernicus University, Grudziadzka 5, 87-100 Torun, Poland*

In this work we use atomistic tight-binding approach to study excitonic fine structure of nanowire quantum dot molecule formed by a double InAs disk-shaped nanowire quantum dot [1] embedded into a [001] or [111] oriented InP nanowire. We show that in a case of identical quantum dots, the quantum dot molecule inherits the symmetry properties of individual quantum dots. For example, in case of identical height quantum dots we don't observe the bright exciton splitting [2]. Next, we change the height of one of quantum dots. For the [001] grown quantum dot molecule this effectively lowers the overall symmetry from D_{2d} to C_{2v} and triggers the bright exciton splitting. On the contrary, for nanowire quantum dot molecules grown on [111] direction, despite different heights of quantum dots forming a molecule the double quantum dot retains its high C_{3v} symmetry. This again indicates no fine structure splitting. We complete our analysis by studies of the external electric field: in the case of [001] substrate the vertical electric field cancels the bright exciton degeneracy, whereas [111] quantum dot molecules are immune to the vertical field and show no fine structure splitting.
Finally, we conclude that nanowire quantum dot molecules combine the advantages of double quantum dots, such as suppression of spin relaxation [3] and wavelength tenability [4], with qualities on nanowire quantum dots [1] such as highly reduced fine structure splitting [2].

[1] M. T. Borgström, V. Zwiller, E. Müller, and A. Imamoglu, Nano Lett. 5(7) (2005).
[2] R. Singh, G. Bester, Phys. Rev. Lett. 103, 063601 (2009).
[3] A. Pfund, I. Shorubalko, K. Ensslin, and R. Leturcq, Phys. Rev. Lett. 99, 036801 (2007).
[4] A. N. Vamivakas, C. Y. Lu, C. Matthiesen, Y. Zhao, S. Falt, A. Badolato, and M. Atatuere, Nature 467, 297 (2010).

Numerical simulations of the Coulomb blockade microscopy experiments: probing the local properties of the planar quantum dots using the scanning gate technique

Elżbieta Wach and Bartłomiej Szafran

AGH University of Science and Technology,
Faculty of Physics and Applied Computer Science,
al. Mickiewicza 30, 30-059 Kraków, Poland

Scanning gate microscopy (SGM) is relatively new technique for probing the quantum transport properties [1, 2]. The electrical transport of the nanodevice is probed with a metalized tip of the atomic force microscope used as a floating gate electrode. It scans the nanostructure and couples capacitively to the sample. The tip-induced electrostatic potential perturbs locally the two-dimensional electron gas (2DEG) buried shallow beneath the semiconductor surface. The perturbation modifies the potential landscape seen by the electrons at the Fermi surface and thus the conductance of the system can be changed.

The conductance monitored as a function of the tip position by the SGM technique allows to obtain some important experimental data on the charge transport properties through the nanodevices, including conditions of the current flow through the quantum dots [3-5]. The current flows only in the conditions of the transport window, i.e. lifting the Coulomb blockade.

We simulate the phenomena that occur during the current transport measurements in the semiconductor heterostructures containing quantum dots defined within the two-dimensional electron gas with the perturbation introduced by the metalized tip of the atomic force microscope. Our numerical models are based on the exact diagonalization for the confinement potential and also the DFT calculations to simulate the screening effect of the tip-induced potential by 2DEG. The effect is crucial for describing the scanning gate experiments. We show how this phenomenon decreases the range of the tip-induced potential, which becomes short-ranged effectively.

We determine the considered system properties by inspecting the maps of the current versus the position of the tip and the energy shifts of the confined particles caused by the tip. The mentioned properties include, for example, the unperturbed charge density in the dot and the form of the effective tip-induced potential seen by the electrons in the nanostructure.

[1] D. K. Ferry, A. M. Burke, R. Akis, R. Brunner, T. E. Day, R. Meisels, F. Kuchar, J. P. Bird, B. R. Bennet, *Semicond. Sci. Technol.* **26**, 043001 (2011).
[2] H. Sellier, B. Hackens, M. G. Pala, F. Martins, S. Baltazar, X. Wallart, L. Desplanque, V. Bayot, S. Huant, *Semicond. Sci. Technol.* **26**, 064008 (2011).
[3] M. Huefner, B. Kueng, S. Schnez, K. Ensslin, T. Ihn, M. Reinwald, W. Wegscheider, *Phys. Rev. B* **83**, 235326 (2011).
[4] A. E. Gildemeister, T. Ihn, M. Sigrist, K. Ensslin, D. C. Driscoll, and A. C. Gossard, *Phys. Rev. B* **75**, 195338 (2007).
[5] P. Fallahi, A. C. Bleszynski, R. M. Westervelt, J. Huang, J. D. Walls, E. J. Heller, M. Hanson, A. C. Gossard, *Nano Lett.* **5**, 223 (2005).

Individual Cd(Se,Te)/ZnSe Quantum Dots: Beyond the Crossroad of Se and Te Based Quantum Dot Systems

M. Ściesiek[1], J. Suffczyński[1], W. Pacuski[1], M. Parlińska-Wojtan[2], T. Smoleński[1], P. Kossacki[1], and A. Golnik[1]

[1] *Institute of Experimental Physics, Faculty of Physics, University of Warsaw, Pasteura 5 St., 02-093 Warsaw, Poland*
[2] *Institute of Nuclear Physics, Polish Academy of Sciences, Radzikowskiego 152 St., 31-342 Kraków, Poland*

Epitaxial Cd(Se,Te) Quantum Dots (QD) in ZnSe barrier exhibit typically a very high spectral density, which hinders investigation of a single dot photoluminescence.[1] Here, we design, grow and study individual Cd(Se,Te)/ZnSe QDs of low spectral density of emission lines achieved by implementation of a Mn-assisted growth.[2]

A large variation of parameters being a measure of electron-hole (*e-h*) wavefunctions overlap: exciton (X) radiative lifetime τ_X (280–620 ps), splitting between dark and bright exciton δ_0 (1.5–2.5 meV) and exciton-biexciton energy difference (3 meV $\leq \Delta E_{X-XX} \leq$ 26 meV) is found in the statistics of QDs. Such behavior, untypical for binary II-VI QDs is attributed to a strong variation from dot to dot of electron-hole (*e-h*) separation due to a different degree of localization of electrons and holes in, respectively, CdSe and CdTe rich QD regions. A significant correlation between the exciton radiative decay rate ($1/\tau_X$) and the δ_0 (see Fig. 1a) confirms that dominating contribution to the δ_0 comes from a short-range component of the *e-h* exchange interaction. In contrary to a simple expectation, the Cd(Se,Te)/ZnSe QDs excitonic Landé factor g_X is smaller than Landé factors found previously in case of both, CdSe/ZnSe QDs and CdTe/ZnTe, binary type QD systems (see Fig. 1b). Additionally, a distinct and so far not observed for II-VI QDs, dependencies of the g_X and of the fine structure exchange splitting δ_1 on the ΔE_{X-XX} are found: the g_X increases, while the δ_1 decreases with the increasing ΔE_{X-XX}, that is with the increasing *e-h* wavefunctions overlap (see Fig. 1b). The obtained results demonstrate that values of the δ_1 and of the Landé factor in the studied QDs are dictated primarily by the electron and hole respective spatial shift and wavefunctions overlap.

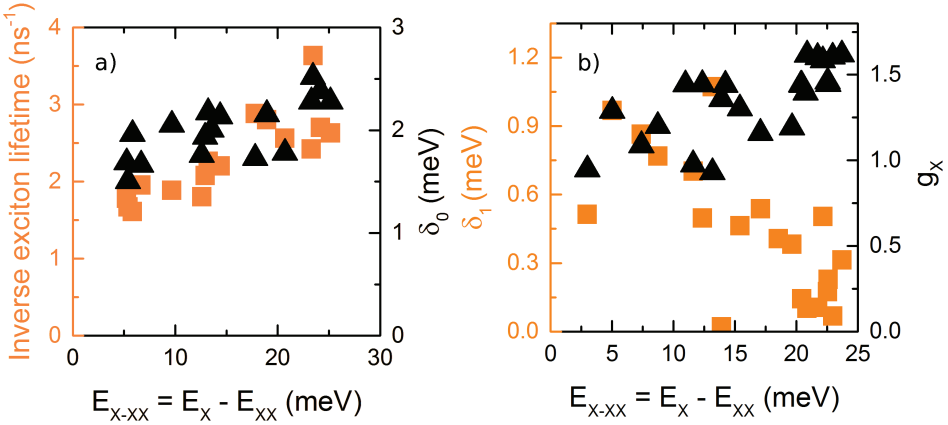

Figure 1: a) Inverse exciton lifetime and δ_0 splitting between bright and dark exciton as a function of energy difference between exciton and biexciton E_{X-XX}. b) Fine structure splitting δ_1 and exciton Landé factor g_X as a function of E_{X-XX}.

[1] A. A. Toropov *et al.*, Appl. Phys. Lett. 89, 123110 (2006).
[2] M. Ściesiek, J. Suffczyński, W. Pacuski, M. Parlińska-Wojtan, T. Smoleński, P. Kossacki, and A. Golnik, arXiv:1623.00313.

Morphology and stability of the C/BN and SiC/GaN interfaces based on *ab initio studies*

M. Sznajder[1], N. Hrushka[1], and J. A. Majewski[2]
[1] *Faculty of Mathematics and Natural Sciences, University of Rzeszów, Pigonia 1, 35-959 Rzeszów, Poland*
[2] *Faculty of Physics, University of Warsaw, ul. Pasteura 5, 02-093 Warszawa, Poland*

Excellent physical properties of boron nitride (c-BN, h-BN) are crucial for technological development of micro-, or nanoelectronic devices, high-temperature ceramic applications, protective coatings, and optoelectronic devices operating in the visible/ultra-violet range [1-3]. The C/BN heterostructures are of importance for these applications, as well as the knowledge on the microscopic details of interfaces' morphology and stability.

In this report, we discuss diamond/BN and 3C-SiC/GaN heterostructure junctions as a prototype of the interfaces between B/C, N/C, Ga/C, Ga/Si and N/Si atomic layers. Our studies are based on *ab-initio* DFT calculations. In the studied heterostructures, we concentrate on the two important growth directions, i.e., [001] and [111] ones. In both cubic directions the abrupt C/N and C/B interfaces contain 'oversaturated' or 'undersaturated' tetrahedral bonds [4]. Such bond heteropolarity results in macroscopically charged interfaces that are mostly energetically unstable and should undergo various reconstructions [4]. We propose some reconstruction patterns, which involve substitution of certain number of either III- or V-valency atoms by carbon atoms in the epitaxially grown BN monolayers, as well as one mixed atomic layer (N/C or B/C), depending on the crystallographic orientation. We employ both a slab and the non-stoichiometric super-lattice approaches by creating super-cells having up to 104 atoms, with lateral 2x2 unit cell. The computations of the total energies of the abrupt and reconstructed interfaces, and laterally averaged distributions of the total potential and charge enabled to find the preferred bonding configurations, as well as the resulting valence electron charge densities in the systems studied. Comparison of the obtained results in the slab approach for C/c-BN, interfaces in the [111] direction with the respective ones for the crystallographically equivalent 3C-SiC/GaN interfaces shows the preferred reconstructed C-Ga(B) interface type. The energy gain resulting from the charge compensation by C atoms mixed in III-valency atom layer is up to 2.8 eV/atom. The computed formation enthalpies, valence band offsets (VBO's), induced interface charges, and electric fields provide microscopic knowledge about C/nitride and SiC/nitride interface morphology.

Finally, we investigate the role of van der Waals interaction between the graphene monolayer on h-BN and c-BN in the inter-planar binding energy.

[1] G. H. Lee, Y. J. Yu, X. Cui *et al*., *ACS Nano* **7**, 7931 (2013).
[2] Z. Liu, Y. Gong, W. Zhou, et al. *Nat. Commun*. **4**, 2541 (2013).
[3] H. X. Jiang and J. Y. Lin, *Semicond. Sci. Technol*. **29** 084003 (2014).
[4] M. Grabowski, M. Sznajder and J.A. Majewski, *Acta Phys. Pol. A*, **129**, 138 (2016).

Temperature-dependent Photoluminescence of Nonpolar ZnO/ZnMgO Quantum Wells

E. Pozingytė[1], A. Rimkus[1], S. Paurazaitė[1], S. Tumėnas[1] R. Nedzinskas[1], L. Chang[2], M. M.C. Chou[2]

[1] *Center for Physical Sciences and Technology, A. Goštauto 11, Vilnius, Lithuania*
[2] *National Sun Yat-Sen University, Lienhai Rd. 70, Kaohsiung, Taiwan (ROC)*

Zinc oxide has drawn great attention recently for its possible applications in a short wavelength optoelectronics. ZnO has a wide direct band-gap of 3.37 eV at room temperature, which also can be tuned towards higher energies by alloying it with MgO [1,2]. In this work, we compared nonpolar m- $[10\bar{1}0]$ and a- $[11\bar{2}0]$ ZnO/ZnMgO QWs grown by molecular beam epitaxy on a lattice-matched (100) and (010) $LiGaO_2$ substrates. Temperature dependent (3–300 K) photoluminescence (PL) spectroscopy was used to study optical properties of QW structures with a particular interest in polarized optical response.

Low temperature PL spectra of m-ZnO/ZnMgO QW show three distinct optical features (see Fig. 1 a). High-energy feature spanning the region 3.5–3.42 eV is associated with the excitonic transition from ZnO/ZnMgO QWs. Then a sharp peak at 3.3 eV is related to the near-band emission from ZnO buffer layer. In the low photon energy region, a broad "green" band centred at 2.5 eV is due to the defects. An optical response from a-ZnO/ZnMgO QW merges with a PL from ZnO epilayer (see Fig. 1 b). It was found that the relative intensity of established features varies with excitation power density due to the saturation of defects for both QW structures. Furthermore, a significant in-plane optical anisotropy was found for both nonpolar QWs and is discussed in detail.

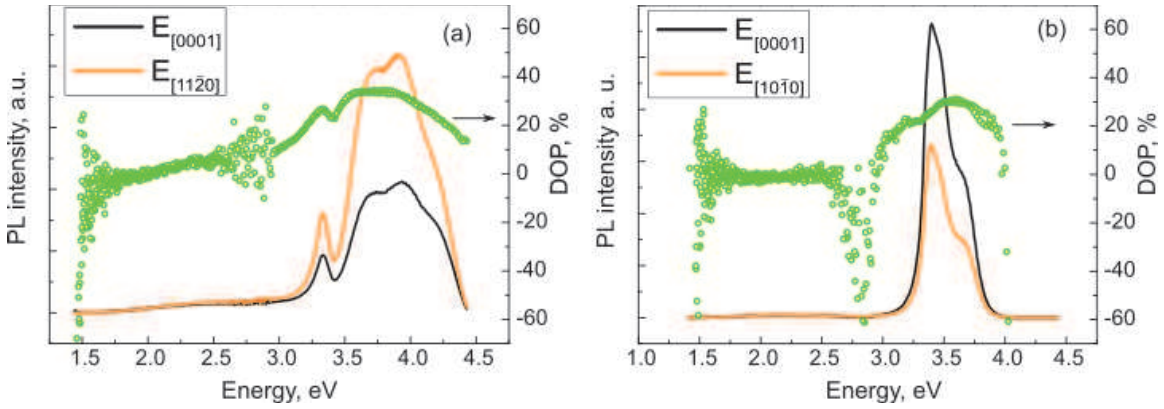

Figure 1: Polarized PL emission and degree of polarization (DOP) of (a) m-ZnO/ZnMgO QW and (b) a-ZnO/ZnMgO QW.

[1]M. M. C. Cou, D.-R. Hang, C. Chen, Y.-H. Liao, *Thin Solid Films* **519**, 3627-3631 (2011).
[2] J. Chen, W. Z. Shen, N. B. Chen, D. J. Qiu, H. Z. Wu, *J. Phys. Condens. Matter* 15(**30**), L45 (2003).

Influence of superlattice period thickness on strain distribution in GaN/AlN multi-quantum-wells

A. Wierzbicka[1], A. Kaminska[1,2], J. Borysiuk[1], D. Jankowski[1], K. Koronski[1], M. Sobanska[1], K. Klosek[1], Z. R. Zytkiewicz[1]

[1] *Institute of Physics, Polish Academy of Sciences, Al. Lotników 32/46, 01-142 Warsaw, Poland*
[2] *Cardinal Stefan Wyszynski University, College of Science, Department of Mathematics and Natural Sciences, Dewajtis 5, 01-815 Warsaw, Poland*

Aim of this work was to study influence of the thickness of superlattice period on strain distribution in GaN/AlN multi-quantum-wells (MQWs) by X-ray diffraction (XRD), photoluminescence (PL) and transmission electron microscopy (TEM) techniques. A series of samples consisting of 10 periods of GaN/AlN MQWs were grown by plasma-assisted molecular beam epitaxy (PAMBE) on 1μm-thick (0001)-oriented AlN-on-sapphire templates. The MQWs were grown on 500 nm thick Si-doped AlN layer, and were capped by 50 nm of AlN (also Si-doped). The widths of GaN quantum wells and AlN quantum barriers were equal. For different samples they varied from 1 nm up to 4 nm.

XRD measurements were used to examine structural properties of GaN/AlN superlattices in lateral and vertical directions as well as strain distribution. First, for each sample two types of measurements were done: $2\theta/\omega$ scans of 0002 symmetrical reflection and reciprocal space maps of the $\bar{1}\bar{1}24$ asymmetrical reflections. It allows calculation of the accurate values of lattice parameters of supperlattices and substrates. High-resolution XRD maps show that for the narrowest GaN/AlN MQWs *a*-lattice parameter is similar to Si-doped AlN layer lying directly under the MQW, so it is almost fully strained. We observed that with increasing of GaN/AlN MQWs width the average superlattice *a* in-plane lattice parameter increases to values close to GaN lattice parameter *a*. The structures are partially relaxed. Next the $2\theta/\omega$ scans were simulated using Panalytical X'Pert Epitaxy software utilizing dynamical diffraction theory. We observed the interference oscillations, so-called thickness fringes from experimental and theoretical data coming from MQWs. The fit of these two curves allows us to determine thicknesses of the GaN quantum wells and AlN barriers and the quality of the interfaces. The blurring of the interfaces causes deviations between experimental and calculated data, so TEM measurements help to check the quality of the interfaces in MQWs.

Photoluminescence spectra show that due to Quantum-Confined Stark Effect (QCSE) the PL peak energies of the MQWs decreased with increasing of the width of the AlN quantum barriers and GaN quantum wells.

Acknowledgements: The authors acknowledge support of the Polish National Science Centre by grant No. DEC-2012/05/B/ST3/03113.

A transition from 0D to Extended Ground State in InP-Substrate-Based Coupled Quantum Well - Quantum Dash System at 1.55 μm

M. Syperek,[1] J. Andrzejewski[1], A. Maryński[1], W. Rudno-Rudziński[1], J. Misiewicz[1], S. Hein[2], S. Höfling[2], and G. Sęk[1]

[1]*Laboratory OSN, Division of Experimental Physics, Faculty of Fundamental Problems of Technology, Wrocław University of Science and Technology, Poland*
[2]*Technische Physik, Univ. of Würzburg and Wilhelm-Conrad-Röntgen-Research Center for Complex Material Systems, Am Hubland, Würzburg, Germany*
[3]*School of Physics and Astronomy, University of St. Andrews, St. Andrews, UK*

The concept of a coupled quantum-well quantum dot/dash system (QW-QD/QDash) remains a challenging issue in the context of its band structure engineering desired for specific applications. In the case of QW-QD/QDash-based lasers one of the problem is to preserve a quasi-0D-like character of the gain medium that results from a full 3D confinement of carriers. However, in the case of some QD/QDash memory applications there is required a weaker confinement in the dot allowing out tunnelling of carriers into the neighbouring QW. In this work we investigate a system based on InP substrate in which both scenarios can be realized by tailoring the well width (d_{well}).

The system under study consists of $In_{0.53}Ga_{0.47}As$ QW separated from a layer of InAs QDashes by 1.7-nm-wide InAlAs barrier. Four structures were investigated with d_{well} equal 4.5, 5.5 and 6.5 nm, and a reference structure with QDashes only. In all cases, the ground state (GS) emission of the entire system occurs at 1.55 μm. The electronic coupling is examined at T = 5 K by combination of various optical spectroscopy techniques, with the major role of time-resolved photoluminescence, supported by eight-band **k·p** calculations of the coupled system's band structure.

The experimental results show that with increasing d_{well} the electronic coupling between the QW and QDash parts at the GS increases considerably, as it is viewed by elongation of the PL lifetime (τ_{PL}). For d_{well}=4.5 nm the $\tau_{PL}\approx$1.8 ns is comparable with the one registered for the reference structure that resembles the Coulomb-correlated electron-hole recombination lifetime in quasi-0D confinement of a QDash. However, when the d_{well} increases to 5.5 nm, and 6.5 nm, the τ_{PL} increases up to ~4.9 ns, and ~9.7 ns, respectively. This indicates an extension of the GS of either electrons or holes from QDashes to the well. A similar effect has been observed in (In,Ga)As/GaAs coupled QW-QDs system [1] where mainly electrons have tendency to be smeared over QW and QD potential. For the system under study a reversed trend is expected as confirmed by the theoretical calculations: the electrons are strongly confined in dahs whereas the holes are leaking out into the well.

This experimental founding opens the rout towards exploration of an electron spin memory in a coupled system at 1.55 μm where initially addressed electron spin state through creation of a positively charged exciton can be left in the dash while holes can be removed away due to their tunnelling into a QW.

[1] M. Syperek, J. Andrzejewski, W. Rudno-Rudziński, G. Sęk, J. Misiewicz, E. M. Pavelescu, C. Gilfert, and J. P. Reithmaier *Phys. Rev. B* ***85****, 125311 (2012).*

The work has been supported by the grants No. 2013/10/M/ST3/00636 and 2011/02/A/ST3/00152 of the National Science Centre in Poland.

Room Temperature Carrier Dynamics in the W-type GaInSb/InAs/AlSb Quantum Well Structure Emitting in Mid-Infrared Spectral Range

M. Syperek [1], K. Ryczko[1], R. Weih[2], M. Dyksik[1], M. Kamp[2], S. Höfling[2,3], J. Misiewicz[1], and G. Sęk[1]

[1] *Laboratory OSN, Division of Experimental Physics, Faculty of Fundamental Problems of Technology, Wrocław Univ. of Science and Technology, Wrocław, Poland*
[2] *Technische Physik, University of Würzburg and Wilhelm-Conrad-Röntgen-Research Center for Complex Material Systems, Würzburg, Germany*
[3] *School of Physics and Astronomy, University of St. Andrews, St. Andrews, UK*

The type II W-design quantum wells (QW) based on InAs/GaInSb broken gap materials' combination have been developed as a key element of the gain medium of interband cascade lasers (ICLs) emitting in mid-infrared spectral range [1]. The ICLs have been proven to have has a huge application potential in optical gas sensing of medically and environmentally relevant gasses, and overwhelming in some performances the systems based on quantum cascade lasers. In spite of that, some of the properties of the active region in this experimentally demanding spectral range are still not well known, and this concerns also carrier dynamics, on which only a very initial work has been reported [2]. In this work, we use experimentally challenging pump-probe technique utilizing pJ pulses in order to study at carrier dynamics at room temperature in the W-type QWs to get a set of characteristic laser-performance-related time constants.

The transient reflectivity (TR) experiment based on a pump-probe scheme has been used in order to test carrier relaxation dynamics in such a W-design QW structure. The QW is excited by a train of 140 fs-long pulses with the photon wavelength of 830 nm, and ~13.2 ns pulse-to-pulse distance that produces certain carrier population at the higher energy states in the well. Subsequent carrier relaxation is tested by a train of 200 fs-long probe pulses that are tuned to the ground state (GS) emission of the QW occurring at 2.5 μm. The TR signal reveals two characteristic processes: (i) population of the GS hindered in the rise of the TR signal, and (ii) its subsequent depopulation represented by the decay of the transient reflectivity amplitude. The measured TR rise time is 2.3±0.2 ps and it is supposed to be related to the longitudinal phonon-assisted relaxation channel since the initial population of photo-injected carriers is insufficient for the Auger-type relaxation. The GS depopulation occurs via two processes of a significantly different time scale. The long-lasting one in the nanosecond range is attributed to the radiative recombination of spatially separated electrons and holes - expected for the W-type QW structure. However, the origin of a short decay component of 240±0.2 ps time constant is not clear and has not been observed for such type of QWs. It can be attributed to the carrier escape process from the QW GS to some localized states at the InAs/GaInSb interfaces caused by the intermixing effect, which has been predicted previously [3].

[1] I. Vurgaftman et al. *Nat. Commun.* **2**, 585 (2011).
[2] S. W. McCahon et al. *Appl. Phys. Lett.* **68**, 2135 (1996).
[3] M. Motyka et al. *Nano Research Letters* **10**, 471 (2015).

Work supported by the iCspec project of the European Union's Horizon 2020 research and innovation programme under grant agreement No 636930 and by the National Science Centre of Poland within Grant No. 2014/15/B/ST7/04663.

Natural quantum dots formed in GaN nanowire-UV-LED

E. M. Łacińska[1], P. Kaźmierczak[1], K. P. Korona[1], M. Sobańska[2], K. Kłosek[2], Z. R. Zytkiewicz[2], A. Wysmołek[1]

[1]Faculty of Physics, University of Warsaw, Pasteura 5, 02-093 Warsaw, Poland
[2]Institute of Physics, Polish Academy of Sciences, Al. Lotników 32/46, 02-668 Warsaw, Poland

Semiconductor nanowires provide a number of possibilities for the design of various sophisticated heterostructures and consequently enable development of advanced electronic and optoelectronic devices. They are both efficient light harvesters and emitters, which makes them suitable building blocks for production of solar cells as well as light emitting diodes (LED) and lasers. It is known that incorporation of quantum wells, which enable carrier confinement, improves the efficiency of light emitting devices.

In this communication we present our research on GaN-nanowire-UV-LED with built-in quantum wells. Our sample is grown by plasma-assisted molecular beam epitaxy (PAMBE) on n-type Si, and consists of two sections. The bottom section are n-type AlGaN nanowires with AlN composition gradient from 0 to 15 %. The sample's top part consists of fully-coalesced p-type $Al_{0.2}Ga_{0.8}N$ nanowires forming a p-n junction. Three GaN quantum wells with width of 3,5 nm separated by 15 % AlGaN barriers are built in the active part of the structure.

The sample was studied using electroluminescence and microphotoluminescence spectroscopy. As expected, electroluminescence measurements showed bright room-temperature emission originating from quantum wells near energy of 3,25 eV. Low-temperature photoluminescence spectra obtained for different excitation power are shown in Fig. 1. They are dominated by emission bands originating from AlGaN barriers with different Al concentrations observed at energies of 3,5 – 3,65 eV, as well as GaN buffer emission clearly observed at 3,47 eV. In the low energy part of the spectrum less intensive emission which could be assigned to GaN/AlGaN QWs is observed. Interestingly enough, a number of sharp lines with halfwidths of about 0,5 meV appear at random energies in the middle part of the spectrum. As shown in Fig. 2, these lines are clearly visible for rather small excitation power and saturate for high power excitation. We propose that these sharp emission lines originate from natural quantum dots formed within our structure. The QWs form disks of 3,5 nm thickness and 50 nm diameter. In such disk, even small potential fluctuation is enough to reduce space available for electrons to quantum dimensions and create a quantum dot. Fluctuations can be due to AlGaN barrier composition, defects or strain caused by overgrowth of $Al_{0.2}Ga_{0.8}N$ layer.

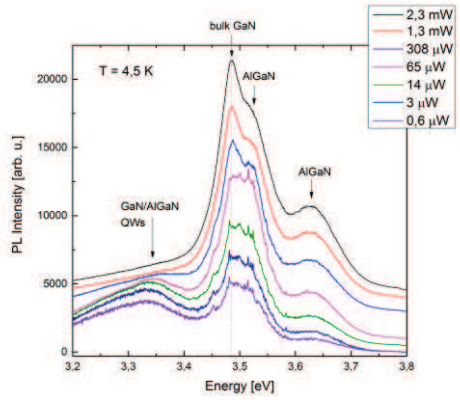

Fig. 1. Photoluminescence spectra obtained for different excitation power.

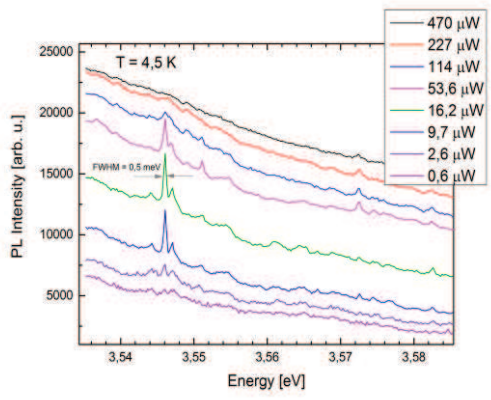

Fig. 2. Photoluminescence spectra with sharp emission lines measured for different excitation power.

Single CdSe quantum dot containing a single copper ion

J. Mikulski[1], P. Wojnar [1]Ł. Kłopotowski[1], T. Smoleński[2], T. Kazimierczuk[2], B. Sikora[1], K. Fronc[1], J. Kossut[1]

[1] *Institute of Physics, Polish Academy of Sciences, Al. Lotników 32/46, 02-668 Warsaw, Poland*
[2]*Faculty of Physics, University of Warsaw, Pasteura 5,02-093 Warsaw, Poland*

In this work, we report photoluminescence (PL) measurements performed on CdSe quantum dots (QDs) doped with copper. The PL behavior in magnetic field is consistent with the one expected for a QD with a single Cu ion in a d^9 configuration. Our results underline the possibility of employing Cu as magnetic dopants in II-VI semiconductors.

Self-assembled CdSe/ZnSe QDs were grown by molecular beam epitaxy. First, a ZnSe barrier layer is grown on 100-GaAs substrate and is followed by 3 monolayers of CdSe grown by alternating opening of Cd and Se effusion cells for 5 seconds at 280C. Simultaneously to the Cd flux the copper effusion cell has been opened for 5 seconds. Its flux is characterized by the beam equivalent pressure being of the order of 10^{-9} – 10^{-8} torr depending on the sample. The quantum dots formation process is induced by the Se-covering at low temperature and its subsequent thermal desorption. The QDs are finally capped with 50nm ZnSe barrier layer.

The PL was measured at 5 K in magnetic fields up to 10 T in Faraday configuration in two circular polarizations. The measurements were carried out in the system with a spatial resolution of the order of 1 micrometre allowing for investigations of individual QD.

In order to distinguish the CdSe dots with no copper ions from those containing the dopants we searched for appearance of the line splitting in the absence of the magnetic field, the splitting being the result of copper–exciton exchange sp-d interaction combined with the anisotropic electron-hole exchange interaction. The PL dependence on the magnetic field is then compared to calculations within a model based on the following Hamiltonian:

$$\hat{H} = \hat{H}_{Cu-e} + \hat{H}_{Cu-h} + \hat{H}_{e-h} + \hat{H}_{Zeeman} + \gamma B^2 \quad (1)$$

where the first two terms describe the s-d and p-d exchange interaction between the Cu^{2+} ion and the carriers, while the third term describes the electron-hole exchange interaction (both the isotropic and anisotropic one, the latter causing a mixing of the two spin states of the bright exciton. The last two terms describe the interaction of carriers and the ion with the field. Comparison between the measured and calculated PL dependence on magnetic field allows to conclude that the investigated QD indeed contains a single Cu ion with a spin ½ resulting from the 9 electrons occupying the ion d shell. The anticrossings observed at ~5 T are due to a compensation of the exchange field by the external one, whereupon the anisotropic exchange splitting is resolved.

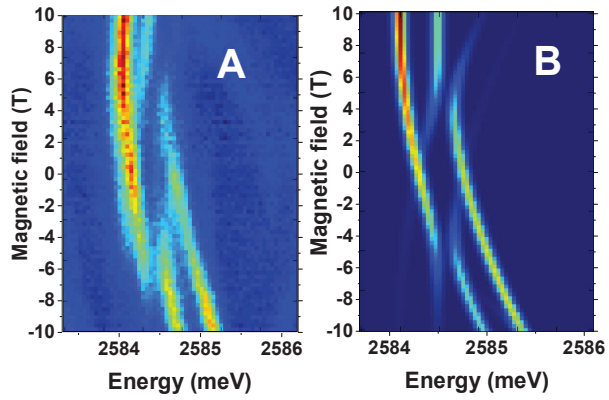

Figure 1. Magnetic field dependence of the μ-PL spectra of a CdSe QD doped with a single Cu ion (A - experiment, B - calculation). Positive/negative fields correspond to $\sigma_+/\sigma-$ PL detection polarizations.

The research has been supported by National Centre of Science (Poland) grant 2013/08/A/ST3/00297.

Polariton lasing of semimagnetic exciton-polaritons.

K. Lekenta, R. Mirek, M. Król, J.-G. Rousset, M. Nawrocki,
W. Pacuski, J. Szczytko and B. Piętka

Institute of Experimental Physics, Faculty of Physics, University of Warsaw, Poland

The past decade has encounter extremely fast development in the studies on quantum phenomena in a semiconductor microcavity field. The works devoted to the interaction between light and matter show that as a result of strong coupling between a photonic and an excitonic ground state, two new states arise: upper and lower exciton-polaritons. Studies include the area of nonlinear interactions as Bose-Einstein condensation [1], polariton lasing [2] or superfluidity [3].
In our work we investigate polariton lasing in a semimagnetic semiconductor microcavity. Our microcavity sample consist of two Bragg mirrors consisting of alternating (Cd,Zn,Mg)Te layers with various magnesium concentration embedding a cavity with four quantum wells containing 1% of manganese [4,5]. We modified a confocal optical microscopy setup to detect angularly resolved photoluminescence spectra. Sample was pumped nonresonantly with a fs laser pulses. The II-VI semiconductor structures suffer from photonic disorder, more pronounced than in III-V semiconductors. However in the confocal microscopy setup we have the ability to a precise positioning of the excitation spot on the sample surface and we could determine the places with homogenous (over tens of μm) potential distribution.
We observe different effects depending on excitation power (Figure). Starting from low power we could observe accumulation of polaritons at the bottleneck at lower polariton branch. For higher excitation power the population at the bottleneck decreases and the polaritons accumulate at the bottom of lower polariton branch, where the intensity starts to dominate over the intensity at the bottleneck. Above threshold we observe polariton lasing, what turn on to the nonlinear interaction regime. The energy shift due to polariton - polariton interactions is clearly visible. In our work we demonstrate a detailed study of the threshold of polariton lasing in semimagnetic semiconductor microcavity for large excitation spots and in a localised minima, where the non-linear effects are much stronger.

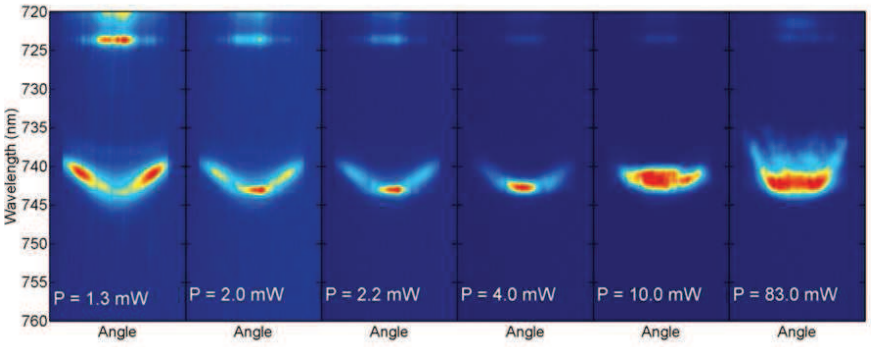

Figure: Angularly resolved photoluminescence maps of semimagnetic exciton-polariton lasing as a function of power excitation in a homogenous photonic potential distribution.

[1] J. Kasprzak et al. *Nature* **443**, 409 (2006). [2] R. Balili et al., *Science* **316**, 1007 (2007). [3] A. Amo et al. *Nature Phys.* **5**, 805 (2009) [4] J.-G. Rousset et al., J. Cryst. Growth 378, 266 (2013). [5] J.-G. Rousset et al., Appl. Phys. Lett. 107, 201109 (2015).

Optically detected cyclotron resonance in a GaAs/GaAlAs heterostructure

M. Deresz[1], D. Yavorskiy[1], K.-J. Friedland[2], R. Hey[2], and J. Łusakowski[1]

[1] *Faculty of Physics, University of Warsaw, Pasteura 5, 02-063 Poland*
[2] *Paul-Drude Institut, Hausvogteiplatz 5-7, DE-10117 Berlin, Germany*

Optically detected magnetic resonance is an experimental technique combining simultaneous excitations with visible and THz radiation. In particular, it allows to detect low-energy transitions by studying a near - band luminescence. In the present experiment, this technique is used to observe an influence of a cyclotron resonance transition in a two-dimensional electron gas (2DEG) on a luminescence originating from recombination of a 2DEG electron with acceptor-bound photoexcited hole.

The sample under investigation was a GaAs/$Ga_{0.67}Al_{0.33}As$ heterostructure grown on a GaAs substrate. At the distance of 30 nm from the GaAlAs barrier, a δ layer of Be atoms in the GaAs channel was introduced with the concentration of 10^9 cm^{-2}. A 2DEG appears at the GaAs/GaAlAs interface due to doping of the GaAlAs barrier with Si donors. The structure was previous studied with luminescence experiments. The electron population on the first and second subbands under optical excitaion conditions was determined [1] as well as a dependence of the degree of polarization of luminescence on the electron concentration [2].

The experiment was carried out in an optical helium cryostat supplied with a split coil. The measurements were done at 1.6 K and magnetic field from 0.5 T to 1.2 T. A photoluminescence was excited with a Ar+ laser, with the power of excitation less than 0.1mWcm^{-2}. The spectra were detected with a spectrometer supplied with a CCD camera. At each magnetic field, two spectra were measured: one with and the other without illumination of the sample with a 336 GHz(1.37 meV) radiation which corresponds to a CR transition in GaAs at 0.84 T.

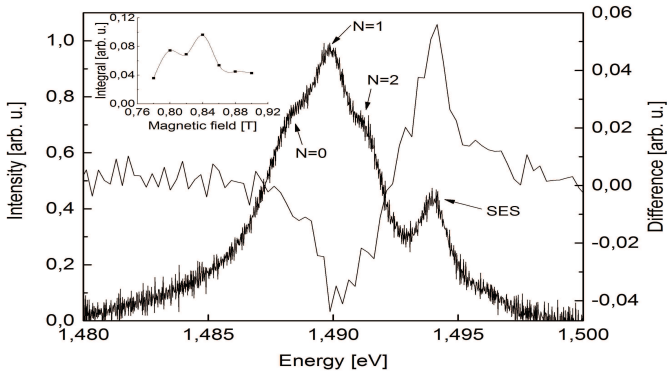

Fig.1: PL (THz off) and a difference spectrum at B = 0.84 T. Inset: integral of the modulus of the difference signal.

The spectra reflect a Landau quantization of the first electrical subband (FES) and a peak resulting from transitions from the second electrical subband (SES). A diffrence spectra (I_{on} - I_{off}; where I is a PL intensity) show a shift of the intensity from the FES to the SES. We note that occupation of all Landau levels on the FES is influenced by the THz radiation, even of these which are fully occupied at THz-off conditions. An integral of the modulus of difference spectra is shown in the inset as a function of the magnetic field and clearly exhibits a resonant character of the observed THz transition. The work opens the possiblity to optically detect low-energy resonances in a 2DEG and also carry out spectroscopy on the acceptor-bound hole.

[1] J. Łusakowski *et al.*, *Phys. Rev. B* **83**, 245313 (2011).
[2] J. Łusakowski *et al., J. Phys C* **19** 236205 (2007).
This work was partially supported by a Polish National Science Centre grant UMO-2015/17/B/ST7/03630.

Cavity quantum electrodynamics effects in resonantly excited strongly-coupled quantum dot – micropillar cavities

Caspar Hopfmann[1], Alexander Carmele[2], Anna Musiał[1,3], Micha Strauß[4], Christian Schneider[4], Sven Höfling[4,5], Martin Kamp[4], Andreas Knorr[2], and Stephan Reitzenstein[1]

[1] *Institute of Solid State Physics, Technische Universität Berlin, Hardenbergstr 36, Germany*
[2] *Institute of Theoretical Physics, Technische Universität Berlin, Hardenbergstr 36, Germany*
[3] *Laboratory for Optical Spectroscopy of Nanostructures, Faculty of Fundamental Problems of Technology, Wrocław University of Science and Technology, Wyb Wyspiańskiego 27, Poland*
[4] *Technische Physik, Universität Würzburg, Am Hubland, Würzburg, Germany*
[5] *School of Physics and Astronomy, University of St. Andrews, St. Andrews, United Kingdom*

Resonant excitation of quantum systems offers the unprecedented possibility of coherent control important for both fundamental study and applications due to minimized dephasing and direct addressing of a chosen state, enabling observation of phenomena not accessible otherwise. In the active field of cavity quantum electrodynamics (cQED) resonant excitation has so far been used to observe strong coupling between quantum dot (QD) exciton (X) and cavity mode (CM) [1] as well as cavity-enhanced dressing of QD X and biexciton [2].

We employed resonance fluorescence (RF) to study cQED effects in strongly coupled InGaAs/GaAs QD-micropillar system. An advanced 90 degree excitation/detection scheme enabled to drive directly the QD X (in-plane excitation) which then couples to the cavity. Spatial and polarization filtering was used to extract the signal. Driving the QD X directly enables realization and observation of fingerprints of the strongly-coupled system for arbitrary laser detunings as the system is not pumped through the CM. Continuous wave excitation with tunable semiconductor laser with 100 kHz linewidth was used to excite the system and cavity spectrum (losses through the upper DBR) was measured in the vertical direction (parallel to the micropillar axis). For QD off-resonant with respect to the cavity a typical saturation behavior was observed. Both direct RF and CM-mediated signal was measured providing info about off-resonant QD X-CM coupling. When QD X transition is resonant with the CM it can be most efficiently excited through the bare (uncoupled) QD state (laser on resonance with the QD X) due to small pure dephasing and purely excitonic character of the pumped state being eigenstate of the system. In that case clear Rabi doublet can be observed. When the QD-laser detuning is varied and the laser energy is scanned over the strongly-coupled system, much weaker and asymmetric response at the energy of the two polariton branches was detected. Varying the excitation power on mutual resonance of the laser field QD X and the CM shows that the eigenstates of the system are determined by relative coupling strengths in the system: At low excitation the laser field is used only to populate the system and clear features of the strong QD X-CM coupling are visible. In the intermediate regime a hybrid system is formed whereas for higher excitation dressing of the polariton branches takes place and a related Mollow triplet-like can be observed in the spectrum. The transition between the regimes was proven experimentally by observation of a clear maximum in the RF signal of the strongly-coupled system as a function of excitation power. Theoretical analysis of the system was performed within the Fourier-transformed first-order autocorrelation function approach including multi-photon scattering.

[1] L. Greuter, S. Starosielec, A. V. Kuhlmann, and R. Warburton, *Phys. Rev. B* **92**, 045302 (2015).
[2] F. Hargart, M. Müller, K. Roy-Choudhury, S. L. Portalupi, C. Schneider, S. Höfling, M. Kamp, S. Hughes, and P. Michler, *Phys. Rev. B* **93**, 115308 (2016).

Mechanism and dynamics of biexciton formation from a long-lived dark exciton in a CdTe quantum dot

Tomasz Smoleński [1], Mateusz Goryca [1], Tomasz Kazimierczuk [1], Piotr Wojnar [2], Piotr Kossacki [1]

[1] *University of Warsaw, Faculty of Physics, Institute of Experimental Physics, ul. Pasteura 5, 02-093 Warsaw, Poland*
[2] *Polish Academy of Sciences, Institute of Physics, al. Lotników 32/64, 02-688 Warsaw, Poland*

Numerous optical studies of various quantum dot (QD) systems established a toolbox of techniques effective in characterization of single-dot photoluminescence (PL) spectra. In particular, measurement of the PL spectrum as a function of the excitation intensity is often employed to distinguish between spectroscopic lines related to different excitonic complexes [1]. The results are usually discussed in terms of a power-law behavior of the PL intensity. The simplistic stochastic model states for example that the formation of the biexciton requires a coincidence of two exciton formation events [2], and thus the biexciton PL intensity should increase quadratically with the excitation power. In real experiments, however, the biexciton PL intensity does not follow this prediction and exhibits less steep dependence [3].

Here we analyze the dependence of a single CdTe QD PL on pulsed excitation intensity and demonstrate contributions of two mechanisms of the biexciton formation: either from an empty dot by capture of two electron-hole pairs within a single excitation pulse or from a resident dark exciton created earlier [4]. We show that in the wide range of intensities the latter mechanism is dominant, which provides a natural explanation for subquadratic biexciton PL intensity power dependence. It is also a general example of the importance of the dark exciton state, which is often neglected [3,5], but should be taken into account in the rate-equation models to correctly describe the QD physics under various excitation regimes, including the CW excitation.

The discussed mechanism allows us to create the single biexciton with the use of two different laser pulses, polarization of which can be controlled independently. We exploit this possibility in the time-resolved experiments to study the impact of a carrier spin-blockade effect on the biexciton (and other excitonic complexes) formation dynamics. Our results show that the formation of the biexciton is slowed down when the two consecutive pulses used to create this complex have opposite circular polarization. Such effect is caused by relatively long relaxation time of a spin blockaded electron pair, while the spin-blockaded holes relax rapidly to their ground state.

[1] P. Michler, *Single Semiconductor Quantum Dots* (Springer, Heidelberg, 2009).
[2] M. Grundmann et al., *Phys. Rev. B* **55**, 9740 (1997).
[3] J. Suffczyński et al., *Phys. Rev. B* **74**, 085319 (2006).
[4] T. Smoleński et al., *Phys. Rev. B* **91**, 155430 (2015).
[5] T. Kazimierczuk et al., *Phys. Rev. B* **81**, 155313 (2010).

GaAs-Ga(As,Bi) Core-Shell Nanowires – Structural and Optical Properties

J. Sadowski [1,2,3], A. Siusys [1], T. Wojciechowski [1], M. Szot[1], A. Kaleta[1], A. Sanchez[4], S. Kret[1]

[1] *Institute of Physics, Polish Academy of Sciences, PL-02-668 Warszawa, Poland*
[2] *MAX-IV laboratory, Lund University, SE-221 00 Lund, Sweden*
[3] *Linnaeus University, SE-351 95 Växjö. Sweden*
[4] *Department of Physics, University of Warwick, Coventry, CV4 7AL, UK*

Alloying GaAs with Bi results in a ternary alloy with interesting optical properties, due to the important band-gap reduction and enhancement of the spin-orbit splitting in Ga(As,Bi). Both features make this ternary alloy interesting for optoelectronic applications in near-infrared energy range, and suitable for solar cell applications. The maximum Bi content in uniform Ga(As,Bi) compound reported so far reaches about 10%. Attempts to obtain higher composition of Ga(As,Bi) solid solution lead to Bi segregation either at the growth front or inside the volume of the growing crystal [1, 2]. We have investigated Bi incorporation into thin Ga(As,Bi) shells deposited around GaAs nanowire (NW) cores. The NWs have been grown by molecular beam epitaxy (MBE) using Au-catalysed growth mode. First the GaAs core NWs were grown at optimum conditions, then Ga(As,Bi) NW shells were deposited at low temperatures (300 – 350 ^{o}C) and close-to-stoichiometric As/Ga flux ratio. The NWs were grown in two distinct crystallographic structures – zinc-blende (ZB), typical for GaAs bulk crystals and layers, and hexagonal wurtizte (WZ) structure, possible to obtain in NWs grown in suitable conditions. Bi incorporation limits into ZB and WZ GaAs will be compared. For the NW Ga(As,Bi) NW cores grown at the highest As/Bi flux ratio we have observed segregation of Bi nanodroplets at the NW side-walls (see Fig. 1). These nanodroplets act as the catalyst for the growth of NW branches, perpendicular to main GaAs NW truncs.

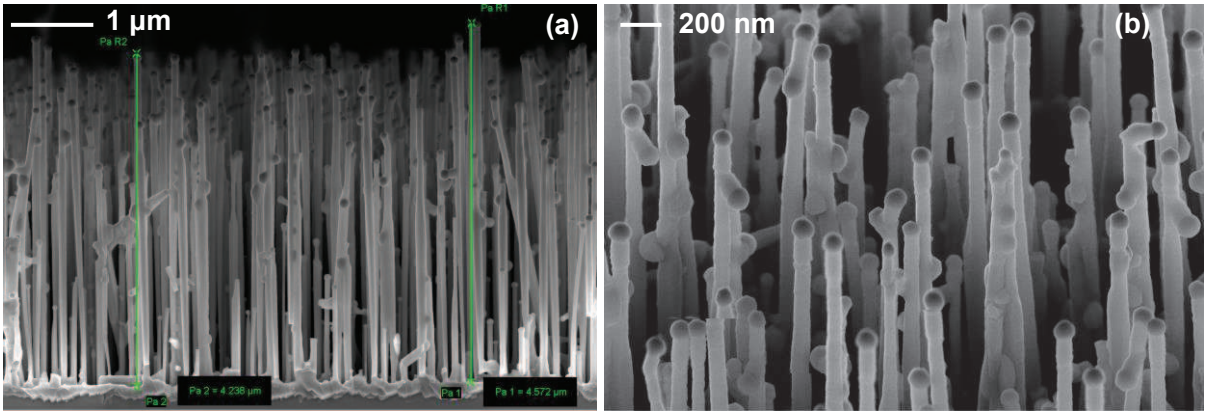

Fig.1. SEM images of GaAs-Ga(As,Bi) core shell NWs grown above Bi surface segregation threshold. (a) – cross-sectional view, (b) 45^{o} view.

This work has been partially supported by the research Project No. 2014/13/B/ST3/04489 financed through the Polish National Science Centre (NCN).

[1] E. Sterzer, N. Knaub , P. Ludewig, R. Straubinger, A. Beyer, K. Volz, *J. Crystal Growth*, **408**, 71 (2014).
[2] E. Luna, M. Wu, J. Puustinen, M. Guina, and A. Trampert, *J. Appl. Phys*. **117**, 185302 (2015).

Growth of CdTe/(Cd,Mg)Te core/shell nanowires with high optical quality

P. Wojnar, J. Płachta, A. Kaleta, S. Kret, M. Szymura, R. Rudniewski, W. Zaleszczyk, L.T. Baczewski, G Karczewski, T Wojtowicz and J. Kossut

Institute of Physics, Polish Academy of Sciences, Warsaw, Poland

CdTe is commonly recognized as a semiconductor particularly well suited for photovoltaic applications due to its direct band gap of 1.5 eV at room temperature which ensures an effective absorption of the solar light spectrum. Although planar CdTe-based solar cells reach efficiencies up to 21% [1], the implementation of CdTe into efficient nanowire-based photovoltaic devices remains still a challenge. This is our main motivation for the growth of CdTe nanowires using Au-catalyzed vapor-liquid-solid growth mechanism in a system for molecular beam epitaxy.

Our previous attempts to grow CdTe nanowires by employing this technique resulted in poor quality 'crooked' nanowires travelling on the surface, whereas only a small percentage of nano-droplets developed into proper straight CdTe nanowires. Here, we have found that initializing the growth with a short ZnTe deposition helps to develop high density straight CdTe nanowire arrays. In the optical spectrum of CdTe nanowires, however, any emission close to the CdTe energy gap is not observable. That is the reason why CdTe nanowires are coated with a (Cd,Mg)Te shell, in the following step. As result a near band edge emission from CdTe nanowires is activated. This is most likely due to the passivation of surface states.

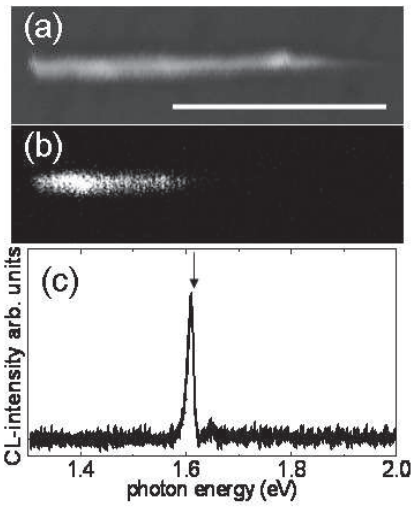

Figure 1. Cathodoluminescence (CL) from an individual CdTe/(Cd,MgTe) core/shell nanowire. Scanning electron microscope image of the investigated nanowire (a); monochromatic CL mapping at 1.61 eV (b); CL spectrum of this individual nanowire (c); scale bar is 1 μm

High optical quality of CdTe/(Cd,MgTe) individual nanowires is revealed by means of low temperature cathodoluminescence, Figure 1, and micro-photoluminescence. The optical emission spectrum from an individual nanowire consists only of the near band edge emission line without any significant contribution of defect related luminescence. Moreover, the role of the strain acting on CdTe nanowire core originating from the lattice mismatched shell is manifested by the increase of the emission energy with increasing shell thickness and Mg concentration in the shell. Microphotoluminescence study reveals that the CdTe near band edge emission is strongly linearly polarized along the nanowire axis, which is most likely due to the dielectric confinement.

The research has been partially supported by National Centre of Science (Poland) grant 2011/01/D/ST5/05039

References:

[1] Green M A, Emery K, Hishikawa Y, Warta W, and Dunlop E D 2015 *Progress in Photovoltaics* **23** 805

(1e,1h) states of carbon nanotube quantum dots

Edyta N. Osika[1,2], **Bartłomiej Szafran** [1]

[1] *AGH University of Science and Technology, Faculty of Physics and Applied Computer Science, al. Mickiewicza 30, 30-059 Kraków, Poland*
[2] *ICFO-Institut de Ciéncies Fotóniques, The Barcelona Institute of Science and Technology, 08860 Castelldefels (Barcelona), Spain*

The idea of single electron spin manipulation in carbon nanotube (CNT) quantum dots has been exploited recently in many experimental and theoretical works [1-3]. CNTs provide very attractive medium for that kind of manipulation due to the presence of the spin-orbit interacion [4], arising from the curvature of graphene plane, as well as an absence of the important decoherence source - the nuclear field. That makes the CNT quantum dots a good candidate for e.g. qubits for future quantum information.

In this work we investigate a few-carriers ambipolar (n-p) quantum dots defined electrostatically in carbon nanotubes. We focus on (1e,1h) electron configuration, since that is the only system in which the Pauli spin-valley blockade has been observed experimentally. The blockade has been used to observe manipulation of spin and valley states of the carriers due to electric dipole spin resonance (EDSR).

We model the system of carbon nanotube n-p quantum dot using the exact diagonalization within the tight-binding approximation. We use single electron energy states and configuration interaction method to calculate few-electron energy spectra. In the model we take into account external fields - electric and magnetic, the spin-orbit coupling, the electron-electron interaction and intervalley scattering. By solving the time-dependent Schroedinger equation we simulate spin-valley dynamics of the system due to EDSR.

We describe the lowest energy states of the (1e,1h) system and compare them with other electronic configurations of the n-p quantum dots. The transitions between Pauli blocked and non-blocked states due to EDSR are calculated and compared explicitly with the experimental data. The magnetic field magnitude and orientation dependence of the presented transitions are discussed. We show also the effect of the nanotube bending on the transition spectra and demonstrate that we can significantly improve the agreement with the experiment by bending the nanotube locally over the gates.

[1] F. Pei, E. A. Laird, G. A. Steele, and L. P. Kouwenhoven, *Nature Nano.* **7**, 630 (2012).
[2] E. A. Laird, F. Pei, and L. P. Kouwenhoven, *Nature Nano.* **8**, 565 (2013).
[3] E. A. Laird, F. Kuemmeth, G. A. Steele, K. Grove-Rasmussen, J. Nygård, K. Flensberg, and L. P. Kouwenhoven, *Rev. Mod. Phys.* **87**, 703 (2015).
[4] T. Ando, *J. Phys. Soc. Jpn.* **69**, 1757 (2000).

Charge and spin injection in a quantum well–quantum dot system

Adam Mielnik–Pyszczorski, Krzysztof Gawarecki, Paweł Machnikowski

Department of Theoretical Physics, Faculty of Fundamental Problems of Technology, Wrocław University of Technology, Wybrzeże Wyspiańskiego 27, 50-370 Wrocław, Poland

The system composed of a quantum well and a quantum dot (QW–QD) has been studied in experiment and theory [1,2]. It turns out that the high density of states in the QW increases efficiency of injection of carriers into QDs. The observed efficient tunneling of carriers combined with techniques of optical orientation and coherent spin control suggest that the QW could also serve as an effective spin injector for the QD structures.

In this contribution we theoretically investigate the process of electron tunneling from a QW to a nearby QD. In order to study the charge and spin dynamics we first determine the strain distribution in the system [3]. The lattice deformation is important in the consideration of a realistic structure since it has strong influence on the band edges, generates a piezoelectric field, which results in additional localization of electrons in the vicinity of the QD, and also, in an external magnetic field, contributes to the effective g–factor. We calculate electronic wave functions within 8–band $k\cdot p$ Hamiltonian including the strain field and the spin–orbit interaction, reduced to a 2–band ($|e\uparrow\rangle$, $|e\downarrow\rangle$) model by Löwdin perturbation theory. We then use the resulting single electron spinor wave functions to calculate the electron evolution within the correlation expansion approach.

We study phonon–induced system relaxation to its ground state localized in the QD (carrier injection), as well as the spin dynamics during this process (spin injection). For carrier injection, we obtained non–monotonic dependence of the relaxation rate on the distance between the QD and the QW. We found an exponential evolution of the average number of electrons in the dot and a non–exponential evolution of the state occupations in the well [1]. We study also the spin evolution during tunneling in order to estimate the spin–flip probability and assess the efficiency of spin injection. We compare spin flip processes generated by various spin–phonon coupling mechanisms.

[1] A. Mielnik–Pyszczorski, K. Gawarecki, P. Machnikowski, Phys. Rev. B **91**, 195421 (2015).
[2] W. Rudno–Rudzinski, G. Sek, J. Andrzejewski, J. Misiewicz, F. Lelarge, B. Rousseau, Semicond. Sci. Technol. **27**, 10 (2012)
[3] C. Pryor, J. Kim, L. W. Wang, A. J. Williamson, and A.Zunger, J. Appl. Phys. **83**, 2548 (1998).

Protection of entangled states of N qubits with dynamical decoupling

Jan Krzywda[1], Piotr Szańkowski[2], and Łukasz Cywiński[2]

[1] *Faculty of Physics, University of Warsaw, 02-093 Warsaw, Poland*
[2] *Laboratory for Cryogenic and Spintronic Research, Insitute of Physics, Polish Academy of Sciences, Warsaw, Poland*

Decoherence of a qubit can be suppressed by subjecting it to a sequence of dynamical decoupling pulses - π rotations effectively interchanging the amplitudes of qubit being in state "0" and "1". For a single spin qubits (quantum dot based [1,2], NV centers [3], phosphorous donors in silicon [4]) dynamical decoupling has led to a substantial (orders of magnitude) increase in coherence times. Furthermore, the dephasing of the qubit due to interaction with its environment was shown to be often well-described under assumption that the environment is a source of classical noise.

Recently, the dynamical decoupling of two qubits from two partially correlated noises was considered theoretically [5]. We extend this theory to the case of N entangled qubits driven by various sequences of pulses. We consider initial states including so-called W, GHZ, and cluster states [6], and noise spectra typically encountered for solid-state based qubits, e.g. Ornstein-Uhlenbeck noise and $1/f^{\alpha}$ noise with $\alpha \in [0.5, 3]$. The relative efficiency of entanglement protection offered by various pulse sequences will be analyzed. We will also investigate which N qubit entangled states can be used for sensing of presence of cross-correlations of noises affecting distinct qubits, thus paving the way for multi-qubit generalization of two-qubit noise correlation sensing protocol described in [5].

This research is supported by funds of Polish National Science Center (NCN), grant no. DEC-2012/07/B/ST3/03616.

[1] J. Medford, Ł. Cywiński, C. Barthel, C. M. Marcus, M. P. Hanson, and A. C. Gossard, *Phys. Rev. Lett.* **108**, 086802 (2012).
[2] F. K. Malinowski, F. Martins, P. D. Nissen, E. Barnes, M. S. Rudner, S. Fallahi, G. C. Gardner, M. J. Manfra, C. M. Marcus, and F. Kuemmeth, *arXiv:1601.06677* (2015).
[3] Y. Romach et al., *Phys. Rev. Lett.* **114**, 017601 (2015).
[4] J. T. Muhonen et al., *Nature Nanotechnology* **9**, 986 (2014).
[5] P. Szańkowski, M. Trippenbach, and Ł. Cywiński, *arXiv:1507.03897* (2015).
[6] L. Aolita, F. de Melo, and L. Davidovich, *Rep. Prog. Phys.* **78**, 042001 (2015).

Accuracy tests of EXX+RPA scheme in r-space implementation of KS-DFT

M. Marchwiany[1,2], M. Popielska[1], M. Kruk[1], and J. A. Majewski[1]

[1]Faculty of Physics, University of Warsaw, ul. Pasteura 5, 02-093 Warsaw, Poland
[2]Interdisciplinary Centre for Mathematical and Computational Modelling (ICM), University of Warsaw, Pawinskiego 5a, 02-106 Warsaw, Poland

In this communications, we present technical details of the implementation of the exact-exchange (EXX) [1] contribution to the Kohn-Sham potential, with correlation energy calculated employing the random phase approximations (RPA), which have proved to account for correct description of the Van der Waals interactions [2]. This implementation is done on the newly developed code in our group, in which the Kohn-Sham equations [3] are directly solved on a grid in the r-space. Calculations in r-space, in contrast to the majority of available commercial and under GNU license available computer codes, allows for employing the periodic boundary conditions only along physically periodic directions, i.e., without the necessity of placing partly periodic systems into an artificial three-dimensional super-cell. This allows for more efficient computations of the electronic properties.

In order to check the efficiency (computational burden, time consuming) and the accuracy of our real space code, we study representative systems of carbon-based materials, in which the Van der Waals interactions are of particular importance, such as graphite; bi- and tri-monolayers of graphene, carbon nanotubes, and simple molecules C_2. These systems exhibit different types of periodicity, therefore, we also compare the obtained results with the ones obtained within standard supercell calculations. Moreover, in all of these cases we examine the accuracy of the pseudopotential EXX scheme with the all electron approach (commercial all-electron code FHI-aims [4]), by comparing the structural and electronic properties of representative systems.

[1] T. W. Hollins, S. J. Clark, K. Refson, and N. I. Gidopoulos, *Phys. Rev. B* **85**, 235126 (2012).
[2] H. V. Nguyen, G. Galli, *J. Chem. Phys*. **132**, 044109 (2010).
[3] W. Kohn, and L. J. Sham, *Phys. Rev*. **140**, A1133 (1965).
[4] Volker Blum, Ralf Gehrke, Felix Hanke, Paula Havu, Ville Havu, Xinguo Ren, Karsten Reuter, and Matthias Scheffler, *Comp. Phys. Comm*. **180**, 2175 (2009).

The effect of localized electric field in the type-II InAs/GaAsSb quantum dot using photoreflectance spectroscopy

S. H .Lee [1], J. S. Kim[1*], Y. H. Kim [2] and Christiana B. Honsberg[3]
[1] *Department of Physics, Yeungnam University, Gyeongsan 712-749, South Korea*
[2] *Division of Convergence Technology, Korea Research Institute of Standards and Science, Daejeon 305-340, South Korea*
[3] *School of Electrical, Computer and Energy Engineering, Arizona State University, Tempe, Arizona 85287, USA*
***E-mail:** jongsukim@ynu.ac.kr*

We investigated the effect of localized electric field in the type-II InAs/GaAsSb quantum dot (QD) in GaAs matrix by photoreflectance (PR) spectroscopy. Excitation laser intensity dependent-PR experiment was performed at 10 K to enhance confinement effect of carriers which are spatially separated into electrons in InAs and holes in GaAsSb due to the type-II band alignment. In addition, the PR results of InAs/GaAsSb type-II system were compared with those of InAs/GaAs type-I system.

Figure. 1 shows PR spectrum of (a) type-II InAs/GaAsSb submonolayer (SML) QD and (b) type-I InAs/GaAs SML QD. Each transition such as GaAs, spin orbit splitting, QD and FKO was addressed.

The inset of Fig. 1 (a) shows that as increasing the excitation laser intensity the Franz-Keldysh oscillations (FKOs) start to appear and their periods are extended for InAs/GaAsSb type-II sample. This phenomenon is attributed to the localized electric field due to the bend bending effect caused by the spatially separated photo-excited carriers in the interface region of type-II band alignment structure [1], because appearance of FKOs in the PR spectrum above bulk band gap is caused by an existence of electric field in an interface of a sample [2]. In contrast, for InAs/GaAs type-I system, the PR spectra in the inset of Fig. 1 (b) show that FKOs do not change even at high excitation laser intensity due to the absence of localized electric field in the interface region. The presence of localized electric field was proved and the field's magnitude can approximately be obtained.

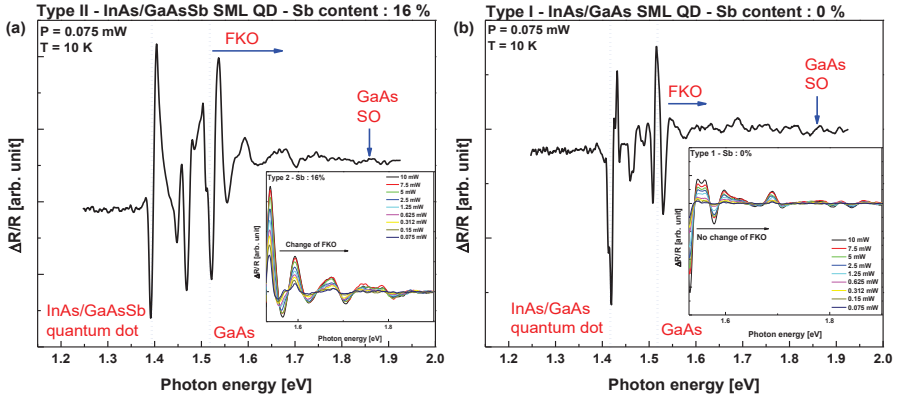

Figure 1. Photoreflectance spectra of (a) type-II InAs/GaAsSb SML QD and (b) type-I InAs/GaAs SML QD. The insets of (a) and (b) show the change of FKOs with various excitation laser intensities.

[1] T. T. Chen, C. L. Cheng, Y. F. Chen, F. Y. Chang, H. H. Lin, C.–Y. Wu and C.-H. Chen, *Phys. Rev. B.* 75, **03310** (2007).
[2] C. Van Hoof, K. Deneffe, J. De Boeck, J. D. Arent and G. Borghs, *Appl. Phys. Lett*. 54, **608** (1989).

Photoelectrical Properties of CdS/CdMgTe Heterostructure for Tandem Solar Cells

T.I. Mykytyuk [1], I.M. Fodchuk [1], V.V. Kulchynsky [1], O.L. Maslyanchuk [1] X. Mathew [2]

[1] *Chernivtsi National University, 2 Kotsyubinsky Str., Chernivtsi 58012, Ukraine*
[2] *Instituto de Energías Renovables, Universidad Nacional Autonoma de Mexico, Temixco, Morelos 62580, México*

For several decades, solar cells based on CdTe keep a stable position in thin-film photovoltaics as an alternative to solar modules based on mono- and poly-silicon wafers. Thin film tandem solar cells are one of alternative way for increasing solar cells efficiency. Many experts in the field of photovoltaic considered that thin film CdS/CdMgTe heterostructure with an absorbing layer of CdMgTe one of the most promising semiconductor materials for developing the top sub-cell in a tandem device [1,2]. For the above top-cell, a suitable absorber material for the bottom sub-cell can be the well-studied CIGS and $Hg_xCd_{1-x}Te$ alloys with a bandgap in the range of 1-1.1 eV. $Cd_{1-x}Mg_xTe$ is an alloy of MgTe and CdTe and can be made with a wide tolerance to variations of Cd/Mg ratio, when the semiconductor bandgap varies continuously with *x* from about 1.5 eV for CdTe to about 3.5 eV for MgTe. Whatever the material composition, $Cd_{1-x}Mg_xTe$ is a direct-bandgap semiconductor and strongly absorbs sunlight. Because of this, a much thinner film in CdMgTe-based solar devices is required than of other indirect-bandgap semiconductor materials. In this case important to take into account physical factors which occurs when thinning absorber layer, such as: decrease in absorptive capacity, recombination losses at the surfaces and in the space charge region of p-n heterojunction.

The analysis is complicated by the fact that transmission spectra of the CdS/CdMgTe layers differ from the spectra of monolithic thin-film structures since the reflection coefficients at the interfaces: semiconductor/air and semiconductor/semiconductor can vary significantly. This problem can be solved by calculations based on the optical constants of materials that take into account reflections from all interfaces and absorption in the materials.

This paper presents calculations which gives quantitative description of the spectral distribution of the quantum efficiency of CdS/CdMgTe heterostructure. A theoretical analysis of the optical and recombination losses in thin film CdS/CdMgTe solar cells and its impact on short-circuit current are carried out. Our results show, at which thickness of the absorber layer and the width of the space-charge region the limiting factors can be ignored. The spectra of the optical transmission the CdS/CdMgTe structure with taking into account optical constants dependencies have been calculated**.** Quantum efficiency the CdS/CdMgTe solar cell and the losses due to the recombination of charge carriers at the front and back surfaces of the absorbing layer, in its neutral part and in the space charge region of p-n heterojunction have been determined.

[1] S. Omar, A. Martínez, L. Remolina, G. Huerta, N.R. Santana, M. Mathews, L. Ramon-Garcia, E.R. Morales, X. Mathew, *Materials Chemistry and Physics*, **132**, 559 (2012).
[2] X. Mathew, J. Drayton, V. Parikh, N.R. Mathews, Xiangxin Liu, A.D. Compaan, *Semiconductor Science and Technology*, **24**, 015012 (2009).

Phase Tuned TiO_2 Nanotubes for Enhanced Photocatalytic Hydrogen Generation: Anatase → Anatase-Rutile → Anatase-Rutile-Brookite.

Preethi L K and T Mathews.

Thin Films & Coatings Section, Surface and Nanoscience Division, Indira Gandhi Centre for Atomic Research, Kalpakkam, India – 603102.

TiO_2 is a well known photocatalyst for wide applications such as water splitting, pollutant degradation, solar cell etc due to its high chemical stability, band level positioning, and abundant availability. However, the material absorbs only the UV part of sunlight, and suffers high electron-hole recombination rate which needs substantial improvement. Among various modifications adopted, the mixed phase TiO_2 is widely recognized due to the efficient electron-hole pair separation, which results in an enhanced photocatalytic activity, when compared to single phase TiO_2. Even though there are many literatures reporting the synthesis of TiO_2 mixed phases and their enhanced photocatalytic activity, development of more facile and simple methods for the synthesis of tunable phase-junction TiO_2 is still under progress. Herein, we report a novel synthesis method to prepare anatase, anatase-rutile and anatase-rutile-brookite heterojunctions porous TiO_2 nanotubes by simply tuning the voltage in electrochemical anodization technique. The phase evolution with respect to voltage is confirmed by the X-ray diffraction analysis. It is observed that the anatase-rutile-brookite phase junction TiO_2 nanotubes are highly efficient compared to anatase-rutile or anatase TiO_2 nanotubes in hydrogen generation by water splitting. The results suggest that the anatase-rutile-brookite having two junction interfaces highly facilitate inter-particle charge transfer due to the synergistic effect among the phases compared to single junction anatase-rutile or bare anatase TiO_2 nanotubes. This opens a pathway for the simple synthesis and study of tri-phase TiO_2 for efficient photocatalytic water splitting.

Spin injection and spin transport in a high mobility 2D electron gas

Mariusz Ciorga

Institute for Experimental and Applied Physics, University of Regensburg, Universitaetsstrasse 31, 93053 Regensburg, Germany

Electrical generation and control of electron spins in semiconductors is the central theme in semiconductor spintronics. Effective spin injection into a two-dimensional electron gas (2DEG) is particularly desirable as it is prerequisite for many new functionalities in potential devices, with a Datta-Das spin field effect transistor [1] being a primary example. Whereas real progress in understanding of spin injection phenomena in bulk semiconductors has been achieved, effective spin injection into high mobility 2DEGs remains a relatively open matter.

In the first part of the talk I will discuss general issues related to electrical spin injection and detection in semiconductors, addressed in the so-called standard model of spin injection based on spin drift-diffusion equations. I will illustrate the discussion mainly with the results of our experiments on bulk GaAs-based structures with (Ga,Mn)As/GaAs spin Esaki diodes employed as spin injecting and detecting contacts.

In the second part I will focus on different aspects of experiments on spin injection in high mobility 2DEGs, while presenting the results of our investigations of structures with a 2DEG confined in an inverted (Al,Ga)As/GaAs heterojunction [2]. I will show and discuss large spin-valve signals observed in the investigated structures, measured both in *nonlocal* and *local* experimental configurations. I will consider the importance of ballistic effects in a spin injection process [3], which in some cases can be responsible for enhancement of the spin signal in comparison with the prediction of the standard model of spin injection. Furthermore, I will discuss conditions required for succesfull observation of a spin precession signal in high mobility 2DEG channels. Reliable spin precession measurements are of particular importance because they provide us direct information about spin transport parameters of the channel, like spin relaxation times or the spin diffusion constant.

The work has been supported by Deutsche Forschungsgemeinschaft (DFG) through SFB689.

[1] S. Datta and B. Das, *Appl. Phys. Lett.* **56**, 665 (1990).
[2] M. Oltscher *et al.*, *Phys. Rev. Lett.* **113**, 236602 (2014).
[3] K. Cheng and S. Zhang, *Phys. Rev. B* **92**, 214402 (2015).

Advances and Prospects of High-Mobility 2D Electrons in ZnO Heterostructures

Y. Kozuka [1]

[1] *Department of Applied Physics and Quantum-Phase Electronics Center (QPEC), University of Tokyo, Tokyo 113-8656, Japan*

High-mobility 2D electron systems (2DES) have offered fertile playgrounds for novel quantum transport phenomena such as quantum Hall effect. GaAs is one of the best materials exhibiting the highest electron mobility exceeding 30 million cm^2/Vs. On the other hand, other semiconductor materials give opportunities to incorporate their own characteristic properties in quantum Hall physics.

Here we present the latest results on high-mobility 2DES created at the (Mg,Zn)O/ZnO heterointerfaces [1]. Owing to longstanding efforts to fabricate high-quality ZnO thin films, the maximum electron mobility of the 2DES reaches 1 million cm^2/Vs (Fig. 1), which corresponds to a mobility of ~ 5 million cm^2/Vs for GaAs 2DES in terms of transport scattering time [2]. This dramatic improvement leads to the recent observation of the even-denominator fractional quantum Hall state [3], which has been exclusively studied in GaAs 2DES. Given such high-mobility 2DES in ZnO, we can further explore new physics incorporating strong electron correlation, long spin relaxation time, superconducting proximity effect and so on.

[1] Y. Kozuka, A. Tsukazaki, and M. Kawasaki, Appl. Phys. Rev. **1**, 011303 (2014).
[2] J. Falson, Y. Kozuka, J. H. Smet, T. Arima, A. Tsukazaki, and M. Kawasaki, Appl. Phys. Lett. **107**, 082102 (2015).
[3] [2] J. Falson, D. Maryenko, B. Friess, D. Zhang, Y. Kozuka, A. Tsukazaki, J. H. Smet, and M. Kawasaki, Nature Phys. **11**, 347 (2015).

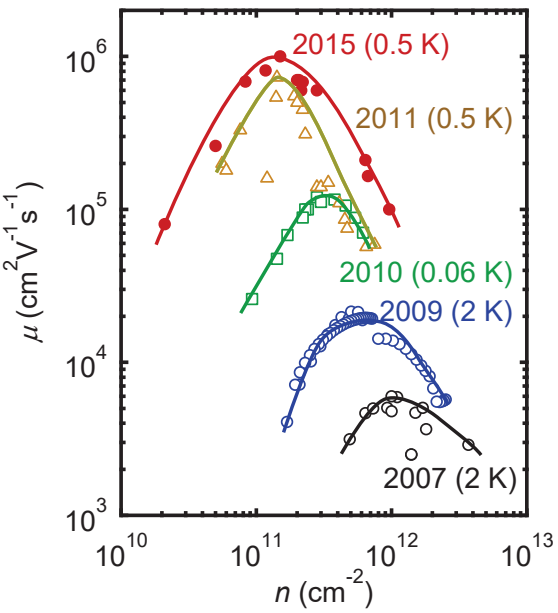

Fig. 1: Improvement in the electron mobility (μ) of 2DES in (Mg,Zn)O/ZnO heterinterfaces.

Local conductance and ultrafast dynamics of MBE grown Bi_2Te_3 films

J. Szade[1,2], M. Weis[1,2], R. Rapacz[1,2], K. Balin[1,2], M. Wojtyniak[1,2], A. Nowak[1,2], B. Wilk[1,2] and P. Ruello[3]

[1] *A. Chełkowski Institute of Physics, University of Silesia, Uniwersytecka 4, 40-007 Katowice, Poland*
[2] *Silesian Center for Education and Interdisciplinary Research, 75 Pułku Piechoty 1A, 41-500 Chorzów, University of Silesia, Poland*
[3] *Institut des Molecules et Materiaux du Mans, UMR CNRS 6283, Universite du Maine, 72085 Le Mans, France.*

Topological insulators (TI) are a new class of materials with semiconducting bulk solid while conducting on the surface. The surface Dirac electronic states exhibit natural spin-polarized current and appear to be protected against backward non-magnetic scattering. This makes them very attractive in applications for next generation spintronic devices [1].
The spin-orbit and electron-phonon coupling effects play a pivotal role in the transport properties of surface and bulk electrons. The detection and control of spin-momentum-locking of the surface states, as well as understanding the electron dynamics are the crucial problems determining the future applications.

In this work we studied thin films of Bi_2Te_3 belonging to the group of three-dimensional TIs. The films were grown on Si(100) or mica (muscovite) substrates by thermal evaporation with the use of Molecular Beam Epitaxy (MBE). For the films grown on Si polycrystalline structure was found while the deposition on the mica substrate lead to the formation of high quality single crystal films with the thickness in the range 4-20 nm [2-4].
The correlations between structural properties and morphology of the deposited films and their local electrical conductivity were studied with the use of AFM microscopy with the conducting tip (LC AFM) [3]. Application of LC-AFM allowed us to show the extremely high conductivity (very high contact currents) and metallic behavior (linear I–V curves) of the Bi_2Te_3 film surface, which most likely is an effect of the presence of the Dirac surface states. Moreover, we were able to localize small regions with reduced conductance, which were attributed to the local changes of the electronic structure caused by various defects.

By applying femtosecond pump-probe optical spectroscopy we demonstrated that it is possible to generate coherent optical phonons in Bi-Te nanostructures both in poly and single crystalline samples [4]. We show the effect of critical thickness of the film limiting the generation of the optical phonons. A new insights on the out-of-equilibrium electron- phonon coupling and phonons dynamics in confined TI was achieved. Additionally, by testing the effect of cap layer we were able to detect a strong dependence of the electronic excitation relaxation time on the element forming the overlayer.

[1] Y.-Y. Li, et al. *Adv. Mater*., 2010, 22, 4002– 4007.
[2] R. Rapacz, K. Balin, A. Nowak and J. Szade, *J. Cryst. Growth*, 2014, 401, 567–572.
[3] R. Rapacz, K. Balin, M. Wojtyniak and J. Szade, *Nanoscale*, 2015,7, 16034-16038
[4] M. Weis, K. Balin, R. Rapacz, A. Nowak, M. Lejman, J. Szade, and P. Ruello, *Phys. Rev. B* 92, 2015, 014301.

Simulations of scanning gate microscopy imaging of the spin-orbit interaction in 2DEG in presence of in-plane magnetic field

K. Kolasiński, B. Szafran

AGH University of Science and Technology, Faculty of Physics and Applied Computer Science, al. Mickiewicza 30, 30-059 Kraków, Poland

In the scanning gate microscopy (SGM) a negatively charged tip of an atomic force microscope scans the area above the sample inducing a local depletion of the two dimensional electron gas (2DEG) buried shallow beneath the surface. This depletion behaves as a movable scatterer for the Fermi level electrons which affects the conductance G of the device. By measuring G as a function of tip parameters (position/voltage) one records conductance maps which reveal properties of the coherent charge and spin transport within 2DEG.

We investigate the possibility of mapping of the electron band structure near the Fermi level exploiting the spin-dependent backscattering induced by the tip and the resulting interference with the incident electron waves from SGM conductance maps of mesoscopic devices with quantum point contacts (QPC) [1]. For the systems with large Lande factor and in the presence of the external in-plane magnetic field the interference fringes in the conductance maps form beating pattern due to spin-dependence of the Fermi wavelengths [2], but this pattern does not depend on the magnetic field orientation, unless the spin-orbit coupling SO is present. In presence of the SO coupling the electron when scattered experiences precession of its spin due to rotation of the momentum-dependent effective magnetic field [3], and the interference potentially involve both spin branches. In case of the presence of the in-plane magnetic field and SO interaction the spin mixing becomes possible. Its consequence is an appearance of the dependence of the beating patterns on the orientation of the magnetic field. We demonstrate that the shape of the Fermi level structure can be traced back from the beatings using the Fourier transform analysis. As a result one should be able to extract the SO coupling constant from conductance mapping in the real space.

[1] M. A. Topinka, et al., Nature, 183-186. (2001)
[2] A. Kleshchonok, et al.,Phys. Rev. B 91, 125416 (2015)
[3] L. Meier, et al., Nature Phys., 650-654. (2007)

On the spin memory effect in InAs quantum dash emitting at 1.55 μm

M. Syperek [1], Ł. Dusanowski[1], J. Misiewicz[1], A. Somers[2], J. P. Reithmaier[2,3]
S. Höfling[2,4], and G. Sęk[1]

[1] *Laboratory OSN, Division of Experimental Physics, Wrocław Univ. of Science and Technology, Wrocław, Poland*
[2] *Technische Physik, University of Würzburg and Wilhelm-Conrad-Röntgen-Research Center for Complex Material Systems, Würzburg, Germany*
[3]*INA, University of Kassel, Kassel, Germany*
[4]*School of Physics and Astronomy, University of St. Andrews, St. Andrews, UK*

Recently, the InAs on InP QDash-based non-classical single photon emitter operating at 1.55 μm has been demonstrated [1] along with the possibility to diminish the confined exciton fine structure splitting [2]. While the former clearly shows QDash capabilities to generate single photons at a time, the latter can lead soon to demonstration of polarization-entangled photons at telecommunication wavelengths, essential for e.g. quantum repeater technology. Since epitaxial nanostructures as QDashes can be considered as a bridge platform between the solid-state quantum information storage/operation and the quantum state of light, it is crucial to investigate properties of the confined spin state that can mediate the exchange process of quantum information and constitute the spin memory element.

We demonstrate an impact of different spin-injection scenarios on the possibility to read-out the written exciton/electron spin state confined in a QDash. The spin initialization as well as read-out processes are realized by all-optical means. A properly polarized train of femtosecond or picosecond laser pulses creates the spin excitation in a QDash, whereas analysis of the photoluminescence signal (degree of polarization-DOP as a function of time or averaged in time) provides information about the confined spin state, e.g. existence of the spin memory and its storage time. First, we have focused on the possibility to observe an exciton spin memory (ESM) under non-resonant photo-injection. This revealed existence of a strong DOP "background" of ~27% that is not connected to population of a spin state but it is due to intrinsic properties of QDashes. The ESM is observed after the spin injection into the wetting layer as indicated by enhanced DOP in respect to the intrinsic one. This result shows partial preservation of the exciton spin state after relaxation process down to the QDash ground state, with the further possibilities to be recovered in the emission. The most pronounced ESM is obtained by utilizing a single longitudinal optical phonon-mediated process for the spin injection scheme. This led to further increase in the contrast between the "background" DOP and the actual one by ~35%, i.e. indicates on easy recovery of the spin memory state. Despite existence of the ESM effect the measured spin relaxation time reaches 1.7 ns that is comparable to the exciton decay time. It raises the question about possible spin relaxation mechanisms for such types of quantum structures. A high "background" DOP suggests that strong heavy-light hole mixing might be responsible for efficient relaxation channel of the spin state injected into such large nanostructures made of InAs on InP(001). In order to omit the above-mentioned limitation we propose to use a spin state of a resident electron that is addressed by utilizing the intermediate trion state. Initial results show a long spin memory effect that overcomes significantly the exciton spin lifetime.

[1] Ł. Dusanowski, et al. *Appl. Phys. Lett.* **105**, 021909 (2014).
[2] P. Mrowiński, et al. *Appl. Phys. Lett.* **106** 053114 (2015).
Work is supported by grant No. 2011/02/A/ST3/00152 of the National Science Centre in Poland.

Spin properties of the indirect exciton in indirect band-gap (In,Al)As/AlAs quantum dot ensembles

J. Debus[1], T. S. Shamirzaev[2], D. Dunker[1], J. Rautert[1], V. F. Sapega[3], D. R. Yakovlev[1,3], and M. Bayer[1,3]

[1] *Experimental Physics 2, TU Dortmund University, Dortmund, Germany*
[2] *Institute of Semiconductor Physics, Russian Academy of Sciences, Novosibirsk, Russia*
[3] *Ioffe Institute, Russian Academy of Sciences, St. Petersburg, Russia*

While semiconductor quantum dots (QDs) have been established as efficient light emitters and detectors in optoelectronics, other applications are only prospective so far. Particular examples are implementations in spin electronics and quantum information technologies. For these purposes, the QDs are typically loaded with resident carriers whose spins are well protected from relaxation by the three-dimensional confinement. In this context, exciton complexes are often used for spin manipulation, but are considered as less perspective as information carriers. This reservation is primarily related to the limited exciton lifetime of about a nanosecond, being too short to provide sufficient coherent manipulation for quantum information. This situation may change if the exciton lifetime could be extended significantly.

An appealing possibility is the realization of QDs with a band gap which is indirect in real or momentum space. We focus on self-assembled (In,Al)As/AlAs QDs, for which dependent on the dot size a crossover of the lowest conduction band states between the Γ- and X-valley occurs, reflected by the lifetime of the corresponding exciton: this exciton is formed by a Γ-valley heavy-hole and an electron contributed by the Γ- and X-valley, whereby both carriers are located within the QD. If the Γ- and X-electron states become admixed, the lifetime of that exciton can be as long as hundreds of μs [1], which may allow for sufficient manipulation within this time span.

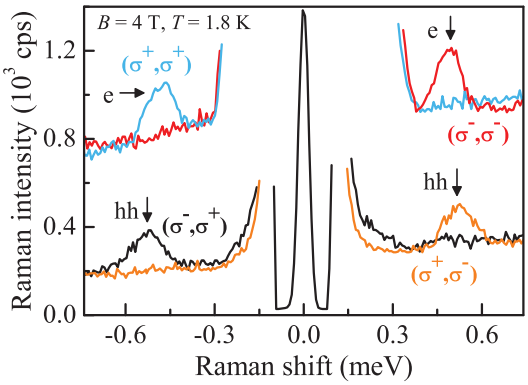

We report on spin properties of the indirect exciton in undoped (In,Al)As/AlAs quantum dots studied by time-resolved photoluminescence and resonant spin-flip Raman scattering (SFRS). The SFRS is used to characterize the Γ-X-state mixing and, as shown in the figure, it allows for initializing as well as orienting the spins of the electron (e), heavy hole (hh), and, in particular, indirect exciton with coherent manipulation efficiencies of up to 20 % [2]. Besides a long and thermally robust spin relaxation time T_1 of up to 200 μs at an external magnetic field of $B = 4$ T [3], we have recently found a high optical orientation degree for the indirect exciton under quasi-resonant excitation at low fields in the mT-range. It ranges around 80 % at 50 mT depending strongly on the excitation and detection energies as well as optical excitation density. Furthermore, the temporal evolution of the circular polarization degree of the photoluminescence changes its sign in the μs-range thus hinting at dark and bright indirect excitons contributing by their different spin dynamics.

[1] T. S. Shamirzaev, J. Debus, D. S. Abramkin et al., *Phys. Rev. B* **84**, 155318 (2011).
[2] J. Debus, T. S. Shamirzaev, D. Dunker et al., *Phys. Rev. B* **90**, 125431 (2014).
[3] D. Dunker, T. S. Shamirzaev, J. Debus et al., *Appl. Phys. Lett.* **101**, 142108 (2012).

Application of Ion Beams to Fabricate and Tune Properties of Dilute Ferromagnetic Semiconductors

Shengqiang Zhou[1], Ye Yuan[1], M. Sawicki[2], A. W. Rushforth[3], K. W. Edmonds[3], R. P. Campion[3] and B. L. Gallagher[3], C. Timm[4], M. Helm[1]

[1] *Helmholtz-Zentrum Dresden-Rossendorf, Dresden, 01328, Germany*
[2] *Institute of Physics, Polish Academy of Sciences, Warszawa, Poland*
[3] *University of Nottingham, Nottingham NG7 2RD, UK*
[4] *Technische Universität Dresden, 01062 Dresden, Germany*

Combining semiconducting and ferromagnetic properties, dilute ferromagnetic semiconductors (DFS) have been under intensive investigation for more than two decades. Mn doped III-V compound semiconductors have been regarded as the prototype of the type. In this contribution, we will show how the implantation technique, a standard method for doping Si in microelectronic industry, can be utilized in fabricating and deeper understanding of DFS. First, ion implantation followed by pulsed laser melting (II-PLM) provides an alternative to the widely used low-temperature molecular beam epitaxy (LTMBE) approach in the preparation of diverse DFS. The prepared DFS materials exhibit pronounced magnetic anisotropy, large X-ray magnetic circular dichroism as well as anomalous Hall effect and magnetoresistance [1-9]. Going beyond LT-MBE, II-PLM is successful to bring two new members, GaMnP and InMnP, into the family of III-Mn-V. Both GaMnP and InMnP films show clear signatures of ferromagnetic coupling and an insulating behavior. Second, helium ions can be used to precisely compensate the holes while keeping the Mn concentration constant [10-12]. We monitor the change of Curie temperature (T_C) and conductivity. For a broad range of samples including (Ga,Mn)As and (Ga,Mn)(As,P) with various Mn and P concentrations, we observe a smooth decrease of T_C over a wide temperature range with carrier compensation while the conduction is changed from metallic to insulating. In the low compensation regime, we can tune the uniaxial magnetic easy axis of (Ga,Mn)(As,P) from out-of-plane to in-plane with an isotropic-like intermediate state. These materials synthesized or tailored by ion beams provide an alternative avenue to understand how carrier-mediated ferromagnetism is influenced by localization.

[1] M. Scarpula, et al., *Phys. Rev. Lett.* 95, 207204 (2005).
[2] D. Bürger, S. Zhou, et al., *Phys. Rev. B* 81, 115202 (2010).
[3] S. Zhou, et al., *Appl. Phys. Express* 5, 093007 (2012).
[4] M. Khalid, …, S. Zhou, *Phys. Rev. B* 89, 121301(R) (2014).
[5] Y. Yuan, … S. Zhou, *IEEE Trans. Magn.* 50, 2401304 (2014).
[6] M. Khalid, …, S. Zhou, *J. Appl. Phys*. 117, 043906 (2015).
[7] Y. Yuan, …, S. Zhou, *J. Phys. D: Appl. Phys.* 48, 235002 (2015).
[8] S. Zhou, *J. Phys. D: Appl. Phys.* 48, 263001 (2015).
[9] Y. Yuan, …, S. Zhou, ACS Appl. Mater. Interfaces, 8, 3912 (2016).
[10] L. Li, S. Yao, S. Zhou, et al., *J. Phys. D: Appl. Phys.* 44 099501 (2011).
[11] L. Li, …, Shengqiang Zhou, *Nucl. Instr. Meth. B* 269, 2469-2473 (2011).
[12] S. Zhou, et al., *arXiv:1602.06790* (2016).

Phonon-mediated generation of quantum correlations between quantum dot qubits

Jan Krzywda[1,2], Katarzyna Roszak[1]

[1] *Department of Theoretical Physics, Faculty of Fundamental Problems of Technology, Wrocław University of Technology, 50-370 Wrocław, Poland*
[2] *Faculty of Physics, University of Warsaw, 02-093 Warsaw, Poland*

Quantum correlations play a crucial role in the understanding and possible implementation of any quantum computation algorithm. Unfortunately the influence of the environment is usually hostile to entanglement [2], which is the standard type of quantum correlations used for quantum computation.

It has been recently shown that a weaker type of quantum correlations, those which are measured by the quantum discord and which are sometimes present in separable (non-entangled) states, are also useful from the perspective of quantum computation [3]. Nevertheless while an interaction with the environment is also detrimental to the quantum discord, the latter is expected to be much more robust against the influence of environment compared to entanglement, and it may even be enhanced, under some special conditions.

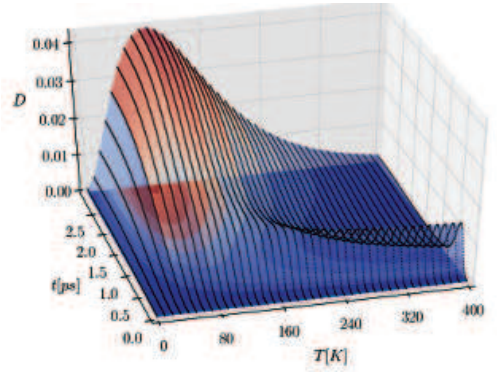

Figure 1: Exemplary time and temperature dependence of the rescaled discord for the initial equal superposition qubit state and thermal state of the environment.

In order to investigate the following idea, we study the generation of quantum correlations between two excitonic quantum dot qubits due to their interaction with the same phonon environment [1]. Such generation results from the fact that during the pure dephasing process at finite temperatures, each exciton becomes entangled with the phonon environment [4]. The extent to which the correlations are generated at different temperatures is a trade-off between the phonon effects being small at low temperatures, and small entanglement generation for a high - temperature environment.

During the study, we show that such an interaction will lead to the creation of finite quantum discord values between the two qubits, if the distance between them is small enough the environments cannot be treated as separate, and the temperature is modest. Because the phonon-induced dephasing of quantum states is partial [5], the generated discord is robust until the influence of other, slower decoherence mechanisms become dominant.

Finally we identify two most prominent features of the evolution during the generation of the quantum discord, their origin and parameter dependence (which are both different) and interpret them with the help of X-states whose quantum correlations are easier to quantify.

[1] J. Krzywda and K. Roszak *Sci. Rep.* **6**, 23753 2016. *ArXiv:1511.08434*
[2] T. Yu and J. H. Eberly, *Phys. Rev. Lett.* **93**; 140404, 2004.
[3] H. Olivier and W. Żurek *Phys. Rev. Lett.* **88**; 117901, 2001.
[4] K. Roszak and P. Machnikowski, *Phys. Rev. A* **73**, 022313 2006.
[5] K. Koszak and Ł. Cywiński, *Phys. Rev. A* **92**; 032310, 2015.

P-shell exciton complexes with neutral-exciton-like exchange interaction in CdTe/ZnTe quantum dots

T. Smoleński[1], T. Kazimierczuk[1], M. Goryca[1], M. Koperski[1], P. Wojnar[2], A. Golnik[1], P. Kossacki[1]

[1] *Institute of Experimental Physics, Faculty of Physics, University of Warsaw, Poland*
[2] *Institute of Physics, Polish Academy of Sciences, Warsaw, Poland*

Carrier-carrier interactions are an important factor determining energy of exciton complexes in self-assembled quantum dots (QDs). In particular, the fine structure of a given excitonic complex is a result of the exchange interaction. For example, in the simplest case of the neutral exciton consisting of a single electron and a single hole there are four eigenstates with characteristic energy spectrum of a pair of bright states separated from a pair of dark states by energy commonly denoted by δ_0. This *isotropic* exchange splitting is usually accompanied by a smaller *anisotropic* exchange splitting of the two bright states by energy δ_1. Such a picture is known to be valid for the ground state neutral exciton in different material systems. In general, more complex excitons exhibit more complex spectra. However, in our work we demonstrate that the same pattern of exchange interaction can be observed for a few other excitonic complexes.

Here we focus on two exciton complexes: a "hot" neutral exciton with both carriers on the *p*-shell and a doubly negatively charged exciton (X^{2-}) recombining to a two-electron singlet state. By using either the excitation spectroscopy or the non-resonant photoluminescence we show that in both cases the optical spectrum features a single pair of orthogonally polarized lines, in close analogy to the neutral exciton. Similarly, in each case the magnetic field in Faraday configuration increases the observed splitting according to a general formula: $\sqrt{(g\mu_B B)^2 + \delta_1^2}$. By applying the magnetic field in Voigt configuration or by comparison against the emission to the triplet state in the case of X^{2-} we additionally determine the corresponding isotropic exchange constant δ_0. As a result, we fully describe three cases of exchange interaction: between *s*-shell electron and *s*-shell hole (from the neutral exciton), between *p*-shell electron and *p*-shell hole (from the "hot" neutral exciton), and between *p*-shell electron and *s*-shell hole (from the doubly negatively charged exciton).

We conclude that both *p*-shell neutral exciton and doubly negatively charged exciton are viable substitutes for the neutral exciton regarding the structure of the energy spectrum, which opens a possibility to explore different regimes of exchange parameter values. A proof-of-concept for this idea is an observation of a characteristic 6-fold splitting of doubly negatively charged exciton in a QD doped with a single Mn^{2+} ion.

[1] T. Smoleński, M. Koperski, M. Goryca, P. Wojnar, P. Kossacki, T. Kazimierczuk, *Phys. Rev. B* **92**, 085415 (2015).
[2] T. Kazimierczuk, T. Smoleński, J. Kobak, M. Goryca, W. Pacuski, A. Golnik, K. Fronc, Ł. Kłopotowski, P. Wojnar, P. Kossacki, *Phys. Rev. B* **87**, 195302 (2013).

Room temperature polariton lasing in a ZnTe based microcavity containing a single CdSe/(Cd,Mg)Se quantum well

K. Sawicki, J.-G. Rousset, R. Rudniewski, W. Pacuski, J. Suffczyński and M. Nawrocki

Institute of Experimental Physics, Faculty of Physics, University of Warsaw
Pasteura 5 St., PL-02-093 Warsaw, Poland

Exciton-polariton condensates exhibit several unique features motivating researchers to develop new microcavity systems. One of the most important observations in this field was a polariton lasing achieved under either optical or electrical pumping. Reports on polariton lasing at room temperature, which is a prerequisite for device implementations are, however, still limited to UV and blue spectral range. They concentrate on GaN, ZnO and ZnSe based structures, where exciton binding energy is much higher than in semiconductors with moderate band gaps.

In this work, we report on a room temperature polariton lasing in red spectral range. It is achieved under optical pumping in a new microcavity system with a CdSe quantum well (QW). Studied structures contain a single $(Cd_{0.8},Mg_{0.2})Se$ $\lambda/2$-microcavity embedded between Distributed Bragg Reflectors (DBR). The DBRs are constituted by ZnTe layers and short period superlattices MgSe|ZnTe|MgTe|ZnTe. A 10 nm thick CdSe QW is placed inside the microcavity with Q over 3700 (determined at T = 7 K). The DBRs, and both the CdSe QW and (Cd,Mg)Se are almost lattice matched to ZnTe, which enables pseudomorphic growth mode, without relaxation. The sample does not exhibit degradation when exposed to the ambient atmosphere, despite a relatively high Mg content in the DBRs and barriers. The micro-photoluminescence is excited at 300 K or 10 K using a femtosecond laser (λ_{exc} = 580 nm).

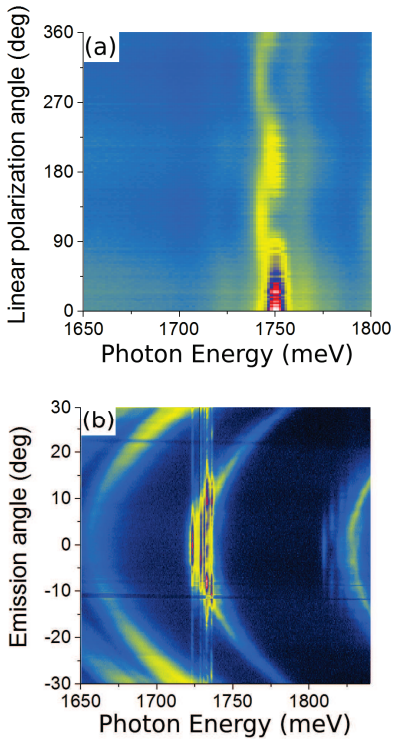

Figure 1: μ-Photoluminescence spectra as a function of a) linear polarization angle and b) emission angle.

The emission intensity *vs* the excitation power reveals a complex dependence including two lasing thresholds. The lower one is attributed to the polariton lasing characteristic for the strong coupling regime, due to the observed emission blueshift and narrowing being the signature of massive occupation of the lowest energy polariton states. The higher threshold is associated with the photon lasing, when the conditions of strong coupling vanish due to a heating of the sample and the increase of carrier concentration. The threshold powers at 300 K are about 42 kW/cm^2 for polariton lasing and about 707 kW/cm^2 for photon lasing. The thresholds decrease with the temperature, attaining respectively 7 kW/cm^2 and 28 W/cm^2 for 10 K. Expected linear polarization of the polariton lasing (Figure 1a) is observed. Momentum space measurements reveal a quantization of energy levels from which the lasing occurs (Figure 1b), which suggests that local traps might be responsible for spontaneous condensation of polaritons triggering the lasing action.

The presented new type of structure enabling the polariton lasing at room temperature provides new perspectives into the both fundamental studies and applications.

Coulomb mediated hybridization of excitons in quantum dot molecules

P.-L. Ardelt[1,2], K. Gawarecki[3], K. Müller[1,4], A.M. Waeber[1], A. Bechtold[1], K. Oberhofer[1], J.M. Daniels[5], F. Klotz[1], M. Bichler[1], T. Kuhn[5], H.J. Krenner[2,6], P. Machnikowski[3], J.J. Finley[1,2]

[1] *Walter Schottky Institut and Physik-Department, Technische Universität München, Am Coulombwall 4, 85748 Garching, Germany*

[2] *Nanosystems Initiative Munich (NIM), Schellingstrasse 4, 80339 Mnchen, Germany*

[3] *Department of Theoretical Physics, Faculty of Fundamental Problems of Technology, Wrocław University of Technology, Wybrzeże Wyspiańskiego 27, 50-370 Wrocław, Poland*

[4] *E.L.Ginzton Laboratory, Stanford University, Stanford, CA 94305, USA*

[5] *Institut für Festkörpertheorie, Westfälische Wilhelms-Universität Münster, Wilhelm-Klemm-Strasse 10, 48149 Münster, Germany*

[6] *Lehrstuhl für Experimentalphysik 1 and Augsburg Centre for Innovative Technologies (ACIT), Universität Augsburg, Universitätsstr. 1, 86159 Augsburg, Germany*

In this contribution we present the results of experimental and theoretical analysis of Coulomb mediated hybridization of exciton states in InGaAs double QDs [1]. The combined PL, PLE and photocurrent response of a QD molecule as a function of the axial electric field reveals avoided level crossings that do not arise from the dominant single-particle tunnel coupling. We identify a new few-particle coupling mechanism stemming from Coulomb interactions between different neutral exciton states [2]. Such Coulomb resonances hybridize the exciton wave function over four different electron and hole single-particle orbitals.

Here, we focus on the comparison between the experimental results and theoretical modeling based on the kp method: the electron and hole states are calculated within 8-band kp method in the presence of strain and piezoelectric field in the 2nd order in strain tensor elements. We take into account non-uniform InGaAs distribution in the dots according to the trumpet-shape composition [3]. Then, the exciton states are calculated using the configuration interaction method.

We find out that microscopic eight-band kp calculations correctly reproduce experimental observations only if a realistic quantum dot geometry is taken into account. Our theoretical analysis reveals that the Coulomb resonances arise from broken axial symmetry in the QD molecule.

[1] P.-L. Ardelt, K. Gawarecki, K. Müller, A.M. Waeber, A. Bechtold, K. Oberhofer, J.M. Daniels, F. Klotz, M. Bichler, T. Kuhn, H.J. Krenner, P. Machnikowski, G. Abstreiter, J.J. Finley, Phys. Rev. Lett. **116**, 077401 (2016),

[2] J. M. Daniels, P. Machnikowski, and T. Kuhn, Phys. Rev. B **88**, 205307 (2015).

[3] M. A. Migliorato, A. G. Cullis, M. Fearn, and J. H. Jefferson, Phys. Rev. B **65**, 115316 (2002).

Stability of Laughlin type and composite fermion states in Chern insulators

Pawel Potasz and Błażej Jaworowski[1]

[1] *Wroclaw University of Science and Technology, Wrocław, Poland*

Chern insulators are band insulators exhibiting a nonzero Hall conductance but preserving the lattice translational symmetry. [1] Fractional Chern Insulators (FCI) are partially filled Chern Insulators that exhibit fractional quantum Hall effect. [3-5] This happens when energy of two particle interaction substantially exceed energy dispersion of topologically nontrivial band. In this work, we consider Lieb lattice within tight-binding model which characterizes by three energy bands with a peculiar perfectly flat middle band. We show that the topology of the energy bands can be controlled by next-nearest-neighbor hoppings in the Haldane model and a staggered sublattice potential. [6] We analyze an existence of Laughlin type and composite fermion (CF) states in Fractional Chern Insulators (FCI) using exact diagonalization. We first show that the system at 1/3 filling of quasi flat band with nontrivial topology exhibits an incompressible phase characterized by a 3-fold degenerate ground state with spectral flow upon flux insertion, constant density, and counting of levels below the gap identical to that of Laughlin 1=3 quasiholes. This Laughlin type phase exists in a large region of parameter space which we show is related to constant standard deviation of Berry curvature [7]. Next, we consider different filling factors searching for CF phases. We analyze many-body energy spectra for 2/5 and 3/7 filling factors, identify CF states and look for factors responsible for their stability.

[1] F. D. M. Haldane, *Phys. Rev. Lett*. **61**, 2015 (1988).
[2] K. Sun, Z. Gu, H. Katsura, and S. Das Sarma, *Phys. Rev. Lett.* **106**, 236803 (2011).
[3] T. Neupert, L. Santos, C. Chamon, and C. Mudry, *Phys. Rev. Lett.* **106**, 236804 (2011).
[4] D. Sheng, Z.-C. Gu, Gu, K. Sun, and L. Sheng, *Nat. Commun.* **2**, 389 (2011).
[5] N. Regnault and B. A. Bernevig, *Phys. Rev. X* **1**, 021014 (2011).
[6] A. Zhao and S.-Q. Shen, *Phys. Rev. B* **85**, 085209 (2012).
[7] B. Jaworowski, A. Manolescu, and P. Potasz, *Phys. Rev. B* **92**, 245119 (2015).

Double-Weyl Nodes And Fermi Arcs In Magnetically Doped Cd_3As_2

Rafał Rechciński and Jakub Tworzydło

Faculty of Physics, University of Warsaw, L. Pasteura 5, 02-093 Warszawa, Poland

The well-known semiconductor compound cadmium arsenide (Cd_3As_2) has recently attracted new interest due to topological properties of its band structure, which place it within the class of Dirac semimetals, a 3D analogue of graphene [1].

The two Dirac cones present in the band structure (along the k_z axis) can be split into a number of Weyl cones (their non-spin-degenerate counterparts) by lifting the spin-degeneracy with the magnetic field. To demonstrate this we consider an 8-band $\mathbf{k} \cdot \mathbf{p}$ model of Cd_3As_2 doped with manganese atoms (Mn). The giant Zeeman splitting, arising due to the presence of magnetic impurities, allows for a robust separation of the Weyl points in momentum space.

We observe that under magnetic field parallel to the z axis each of the cones splits into the four Weyl nodes, two with the chiral charge ± 1 and other two with the chiral charge ± 2 (double-Weyl nodes). The chiral charges are confirmed by a numerical calculation of associated Chern numbers. The double-Weyl nodes exhibit quadratic dispersion in two directions, in contrast to the single-Weyl nodes, around which the bands disperse linearly [2]. The surface Fermi arcs, although present, are not very distinct from the bulk bands.

With the magnetic field parallel to the y axis (and breaking the C_4 symmetry) the cones split into pairs of single-Weyl nodes. The nodes are connected by well-defined, though unusually shaped, Fermi arcs, located on the opposite sides of the sample. The distinctive shape is associated with emergence of two additional Weyl nodes, higher in the energy spectrum.

[1] Z. Wang, H. Weng, Q. Wu, X. Dai, and Z. Fang, *Phys. Rev. B* **88**, 125427 (2013).
[2] C. Fang, M. Gilbert, X. Dai, and B. A. Bernevig, *Phys. Rev. Lett.* **108**, 266802 (2012).

Electric field driven topological phase transition in InN/GaN quantum wells

Sławomir P. Łepkowski [1] **and Witold Bardyszewski** [2]

[1] *Institute of High Pressure Physics - Unipress, Polish Academy of Sciences, ul. Sokołowska 29, 01-142 Warsaw, Poland*
[2] *Faculty of Physics, University of Warsaw, ul. Pasteura 5, 02-093 Warszawa, Poland*

The topological insulators, existing in two-dimensional (2D) and three-dimensional material systems, are a new state of matter characterized by a bulk excitation gap and topologically protected metallic states on their surface or edge [1]. The 2D TIs have so far been realized only in HgTe/CdTe and InAs/GaSb quantum well (QW) systems [2]. However, it was theoretically predicted that also in narrow InN/GaN QWs grown along (0001) crystallographic direction of the wurtzite structure, due to the extremely large built-in electric field originating from the piezoelectric effect and the spontaneous polarization, one may close the energy gap and induce the 2D TI state [3]. Recently, we have shown that due to negative band gap pressure coefficient of InN/GaN QWs, it is possible to close the band gap in these structures by applying hydrostatic pressure, which allows for an observation of pressure-induce topological phase transition from the normal insulator phase to the TI state [4].

In this work, we present a theoretical study showing that the topological phase transition in InN/GaN QWs can be also effectively driven by applying external electric field. We use eight band k·p method to construct a two-dimensional six-band effective Hamiltonian, which takes into account the coupling between the conduction, light hole and heavy hole states [3,4].The effective Hamiltonian is used to calculate the electronic states in Hall bar structures of different widths. The calculations have been performed for two multiple InN/GaN QW structures, one with the QW width of 1.35 nm and the barrier thickness of 40 nm and the other, having the widths of QWs and barriers equal to 1.4 nm and 20 nm, respectively. The thickness of Hall bar structures was varied from 100 to 1000 nm. The obtained results show that applying positive gate voltage in the range from 0 to 2 V to the first QW structure, one can tune the system from normal insulator to the TI state, whereas applying negative voltage from 0 to –1.5V to the second QW structure, it is possible to observe the reverse transition from the TI state to the normal insulator phase. In both cases, the critical value of the gate voltage for the topological phase transition depends also on the width of a Hall bar and e.g. in the case of 1.4 nm-wide QWs, it varies from –0.9 to -.1.25 V for Hall bars with the width changing from 100 to 1000 nm, respectively.

We also study the influence of the external electric field on the dispersion of the edge states. Our calculations show that near the topological phase transition, there is a significant spin splitting of the upper and lower branches of the edge states dispersion curve, which originates from the lack of mirror symmetry of the QW potential. This effect depends significantly on the Hall bar width, which determines the coupling between the edge states localized at the opposite edges. Interestingly, we observe that spin splitting of the edge states unexpectedly decreases with applying external gate voltage, although the electric field in the QW layer increases simultaneously.

This work was supported by the Polish National Science Center, Project No. 2012/07/B/ST3/03174.

[1] M. Z. Hasan and C. L. Kane, *Rev. Mod. Phys.* **82**, 3045 (2010).
[2] M. Konig et al., *Science* **318**, 766 (2007);L. Du et al., *Phys .Rev. Lett.* **114**, 096802 (2015).
[3] M. S. Miao et al., *Phys. Rev. Lett.* **109**, 186803 (2012).
[4] S. P. Łepkowski and W. Bardyszewski, submitted to *Phys. Rev. B.*

1-D Fe-rich Konbu phase in InAs obtained by Fe ion implantation and pulsed laser melting

Y. Yuan[1], M. Sawicki[2], R. Hübner[1], K. Potzger[1], E. Weschke[3], T. Dietl[2], M. Helm[1], and S. Zhou[1]

1 Helmholtz-Zentrum Dresden-Rossendorf, Dresden, Germany

2 Institute of Physics, Polish Academy of Sciences, Warszawa, Poland

3 Helmholtz-Zentrum Berlin fur Materialien und Energie, Berlin, Germany

Transition-metal rich semiconductor nanostructures driven by spinodal decomposition are drawing considerable attention due to wide prospects of functionalization [1]. However, the complexity of the magnetic cations aggregation (e.g. the competition between *p-d* hybridization driven attractive force between magnetic cation, entropy terms, and kinetic barriers) hinders obtaining nano-clusters with the desirable structure. Here, a 1-dimensional (In,Fe)As mixed Konbu phase is tailoring by employing ion implantation and subsequent pulsed laser melting (shown in Fig. 1). These Fe-rich nano-columns are fully commensurate with the InAs host lattice and exhibit an isotropic super-paramagnetic behavior. The XAS/XMCD result shows that Fe atoms with valence +2 and +3 are co-existing and both are spin-polarized. Therefore, it is likely that the magnetism in these Fe-rich nano-columns can be provided via the double exchange mechanism as previously described for the Cr-rich phase in (Zn, Cr)Te [2]. However, it still remains to be clarified why these distinctive structures are formed only in InAs: Fe, but not in other III-Mn-V systems obtained by the same method.

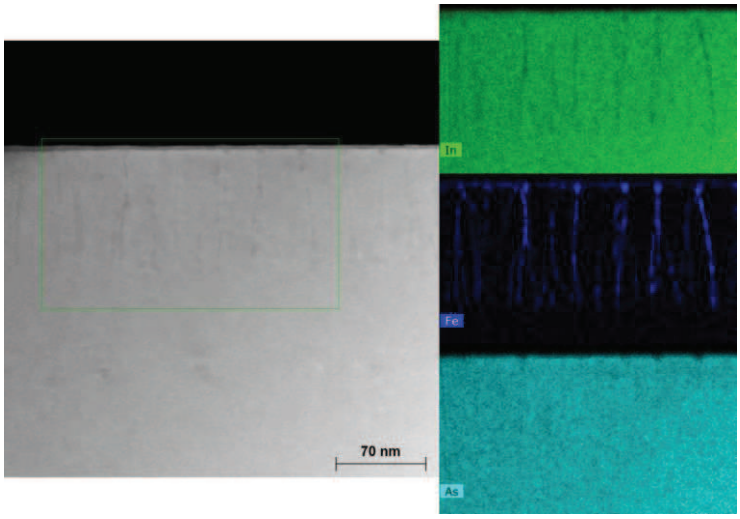

Fig. 1. Cross-sectional TEM image of the (In, Fe)As sample after PLM, and the insets show the EDXS (green: In, deep blue: Fe, and light blue: As) mapping images of the selected region.

[1]. T. Dietl, et al., *Rev. Mod. Phys.*, **87**, 1311-1377 (2015)

[2]. K. Kanazawa, et al., *Nanoscale*, **6**, 14667-14673 (2014)

Galvanomagnetic methods of Curie Temperature determination in low-T_C (Ga,Mn)As samples.

A. Kwiatkowski[1], M. Gryglas-Borysiewicz[1], P. Juszyński[1], J. Przybytek[1], M. Sawicki[2], J. Sadowski[2,3], D. Wasik[1] and M. Baj[1]

[1]*Institute of Experimental Physics, Faculty of Physics, University of Warsaw, Pasteura 5, 02-093 Warsaw, Poland*
[2]*Institute of Physics, Polish Academy of Sciences, al. Lotników 32/46, 02-668 Warsaw, Poland*
[3]*MAX-IV laboratory, Lund University, P.O. Box 118, 221 00 Lund, Sweden*

Nowadays, it is quite common to use the measurement of resistivity tensor (ρ_{xx} and ρ_{xy}) to study magnetic phase transition in (Ga,Mn)As [1, 2, 3], since it is relatively easy to implement especially in the investigations of the influence of external physical parameters (e.g electric field or pressure) on the Curie temperature (T_C). There are two basic methods to determine T_C: 1) the analysis of the peak in the $d\rho_{xx}/dT$ versus T dependence [1, 2, 4] and 2) the analysis of Arrot plots prepared on the basis of $\rho_{xx}(B)$ and $\rho_{xy}(B)$ isotherms measured at high magnetic fields [3]. In this work we critically analyze applicability of these methods for a set of (Ga,Mn)As samples with Curie temperatures in the range from 15 K to 105 K, and two types of magnetocrystalline anisotropies (easy axis in plane and out of plane). We show that the first method works very well in the case of samples with metallic character of resistivity but it is useless in the case when the resistivity has semiconducting character. Next, considering the second of the above methods, we show that in the case of samples with in-plane easy axis of magnetic anisotropy it leads to a large divergence of T_C values (of the order of 10 K) obtained under different assumptions which are necessary while preparing the Arrot plot. In the case of samples with out-of-plane easy axis these assumptions do not have such an impact on the obtained values of T_C as in the first case. Moreover in this work we show a number of ways (other than Arrot plots) to get some characteristic and clear features (observables) from high magnetic field isotherms $\rho_{xx}(B)$ and $\rho_{xy}(B)$, that are closely related to the ferromagnetic – paramagnetic phase transition. These features are very easy to follow as a function of external physical factors. We also show that the measurement of $\rho_{xx}(B)$ and $\rho_{xy}(B)$ in the regime of small magnetic fields allows for the indirect determination of magnetic susceptibility, which in the vicinity of the phase transition is in the form of a characteristic peak. Finally, we discuss the influence of magnetic inhomogeneity of the samples on the results obtained.

[1] V. Novák, K. Olejník, J. Wunderlich, M. Cukr, K.Výborný, A. W. Rushforth, K. W. Edmonds, R. P. Campion, B. L. Gallagher, J. Sinova and T. Jungwirth, *Phys. Rev. Lett.* **101**, 077201 (2008).
[2] M. Wang, R. A. Marshall, K. W. Edmonds, A. W. Rushforth, R. P. Campion, and B. L. Gallagher, *Appl. Phys. Lett.* **104**, 132406 (2014).
[3] Y. Nishitani, D. Chiba, M. Endo, M. Sawicki, F. Matsukura, T. Dietl and H. Ohno, *Phys. Rev. B* **81**, 045208 (2010)
[4] M. Gryglas-Borysiewicz, A. Kwiatkowski, M. Baj, D. Wasik, J. Przybytek, and J. Sadowski, *Phys. Rev. B* **82**, 153204 (2010)

Hydrostatic pressure induced band inversion in $Pb_{1-x}Sn_xSe$ substitutional alloys

A. Kwiatkowski[1], K. Puźniak[1], D. Wasik[1], K. Dybko[2], M. Szot[2], A. Szczerbakow[2], T. Story[2], P. Pfeffer[2] and W. Zawadzki[2]

[1]*Faculty of Physics, University of Warsaw, Pasteura 5, 02-093 Warsaw, Poland*
[2]*Institute of Physics, Polish Academy of Sciences, 02-668 Warsaw, Poland*

It has been shown theoretically and experimentally that topologically protected surface states appear in prototypical topological crystalline insulator SnTe [1,2]. These states are inevitably related to relativistic effects of bulk band theory and specific mirror symmetry of crystal unit cell. The energy gap in rock-salt SnTe is located at four equivalent L points of Brillouin zone and conduction and valence bands are in inverted order with respect to PbTe. In consequence, the $Pb_{1-x}Sn_xTe$ substitutional alloy exhibits gap closure and opening as a function of composition x [3], which in turn is equivalent to transforming system from topologically trivial to nontrivial band ordering.

Analogous situation takes place in $Pb_{1-x}Sn_xSe$. For a given composition x, band inversion can be reached either by temperature or pressure [4]. Here we report on transport study of two bulk $Pb_{1-x}Sn_xSe$ (x=0.14, x=0.20) monocrystals obtained by self selecting vapour growth method. The composition x=0.14 was chosen in order that the energy gap (E_g) does not vanish as a function of temperature but pressure only. On the other hand, the composition x=0.20 allows E_g=0 condition to be fulfilled by lowering temperature and applying pressure as well. Both samples were investigated in temperatures ranging from 4.2 K to 300 K and hydrostatic pressures up to 10 kbar. Each time the low-field Hall constant and Hall mobility were measured. The mobility data vs pressure and temperature were analysed within nonparabolic two-band Kane model [3] considering energy dependent relaxation time approximation for various scattering modes [5].

Work supported in part by the Polish National Science Centre Grant No. 2012/07/B/ST3/03607

[1] T.H. Hsieh et al, *Nature Comm.* **3**, 982 (2012).
[2] Y. Tanaka et al, *Nature Physics*, **8**, 800 (2012).
[3] J.O. Dimmock et al, *Phys. Rev. Lett.* **16**, 1193 (1966).
[4] G. Martinez, *Phys. Rev. B* **8**, 4686 (1973).
[5] K. Dybko et al, New J. Phys. **18**, 013047 (2016).

Plasmonic Enhancement of Photoluminescence Intensity in Liquid Exfoliated WS_2 – Silver Island Film Hybrid Structure

Nikodem Czechowski [1], Claudia Backes [2,3], Jonathan N. Coleman [3], Paulina Płochocka [4] and Łukasz Kłopotowski [1]

[1] *Institute of Physics, PAS, al. Lotnikow 32/46, 02-668 Warszawa, Poland*
[2] *Applied Physical Chemistry, Ruprecht Karls University Heidelberg, Im Neuenheimer Feld 253, 69120 Heidelberg, Germany*
[3] *School of Physics and CRANN, Trinity College Dublin, Dublin 2, Ireland*
[4] *LNCMI-T, 143 Avenue de Rangueil, 31400 Toulouse, France*

Hybrid structures, composed of semiconductors and metallic nanoparticles are a group in which plasmon excitation allows for tailoring the optical response of semiconductor [1]. One of the vast possibilities is to use the plasmon excitation to enhance the photoluminescence response of the semiconductor.

Since graphene discovery in 2004, 2D materials focus much attention of the scientific community. Various atomically flat materials are investigated; among them transition metal dichalcogenides (TMD) monolayers form a distinct family of 2D semiconductors with open and direct bandgap, exhibiting photoluminescence at room temperature [2]. Advances in liquid exfoliation of 2D materials and subsequent size selection allows for the preparation of monolayer-enriched dispersions with well-defined size [3]. Such materials are promising candidates to study optical properties as well as fabricate hybrid structures due to the possibility of solution processing.

In this work we report the enhancement of PL intensity of liquid exfoliated WS_2 monolayers, coupled with Silver Island Film (SIF). The hybrid structure was prepared by drop-casting WS_2 on SIF, prepared by reduction of silver nitrate with glucose.

To quantify the enhancement and its spectral dependence, WS_2 PL was measured for three excitation wavelengths (405, 485 and 532 nm) on SIF and on glass. In order to collect statistically significant data, 400 emission spectra for each excitation and substrate was acquired by mapping a 200 μm x 200 μm sample region with 10 μm step for each substrate. Spatial resolution equals to 2 μm. The experiment was carried out at temperature of 7 K.

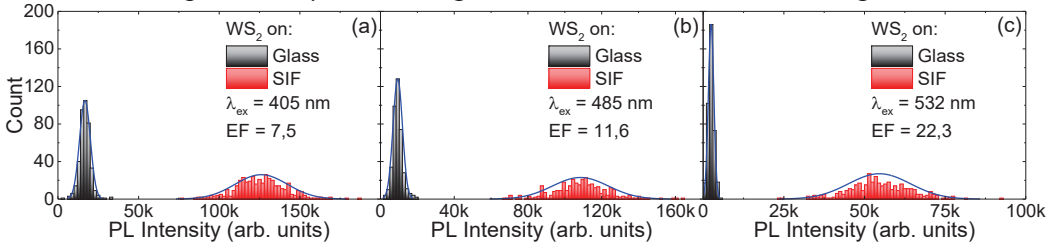

Fig.1. Intensity distributions of monolayer WS_2 PL measured on glass (black bars) and SIF (red bars) for excitation of (a) 405 nm, (b) 485 nm and (c) 532 nm.

This measurement allowed to calculate the enhancement factor; it varies between 8, and 22. Spectral dependence of the EF suggests presence of effects beyond excitation rate enhancement – e.g. Purcell effect. Significant broadening of PL intensity distribution on SIF is observed, revealing SIF inhomogeneity, that is well known from literature.

[1] R. Jiang et al., *Adv. Matt.* **26** (2014), 5274.
[2] Q. H. Wang, et al., *Nat. Nanotechnol.* **7** (2012), 699.
[3] C. Backes et al., ACS Nano 10 (2016), 1589.

Laplace pressure on Co nanopaticles distributed in alumina matrix (Co/Al_2O_3)

G.V. Lashkarev[1], V.P. Kladko[2], M.V. Radchenko[1], M.E. Bugayova[1], Y.Stelmakh[3], L. Krushinskaya[3], A.E.Baibara[1], A.I.Gudymenko[1], L.I.Petrosian[1], T.Osmanov[1], D.Fedorchenko[1]

[1]I.M. Frantsevych Institute for Problems of Material Science, National Academy of Sciences of Ukraine, 3 Krzhizhanovskogo str., Kyiv, Ukraine
[2]V.E. Lashkarev Institute of Semiconductor Physics, av. Nauky 45, Kyiv, Ukraine
[3]E.O. Paton Electric Welding Institute, Academy of Sciences of Ukraine, 68 Antonowich str., Kyiv, Ukraine

Ferromagnetic nanocomposites (FMNC) represent nanoparticles (NP) of ferromagnetic metal (FMM) distributed in diamagnetic matrix. They are related to diluted magnetic semiconductors exposed spinodal decomposition of d-transition metal solution in diamagnetic semiconductors. FMNC layers were deposited by two crucible electron beam evaporation on polycore substrates.

Studies of their magnetic and galvanomagnetic properties demonstrated essential negative magnetoresistivity, obliged to spin-dependent electron tunneling between FMM NP′s through dielectric layer. During our FMNC researches we discovered the following phenomena in these materials: the transition to the spin-glass state, giant thermoelectric power in magnetic field. FMNC layers growing in magnetic field changes the percolation threshold and a temperature of the transition to spin-glass state. Such abundance of spin-dependent phenomena generates the interest to the influence of FM NP′s dimensions on interatomic distances between FMM atoms in NP.

Diminishing of unit cell dimension for NP′s is due to surface tension what leads to Laplace pressure. For the investigation of Laplace pressure effect on Co NP′s we carried out XRD studies of FMNC with Co content of 16,3 and 25,6 at. %, what corresponds to evaluated dimensions of Co nanoparticles about ~ 10 nm[1]. For XRD studies of the facility ARLX′tra (thermo scientific) CuKα irradiation was used. Scanning was fulfilled with a step of 0,005° and signal accumulation time of 1,5 s. The results were compared with the reference XRD in ICDD for bulk Co with hexagonal singony. XRD reflexes of γ-Co are spreaded due to nanosize dimensions of Co NP′s in the accordance with Debye-Sherer equation. On the background of signal fluctuations the generalized diffraction maximum is clearly seen. It is shifted to the side of larger angles for the magnitude of $\Delta 2\theta = 0{,}77°$ in a comparison with the maximum of the reference XRD envelope of bulk γ-Co and testifies to the existence of Co NP′s compression.

The evaluation of surface tension σ according to [2] gives the value about 20kJ/m^2 what is close to the magnitude of 27 kJ/m^2 for Co NP′s in[3]. For their dimensions about ~ 10 nm one receives the Laplace pressure of 8000GPa.

Thus the fulfilled evaluations demonstrate extraordinary high pressure, acting on Co NP′s crystal lattice magnified possibly by the pressure from the side of Co/Al_2O_3 matrix.

Such high pressure leads to diminishing of interatomic distances and to the influence on Curie temperature for Co NP′s.

[1] G. V. Lashkarev, M. V. Radchenko, M. E. Bugaiova, A. I. Dmitriev, V. I. Lazorenko, V. I. Sichkovskyi, W. Knoff, T. Story, Y. A. Stelmakh, and L. A. Krushynskaya., Low Temperature Physics **39**, 66 (2013)

[2] Kliachko Y.A., Kunin L.L., Reports of the USSR Academy of Sciences, **64**, 85 (1949)

[3] *Hong S.,*Curr. Appl. Phys. **3**, 457 (2003)

Electrical and galvanomagnetic properties of ferromagnetic composites Co/Al_2O_3 in magnetic field

G.V.Lashkarev[1], M.V.Radchenko[1], M.E.Bugayova[1], Y.Stelmakh[3], L. Krushinskaya[3], A.E.Baibara[1], T.Story[2], W.Knoff[2], L.I.Petrosian[1], T.Osmanov[1], D.Fedorchenko[1]

[1]I.M. Frantsevych Institute for Problems of Material Science, National Academy of Sciences of Ukraine, 3 Krzhizhanovskogo str., Kyiv, Ukraine
[2]Institute of Physics, Polish Academy of Sciences, Al. Lotnikow 32/46, Warsaw, Poland
[3]E.O. Paton Electric Welding Institute, Academy of Sciences of Ukraine, 68 Antonowich str., Kyiv, Ukraine

Among nanocrystalline magnetic materials the separate place is occupied by ferromagnetic nanocomposites (FMNC), which consist of magnetic nanoparticles (NP′s) distributed in a diamagnetic matrix. Scientific and applied interest in these materials is caused by the possibility of controlling their magnetic and electrical properties by changing the size, shape and concentration of ferromagnetic nanoparticles.

Co/Al_2O_3 FMNC layers were grown by two-crucible electron beam evaporation technique with Co and Al_2O_3 vapors condensation in vacuum on polycore substrates placed in a magnetic field of different directions [1]. The growth of FMNC layers in magnetic field H leads to the their characteristic microstructure with Co NP′s oriented along magnetic field with their longer axes forming fibers observed by electronic microscopy techniques. This magnetoactive technology of ferromagnetic nanocomposites opens new possibilities for the control of materials properties.

In this work, we show how anisotropic magnetic microstructure influences electrical and galvanomagnetic properties of FMNC. At Co concentration higher than percolation threshold electron transport between magnetic fibers occurs by hopping mechanism, instead of metallic conductivity observed in FMNC without fiber microstructure.

For low Co content their electric resistivity follows the $\rho \sim \exp(1/T)$ dependence whereas for high Co content (> 30 at.%) electrical resistivity is described by the law $\rho \sim \exp(T^{-1/4})$. At low Co concentration (and small number of ferromagnetic NP′s) electronic transport through localization centers in Al_2O_3 matrix with a thermal activation character is predominating one. In contrast, at high concentration of Co NP′s electronic transport proceeds via variable range hopping mechanism.

We observed the regularity of higher longitudinal magnetoresistance (MR) values in the case of FMNC′s grown in perpendicular magnetic field and vice versa for transverse MR. These peculiarities are related to such arrangement of electron trajectories in magnetic field at which they cross predominantly the streaks between fibers of Co NP′s.

Thus growth of FMNC in magnetic field modifies essentially their properties.

[1] M.V.Radchenko, G.V.Lashkarev, M. E. Bugaiova, S.V.Trushkin, W.Knoff,T. Story, L.I.Petrosian, Nanostructured material science **3-4**, 42 (2014)

Comparative analysis of superparamagnetic and ferromagnetic resonance in Co/Al_2O_3 nanocomposite films

A.I. Dmitriev[1], M.V. Radchenko[1], M.E. Bugaiova[1], D.A. Fedorchenko[1]
W. Knoff[2], T. Story[2] G.V. Lashkarev[1].

[1]*I.M. Frantsevych Institute for Problems of Material Science, National Academy of Sciences of Ukraine, 3 Krzhizhanovskogo str., Kyiv, Ukraine. e-mail: <dmitr.kiev@gmail.com>*
[2]*Institute of Physics, Polish Academy of Sciences, Al. Lotnikow 32/46, Warsaw, Poland*

Magnetic resonance in ferromagnetic (FM) and superparamagnetic (SPM) nanocomposite (NC) systems can be analyzed in the framework of phenomenological Landau-Lifshitz (LL) theory taking into account various magnetization damping mechanisms and perturbations with peculiar temperature dependence [1-3].

Magnetic NC containing Co in the form of nanoparticles (NPs) were grown on policore substrates using two-crucible electron beam facility. This technology allows to obtain Co_X/Al_2O_3 samples with various Co content X = (16 - 41) at. % covering both FM and SPM films. The experimental studies of the temperature dependence of the resonance peak width (RPW) in FM and SPM nanocomposites were performed in the temperature range T=(3÷270) K with the Bruker spectrometer operating at 9.4 GHz. The pronounced increase of the RPW was observed at low temperatures indicating strong damping of magnetization precession. Figure presents the comparison of theoretical predictions for the correlation between the resonant field, the RPW and our experimental data. In the case of SPM film the RPW changes can be explained by the LL model (modification c), whereas for FM film the behavior of the discussed dependence is in conflict with all regimes proposed in theoretical calculations [1].

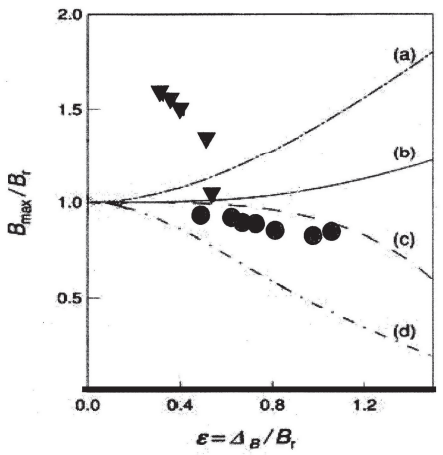

Fig. Lines a-d – LL theory with modifications [1]. Experiment: ▼ - FMR, Co41%; ● – SPR, Co16%. B_{max} - resonant field, B_r = 3.39 kOe - the field corresponding to g = 2, Δ_B - the half-width at half maximum of the resonance peak.

The observed damping was analyzed taking into account the complicated structure of NPs interface, the volume of which is 2.5 - 4 times larger than the one of Co core. This gives a rise to internal disturbing magnetic fields that violate the resonance conditions.

The possible sources of precession perturbations are the following: (1) an antiferromagnetic layer CoO; (2) an ensemble of magnetic oxygen vacancies on the interface $CoO-Al_2O_3$ [4]; (3) an ensemble of Co single atoms or their small clusters in the Al_2O_3 matrix. Therefore nontrivial changes of magnetization damping in SPR and FMR films probably is due to the conflict between ferromagnetic Co NPs and magnetic state of their shells.

[1] S. P. Gubin. John Wiley & Sons, 18.11ISBN: 978-3-527-40790-31 (2009).
[2] Orhan Yalçın ISBN: 978-953-51-1186-3, InTech. DOI: 10.5772/56134 (2013).
[3] L. Landau, E. Lifshitz, Phys. Z. Sowjetunion 8, 153, (1935)
[4] A.N. Morozovska, E.A. Eliseev, M.D. Glinchuk, R. Blinc. Phys. B 406, 1673 (2011).

Structural Investigations of Graphene Layers Grown on 4H-SiC - Buffer Layer Engineering

M.Tokarczyk[1, a)], G.Kowalski[1] , M.Gryglas-Borysiewicz[1], P.Ciepielewski[2], M.Możdżonek[2], W.Strupiński[2] and J.M.Baranowski [1,2]

[1] Faculty of Physics, University of Warsaw, Pasteura 502-093 Warsaw, Poland
[2]Institute of Electronic Materials Technology, Wólczyńska 133, 01-919 Warsaw, Poland

Intercalation of the various elements or compounds into the few layer graphene structure shows the way for future graphene electronic applications. That also includes functionalized graphene which may be suitable for the specific applications like bio-sensors, liquid and gas sensors etc. X-ray diffraction and X-ray reflectometry measurements presented here regarding few layer graphene structures are based on standard laboratory X-ray source equipped with parallel beam Bragg reflection mirror and standard Phillips diffractometer [1]. Samples were grown either by Chemical Vapor Deposition (CVD) or sublimation methods at 1600^{o}C under an argon laminar flow in an Aixtron VP508 hot-wall reactor. Graphene growth was preceded by H_2 etching of the SiC substrate. SiC surface was atomically stepped [2], although substrate was nominally on-axis (0001) oriented. Graphene intercalated with hydrogen [1], oxygen [3], and nitrogen, together with graphene oxide are prime examples of such graphene treatments which can led to specific graphene properties necessary for the wide spectra of applications. We have shown that in all samples investigated one can observe presence of non intentional water layers between the SiC and first carbon layer. Positioning and type of bonding of the intercalate, within the few layer graphene structure, is a crucial aspect of the whole functionalization. Using X-ray laboratory setup we have measured standard diffraction pattern as well as low angle reflectometry signal allowing for the precise evaluation of the buffer region above SiC substrate. We have shown that one can manipulate the positioning and presence of the intercalates, within the graphene structure, by thermal treatment and UV light. We have also observed a clear resistance changes upon UV illumination. This may be connected with the presence of water layers within the buffer volume. It will be shown that hydrogen, oxygen and nitrogen intercalate differently and positions itself at completely different lattice sites within the layer. X-ray measurements are compared with Raman spectroscopy, and ATR measurements to cross-reference the presence and positions of the intercalate.

[1] Tokarczyk, M. et al., *Appl. Phys. Lett*. **103**, 241915 (2013)
[2] Grodecki, K. et al., *Appl. Phys. Lett*. **100**, 261604 (2012)
[3] Kowalski, G et al. *J. Appl. Phys*. **117,** 105301 (2015)

[a)] Electronic mail: Mateusz.Tokarczyk@fuw.edu.pl

Lattice dynamics and photoluminescence emission of the two-dimensional $Mo_{1-x}W_xS_2$ alloys

Joanna Kutrowska-Girzycka [1], Joanna Jadczak [1], Ewelina Zdanowicz [1], Ying-Sheng Huang [2], Leszek Bryja [1]

[1] *Laboratory for Optical Spectroscopy of Semiconductors, Department of Experimental Physics, Department of Fundamental Problems of Technology, Wrocław University of Science and Technology, Wyb. Wyspiańskiego 27, 50-370 Wrocław, Poland*
[2] *Department of Electronic Engineering, National Taiwan University of Science and Technology, Taipei 10607, Taiwan*

The family of the transition metal dichalcogenides (TMDs) such as MoS_2 and WS_2 have recently attracted a big attention due to two dimensional character of covalently bonded layers held together by weaker van der Waals forces. A single layer of MX_2 (M = Mo or W and X=S, Se or Te) consist of one atomic layer of metal atoms hexagonally packed between two trigonal atomic layers of chalcogenide atoms. In single-layer form the lack of inversion symmetry leads to remarkable optical and electronic properties different from those of bulk form. Unlike different 2D crystals, such as graphene and boron nitride, they are semiconductors, hence they reveal properties more attractive for specific application e.g. in optoelectronic devices.

In this work we focus on optical properties of $Mo_{1-x}W_xS_2$ monolayers. The studied flakes were mechanically exfoliated from bulk crystals grown by chemical vapour transport method (CVT) and transferred on Si/SiO_2 substrates. Prepared samples were identified and characterized by optical microscopy and atomic force microscopy (AFM). The micro-photoluminescence (μ-PL) measurements were performed for the wide range of temperatures (from 6 to 300 K). The power-dependent micro-Raman scattering investigations were carried out in backscattering geometry at room temperature under different conditions: ambient, acetone, water and saturated NaCl water solution. The excitation power varied from 12.5 μW to 1.25 mW and from 25 μW to 25 mW for the laser lines λ=633 nm and λ=532 nm, respectively.

The Raman spectra of the binary MoS_2 and WS_2 reveal two prominent first-order phonon modes: the E^1_{2g} and the A_{1g} modes. The E^1_{2g} mode is an in-plane vibration, for which the atoms are oscillating parallel to the basal plane of the van-der Waals coupled crystal layers. The A_{1g} mode is an out-of plane vibration, where the sulfur atoms are moving in opposite directions. In case of ternary materials the A_{1g} mode exhibits one-mode behavior whereas the E^1_{2g} mode exhibits two-mode behavior. We observe that in case of the WS_2 monolayer, similarly to MoS_2, the A'_1 mode shifts towards lower energies when the power density of the laser increases, whereas E' phonon mode remains essentially inert. This is likely due to stronger coupling of A'_1 mode with the excited d_{z^2} states. These results are consistent with previous studies of MoS_2 in FET geometry [1]. The comparison of the studied materials reveals that WS_2 is more sensitive to change of the carrier concentration than MoS_2. This tendency decreases linearly with increasing Mo content in $Mo_{1-x}W_xS_2$ alloys. Our results show that the charge carrier density can be effectively tuned by the light intensity.

[1] B. Miller, E. Parzinger, A. Vernickel, A. W. Holleitner, U. Wurstbauer, Appl. Phys. Lett. **106**, 122103 (2015).

Optical Properties of Defects in Exfoliated MoS_2 Measured by Reflectometry and Raman Scattering

K.Norowski[1], K.Gołasa[1], M. Grzeszczyk[1], M.Król[1], K. Nogajewski[2], M. Potemski[2], B. Piętka[1], J.Szczytko[1]

[1]Institute of Experimental Physics, Faculty of Physics, University of Warsaw, ulPasteura 5 02-093 Warsaw, Poland
[2]Laboratoire National des Champs MagnétiquesIntenses, CNRS-UJF-UPS-INSA, Grenoble, France

Scotch tape exfoliation is a widely used technique of obtaining two-dimensional crystals from bulk materials of layered structure like graphite or transition metal dichalcogenides (TMDCs). A typical representative of the TMDC family is molybdenum disulphide (MoS_2), a naturally occurring mineral, whose structure is characterized by strong intralayerion-covalent bonds between sulphur and molybdenum atoms and by weak van der Waals bonds between S-Mo-S layers.

A confocal microscope was used for scanning the surface of MoS_2 samples and for studying different defects formed during the exfoliation process. The measurements were carried out at room temperature with the aid of red (633 nm) and green (532 nm) laser light illumination. Our experimental setup enabled us to obtain images with a spatial resolution up to about 300 nm(see Figure). Different light sources allowed for highlighting different defects as: folding, cracking, or displacement, whose visibility turned out to be wavelength-dependent. The reflectivity of MoS_2 flakes was compared with the Raman spectroscopy measurements used for sample's thickness estimation. We demonstrate that the correlation between the number of layers in a flake and the intensity of light reflected from the flake can be used for preliminary determination of the flake's thickness.

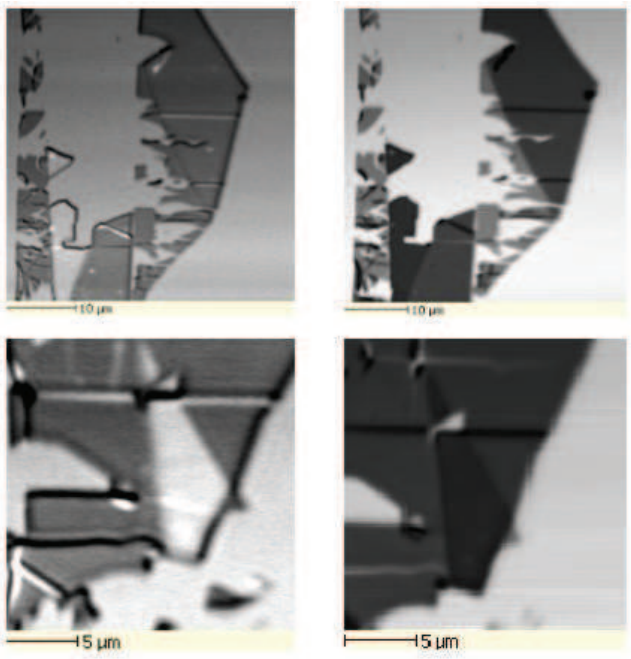

Figure. Microscopic images of exfoliated MoS2 illuminated by red (left) and green (right) laser. Different defects are determined: folding, cracking, displacement. The thickness of these defects was determined by Raman spectroscopy.

Resonant Raman spectra of suspended MoS_2

K. Gołasa [1], M. Grzeszczyk [1], M. Zinkiewicz [1], K. Nogajewski [2], A. Wysmołek [1], M. Potemski [2], and A. Babiński [1]

[1] *Faculty of Physics, University of Warsaw, ul. Pasteura 5, 02-093 Warsaw, Poland*
[2] *LNCMI, CNRS-UJF-UPS-INSA,25 rue des Martyrs, 38042 Grenoble, France*

Layered transition metal dichalcogenides (TMDs) have recently attracted a great interest due to their remarkable properties [1] and relatively easy synthesis methods. Typical representatives of TMDs family, such as MoS_2, WS_2 or $MoSe_2$ are direct band-gap semiconductors in their monolayer form, which makes them suitable for nanoelectronics and optoelectronics device applications [2,3]. The layered structure of thin flakes means that, when considering the properties of the material, the interaction with the substrate cannot be neglected. In a number of reports, the properties of suspended MoS_2 flakes have been studied [4]. In particular, these measurements revealed that with the resonant excitation (λ= 632.8 nm) no significant difference between the Raman scattering on the suspended and the supported flakes can be noticed.

In this communication we report on our measurements of the crystal lattice dynamics in freely suspended thin MoS_2 layers. We analyze resonant (λ=632.8 nm) Raman spectra of suspended and supported (SiO_2/Si substrate) few-layer (4ML-6ML) MoS_2 flakes and bulk material. While our experimental results agree, in general, with the previous reports, we observe the effect of the substrate on two structures, which can be detected in Raman scattering spectrum at ~420 cm^{-1} and ~460 cm^{-1}. First 'b' peak is due to the combined process involving phonons with wavevectors parallel to the c-axis. The 'b' peak indicated by triangles (Fig. 1) exhibits a clear displacement between suspended and supported samples. The second, broad and asymmetric peak at ~460 nm^{-1} is a convolution of several components. The intensity of a low-energy component, which is related to a combined 2LA(M) process, is significantly lower in suspended as compared to supported MoS_2 flakes.

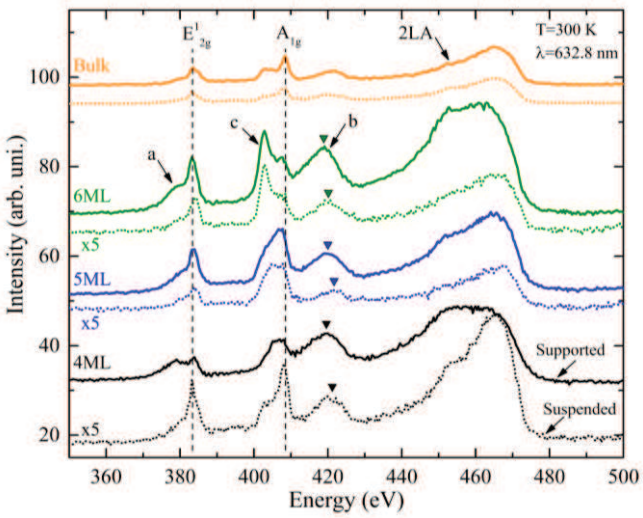

Figure 1. Resonant Raman spectra measured at room temperature for few-layer MoS_2 flakes and bulk material. Dashed and solid lines indicate samples suspended and supported, respectively.

We analyze the possible sources of observed differences between supported and suspended MoS_2 flakes. We consider the influence of the resonant character of the excitation and the effect of substrate interactions. We propose a physical model to explain the observed phenomena.

[1] K. Mak et al., *Nat. Nanotech. 7*, 494 (2012); T. Cao et al., *Nat. Comm.* ***3***, 887 (2012).
[2] B. Radisavljevic et al., *Nat. Nanotech*. ***6***, 147 (2011).
[3] Z. Yin et al., *ACS Nano* **6**, 74 (2012); M. Bernardi et al., *Nano Lett*. ***13***, 3664 (2013).
[4] H. Shi et al., *ACS Nano* **7**, 1072 (2013); J.-U. Lee et al., *2D Mater.* ***2***, 044003 (2015); M. Buscema et al., *Nano Research 7*, 561 (2014).

Magneto-optics of Massive Dirac Fermions in Strong Magnetic Fields.

Ludmiła Szulakowska[2], Paweł Potasz[1], Paweł Hawrylak[2]

[1]Wrocław University of Science and Technology, ul. Wybrzeże Wyspiańskiego 27, Wrocław, Poland
[2]Department of Physics, Advanced Research Complex, 25 Templeton Str.,University of Ottawa, Ottawa, Ontario, K1N 6N5, Canada

Massive Dirac Fermions (mDF) describe the low energy electronic properties of a class of two-dimensional crystals, from graphene in a staggered potential to transition metal dichalcogenides (TMDCs), such as MoS2 and WS2 [1-6]. In the energy structure of staggered graphene and TMDCs there exist two non-equivalent valleys, K and –K, with valence and conduction band separated by an energy gap E_g and split by a strong spin-orbit (SO) coupling. Recent experiments on TMDCs have shown that the optical transitions in these valleys couple to the oppositely circularly polarised light [2-4], which allows to address them independently.

The massive Dirac Fermions in strong perpendicular external magnetic field and their interaction with light have been studied in Refs. [6,7]. The magnetic field leads to the formation of degenerate levels, each being a mixture of different Landau levels (LLs) from the valence and conduction band. The mixing is controlled by the ratio of energy gap to Fermi velocity and by the strength of the SO coupling. The characteristic feature of Massive Dirac Fermions is the splitting of the two zero LLs of graphene into one attached to the top of the valence band in K valley and one attached to the bottom of the conduction band in the –K valley. In addition, topological magnetic moment, atomic magnetic moments and Zeeman splitting appear.

In this work we investigate the effect of electron-electron interactions on the optical properties of massive Dirac Fermions [8]. We start with the single-electron picture, using the massive Dirac equation with spin-valley-dependent low-energy gap [7]. We populate the N valence mDF levels and construct the Hartree-Fock (HF) ground state. We create quasi-electron and quasi-hole excitations out of the HF ground state, calculate self-energy, direct and exchange vertex corrections and solve numerically the Bethe-Salpeter equation to obtain the magneto-exciton spectrum in the two non-equivalent valleys. Using the selection rules for each spin, valley and polarisation of radiation, the absorption and emission spectra are calculated as a function of the mass-term, from massive to massless Dirac fermions. The magneto-exciton spectra will be compared with positively and negatively charged trions.

[1] E. Kadantsev, P. Hawrylak , *Solid St. Com,* **152,** (2012).
[2] X. Xu, W. Yao, D. Xiao, T. F. Heinz, *Nature Phys*, **10**, (2014).
[3] T. Scrace, Y. Tsai, B. Barman, L. Schweidenback, A. Petrou, G. Kioseoglou, I. Ozfidan, M. Korkusinski, P. Hawrylak, *Nature Nanotechnology*, **10**, (2015).
[4] D. MacNeill, C. Heikes, K. F. Mak, Z. Anderson, A. Kormányos, *Phys. Rev. Lett*, **114**, (2015).
[5] A. Kormanyos, V. Zolyomi, N. D. Drummond, P. Rakyta, G. Burkard, V. I. Falko, *Phys. Rev. B*, **88**, (2013)
[6] T. Cai, S. A. Yang, X. Li, F. Zhang, J. Shi, W. Yao, Q. Niu, *Phys. Rev. B*, **88**, (2013).
[7] F. Rose, M. O. Goerbig, F. Piechon, *Phys. Rev. B*, **88**, (2013).
[8] P. Hawrylak, M. Potemski, *Phys. Rev. B*, **56**, (1997).

Anomalous effect of temperature on the Raman scattering in few-layer $MoTe_2$

M. Grzeszczyk[1], K. Gołasa[1], M. Zinkiewicz[1], K. Nogajewski[2], M. R. Molas[2], M. Potemski[2], A. Wysmołek[1] and A. Babiński[1]

[1]Faculty of Physics, University of Warsaw, Pasteura 5, 02-093 Warsaw, Poland
[2]LNCMI, CNRS-UJF-UPS-INSA,25 rue des Martyrs, 38042 Grenoble, France
Magdalena.Grzeszczyk@fuw.edu.pl

Molybdenum ditelluride ($MoTe_2$), like other layered transition metal dichalcogenides (LTMDs), exhibit unique physical properties. Their layered structure results e.g. in a complicated spectrum of the Raman scattering due to out–of–plane A_{1g}–related modes.[1] It has been shown that the number of those features increases with the thickness of the material, which is related to the interlayer interactions. In particular there are two out–of–plane Raman active modes in 3L and 4L of $MoTe_2$. The higher energy mode (i) corresponds to vibrations in which Te atoms in all $MoTe_2$ layers move in phase. In the lower energy mode (j) in 3L (4L) Te atoms in the central (two central) $MoTe_2$ planes vibrate out–of–phase with respect to vibrations of Te atoms in the outer layers. In our recent communication[2] we shown a significant enhancement of the anti-Stokes scattering due to the (i) mode in 3L $MoTe_2$.

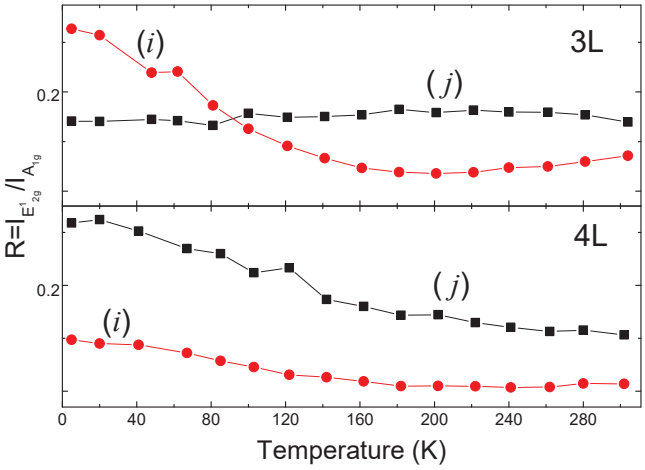

Fig. 1. The relative intensity of the out-of-plane modes in 3L and 4L $MoTe_2$ as a function of temperature.

In this report we further investigate the effect with temperature dependent measurements of Raman scattering. We study the effect of temperature on the out–of–plane modes in 3L and 4L of $MoTe_2$. In our experiment we observe that while in 4L both modes gain intensity with the decreasing temperature, in the 3L the evolution of (i) and (j) modes differs. The intensity of the (j) mode is not affected significantly by temperature. Simultaneously the non-monotonic dependence of the (i) mode can be noted. We relate this effect to the resonance of the excitation light with the electron-hole transition at the M point of the Brillouin zone.

The difference between the results for 3L and 4L is explained in terms of specific effect of the layer parity on the band structure of few-layer $MoTe_2$.

[1]G. Froehlicher et al., *Nano Letters* **15**, 6481 (2015).
[2] M. Grzeszczyk et al., *ArXive* 1511:07184.

Wednesday

Ab initio studies of dynamical properties of chosen group VI-B transition metal dichalcogenides systems

T. Woźniak[1], J. Jadczak[1], P. Scharoch[1], A. Wójs[1]

[1] *Faculty of Fundamental Problems of Technology, Wrocław University of Technology, wyb. Wyspiańskiego 27, 50–370 Wrocław*

Recently, group-VIB transition metal dichalcogenides (TMDCs) attract significant interest due to their extraordinary and tunable electronic and optical properties [1, 2]. Their quasi two-dimensional character leads to the anisotropy of their physical properties, which has various technological applications. Moreover, the mixed layered crystals allow for continuous tuning of the optical bandgap, rendering the TMDCs alloys the appealing materials for applications in electronic and optoelectronic devices. Hence, an experimental characterization and theoretical analysis of the properties of mixed crystals is of fundamental importance. This work is focused on the phonon properties of chosen TMDC systems, especially the influence of composition variations in mixed crystals.

We study from first principles (DFT) dynamical properties of several MX_2 bulk crystals and thin films (M=Mo, W, Re; X=S, Se, Te). Dynamical properties of $MX1_{2(1-x)}X2_{2x}$ alloys are investigated within a supercell model for different compositions x. The calculated phonon dispersions and densities of states reproduce well the measured Raman spectra [3]. We are able to explain the evolution of Raman modes by analysing the projected phonon density of states at Γ point of reciprocal space. Additionally, we develop a phonon vector unfolding technique at the center of the Brillouin zone. It simplifies the crowded supercell phonon dispersions and allows for a direct comparison with experimental data.

[1] H. Wang, H. Yuan, S. S. Hong, Y. Lib and Y. Cui, Chem. Soc. Rev. **44**, 2664 (2015).
[2] T. Woźniak, P. Scharoch and M. J. Winiarski, Acta Phys. Pol. A **129**, 56 (2016).
[3] J. Jadczak, D. O. Dumcenco, Y. S. Huang, Y. C. Lin, K. Suenaga, P. H. Wu, H. P. Hsu and K. K. Tiong, J. Appl. Phys. **116**, 193505 (2014).

WSe_2 monolayers in dielectric cavities

M. Król[1], R. Mirek[1], K. Lekenta[1], K. Nogajewski[2], A. Babiński[1], M. Potemski[2], J. Szczytko[1] and B. Piętka[1]

[1]*Institute of Experimental Physics, Faculty of Physics, University of Warsaw, Poland*

[2]*Laboratoire National des Champs Magnétiques Intenses, CNRS-UJF-UPS-INSA, Grenoble, France*

Thin layers of transition metal dichalcogenides (TMDs) such as MoS_2, WS_2 or WSe_2 have recently attracted considerable attention. Single layers of TMDs exhibit a direct band-gap, which make them a very appealing group of materials with potential applications in opto-electronic devices. We demonstrate a possible realization of optical cavities designed for one particular representative of this group i.e. for tungsten diselenide, WSe_2.

In our work we present the processing and optical properties of dielectric cavities incorporating WSe_2 monolayers. The procedure of sample fabrication consists of two independent growth processes of subsequent TiO_2 and SiO_2 layers which constitute two distributed Bragg reflectors (DBRs) and a $\lambda/2$ SiO_2 cavity. After completing the first DBR terminated by the bottom half of the cavity, exfoliated monolayers of WSe_2 are deposited on its top surface by means of an all-dry polydimethylsiloxane-based transfer technique, and then the second half of the cavity along with the top DBR are grown. Previously performed numerical simulations based on transfer matrix method gave us widths of dielectrics layers needed to achieve desired samples properties. The cavity mode energy at liquid helium temperature should be close to the exciton resonance in 1 ML-thick WSe_2 with the maximum of the electric field amplitude exactly at the position of the monolayer. Microscopic images of a selected sample in Fig. a demonstrate that WSe_2 monolayers are not affected by the growth process of the top DBR. Shown in Fig. b are measured reflectance spectra at cryogenic temperatures that gave us the cavity mode at an energy of 1.74 eV, which is very close to that of 2-D excitons in WSe_2 monolayers (1.75 eV).

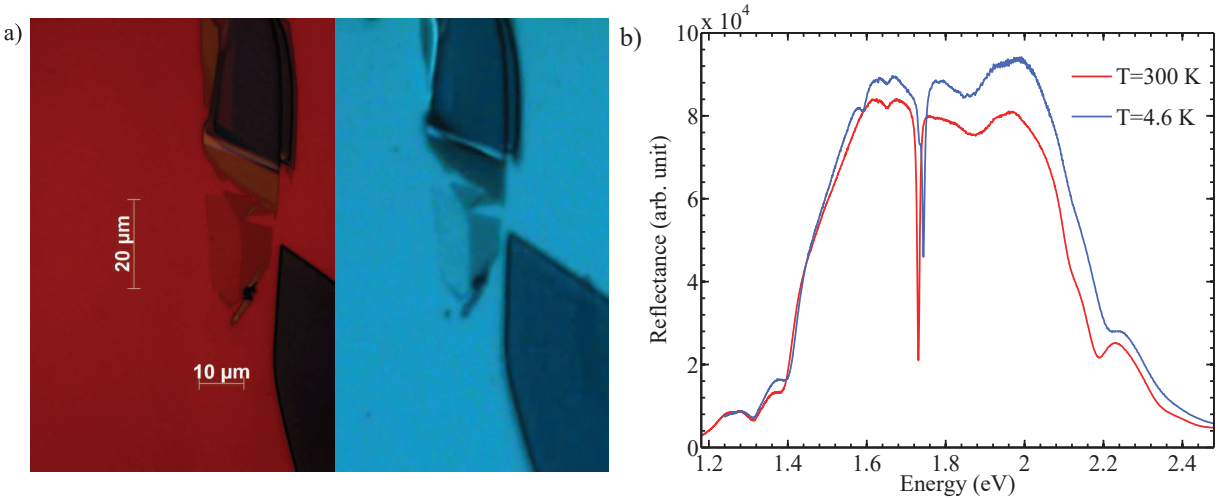

Figure: a) Image of a WSe_2 single layer before (left) and after (right) growth of the top DBR b) reflectance spectra in low and high temperature from cavity structure in the vicinity of the WSe_2 single layer.

Wednesday

Strong interaction of GaN nanowires with bulk MoS_2: Raman and photoluminescence studies

J. Łysiak[1,2], P. Perkowska[1], A. Wysmołek[1], A. Reszka[3], M. Sobanska[3], K. Klosek[3] and Z. R. Zytkiewicz[3]

[1] *Faculty of Physics, University of Warsaw, Pasteura 5, 02-093 Warsaw, Poland*

[2] *College of Intern-Faculty Individual Studies in Mathematics and Natural Sciences, University of Warsaw, Banacha 2C, 02-097 Warsaw, Poland*

[3] *Institute of Physics, Polish Academy of Sciences, Al. Lotników 32/46, 02–668 Warsaw, Poland*

Disulfide molybdenum (MoS_2) crystal has very interesting physical properties. It is commonly known that luminescence of disulfide molybdenum strongly depends on its thickness. Decreasing the number of MoS_2 layers leads to strong increase of photoluminescence intensity which is explained as transformation of indirect to direct bandgap semiconductor.

In this work, we show that substantial enhancement of both Raman and photoluminescence spectra of MoS2 crystals can be achieved by deposition of gallium nitride (GaN) nanowires on top of them.

The MoS_2 samples were exfoliated from synthetic bulk crystal and placed on silicon substrate covered with silicon dioxide. The GaN nanowires of length of 1-2μm and diameter of 30-50nm were grown by MBE on Si(111). Subsequently they were separated from the Si substrate using methanol ultrasonic bath and deposited on MoS_2 surface.

Presence of GaN nanowires on the MoS_2 surface was verified by optical microscopy (see black spots on Fig.1, top part) which matches very well with the Raman signal of E_2 GaN mode.

Interestingly enough, positions of GaN nanowires perfectly correspond to the enhancement of both Raman and photoluminescence of MoS_2 crystal. As presented in Fig.1, E^1_{2g} Raman mode of MoS_2 was amplified by factor of ∼1.5 and PL even by a factor of ∼3.

The obtained results may indicate strong interaction leading to the apperance of photonic effects in Raman and selection rule breaking for emission spectra from MoS_2 bulk crystals.

The observed effect would be important from the point of view of nanooptical devices based on MoS_2 structures.

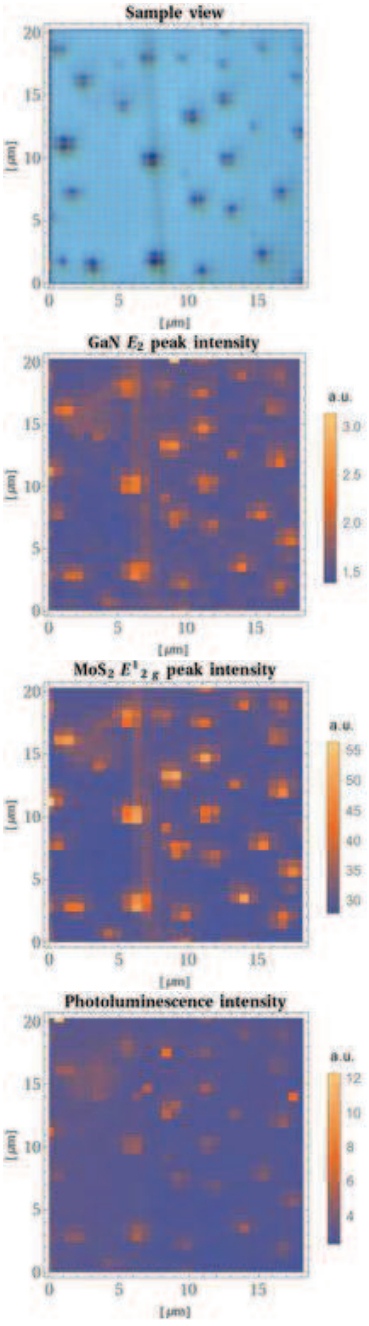

Figure 1: Results of spacially resolved Raman and photoluminescence spectroscopy of GaN nanowires deposited on bulk MoS_2.

Wednesday

Ab initio studies of graphene layers on insulating substrates

Mikołaj Sadek* **and Jacek A. Majewski**

Faculty of Physics, University of Warsaw, ul. L. Pasteura 5, 02-093 Warszawa, Poland

Graphene is one of the most promising materials for applications in the future nanoelectronics and the large-area graphene has been synthetized on metal surfaces by chemical vapor deposition. However, to utilize graphene's unique features in electronic devices, one needs to place it onto an insulating substrate. This procedure requires a multiple step transfer process and, therefore, several attempts have been undertaken to achieve the transfer-free synthesis of graphene. So far, the metal-catalyst-free synthesis of graphene has been tried on the whole plethora of substrates such as MgO, GaN, h-BN, Si_3N_4, Al_2O_3, ZrO_2, HfO_2, and also directly on SiO_2 [1, 2].

However, the deeper understanding of the physicochemistry of graphene/substrate interfaces would facilitate the development of the better growth techniques. Therefore, we have undertaken the *ab initio* studies of the graphene layers of the substrates MgO, GaN, h-BN, Si_3N_4, and SiO_2 substrates. We attempt to find out the possible morphology of these interfaces and the stability of the resulting structures. It is also interesting question to which extent the substrate influences the electronic properties of graphene. Our studies are based on the *ab initio* calculations in the framework of the density functional theory (DFT) with the energy functionals containing van der Waals (vdW) correction that turned out to be important in our studies of the graphene and h-BN vertical heterostructures [3]. To perform the computations, we have employed the *SIESTA* and *VASP* numerical packages with norm-conserving and PAW pseudopotentials, respectively. For systems containing more than 500 atoms, we have used also Density Functional based Tight Binding (DFTB) method [4]. However, the studies are far from being complete yet, we can conclude that they provide hints how the graphene layers can form on the variety of substrates studied.

This research has been supported by the NCN grant *HARMONIA* (Contact No. UMO-2013/10/M/ST3/00793).

[1] Yong Seung Kim, *et al*., *Nanoscale* **6**, 10100-10105 (2014).
[2] Zheng Yan, *et al*., *ACS Nano* **5**, 8187-8192 (2011).
[3] M. Sadek and J. A. Majewski, to be published elsewhere; M. Sadek *et al*., *IWN 2014 Int. workshop on Nitride Semiconductors*, Wroclaw, 2014, p. 176.
[4] www.dftb.org

*email: Mikolaj.Sadek@fuw.edu.pl

Wednesday

Strong Photoluminescence Fluctuations In Laser-thinned Few-layer WS_2

Ł. Bala[1,2], E. M. Łacińska[1], K. Nogajewski[2], A. Wysmołek[1] , M. Potemski[2]

[1]Faculty of Physics, University of Warsaw, Pasteura 5, 02-093 Warsaw, Poland
[2]Laboratoire National des Champs Magnétiques Intenses, CNRS-UJF-UPS-INSA, 25 rue des Martyrs, 38042 Grenoble, France

Transition metal dichalcogenides (TMDs) have recently become a worldwide subject of intensive optical studies. One of the astonishing properties of these materials is that their bandstructures undergo a transformation from indirect-bandgap to direct-bandgap when decreasing the number of layers in the crystal lattice, which is accompanied by a substantial increase of the photoluminescence intensity. Since up to now there are no well-established procedures of synthesizing large-area TMD monolayers, a very desirable would be an efficient and reliable method of fabricating them from bulk TMD flakes.

In this communication we present our results of μ-Raman and μ-photoluminescence (μ-PL) study of few-layer WS_2 flakes that have been locally thinned down by a focused laser beam. The flakes were obtained by means of standard exfoliation of a bulk crystal and then deposited on a Si/SiO_2 substrate. Their actual thickness was determined using optical microscopy. After initial characterization a certain number of WS_2 layers were locally removed with the aid of high-power laser light. In order to get full control over this process spatially-resolved Raman maps were recorded on the locations subjected to laser-thinning (a typical result obtained on a 3-layer flake is shown in Fig. 1). The observed redshift of about 1 cm^{-1}, present in the middle of the map, suggests that the investigated flake was locally thinned down by one layer. We found the Raman spectra in the middle of the laser-induced hole to be very similar to that of an unperturbed two-layer WS_2 film.

In order to verify the quality of the obtained structure low-temperature μ-PL experiments were performed.

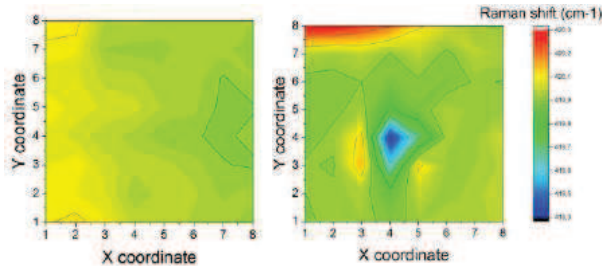

Figure 1. Spatially-resolved maps of the A_{1g} Raman mode of a 3-layer WS_2 flake before (left panel) and after laser-thinning (right panel).

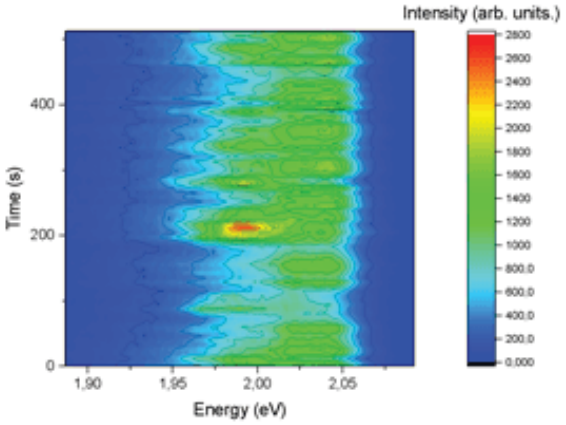

Figure 2. Subsequent photoluminescence spectra measured with 1 s acquisition time for laser excitation spot positioned at the boundary between the 3- and 2-layer parts of the investigated WS_2 flake.

It was found that the luminescence spectra measured outside the laser-thinned region were quite stable. Interestingly, huge intensity and energy fluctuations were detected at the boundary between the 3-layer area of the flake and the laser-thinned region (Fig. 2). Similar effects were found at the edges of a WS_2 monolayer flake, which has not been subjected to laser-thinning. The origin of the observed time evolution of the PL response will be discussed in terms of electrostatic potential fluctuations resulting from light-induced changes of the charge states of defects present in the laser-thinned area.

Temperature dependent studies of Raman modes in few-layer $MoSe_2$

Małgorzata Zinkiewicz [1], Magdalena Grzeszczyk [1], Katarzyna Gołasa [1], Karol Nogajewski [2] and Adam Babiński [1]

[1] *Faculty of Physics, University of Warsaw, Pasteura 5, 02-093 Warsaw, Poland*
[2] *LNCMI, CNRS-UJF-UPS-INSA,25 rue des Martyrs, 38042 Grenoble, France*

The layered structure of molybdenum diselenide ($MoSe_2$) results in a complicated spectrum of the Raman scattering due to out–of–plane A_{1g}–related modes. In 3L of $MoSe_2$ the spectrum excited with 514 nm excitation [1] is composed of two out–of–plane Raman active modes. The higher energy mode (i) corresponds to vibrations in which Se atoms in all $MoSe_2$ layers move in phase. In the lower energy mode (j) in 3L Se atoms in the central MoSe2 planes vibrate out–of–phase with respect to vibrations of Se atoms in the outer layers.

In this work we investigate how the A_{1g} Raman modes in 3L $MoSe_2$ sample evolve with temperature. Both Stokes and anti-Stokes scattering is studied in temperature range from T=4.2K to T=300K. In Stokes scattering the lower energy component (*j*) does not change its intensity with increasing temperature, while the higher one (*i*) varies having its maximum at 60 K. This behaviour does not occur for anti-Stokes spectra, where both peaks increase with temperature. We assume it may be connected with excitonic resonances recently studied in $MoTe_2$ material [2]. Further studies for different thickness of material are being continued.

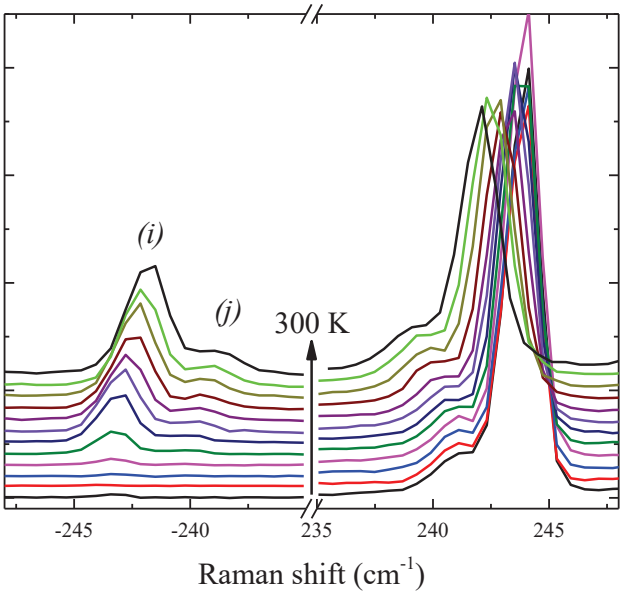

Figure 1: Anti-Stokes and Stokes Raman spectra of A1g mode in 3 layers $MoSe_2$.

[1] P. Tonndorf, R. Schmidt, P. Böttger, X. Zhang, J. Börner, A. Liebig, M. Albrecht, C. Kloc, O. Gordan, D. R. T. Zahn, S. Michaelis de Vasconcellos, and R. Bratschitsch, *Opt. Express* **21**, 4908-4916 (2013)
[2] M. Grzeszczyk, K. Gołasa, M. Zinkiewicz, K. Nogajewski, M. R. Molas, M. Potemski, A. Wysmołek, A. Babiński, *ArXive* 1511:07184.

Deep-level defects in n-type $GaAs_{1-x}Bi_x$ with $0 \le x \le 2.3$ grown on GaAs by MBE

Ł. Gelczuk[1,*], J. Kopaczek[2], T. Rockett[3], R. D. Richards[3] and R. Kudrawiec[2]

[1]Faculty of Microsystem Electronics and Photonics, Wrocław University of Technology, Janiszewskiego 11/17, 50-372 Wrocław, Poland
[2]Faculty of Fundamental Problems of Technology, Wrocław University of Technology, Wybrzeże Wyspiańskiego 27, 50-370 Wrocław, Poland
[3]Department of Electronic and Electrical Engineering, University of Sheffield, Sir Frederick Mappin Building, Mappin Street, Sheffield S1 3JD, United Kingdom

The dilute bismide alloy $GaAs_{1-x}Bi_x$, containing a few percent of Bi atoms, grown on GaAs has attracted a lot of attention in recent years due to its unusual properties [1, 2] including a large band gap reduction (~50-90 meV per percent of Bi) and a strong enhancement of the spin-orbit splitting. These properties make this material system an attractive candidate to develop GaAs-based applications for long-wavelength optoelectronics as well as for spintronics. It is also complementary to the well-studied dilute nitride alloy $GaAs_{1-x}N_x$ because incorporating Bi in GaAs perturbs the valence band, whereas N in GaAs perturbs the conduction band [3]. It is due to the fact that isolated N forms resonant state in the conduction band and N pairs and clusters form bound states in the band gap. On the other hand, isolated Bi forms resonant state in the valence band and Bi pairs or clusters will form bound states in the band gap. Due to a strong carrier scattering at localized states, N alloying affects mainly the electron density and mobility, while Bi alloying affects the hole density and mobility in GaAs [4]. Unfortunately, efficient incorporation of Bi requires low temperatures and nearly stoichiometric growth conditions due to a large immiscibility between Bi atoms and GaAs compound, what then favours the increase of defect density and can further degrade the electro-optical properties of $GaAs_{1-x}Bi_x$ alloy.

In this paper, we present deep level transient spectroscopy (DLTS) measurements on n-type $GaAs_{1-x}Bi_x$ layers having $0 \le x \le 2.3$ grown on GaAs substrate by molecular beam epitaxy (MBE). In the experiment, four Bi-containing samples and one GaAs reference sample grown at the same low temperature equal to 378ºC were investigated. The DLTS temperature spectra show that incorporating Bi suppresses the formation of native electron traps revealed in GaAs, thus reducing the total trap concentration in dilute $GaAs_{1-x}Bi_x$ layers. Moreover, other electron traps are also formed when incorporating Bi, thus they may involve Bi as a constituent. The possible origin of the traps was analyzed with the use of the band gap diagram concept, which considers the reduction of the band gap energy with increasing Bi (or N) concentration. This approach was recently successfully applied for identification of deep electron traps in as-grown and annealed n-type $GaAs_{1-x}N_x$ layers grown by MBE.

* e-mail: lukasz.gelczuk@pwr.edu.pl

[1] S. Francoeur, M.J. Seong, A. Mascatenhas, S. Tixier, M. Adamcyk, and T. Tiedje, *Appl. Phys. Lett.* **82**, 3874 (2003).
[2] B. Fluegel, S. Francoeur, A. Mascarenhas, S. Tixier, E.C. Young, and T. Tiedje, *Phys. Rev. Lett.* **97**, 067205 (2006).
[3] Y. Zhang, A. Mascarenhas, and L. W. Wang, *Phys. Rev. B* **71**, 155201 (2005).
[4] R. N. Kini, A. J. Ptak, B. Fluegel, R. France, R. C. Reedy, and A. Mascarenhas, *Physical Review B* **83**, 075307 (2011).
[5] Ł. Gelczuk, R. Kudrawiec, and M. Henini, *J. Appl. Phys.* **116**, 013705 (2014).

Energy decomposition analysis of 2D boron crystals from first principles

T. Tarkowski[1], J. A. Majewski[1], and N. Gonzalez Szwacki[1]

[1] *Institute of Theoretical Physics, Faculty of Physics, University of Warsaw, ul. Pasteura 5, PL-02-093 Warszawa, Poland*

Very recently, a monolayer boron crystal has been successfully grown on the Ag(111) surface under ultrahigh vacuum [1]. The structure of that crystal can be described as an arrangement of boron atoms on a hexagonal (triangular) lattice with some fraction of atoms missing. The distribution of the missing atoms (vacancy sites in the triangular lattice) depends on many factors, and one of them is the amount of charge that is transferring from the substrate to the 2D crystal. Furthermore, an uncharged freestanding crystal, which is known in the literature as the α-sheet [2], has evenly distributed vacancies as it is shown in Fig. 1.

The purpose of this investigation is to decompose the total energy of a 2D boron crystal into energy contributions coming from the constituent atoms according to their coordination number. We may write:

$$E_{tot}\left(n_3, n_4, n_5, n_6, q\right) = \frac{1}{N}\sum_{i=3}^{6} n_i e_i^q$$

where n_i and e_i^q are the number of boron atoms in the unit cell with i nearest neighbours and their energy, respectively. N is the total number of atoms per unit cell. The individual energy contributions, e_i^q, are found from separate first principles computations for 2D boron crystals in which each atom has i nearest neighbours. One example is the boron graphitic structure from which we calculate e_3^q. We show that by using such a simple energy decomposition it is possible to predict, with reasonable accuracy, the total energy of any 2D boron crystal (with any particular distribution of vacancy sites). Furthermore, the model is extendable to charged structures (with charge q), for which we calculate, from first principles, an appropriate set (e_i^q) of energy values.

For instance the estimated binding energy, $E_b = E(isolated\ \mathrm{B}\ atom) - E_{tot}(n_i, q)$, for the uncharged α-sheet is 6.55 eV, which differs by only 50 meV from the 'true' 6.6 eV value calculated using first principles computations. We also show that in contrast to neutral structures that give preference to coordination number 5, in negatively charged structures the atoms prefer to be 3- and 4-coordinated. A detailed comparison with experimental results will be presented.

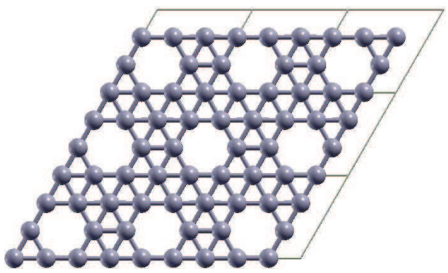

Figure 1: Structure of the α boron sheet.

[1] A. J. Mannix et al., *Science* **350**, 1513 (2015).
[2] H. Tang and S. Ismail-Beigi, *Phys. Rev. Lett.* **99**, 115501 (2001).

Magnetic properties of singlecrystalline $Cd_xMn_yCr_zSe_4$ ($0.03 \leq y \leq 0.12$)

I. Jendrzejewska[1], E. Maciążek[1], T. Groń[2], P. Zajdel[2], H. Duda[2], J. Kusz[2] and A. Kita[1]

[1]*University of Silesia, Institute of Chemistry, ul. Szkolna 9, 40-006 Katowice, Poland,*
[2]*University of Silesia, Institute of Physics, ul. Uniwersytecka 4, 40-007 Katowice, Poland*

$CdCr_2Se_4$ spinel is a ferromagnetic semiconductor with the Curie temperature T_C = 130 K, Curie-Weiss temperature θ = 200 K, saturation magnetization M_S = 5.30 μ_B/f.u. at 4.2 K and the effective magnetic moment μ_{eff} 5.49 = μ_B/f.u. [1-3]. It has a structure of AB_2X_4 type with a lattice constant of 10.721-10.750 Å, in which the Se-anions form a cubic close-packed lattice, with the Cd-cations occupying the tetrahedral sites and the Cr-cations occupying the trigonal antiprismatic sites [2]. In $CdCr_2Se_4$ the magnetic order results from the competition of nearest neighbors positive Cr-Se-Cr interaction and more distant negative Cr-Se-Cd-Se-Cr exchange interaction [3]. Substitution of the manganese for the divalent cadmium ion showed the ferromagnetic order in polycrystalline $Cd_{0.85}Mn_{0.01}Cr_{1.97}Se_4$ spinel with the Curie temperature T_C = 135 K, Curie-Weiss temperature θ = 145 K, saturation magnetization M_S = 7.49 μ_B/f.u. at 4.2 K and the effective magnetic moment μ_{eff} 5.76 = μ_B/f.u. [4].

Magnetization measurements were carried out using a Quantum Design System (MPMS XL). Static (dc) magnetic susceptibility was measured in the magnetic field H_{dc} = 100 Oe and recorded in zero-field-cooled (ZFC) mode. Dynamic (ac) magnetic susceptibility was measured at an internal oscillating magnetic field H_{ac} = 3.9 Oe with an internal frequency f = 300 Hz. Both dc and ac magnetic susceptibility were measured in the temperature range 5–400 K. Magnetization isotherms were measured in the temperature range 5-275 K in static (dc) magnetic fields up to 70 kOe.

Magnetic measurements showed that the $Cd_xMn_yCr_zSe_4$ single crystals (y = 0.03, 0.06, 0.09 and 0.12) are ferromagnets with the Curie temperature T_C = 130 K, Curie-Weiss temperature θ = 161-183 K, saturation magnetization M_S = 3.83-5.45 μ_B/f.u. at 5 K and the effective magnetic moment μ_{eff} 4.62-5.30 = μ_B/f.u., weakly dependent on the manganese substitution. The imaginary component of ac magnetic susceptibility showed strong energy loss in the long range of magnetic order, connected, for example, with the magnetic-domain-wall motion or with rotation of magnetization within domains [5]. The most interesting observation of magnetic measurements was magnetic hysteresis, which showed the existence of spontaneous magnetization and the coercive field in all crystals $Cd_xMn_yCr_zSe_4$, *i.e.* the typical ferromagnetic properties. Based on the experimentally set of magnetic hysteresis loops the values of spontaneous magnetization M_S = 0.08 μ_B/f.u. at 5 K and coercive field H_C 19 Oe were determined. The resulting hysteresis loops have a shape typical for affecting ferromagnetic material containing clusters of different sizes. Similar loops for $Cd_{1-x}Mn_xGeAs_2$ crystals were found [6].

[1] R. Plumier, M. Lecomte, A. Miedan-Gros, and M. Sougi, *Phys. Rev. Lett.* **55**, 239 (1975).
[2] P.K. Baltzer, M. Robbins, and P.J. Wojtowicz, *J. Appl. Phys.* **38**, 953 (1967).
[3] E. Loudghiri, M. Nouges, M. Taibi, and A. Belayachi, *Maroc. J. Cond. Matt.* **5**, 62 (2004).
[4] I. Jendrzejewska, P. Zajdel, J. Mroziński, E. Maciążek, T. Goryczka, A. Hanc, A. Kita, *Sol. State Phenom.* **163**, 204 (2010).
[5] T. Sato, T. Ando, T. Watanabe, S. Itoh, Y. Endoh, and M. Furusaka, *Phys. Rev. B* **48**, 6074 (1993).
[6] R.V. Demin, L.I. Koroleva, S.F. Marenkin, S.G. Mikhailov, V.M. Novotortsev, V.T. Kalinnikov, T.G. Aminov, R. Szymczak, H. Szymczak, and M. Baran, *Tech. Phys. Lett.* **30**, 81 (2004).

Carrier spin dynamics in undoped double quantum dots

Michał Gawełczyk and Paweł Machnikowski

Department of Theoretical Physics, Faculty of Fundamental Problems of Technology, Wrocław University of Technology, Wybrzeże Wyspiańskiego 27, 50-370 Wrocław, Poland

In this contribution, we provide a model of the electron and hole spin dynamics in a double quantum dot structure [1], considering the carrier tunneling between quantum dots, which is enhanced by an electric field. Taking into account also the presence of an in-plane or tilted magnetic field, we provide the simulation of magneto-optical experiments which are performed currently on such structures to probe the temporal spin dynamics.

Probing exciton spin dynamics in neutral structures is limited by recombination much faster than the actual spin dynamics. In doped structures, in turn, the initialization of resident spins is subject to the intrinsic dephasing [2] affecting the results of experiments sensitive to spin coherence [3]. The search for undoped systems with long-living spins brought a proposal and first realizations of double quantum wells and dots, in which exciton is spatially separated due to the carrier tunneling.

In our model of such system, spin precession in the magnetic field is treated exactly, while the dissipative dynamics of the system (spin relaxation, dephasing, carrier tunneling between quantum dots, and recombination) is described in the Markov limit by the universal Lindblad superoperator in the master equation for the density matrix evolution. Moreover, we include the spin-orbit coupling effects, which give rise to the mixing of states with different angular momenta and in cosequence to the probability of spin-flip tunneling of carriers. To obtain the direct correspondence with experimentally measured quantities we employ the numerical solution for the density matrix and construct substantial dynamical variables such as spin polarization and coherences for each of QDs.

We reproduce the experimentally observed effect of the extension of the spin polarization life time caused by the charge separation, which occurs in structures of this type. Moreover, we provide a number of qualitative predictions concerning the necessary conditions for observation of this effect as well as about possible channels of its suppression. We consider also the impact of the magnetic field tilting, which results in an interesting spin polarization dynamics. Finally, we discuss the relevance of the spin-flip tunneling caused by the spin-orbit interaction for typical systems.

We find that the effect of spin polarization life time extension depends essentially on the ratio of tunneling time to direct exciton recombination time. The spin-orbit interactions and spin-flip tunneling caused by it lead to the loss of spin coherence which occurs once during the tunneling process at low temperature and accumulates in time at higher temperature. The strength of this effect scales with the localization length, which makes it negligible for small QDs.

[1] M. Gawełczyk, P. Machnikowski, arXiv:1407.4529.
[2] M. Gawełczyk, P. Machnikowski, *Phys. Rev. B* **87**, 195315 (2013).
[3] M. Syperek, D. R. Yakovlev, A. Greilich, J. Misiewicz, M. Bayer, D. Reuter, and A. D. Wieck, *Phys. Rev. Lett.* **99**, 187401 (2007).

Carrier spin dephasing in coupled quantum dots

M. Krzykowski, M. Gawełczyk, K. Gawarecki, P. Machnikowski

Department of Theoretical Physics, Faculty of Fundamental Problems of Technology, Wrocław University of Technology, Wybrzeże Stanisława Wyspiańskiego 27, 50-370 Wrocław, Poland

Understanding of spin dynamics in a system of coupled quantum dots (QDs) is important due to its potential for future use in spintronic devices. Spin-preserving tunneling in such structures [1] can be exploited to implement a spin-initialization scheme based on exciton dissociation [2].

In this contribution we show that spin coherence is not preserved during carrier tunneling in an external magnetic field if there is a misfit between g-factors in QDs. This decoherence is present even in the absence of direct coupling between the spin and the phonon bath. It is a "welcher-weg" type of decoherence [3], where phonon bath "measures" spin as the carrier tunnels.

Our model consists of a carrier confined in a semiconductor QD coupled to a phonon bath and placed in external magnetic and electric fields. We model spin dynamics using a Markovian master equation in the Redfield form in a broad range of parameters, such as temperature, g-factors and energy levels in QDs, by solving the equation numerically. In further calculations carrier states, g-factors, as well as carrier-phonon couplings were acquired using a multiband $\mathbf{k} \cdot \mathbf{p}$ method [4].

We have found that the decoherence resulting from tunneling of the carrier with the emission of a phonon is strongly correlated to the difference between g-factors in the QDs. Even for a small mismatch of parameters ($\approx 10\%$) effects of decoherence during carrier tunneling become important. We have also studied temperature impact on decoherence. Simulations showed a significant effect in the moderate-temperature regime, with spin decoherence times for a state in thermal equilibrium with respect to the spatial degrees of freedom being 3 orders of magnitude shorter at $T = 30$ K compared to $T = 5$ K. The exponential decay of spin coherence can be attributed to the accumulated coherence loss during repeated thermally activated tunneling between the lowest states in different QDs.

[1] T. Kazimierczuk, J. Suffczyński, A. Golnik, J. A. Gaj, P. Kossacki, and P. Wojnar, Phys. Rev. B **79**, 153301 (2009).
[2] T. M. Godden, J. H. Quilter, A. J. Ramsay, Yanwen Wu, P. Brereton, S. J. Boyle, I. J. Luxmoore, J. Puebla-Nunez, A. M. Fox, M. S. Skolnick, Phys. Rev. Lett. **108**, 017402 (2012).
[3] K. Roszak, P. Machnikowski, Phys. Lett. A **351**, 251 (2006).
[4] K. Gawarecki, P. Machnikowski, Phys. Rev. B **85**, 041305(R) (2012).

Critical temperature of two-dimensional hydrogenated multilayer graphene-based diluted ferromagnet

Karol Szałowski

Department of Solid State Physics, Faculty of Physics and Applied Informatics, University of Łódź, ulica Pomorska 149/153, PL 90-236 Łódź, Poland

Hydrogenated graphene constitutes a promising platform for future spintronics devices [1], thus it attracts increasing attention [2]. One of the natural goals to achieve in such system is the ferromagnetic ordering of localized magnetic moments. As predicted theoretically [3], the long-range ferromagnetic interaction emerges between localized magnetic moments provided by hydrogen atoms deposited over carbon atoms of one sublattice of multilayer graphene.

The aim of the paper is to present the results of numerical calculations of critical temperature of diluted ferromagnet based on multilayer graphene with H adatoms at the surface, over carbon atoms of one sublattice [4]. The calculations of critical (Curie) temperature of continuous phase transition are based on Pair Approximation (PA) for diluted ferromagnetic systems with long-range interactions [5]. For comparison, the results yielded by Mean Field Approximation (MFA) are also presented. The interaction of the form $J(r) \propto (1/r)\exp(-r/\lambda)$ with characteristic exponential decay length λ is assumed. The exponential attenuation can be expected in the presence of disorder in the system.

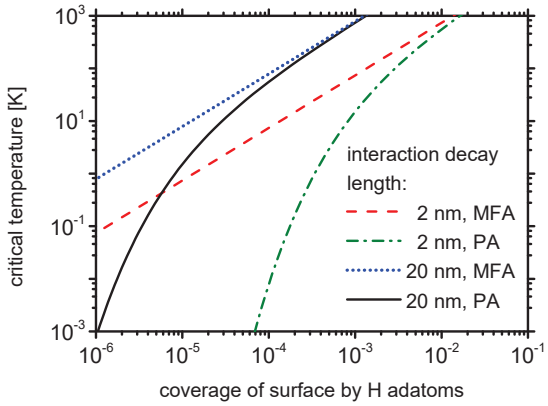

Critical temperature as a function of surface coverage with H adatoms for two interaction decay lengths. Results of MFA and PA (for Heisenberg coupling) are compared.

The wide range of adatom concentrations and attenuation lengths is considered. The dependence of critical temperature on both quantities id thoroughly analysed. In particular, a highly non-linear dependence of critical temperature on impurity concentration (surface coverage by H atoms) is predicted, as illustrated in the figure. Moreover, it is demonstrated that MFA, commonly applied to systems with long-range interactions, heavily overestimates the critical temperature values compared to PA. In addition, PA is capable of taking into account the interaction anisotropy in spin space, ranging from anisotropic Ising to isotropic Heisenberg couplings. Thus, the importance of such anisotropy can be discussed.

The computational support on Hugo cluster at Laboratory of Theoretical Aspects of Quantum Magnetism and Statistical Physics, P. J. Šafárik University in Košice is gratefully acknowledged.

This work has been supported by Polish Ministry of Science and Higher Education on a special purpose grant to fund the research and development activities and tasks associated with them, serving the development of young scientists and doctoral students.

[1] W. Han, R. K. Kawakami, M. Gmitra, J. Fabian, *Nat. Nanotechnol.* **9**, 794807 (2014).
[2] D. Soriano, D. V. Tuan, S. M.-M. Dubois *et al.*, *2D Mater.* **2**, 022002 (2015).
[3] M. Moaied, J. V. Alvarez, J. J. Palacios, *Phys. Rev. B* **90**, 115441 (2014).
[4] K. Szałowski, arXiv:1603.03810 (2016).
[5] K. Szałowski, and T. Balcerzak, *J. Phys. Soc. Jpn.* **83**, 044002 (2014).

g-factor Properties of Electrons and Holes Confined in InAs Quantum Dots Emitting at Telecom Wavelengths

Janina J. Schindler[1*], V. V. Belykh[1], D. R. Yakovlev[1,2], E. A. Zhukov[1], M. A. Semina[2], M. Yacob[3], J. P. Reithmaier[3], M. Benyoucef[3] and M. Bayer[1,2]

[1]*Experimental Physics 2, TU Dortmund University, Germany*
[2]*Ioffe Institute, Russian Academy of Sciences, St. Petersburg, Russia*
[3]*Institute of Nanostructure Technologies and Analytics, University of Kassel, Germany*

Spins in semiconductor quantum dots (QDs) are considered as very attractive system for future applications in the solid-state quantum information processing. In that context, the characterization of *g*-factors is very important to assess the spin dynamics for the semiconductor physics in general and for tailoring nanostructures in particular, since the dynamics are sensitive to shape anisotropies as well as spin-state mixing. We study electron and hole *g*-factors and dephasing times in a novel InAs/InAlGaAs/InP quantum dot ensemble emitting in the telecom spectral range around 1.5 □m by measuring time-resolved pump-probe ellipticity [1].

All components of the electron and hole *g*-factor tensors are measured via tuning the excitation energy through the inhomogenously broadend QD ensemble. Surprisingly, the electron *g*-factor shows the largest anisotropy so far reported for QDs changing from $g_{e,x} = -1.63$ to $g_{e,z} = -2.52$ between directions perpendicular and parallel to the dot growth axis, respectively, at an energy of 0.82 eV. The hole *g* -factor anisotropy at this energy is even stronger: $|g_{h,x}| = 0.64$ and $|g_{h,z}| = 2.29$. We observe a strong deviation of the electron *g*-factors from the Roth-Lax-Zwerdling equation and a steep dispersion of the hole *g*-factor, which is affected by the strain and size of QDs with large confinement. The out-of-plane anisotropy is even more pronounced for the distribution of the *g*-factors among the QD ensemble, determined from the spin dephasing time [2].

[1] Belykh et al., Phys. Rev. B 92, 165307 (2015)
[2] Belykh et al., arXiv: 1512.03544v2 (2015).

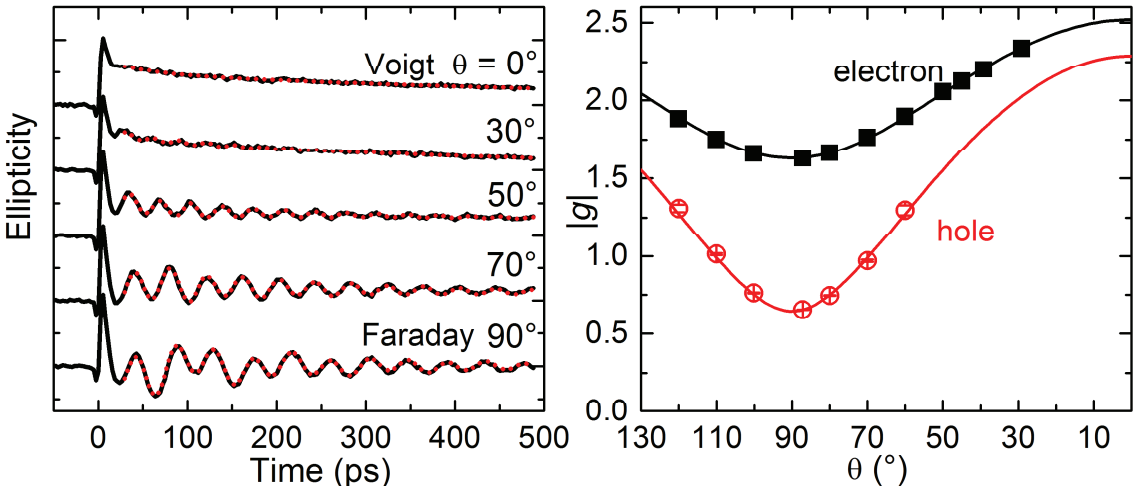

T-shaped spin-separator based on a magnetic two-dimensional electron gas

Z. Adamus[1], D. Sztenkiel[1], J. Wróbel[2,1] and T.Wojtowicz[1]

[1]*Institute of Physics, Polish Academy of Sciences, al. Lotników 32/46, 02-668 Warszawa, Poland*

[2]*Faculty of Mathematics and Natural Sciences, Rzeszów University, al. Rejtana 16A, 35-959 Rzeszów, Poland*

The so-called tree-terminal ballistic junctions (TBJs) consist of three quantum wires connected via ballistic cavity to form a Y-shaped or T-shaped current splitter, which in principle can operate at high speed with a very low power consumption. The interesting and unexpected transport characteristic of TBJs is the almost reflectionless separation of 1D conductance modes, which occurs at the junction area. This spectacular example of the so-called *wave function engineering* has been experimentally demonstrated for T-branch switches, patterned from two-dimensional electron gas [1, 2].

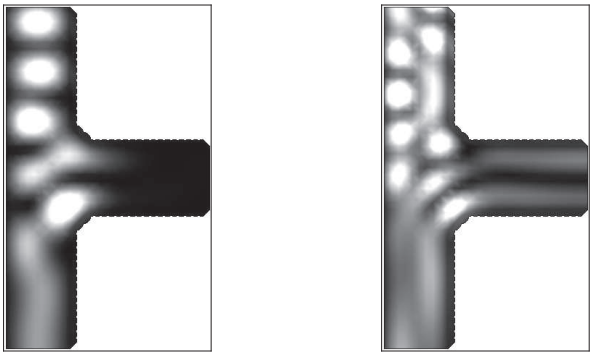

(a) (b)

Fig.1 Squared modulus of the Zeeman splitted wave functions for "up" (a) and "down" (b) spin directions (brighter areas correspond to higher density). Spin-orbit (SO) interaction is not taken into account, note a rounded corners of the central junction area.

Here we propose to extend the idea of reflectionless charge current redirection on the magnetic system where one-dimensional channels are spin polarized (see Fig.1). We present the theoretical model of T-shaped ballistic junction patterned from a high mobility modulation doped CdMgTe/Cd(Mn)Te quantum well. Nanostructure is modeled as a discrete lattice with tight-binding Hamiltonian. To make simulation more realistic, system includes rounded corners and finite edge potential. The numerical calculations are performed using the Kwant code [3]. It is intended that parameters of our model closely reflect the experimental characteristics of a real device. In particular, we carefully examined the role of spin-orbit interaction, which is usually omitted in the theoretical analysis of the ballistic mode separation. Results are discussed in terms of current density, wave function and local density of states (LDOS) with respect to the average spin orientation and magnetic field direction.

The research was partially supported by National Science Centre (Poland) under the grant DEC-2012/06/A/ST3/00247 and Regional Development Program (Poland), grant WND-RPPK. 01.03.00-18-053/12.

[1] J. Wróbel *et al.*, Phys. Rev. B **81**, 233306 (2010).
[2] O. A. Tkachenko *et al.*, Nanotechnology **23**, 095202 (2012).
[3] C. W. Groth, *et.al,*, *New J. Phys.* **16**, 063065 (2014)

Defect induced magnetism in SiC

Yutian Wang, Yu Liu, Sybille Gemming, Manfred Helm, Shengqiang Zhou

Helmholtz-Zentrum Dresden-Rossendorf, Dresden, 01328, Germany

Defect-induced magnetism is attracting intensive research interest. It not only challenges the traditional opinions about magnetism, but also has some potential applications in spin-electronics. SiC is a new candidate for the investigation of defect-induced ferromagnetism after graphitic materials and oxides due to its high material purity and crystalline quality [1, 2]. In this contribution, we made a comprehensive investigation on the structural and magnetic properties of ion implanted and neutron irradiated SiC sample. In combination with X-ray absorption spectroscopy and first-principles calculations, we try to understand the mechanism in a microscopic picture.

For neon or xenon ion implanted SiC, we identify a multi-magnetic-phase nature [3]. The magnetization of SiC can be decomposed into paramagnetic, superparamagnetic and ferromagnetic contributions. The ferromagnetic contribution persists well above room temperature and exhibits a pronounced magnetic anisotropy. By combining X-ray magnetic circular dichroism and first-principles calculations, we clarify that p-electrons of the nearest-neighbor carbon atoms around divacancies are mainly responsible for the long-range ferromagnetic coupling [4]. Thus, we provide a correlation between the collective magnetic phenomena and the specific electrons/orbitals.

With the aim to verify if a sample containing defects through its bulk volume can persist ferromagnetic coupling, we applied neutron irradiation to introduce defects into SiC [5]. Besides a weak ferromagnetic contribution, we observe a strong paramagnetism, scaling up with the neutron fluence. The ferromagnetic contribution only occurs in a narrow fluence window or after annealing. We speculate that defect-induced ferromagnetism rather locally appears in particular regions, like surface/interface/grain boundaries.

[1] L. Li, et al., *Appl. Phys. Lett.* 98, 222508 (2011).
[2] Y. Wang, et al., *Phys. Rev. B* 90, 214435 (2014).
[3] Y. Wang, et al., *Phys. Rev. B* 89, 014417 (2014).
[4] Y. Wang, et al., *Scientific Reports*, 5, 8999 (2015).
[5] Y. Wang, et al., *Phys. Rev. B* 92, 174409 (2015).

Capacitance Studies of GaMnAs / GaAs Esaki diodes

Z. Ogorzałek[1], K. Filipiuk[1], M. Gryglas-Borysiewicz[1], A. Kwiatkowski[1], J. Przybytek[1], A. Lemaître[2], M. Sawicki[3], M. Baj[1], D. Wasik[1]

[1] *Faculty of Physics, University of Warsaw, Pasteura 5, Warsaw, Poland*
[2] *Laboratory for Photonics and Nanostructures (CNRS), Route de Nozay, Marcoussis, France*
[3] *Institute of Physics, Polish Academy of Sciences, Al. Lotników 32/46, Warsaw, Poland*

The GaMnAs / GaAs Esaki diode is an interesting system, in which the electrical properties of GaMnAs may be investigated in a non-standard way. In a typical parallel transport configuration current is passed in the plane of the layer and resistivity tensor is measured, which allows to find fundamental magnetic properties of the layer (e.g. the Curie temperature, magnetic anisotropies, etc.) [1, 2]. In this case the carriers participating in the transport are close to the Fermi energy. For GaMnAs being a part of a diode the situation is quite different. In this case, due to a possibility of tuning band alignment with voltage, different valence band states may contribute to the current, leading to such fine effects like tunneling anisotropic magnetocurrent [3-5].

In our previous studies of (Ga,Mn)As diodes with different Mn content [6] we have observed a qualitative difference between the I(V) curves of ferromagnetic and paramagnetic samples. In particular, ferromagnetic ones showed puzzling biexponenial dependence for forward bias, missing for paramagnetic samples where the current rise was much faster.

To understand these observations, we investigated electrostatic state of the samples by means of capacitance studies. The capacitance was measured as a function of bias at room temperature. The investigations provided us with basic parameters of the diodes, e.g. depletion layer width (DLW) and a built-in potential. The measured bias evolution of the DLW, showed a rapid decrease of the DLW with polarization for ferromagnetic samples, revealing the origin of the biexponenial I(V) curve. Moreover, the evaluation of the built-in potential allowed to estimate the position of the Fermi level in (Ga,Mn)As for different Mn contents. The results enabled to discuss the competing models of GaMnAs valence band structure.

This study was partially supported by the National Science Centre (Poland) under grant No. DEC-2011/03/B/ST3/03287

[1] M. Glunk, J. Daeubler, L. Dreher, S. Schwaiger, W. Schoch, R. Sauer, and W. Limmer, *Phys. Rev. B* **79**, 195206 (2009)
[2] M. Gryglas-Borysiewicz, A. Kwiatkowski, M. Baj, D. Wasik, J. Przybytek, and J. Sadowski, *Phys. Rev. B* **82**, 153204 (2010),
[3] R. Giraud, M. Gryglas, L. Thevenard, A. Lemaître, G. Faini, *Appl. Phys. Lett*., **87**, 242505 (2005)
[4] P. Sankowski, P., Kacman, J. A. Majewski, T. Dietl, Spin-dependent tunneling in modulated structures of (Ga,Mn)As, *Phys. Rev. B* ***75***, 045306 (2007)
[5] M. Gryglas-Borysiewicz, A. Kwiatkowski, A. Lemaître, J. Przybytek, K. Budzik, Ł. Balcerzak, M. Sawicki, D. Wasik, http://dx.doi.org/10.1016/j.apsusc.2016.03.087
[6] Presentation at 44th *Jaszowiec* International School & Conference on the Physics of Semiconductors, to be published

Impact of Mg Doped Cladding Layers on Ferromagnetism of (Ga,Mn)N Thin Films

K. Gas [1,2], G. Kunert [3,4], S. Figge [4], S. Stefanowicz [2], T. Baraniecki [3], P. Dłużewski [2], B. Kurowska [2], R. Jakieła [2], G. Mazur [2], D. Hommel [3,1,4], and M. Sawicki [2]

[1] *Institute of Experimental Physics University of Wrocław, Wrocław, Poland*
[2] *Institute of Physics, Polish Academy of Sciences, Warsaw, Poland*
[3] *Wrocław Research Center EIT+ Sp. z o.o., Wrocław, Poland*
[4] *Institute of Solid State Physics, University of Bremen, Bremen, Germany*

Since GaN has reached the status of the second most important semiconducting material after Si the prospect of spintronics functionalization of GaN have gained in significance. However, the most obvious way of magnetic functionalization of GaN by alloying it with transition metals (mainly Mn) showed that due to a short range of superexchange Mn-Mn interaction the Curie temperature, T_C, does not exceed 13 K even for as high Mn content as 10%, despite exhibiting the highest saturation magnetization in the whole dilute ferromagnetic semiconductors family [1,2]. On the other hand, an extending of the effective range of the magnetic coupling in such a high Mn-content material should lead to a substantial increase of T_C. For example, a presence of mobile holes is expected to bring the T_C above the room temperature (RT) in this material system [3].

Here we show that a substantial, up to 50% increase of the magnitude of T_C in (Ga,Mn)N is possible when a thin (5 nm thick) layer gets sandwiched between Mg-doped GaN. To this end we investigate two sets of GaN:Mg/(Ga,Mn)N/GaN:Mg structures grown by molecular beam epitaxy (MBE) on GaN templated c-plane Al_2O_3. Targeting the same Mn content in the first set we vary the Mg content in the GaN:Mg cladding layers by changing the Mg flux from 0 to 2×10^{-8} Torr. In the second set we vary the Mn incorporation into (Ga,Mn)N film by changing the substrate temperature from 600 to 730°C under a constant Mg flux of 1×10^{-8} Torr. Structural properties are examined by XRD, SIMS and HRTEM. Both Mn concentration and values of T_C are established from highly elaborated and dedicated SQUID magnetometry allowing to fully mitigate spurious magnetic artifacts originating from residual magnetism of MBE substrates and materials used for sample holder construction. Interestingly, whereas the highest Mg flux used to grow GaN:Mg layers practically prevented Mn incorporation into the middle layer, the structures grown with the mid-high Mg flux of 1×10^{-8} Torr show up to 50% higher T_C than equivalent plane thick (Ga,Mn)N films [4]. On the other hand, a very high RT resistivity of these layers preclude a simplistic explanation of hole mediated coupling and calls for more detailed studies of the Mn incorporation and final distribution in GaN during Mg-assisted MBE growth.

[1] M. Sawicki et al., Phys. Rev. B **85**, 205204 (2012).
[2] G. Kunert et al., Appl. Phys. Lett. **100**, 155321 (2012).
[3] T. Dietl and H. Ohno, Rev. Mod. Phys. **86**, 187 (2014).
[4] S. Stefanowicz et al., Phys. Rev. B **88**, 081201(R) (2013).

This work has been supported by the National Science Centre (Poland) through grants FUGA (DEC-2014/12/S/ST3/00549) and OPUS (DEC-2013/09/B/ST3/04175), by the EU 7th Framework Programme "EAgLE" (REGPOT-CT-2013-316014) and by Wrocław Research Center EIT+ within the project "The Application of Nanotechnology in Advanced Materials" - NanoMat (P2IG.01.01.02-02-002/08) co-financed by the European Regional Development Fund (operational Programme Innovative Economy, 1.1.2).

Fe donor in ZnO: a Half-resonant Character Driven by Strong Intracenter Coulomb Coupling

A. Ciechan[2], J. Papierska[1], P. Bogusławski[2,3], M. Boshta[4], M. M. Gomaa[4], E. Chikoidze[5], Y. Dumont[5], A. Drabińska[1], H. Przybylińska[2], A. Gardias[1], J. Szczytko[1], A. Twardowski[1], M. Tokarczyk[1], G. Kowalski[1], B. Witkowski[2], K. Sawicki[1], W. Pacuski[1], M. Nawrocki[1], and J. Suffczyński[1]

[1]Institute of Experimental Physics, Faculty of Physics, University of Warsaw, ul. Pasteura 5, 02-093 Warsaw, Poland
[2]Institute of Physics, Polish Academy of Sciences, al. Lotników 32/46, 02-668 Warsaw, Poland
[3]Institute of Physics, Kazimierz Wielki University, Powstańców Wielkopolskich 2, 85-064 Bydgoszcz, Poland
[4]Solid State Physics Department, National Research Center, Giza, Egypt
[5]Groupe d'Etudes de la Matiere Condensee (GEMaC), Universite de Versailles St-Quentin en Yvelines-CNRS, Universite Paris-Saclay, Versailles, France

Typically, a donor introduced to a semiconductor induces an energy level within the band gap, which is close to the bottom of the conduction band. Some donors are, however, resonant, which means that their donor (0/+) ionization level is situated within the conduction band. As a consequence they autoionize spontaneously even at zero temperature.

According to our first principles calculations, iron dopant in ZnO presents a particular case of a half-resonant donor representing an intermediate situation: Fe^{2+} charge state is unstable because the donor level of Fe^{2+} is within the conduction band continuum, but the autoionization from 2+ to 3+ charge state is only partial because the donor level of the ionized Fe^{3+} is below the bottom of the conduction band. A complete ionization of the Fe would require a non-zero ionization energy of around 0.1-0.2 eV. We find that large, about 1 eV, difference in the donor level energies of the 3+ and 2+ charge states is a consequence of a large intrashell Coulomb coupling between *d*(Fe) electrons.

We confirm the results of theoretical considerations by studies of polycrystalline (Zn,Fe)O films with the Fe content attaining 0.2% using several experimental methods like electron paramagnetic resonance, magnetometry, conductivity, excitonic magnetic circular dichroism (MCD) and magneto-photoluminescence (PL).

The samples are *n*-type, with the room temperature electron concentration increasing from about $5.4*10^{15}$ cm^{-3} to $1.5*10^{16}$ cm^{-3} upon doping with 0.2% of Fe. The donor character of the Fe ions and activation energy of conductivity of 0.14 eV remain in agreement with the theoretical estimations. Relatively low electron concentrations indicate a high degree of compensation of Fe donors, most possibly by the zinc vacancies. The presence of compensating acceptors is also reflected by the DAP recombination observed in the PL.

Brillouin-like dependencies found in measurements of MCD and of PL in magnetic field along with a clear Curie-paramagnetic dependence on temperature of magnetization determined from magnetospectroscopy confirm presence of Fe ions in 3+ valency and the ion-carrier *s,p-d* exchange interaction in the (Zn,Fe)O.

The presented results help explaining the fact that despite transition metal ions in II-VI semiconductors exhibit typically a native 2+ valency, for the case of ZnO 3+ or mixed 3+/2+ valency was previously reported.

[1] arXiv:1603.01123 (submitted to Physical Review B)

Magnetoresistive Effects in Nanostructures Tailored from (Ga,Mn)(Bi,As) Dilute Magnetic Semiconductor

K. Levchenko [1], T. Andrearczyk [1], E. Łusakowska [1], J. Sadowski [1,2], Z. Tkaczyk [1], J. Wróbel [1], T. Figielski [1] and T. Wosiński [1]

[1] *Institute of Physics, Polish Academy of Sciences, 02-668 Warsaw, Poland*
[2] *MAX-IV Laboratory, Lund University, P.O. Box 118, SE-221 00 Lund, Sweden*

The aim of our work is to unleash the potential of (Ga,Mn)(Bi,As) quaternary compound as a prospective dilute ferromagnetic semiconductor. Nearly two decades of intensive studies of the (Ga,Mn)As ternary compound accumulated experience and successful achievements in both theory and experiment, proving that this prototype dilute ferromagnetic semiconductor provides a basis for developing novel spintronic functionalities [1]. As verified in our recent investigations [2], incorporation of a small fraction of bismuth into (Ga,Mn)As layers results in a strong enhancement of magneto-transport effects, owing to increased spin-orbit coupling. Appropriate nano-structurization of thin (Ga,Mn)As layers results in patterning-induced strain relaxation, which introduces into narrow stripes of the material a shape-dependent magnetic anisotropy in addition to the magneto-crystalline anisotropy of the layers. This patterning-induced magnetic anisotropy offers an additional degree of freedom that can be used in device operation. Our recent studies on several types of nanostructures tailored from (Ga,Mn)As layers, pointed to their utility for spintronic applications [3].

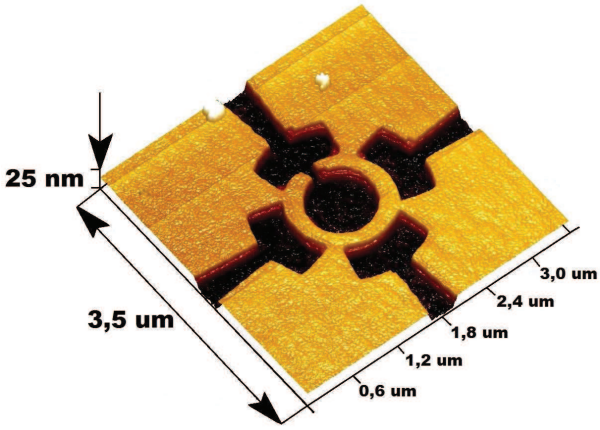

Fig. 1: Atomic force microscopy image for the ring-shaped nanostructure, consisting of a ring with a slit and four large contact areas connected to the ring periphery.

In the present study we have designed and investigated two types of nanostructures, of the cross-like and ring-shape geometries, tailored using electron-beam lithography patterning and chemical etching from 10-nm thick (Ga,Mn)(Bi,As) epitaxial layers with 6% Mn and 1% Bi contents. In the ring-shape nanostructures, shown in Fig. 1, the easy axis of magnetization is along the ring periphery. It results in two different stable magnetic states in the ring: the flux-closure "vortex" state and the "onion" state with a single domain wall (DW), located across from the slit, which contribute an extra resistance to the ring total electrical resistance, owing to spin-dependent scattering of charge carriers passing through the region of DW. For the two types of nanostructures their resistance, measured under a weak in-plane magnetic field at low temperatures, displays hysteresis-like behaviour, controlled by rearrangement of DWs in the nanostructures, which could be utilized in a new class of nonvolatile two-state memory cells.

This work was supported by the Polish National Science Centre under grant No. 2011/03/B/ST3/02457.

[1] T. Dietl and H. Ohno, *Rev. Mod. Phys*. **86**, 187 (2014).
[2] K. Levchenko, T. Andrearczyk, J. Z. Domagala, T. Wosinski, T. Figielski and J. Sadowski, *Acta Phys. Polon. A* **126**, 1121 (2014).
[3] T. Wosinski, T. Andrearczyk, T. Figielski, J. Wrobel and J. Sadowski, *Physica E* **51**, 128 (2013).

Decoherence of an NV center coupled to a bath of ^{13}C nuclear spins

Damian Kwiatkowski[1], **Łukasz Cywiński**[1]

[1] *Institute of Physics, Polish Academy of Sciences, al. Lotników 32/46, PL 02-668 Warsaw, Poland*

The nitrogen-vacancy (NC) color center in diamond [1] is one of the most actively researched semiconductor-based spin qubits [2]. It is especially promising for applications involving using it as a sensor of magnetic field noise. This noise can either be intrinsic, i.e. caused by other spins present inside the diamond crystal (electronic spins of nearby nitrogen impurities, or nuclear spins of ^{13}C isotopes present among the carbon atoms forming the diamond lattice), or extrinsic, caused e.g. by spins of molecules present close to the surface of the diamond nanocrystal [3]. In the former case a careful analysis of decoherence signal can be used to identify NV centers having a few ^{13}C nuclear spins in close proximity [4], and such complexes of spins can be used as few-qubit quantum registers [5]. Such an identification of environment of the NV center requires a very good theoretical understanding of nuclear-induced decoherence in this system. The best available theory is the Correlated Cluster Expansion (CCE) [6], in which contributions to NV decoherence [7] coming from groups (clusters) of increasing numbers of nuclei are systematically taken into account. We will present our recent progress in implementing this method and using it for calculation of NV center decoherence.

This research is supported by funds of Polish National Science Center (NCN), grant no. DEC-2012/07/B/ST3/03616.

[1] M. W. Doherty, N. B. Manson, P. Delaney, Fedor Jelezko, Jörg Wrachtrup, L. C. L. Hollenberg, Annu. Rev. Condens. Matter Phys. **528**, 1 (2013).
[2] V. V. Dobrovitski, G. D. Fuchs, A. L. Falk, C. Santori, and D. D. Awschalom Phys. Rep. **4**, 23 (2013).
[3] T. Staudacher, F. Shi, S. Pezzagna, J. Meijer, J. Du, C. A. Meriles, F. Reinhard, J. Wrachtrup, Science **339**, 561 (2013).
[4] F. Shi, X. Kong, P. Wang, F. Kong, N. Zhao, R.-B. Liu, and J. Du, Nat. Phys. **10**, 21 (2014).
[5] M. V. Gurudev Dutt, L. Childress, L. Jiang, E. Togan, J. Maze, F. Jelezko, A. S. Zibrov, P. R. Hemmer, and M. D. Lukin, Science **316**, 1312 (2007).
[6] W. Yang and R.-B. Liu, Phys. Rev. B **78**, 085315 (2008); Phys. Rev. B **79**, 115320 (2009).
[7] N. Zhao, S.-W. Ho, and R.-B. Liu, Phys. Rev. B **85**, 115303 (2012).

Measurements of longitudinal relaxation time of electrons in n-doped GaAs by means of spin noise spectroscopy

L. Yu. Beliaev

St.-Petersburg State University, Spin Optics Laboratory, St.-Petersburg, Russia

The computational technologies development of the recent yearsraised a great interest to spin-based, rather than charge-based, logic elements implementations. This area of research is currently referred to as spintronics [1]. One of the prominent systems in this area is n-doped GaAs structures since the fabrication of high-quality GaAs heterostructures is available using the MBE technology. GaAs electronic subsystem is characterized by strong interaction with light, in particular, electron spin state can be controlled with circularly polarized light. Hence the GaAs heterostructures are widely studied, some simple properties, such as thermally equilibrated electrons longitudinal relaxation time remained beyond the scope of experimental investigations.

Noise spectroscopy is an elegant method to unravel properties of a system and was proven to be essentially nonperturbative [2]. Although spin noise spectroscopy (SNS) was firstly demonstrated on atomic systems [3,4], this method is highly applicable to semiconductor physics [5].

In most experimental cases SNS is realized using Voight geometry, when the external magnetic field $\mathbf{B}$ is applied orthogonally to the light propagation axis $\mathbf{L}$, $\boldsymbol{B} \perp \boldsymbol{L}$.Any spontaneous magnetization of the system will start to precess around the magnetic field direction. Noise spectrum of its projection on the light axis, which is detected in the experiment, will reveal a peak at the Larmor frequency with the characteristic transverse relaxation time T_2. To the contrary, the noise spectrum in Faraday geometry $\boldsymbol{B} \parallel \mathbf{L}$ will reveal a peak at zero frequency, which width is controlled by longitudinal relaxation time T_1. However, its direct measurement is technically hindered by the 1/f flicker-noise of the detection system. In this work we present a series of experiments devoted to investigation of the longitudinal relaxation time T_1 in the metallic GaAs ($n \approx 2 \cdot 10^{16} cm^{-3}$).

[1] V. S. Zapasskii, *Adv. Opt. Photonics* **5**, 131 (2013).
[2] B.M. Gorbovitskii, V. I. Perel, *Optics and Spectroscopy* **3**, 123 (1983).
[3] E. B. Aleksandrov and V. S. Zapassky, *JETP* **54**, 64 (1981).
[4] S. A. Crooker, D. G. Rickel, A. V. Balatsky, and D. L. Smith, *Nature* **431**, 49 (2004).
[5] M. Oestreich, M. Römer, R. Haug, and D. Hägele, *Phys. Rev. Lett* **95**, 216603 (2005).

Electric and magnetic properties of Mn-dimers on zb-GaN/ zb-SiC(001) interfaces

M. Popielska[1], M. Sznajder[2], and J. A. Majewski[1]

[1]Faculty of Physics, University of Warsaw, Pasteura 5, 02-093 Warsawa, Poland
[2] Faculty of Mathematics and Natural Sciences, University of Rzeszow, Pigonia 1, 35-959 Rzeszow, Poland.

It has been reported that zinc-blende (zb) phase of the nitrides forms during the growth onto the (001) surface of cubic SiC substrate [1]. Recently, those interfaces have been mostly considered from the side of theirs microelectronics applications [2]. Nowadays, increasing interest in various systems for spintronic applications paves the way to consider the Mn dimers diluted onto the GaN /SiC interface from the point of view of its properties relevant for spintronics. Therefore, in this communication, we focus on Mn dimers diluted onto the SiC/GaN interface considering both its magnetic and electronic properties.

We examine a [Si,Ga] type and [C,N] type GaN/SiC(001) interface with single mixed layer and c(2x2) lateral arrangement predicted to be the most stable in comparison to abrupt and two-mixed interfaces [3]. The mixed layers (co-doped with Si, N, C, Ga atoms) are constructed in such manner to be non-polar on the average, in other words to contain the same number of donor- and acceptor-like bonds. Then, we placed the Mn-atoms at the all non-equivalent substitutional cationic positions at the interfaces, and optimized the all positions of atoms that are in close vicinity of magnetic ions. Further, the stability of arising structures has been investigated. The Mn ions substituted into group III or group IV cationic sites have nominally various charge state (valency). We investigate the influence of the valencies of the Mn ions constituting the Mn-dimers on the magnetic properties of the Mn pairs, in particular the exchange coupling *J* constant. Moreover, the role of the local macroscopic electric field is also considered, by studying the abrupt polar interfaces (i.e., with no mixed layers and with electric charge accomodation).

All of the considered structures have been calculated in the framework of the density functional theory (DFT), with the generalized gradient approximation (GGA) using the Perdew-Burke-Ernzerhof (PBE) [4] form of the exchange-correlation density functional as implemented in the numerical package SIESTA [5].

[1] J. G. Kim, A. C. Frenkel, H. Liu, and R. M. Park, *Appl. Phys. Lett.* **65**, 91 (1994).
[2] A. Rizzi, R. Lantier, H. Luth, *Phys. Status Solidi A* **177**, 165 (2000).
[3] M. Stadadele , J. A. Majewski, and P. Vogl, *Phys. Rev. B* **15**, 6911 (1997).
[4] J. P. Perdew, K. Burke, M. Ernzerhof, *Phys.Rev. Lett.* **77**, 3865 (1996).
[5] M. Soler, et al., *J. Phys.: Condens. Matter* **14**, 2745 (2002).

Exchange bias induced suppression of ferroelectric domain switching in multiferroic GeMnTe

H. Przybylińska[1], A. Grochot[1], G. Springholz[2], A. Ney[2], G. Bauer[2], and W. Jantsch[2]

[1] *Institute of Physics, Polish Academy of Sciences, Al. Lotników 32/46, 02-668 Warsaw, Poland*
[2] *Institute for Semiconductor and Solid State Physics, J. Kepler University, Altenbergerstr. 69, A-4040 Linz, Austria*

GeTe doped with manganese is a multiferroic semiconductor, in which ferroelectric and ferromagnetic orders coexist at low temperatures up to the Mn content of 50 %. We have recently demonstrated with use of ferromagnetic resonance (FMR) that in MBE grown GeMnTe layers deposited on (111) BaF_2 substrates the ferroelectric and ferromagnetic moments are coupled to each other, leading to reversal of ferroelectric polarization under relatively low externally applied magnetic fields [1]. In the present study we show that magnetic field induced ferroelectric polarization reversal can be even entirely suppressed in the presence of exchange bias.

We investigated a series of 500 nm thick $Ge_{1-x}Mn_xTe$ layers (with x ranging from 18 to 30 %) grown at exactly the same conditions as those used in Ref. 1 but terminated with a thin Te/Se cap layer to prevent sample degradation (Mn out diffusion and oxidation). In contrast to previous studies where two ferromagnetic resonance signals were observed, corresponding to two ferroelectric domains differing by rotation of oblique $<11\bar{1}>$ axes by 180º around the [111] growth direction, in the capped samples only one dominant FMR signal is observed. Whereas previously the intensities of the FMR signals could be switched between the two domains by appropriate rotation of the magnetic field, in the capped layers no domain switching occurs. Moreover, in all layers a significant (exceeding 300 G at 3 K) internal, unidirectional magnetic field $\mathbf{H}_{int}$ is detected. This field is tilted with respect to the [111] growth axis (which is the easy magnetization direction in the $Ge_{1-x}Mn_xTe$ composition range investigated) with the tilt angle depending on Mn composition and temperature, and points towards the substrate. We attribute $\mathbf{H}_{int}$ to exchange field induced by uncompensated and pinned Mn spins at the interface between the antiferromagnetic MnSeTe cap and ferromagnetic $Ge_{1-x}Mn_xTe$ layers. This assumption is supported by observation of a similar exchange field but oppositely directed (out of the layer surface) for $Ge_{1-x}Mn_xTe$ grown on a 20 nm thick PbEuSe buffer. Also in these samples no domain switching is observed.

In contrast to typical FM/AFM structures, where the direction of the bias field can be set by cooling below the Neel temperature in an applied magnetic field, in the studied samples the exchange field appears spontaneously with no field cooling and its direction cannot be changed with field cooling up to 1 T available in the experimental setup.

Acknowledgement:
Work supported by National Science Centre grant UMO-2014/15/B/ST3/03928.

[1] H. Przybylińska, G. Springholz, R.T. Lechner, M. Hassan, M. Wegscheider, W. Jantsch, and G. Bauer, *Phys.Rev. Lett.* **112**, 047202 (2014).

Inhomogeneous nuclear spin polarization induced by helicity-modulated optical excitation of fluorine-bound electron spins in ZnSe

E. Kirstein[1], F. Heisterkamp[1], A. Greilich[1], E. A. Zhukov[1], T. Kazimierczuk[1,*], V. L. Korenev[2], I. A. Yugova[3], D. R. Yakovlev[1,2], A. Pawlis[4], and M. Bayer[1,2]

[1] *Experimentelle Physik 2, Technische Universität Dortmund, 44221 Dortmund, Germany*
[2] *Ioffe Institute, Russian Academy of Sciences, 194021 St. Petersburg, Russia*
[3] *Physical Faculty of St. Petersburg State University, 198504 St. Petersburg, Russia*
[4] *Peter Grünberg Institute (PGI-9), Forschungszentrum Jülich, 52425 Jülich, Germany*

In a ZnSe:F epilayer dynamic nuclear polarization (DNP) of the ^{77}Se and ^{67}Zn isotopes with nonzero nuclear spin was observed by all-optical means. The DNP is driven by the optically induced electron spin polarization due to the resulting Knight field. Moreover, the electron spin polarization, induced by excitation of the donor-bound exciton, can be measured by the Kerr rotation technique. In the regime of resonant spin amplification (RSA) the interplay between the electron and nuclear spin systems can be precisely investigated by the Overhauser field resulting in a dispersion-like shift of the RSA peaks. The shift of the RSA peaks cannot be explained by a single dispersive curve, but requires a spatially inhomogeneous Knight field. The DNP process was studied with different parameters and techniques to gain a better understanding, mainly of which electron spin polarization component the DNP is driven. The DNP is described in terms of the spin temperature approach, leading to nuclear spin cooling.

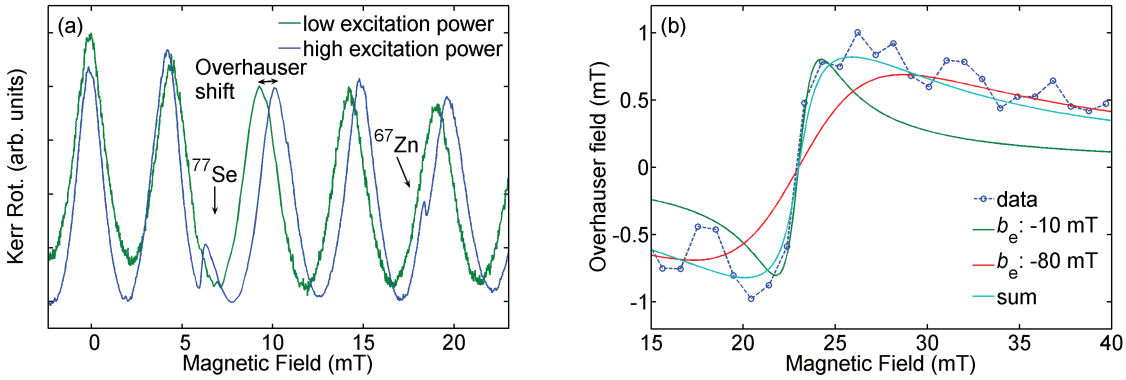

Figure 1: (a) RSA spectra for high and low laser excitation power. The positions of the ^{77}Se and ^{67}Zn resonances are marked by arrows. The shift of the RSA resonances due to nuclear polarization is shown by a horizontal double arrow. (b) The shift of the RSA resonances due to nuclear polarization is shown against the external magnetic field. The dispersive shape of the curve is compared with two theoretical fits and the sum of both curves, showing the development of the spatial inhomogeneous Knight field b_e.

[1] F. Heisterkamp, A. Greilich, E. A. Zhukov, E. Kirstein, T. Kazimierczuk, V. L. Korenev, I. A. Yugova, D. R. Yakovlev, A. Pawlis, and M. Bayer, *Phys. Rev. B* **92**, 245441 (2015).

*__Present address:__ Institute of Experimental Physics, Faculty of Physics, University of Warsaw, 02-093 Warsaw, Poland

Electronic and magnetic properties of isolated Re(vs Mn) ion and Re-Re (vs Mn-Mn) complex in wurtzite - and zinc blende – ZnO in GGA +U approach

O. Volnianska and P. Boguslawski

Institute of Physics PAS, al. Lotnikow 32/46, 02-668 Warsaw, Poland

In the field of spintronics, dilute magnetic semiconductors that combine nonvolatile magnetic storage and traditional electronics can offer the possibility of spin polarized current and electrical control of magnetic effect. Ferromagnetism (FM) in *p*-type Mn-doped ZnO, predicted by T. Dietl in 2000 [1], is one of the most widely studied and controversial transition metal (TM) doped oxide semiconductor systems. Significant array of contradictory results were obtained for this system stating FM [2], AFM, PM, and spin glass phase in ZnMnO [3]. The mechanism of FM in transition metal (TM)-doped oxide semiconductors remains unclear, because the observed magnetism can be either an intrinsic property of the material, or a result of the formation of secondary magnetic phases due to precipitation of TM clusters. At present, two explanations of magnetism in TM-doped ZnO are operative. One approach is based on the Zener model [3], and the second one relies on the first principles calculations showing that the overlap of *d*(TM) with p orbitals of neighboring O atoms form delocalized band levels, and an exchange interaction depends on density of (spin polarizized) states at the Fermi level [4]. It was shown that wave function of Mn ion in ZnO is strongly localized on Mn states and magnetic interaction between Mn-Mn is short range [3]. Delocalization of impurity-induced bands may be responsible for long-range magnetic interactions.

To check this hypothesis we analyzed properties of isolated rhenium Re^{2+} ion in wurtzite (*w*) and zince blende (*zb*) crystals and magnetic interaction Re-Re by Density Functional Theory calculations within the generalized gradient approximation, and compared them with the respective results for Mn. We included the Hubbard-like term +*U* describing the on-site Coulomb interactions [5]. Calculations were performed using QUANTUM-ESPRESSO code [6]. We assumed that $0<U<10$ eV, and applied the correction to *d*(Zn), *d(*Re(Mn)), and 2*p*(O) states. Application of U(Zn) = U(O) = 7 eV gives a correct value of a band gap of ZnO, 3.2 eV. The *w*- (*zb*) - supercell used in calculations contained, 72, 128 (64, 216) atoms.

5*d*(Re) orbital, like 3*d*(Mn), is occupied by 5 electrons. GGA+*U* calculations show that in *w*-ZnO the Re ion introduces a triplet and a doublet in the band gap and that the spin states of isolated ion are high spin (HS) with spins that equal to 5/2 and 2, for neutral (d^5) and 1+(d^4) charge states (*q*), respectively. In *zb*-ZnO, a stable HS configuration with spins 2 and 3/2 are identified for Re in q=0 and 1+, respectively. For small values of *U*, the low spin state is stable. In contrast to Re, Mn ion is in the high spin state within both GGA and GGA+U.

Calculations of spin density indicate a frustrated magnetism for Re ion, since *d*(Re) and *p*(O) of oxygen neighbors have opposite spin polarizations. Calculations of the density of the states of a pair Re-Re were performed. In contrast to the case of a Mn-Mn pair, spin polarization of a Re-Re pair is long-ranged due to the large radius of Re atom. In *p*-ZnO, the 2+ charge state of the Re-Re complex has the FM ground state, in contrast to a neutral pair in intrinsic ZnO, which exhibits a ferrimagnetic ground state. *Finally, the impact of the assumed value of U(Rh) on the magnetic properties of ZnO:Rh is analyzed*.

The work was supported by FNP grant POMOST/2012-5/10, and the National Science Centre, (Poland) Grant No. 2015/17/D/ST3/00971. Calculations were done at Interdisciplinary Center for Mathematical and Computational Modelling, University of Warsaw.

[1] T. Dietl *et al*., Science **287**, 1019 (2000).
[2] P. Sharma *et al*. Mat. Mater. **2**, 673 (2003).
[3] T. Dietl and H. Ohno, Rev. Mod. Phys. **86**, 187 (2014).
[4] L. Petit *et al*. Phys. Rev. B **73**, 045107 (2006).
[5] M. Cococcioni and S. de Gironcoli, Phys. Rev. B **71**, 035105 (2005).
[6] P. Giannozzi *et al*. J. Phys.: Condens. Matter. **21**, 395502 (2009).

Influence of spin polarization of p electrons of anions on a spin state of transition metal ion doped in ZnVI semiconductors. GGA+U calculations

O. Volnianska, P. Boguslawski

Institute of Physics PAS, al. Lotnikow 32/46, 02-668 Warsaw, Poland

II-VI and III-V semiconductors (DMS) doped with transition metals (TM) were the focus of last decade research. A special attention was paid to wide band semiconductors, like ZnO:Mn, due to the predicted ferromagnetism (FM) at room temperature [1, 2]. However semicondictors with p-type conductivity are difficult to fabricate because of the undergoing compensation.

A number of works [3, 4] suggested that *p* orbitals of anions like, N, O or S may play a crucial role in magnetism of DMS. It is obvious if we consider *sp-d* hybridization lying at the base of magnetic properties in DMS [3]. Morever, magnetic properties stem from properties of valence bands that are built mainly from p orbitals of anions. Here, the influence of anions comprising the material matrix is investigated and analyzed within the ab-initio studies. We analyze an electronic structure and magnetic properies of zinc-blende ZnO, ZnS, ZnSe, and ZnTe doped with TM ions as Mn, Fe, Co or Re by Density Functional Theory calculations within the generalized gradient approximation (GGA). We included the Hubbard-like term $+U$ describing the on-site Coulomb interactions [5]. Calculations were performed using QUANTUM-ESPRESSO code [6]. We assumed that U range from 0 to 10 eV, and applied the correction to *d*(Zn), *d(*TM), and 2*p*(O) states. The *zb*-supercell used in calculations contained 64 and 216 atoms.

Electronic structure of TM substituting cation in II-VI crystals is determined by its local atomic configuration and TM-induced bands can be regarded as combinations of the *d*(TM)-*p(*anion*)* states. In *zb*-crystal field a doublet and a triplet (which is higher in energy by ~1 eV) *d*(TM) bands are split into spin-up and spin-down states by the exchange coupling ($\Delta\varepsilon_{ex}$). Stability of high spin state (HS) of defect is determined by an energy of spin polarization (ΔEsp), corresponding to a difference in total energies of spin nonpolarized (PM) and polarized (FM) states.

Calculations of density electronic states and density of spin polarizations for considered system show that spin polarization of defects originates from a spin polarization of *d* orbitals of TM and *p* orbitals of anions, mainly those that are neighbors of the TM ion. Moreover, it is shown that both, ΔEsp and $\Delta\varepsilon_{ex}$ depend on energies of spin polarization of both d(TM) and p(anion) orbitals. We analyzed a dependence of stability of HS state of TM on charge state of TM. Results of GGA+U calculations for neutral TM are shown in Table I.

Table I Energy of spin polarization (eV) and a total spin of TM ions in ZnVI semiconductors

	ZnO	ZnS	ZnSe	ZnTe
Mn_{Zn}	5.93 (S=5/2)	5.5 (S=5/2)	5.4 (S=5/2)	5.6 (S= -5/2)
Fe_{Zn}	4.64 (S=4/2)	3.3 (S=4/2)	2.83 (S=4/2)	3.3 (S= -3.2/2)
Co_{Zn}	3.4 (S=3/2)	2.8 (S=3/2)	2.54 (S=3/2)	2.0 (S=-2.9/2)
Re_{Zn}	4.0 (4.6/2)	3.8 (S=5/2)	0.63 (S=1/2)	4.0 (4.5/2)

The biggest spin polarization energy is reported for ZnO and ZnS and can be associated with strong spin polarization of p orbitals of O (S) atoms near the defects.

Spin density calculations suggest that for defects spin density is localized in the vicinity of both the TM and the nearest-neighbor four anion atoms. A degree of delocalization of a wave function of TM in ZnVI increases with a increasing atomic number of TM and with a decreasing atomic number of anions. In case of Co and Re, spin density function exhibits a long-range and more delocalized character in ZnO and ZnS.

Calculations of spin density indicate a frustrated magnetism for Re ion in ZnO and ZnSe, since d(Re) and p(O) (*p*(Se)) of oxygen neighbors have opposite spin polarizations. In ZnSe, Re_{Zn} is a low spin state with a spin equal to ½. Finally, the impact of the assumed value of U(TM) on the magnetic properties of ZnVI:TM is analyzed.

The work was supported by FNP grant POMOST/2012-5/10, and the National Science Centre, (Poland) Grant No. 2015/17/D/ST3/00971. Calculations were done at Interdisciplinary Center for Mathematical and Computational Modelling, University of Warsaw.

[1] T. Dietl *et al*., Science **287**, 1019 (2000).
[2] T. Dietl and H. Ohno, Rev. Mod. Phys. **86**, 187 (2014).
[3] K. Sato *et al*. Rev. Mod Phys. **82**,1633 (2010).
[4] O. Volnianska, T. Zakrzewski, P. Boguslawski, J. Chem. Phys. 141, 114703 (2014).
[5] M. Cococcioni and S. de Gironcoli, Phys. Rev. B **71**, 035105 (2005).
[6] P. Giannozzi *et al*. J. Phys.: Condens. Matter. **21**, 395502 (2009).

Novel insights into the spin-flip Raman scattering of Mn^{2+} ions

Henning Moldenhauer[1], Carolin Lüders[1], Philipp Waldkirch[1], Dennis Kudlacik[1], Victor Sapega[2], Jörg Debus[1], Andreas Waag[3], Dmitri Yakovlev[1,2], and Manfred Bayer[1,2]

[1] *Experimentelle Physik 2, Technische Universität Dortmund, 44227 Dortmund, Germany*
[2] *Ioffe Institute, Russian Academy of Sciences, 194021 St. Petersburg, Russia*
[3] *Institut für Halbleitertechnik, TU Braunschweig, 38016 Braunschweig, Germany*

Diluted magnetic semiconductors (DMS) are promising materials for devices based on the tailoring of their spin properties leading to the field of semiconductor spintronics. Even though there has been a continuous study on Mn-based DMS during the last decades, several questions on the carrier-Mn ion interactions are still unanswered [1,2]. In that context, we investigate the spin-flip Raman scattering (SFRS) of the Mn^{2+} ions in (Zn,Mn)Se/(Zn,Be)Se quantum wells with Mn ion concentrations below 4 % by precisely analyzing the dependence on the magnetic field geometries.

For tilted geometries, Stühler et al. observed up to fifteen Mn^{2+} SFRS lines [3], which could not be explained by the spin multiplicity of six of the Mn system [4]. It was described in the framework of a collective effect involving several Mn ions, where the decrease in magnetization corresponds to the multiple spin-flips, as observed in the Stokes regime. We measure multiple Mn^{2+} spin-flips also on the anti-Stokes side, which is one argument to extend the proposed model.

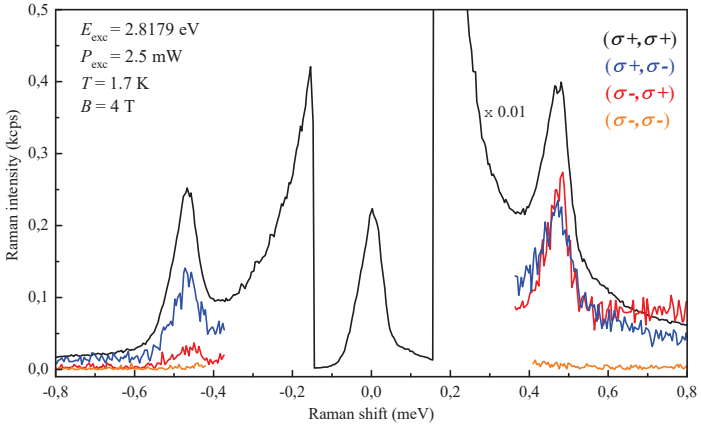

Figure 1: Mn^{2+} SFRS spectra for a $ZnMn_{0.004}Se$ quantum well measured in different circular polarization configurations. The neutral exciton was resonantly excited.

Another argument to reconsider the mechanism of the Mn^{2+} SFRS arises during its study in the Faraday geometry for different circular polarization configurations. As shown in Figure 1, the intensities of the Stokes and anti-Stokes Mn^{2+} SFRS lines are highest for copolarized (σ^+, σ^+) configuration. Moreover, it is dominant for the excitation of the neutral exciton, while at the trion its intensity is negligible. We suggest that the Mn^{2+} SFRS resonance is caused either by anisotropic flip-stop exchange interaction with the electron of the neutral exciton or by a scattering process including isotropic exchange and hyperfine interaction with a nuclear spin. To verify this mechanism we apply radio-frequency fields, combined with resonant SFRS, to observe an impact of the nuclear spin depolarization on the Mn^{2+} SFRS signal.

[1] A. D. McCarty, A. K. Hassan, L.-C. Brunel et al., *Phys. Rev. Lett.* **95**, 157201 (2005)
[2] C. Kehl, G. V. Astakhov, K. V. Kavokin et al., *Phys. Rev. B* **80**, 241203(R) (2009)
[3] J. Stühler, G. Schaack, M. Dahl et al., *Phys. Rev. Lett.* **74**, 2567-2570 (1995).
[4] L. C. Smith, J. J. Davies, D. Wolverson et al., *Phys. Rev. B* **77**, 115341 (2008)

The finite-flake graphene quantum dots in the presence of spin-orbit coupling

D. P. Żebrowski[1,2], B. Szafran [1] and F. M. Peeters [2]

(1) AGH University of Science and Technology, Faculty of Physics and Applied Computer Science, al. Mickiewicza 30, 30-059 Kraków, Poland

(2) Departement Fysica, Universiteit Antwerpen, Groenenborgerlaan 171, B-2020 Antwerpen, Belgium

Due to the long spin decoherence time, graphene is considered as a good candidate for spintronic applications [1]. However, the spin-orbit interaction, that allows for operations on the electron spin, is very weak in the pristine graphene [2]. Hopefully, recent studies showed that adsorbed atoms on the graphene surface give rise to enhanced spin-orbit coupling [2]. The particularly important element is fluorine. Adsorbed on the graphene surface in dilute limit increases the magnitude of the spin-orbit coupling about 1000 times [3].

In this work we present the theoretical study of the quantum dots made of finite graphene flakes. We consider flakes with the top-positioned fluorine adatoms in dilute limit. We use the tight-binding model with p_z orbitals only. It has been shown that these orbitals are sufficient to description the electronic structure near the Fermi level [3]. The one electron wave function are used as a basis to build many-electron wave function in the Slater determinant form. The set of Slater determinants serves as a basis for the many-electron calculations treated by the Configuration Interaction (CI) method.

We show the one- and two- electron energy spectrum in the function of magnetic field and size of the flake. We study the spin structure of the confined states in the dots. We perform the time-dependent calculations in order to simulate the spin-valley transitions driven by the alternating electric field.

References

[1] E. McCann and M. Koshino, Rep. Prog. Phys. **76**, 056503 (2013).

[2] A. Avsar, J. H. Lee, G. K. W. Koon and B. Özyilmaz, 2D Mater. **2** 044009 (2015).

[3] S. Irmer, T. Frank, S. Putz, M. Gmitra, D. Kochan, and J. Fabian, Phys. Rev. B **91**, 115141 (2015).

Condensation of semimagnetic exciton-polaritons in localised potential minima in magnetic field

R. Mirek[1], M. Król[1], K. Lekenta[1], J.-G. Rousset[1], M. Nawrocki[1], W. Pacuski[1], M. Matuszewski[2], J. Szczytko[1] and B. Piętka[1]

[1] *Institute of Experimental Physics, Faculty of Physics, University of Warsaw, Poland*

[2] *The Institute of Physics, Polish Academy of Sciences, Warsaw, Poland*

Over the last years exciton-polaritons are attracting significant attention. Many effects like Bose-Einstein condensation [1] and polariton lasing [2] were observed. However, the investigation on the effect of magnetic field on exciton-polariton coherent phenomena is still at early stage, even though many interesting phenomena such as the Meisner [3] or magnetopolaron [4] effects are predicted.

In our work we focused on magnetic field dependence of exciton-polariton condensate in semimagnetic semiconductor microcavity. Our structure contains four quantum wells (QWs) with 1% of manganese, placed between two Distributed Bragg Reflectors [5, 6]. Excitons confined inside QWs couple to the photonic mode giving rise to two eigenstates called upper and lower exciton-polaritons. Incorporation of manganese in QWs leads to the increased magnetic effects due to the s,p-d exchange interaction between localised electrons of d^5 shell of Mn^{2+} and band electrons. By using a confocal microscope with built in magnet up to 9 T we scanned a large area of a sample surface and detected angularly resolved photoluminescence and reflectivity spectra for different positions on the sample.

The emission maps below and above the condensation threshold in magnetic field are illustrated in the Figure. For small pumping power and low magnetic field we observe incoherent emission distributed over a large area. This map allows to track the potential distribution for polaritons due to the photonic disorder. By increasing the excitation power and/or magnetic field we observe a condensation of exciton-polaritons into potential minima. Above the threshold the condensate gets further localised and we observe the emission from localised spots, multicomponent in energy. In our work we demonstrate the spectral and spatial distributions of exciton-polaritons and we examine the polarisation of emitted light, very sensitive to magnetic field due to semimagnetic semiconductor structure.

Figure: Emission maps (energy integrated) of exciton-polaritons in magnetic field of 8 T below condensation threshold (left panel), at the threshold (center) and above the threshold (right).

[1] J. Kasprzak et al. Nature 443, 409 (2006). [2] R. Balili et al., Science 316, 1007 (2007). [3] Y. G. Rubo, et al., Phys. Lett. A 358, 227 (2006). [4] I. A. Shelykh et al., Phys. Rev. B 80, 201306Í (2009) [5] J.-G. Rousset et al., J. Cryst. Growth 378, 266 (2013). [6] J.-G. Rousset et al., Appl. Phys. Lett. 107, 201109 (2015).

Transport and magnetism at ferromagnetic-paramagnetic critical point in (Ga,Mn)As

G. Mazur[1], J. Sadowski[1,2], T. Dietl[1,3,4], and M. Sawicki[1]

[1] *Institute of Physics, Polish Academy of Sciences, Warsaw, Poland*
[2] *MAX-Lab, Lund University, Lund, Sweden*
[3] *Institute of Theoretical Physics, Faculty of Physics, University of Warsaw, Poland*
[4] *WPI-Advanced Institute for Materials Research, Tohoku University, Sendai, Japan*

The critical behavior of resistivity at the paramagnetic-(anti-)ferromagnetic critical point is one of the open problems in the physics of conducting magnets. In $Ga_{1-x}Mn_xAs$ which has become an archetypical carrier-mediated dilute ferromagnetic semiconductor, a phenomenological approach showed that the singularity in dR/dT at T_C can be consistently interpreted in terms of large wave vector scattering of hole carriers from spin fluctuations [1]. However, the recent studies of *insulating* dilute ferromagnet $Ga_{1-x}Mn_xN$ of similar Mn composition, $x \leq 10\%$ demonstrated a highly nonstandard critical *magnetic* behavior [2]. In this work we re-examine the transport characteristics of $Ga_{1-x}Mn_xAs$ in the vicinity of T_C and relate them to the directly measured magnetization in the same experiment. The magnetic measurements for conducting $Ga_{1-x}Mn_xAs$ material revealed the same departure from the classical, single-value critical exponent, description of the divergence of the initial susceptibility at T_C in $Ga_{1-x}Mn_xAs$ as observed, and explained, for $Ga_{1-x}Mn_xN$ [2]. Its consequences onto the critical behavior of resistivity are examined experimentally and theoretically.

[1] V. Novak *et al*., Phys. Rev. Lett., **101,** 077201 (2008).
[2] S. Stefanowicz, G. Kunert, Tian Li, H. Reuther, C. Kruse, S. Figge, W. Stefanowicz, A. Bonanni, M. Sawicki, T. Dietl, and D. Hommel, Phys. Rev. B **88**, 081201(R) (2013)

Cross-correlations in spin-dependent transport through a quantum dot Cooper pair splitter

P. Trocha[1], K. Wrześniewski[1], and I. Weymann[1]

[1] *Faculty of Physics, Adam Mickiewicz University, ul. Umultowska 85, 61-614 Poznań, Poland*

We investigate Andreev transport through a quantum dot attached to two external ferromagnetic leads and one superconducting electrode [1]. The transport properties of the system are studied by means of the real-time diagrammatic technique in the sequential tunneling regime. In the considered system, two main tunneling processes play role: direct Andreev reflection (DAR) and crossed Andreev reflection (CAR). The former one consists of superpositions of processes: an electron, of energy smaller than superconducting gap, tunnels from the normal metal lead through discrete dots level and it pick up another electron with opposite energy and opposite spin to create a Cooper pair which is able to propagate into the superconductor. During this process, a hole with opposite energy and spin opposite to that of the incident electron is reflected back into the normal metal lead. The latter one consists of such processes where the hole is reflected into the second, spatially separated electrode.

Generally, both DAR and CAR processes contribute to the Andreev current. However, under certain conditions, by properly changing device parameters, one can tune the contributions due to CAR and DAR processes or even suppress one of them. Thus, there is sought a tool which allows to distinguish both contributions. A perfect one seems to be given by current cross-correlations, i.e., correlations calculated between currents flowing through two junctions with normal leads. Thus, we show dependence of current cross-correlations on various parameters of the considered model, both in linear and nonlinear transport regimes. The processes and mechanisms leading to enhancement or suppression of current cross-correlations are examined and discussed.

[1] I. Weymann and P. Trocha, *Phys. Rev B* **89**, 115305 (2014).

Nernst-Ettingshausen effect near zero energy gap in $Pb_{1-x}Sn_xSe$

P. Pfeffer, K. Dybko, M. Szot, A. Szczerbakow, A. Reszka, T. Story, and W. Zawadzki

Institute of Physics, Polish Academy of Sciences
Al.Lotnikow 32/46, 02–668 Warsaw, Poland

The Nernst- Ettingshausen (N-E) effect and electron mobility are investigated theoretically and experimentally in mixed $Pb_{1-x}Sn_xSe$ crystals as functions of temperature and chemical composition in the vicinity of vanishing energy gap E_g. The study is related to the discovery that, by changing the temperature, one arrives at the band ordering in which the topological crystalline insulator states appear on the surface [1]. It is shown theoretically and experimentally for four $Pb_{1-x}Sn_xSe$ samples having x between 0.25 and 0.39 that the bulk N-E effect reaches maximum value as a function of temperature when the energy gap goes through zero [2]. This result contradicts the claim made in the literature that, as the gap vanishes, the N-E effect changes sign [3].

The dc transport phenomena are successfully described theoretically in conditions of extreme bands' nonparabolicity. A situation is reached in which both 2D bands of topological surface states and 3D bands of the bulk crystal are linear in electron **k** vector. The theory uses a spherical approximation to the multi-ellipsoidal bands near the L points of the Brillouin zone. Pertinent scattering modes and their contribution to dc transport phenomena in $Pb_{1-x}Sn_xSe$ are analyzed to reach a proper description of our experimental transport results. Spin-flip scattering transitions for all modes are taken into account. As the gap goes through zero, some transport integrals exhibit a singular nonphysical behavior and it is demonstrated how to deal with this problem by introducing damping. Fitting the theoretical description to experiments in four samples we establish adjustable parameters for the active scattering modes. A very good agreement between the theory and experiment is obtained for critical temperatures at which the gap Eg vanishes for different chemical compositions.

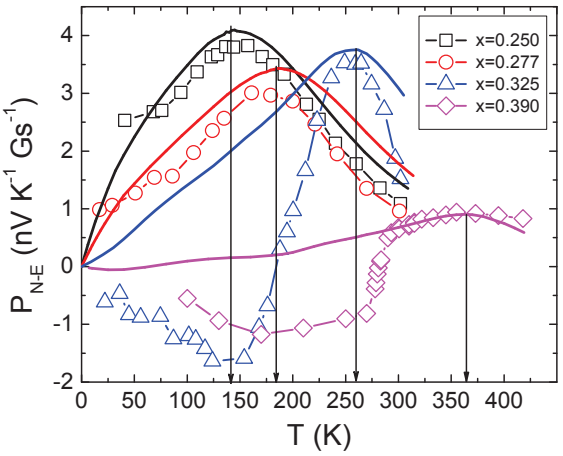

Figure 1: Theoretical and experimental P_{N-E} coefficients versus temperature for four investigated $Pb_{1-x}Sn_xSe$ samples. Solid lines - theory, open symbols - experiment. Vertical arrows point to the temperatures for which the corresponding gaps vanish.

[1] P. Dziawa et al, *Nature Materials* **11**, 1023 (2012).
[2] K. Dybko et al, *New J. Phys.* **18**, 013047 (2016).
[3] T. Liang et al, *Nature Commun.* **4**, 2696 (2013).

Analysis of orderings of partitions in the context of fractional quantum Hall effect

Bartosz Kuśmierz and Arkadiusz Wójs

Wrocław University of Technology, wybrzeże Wyspiańskiego 27, 50-370 Wrocław, Poland

Fractional quantum Hall effect is still highly examined remarkable behavior of electron in solid state. Among many approaches to this problem we focus on based on general trial wave functions, generated by the k-body short-repulsion. Such series, among the Laughlin state (k=2) consists of the Moore-Read „Pfaffian" (k=3) state, believed to be a good description of $\nu = 5/2$ state and Read-Rezayi parafermion ground states (k=4), witch is considered as a description of $\nu = 13/5$ state. Those wave functions are associated to the symmetric functions theory. Connections between the symmetric polynomials theory and quantum Hall effect has been discussed in a series of papers [1-4].

This poster is devoted to the analysis of one aspect of the symmetric polynomials theory in a physics of Hall systems i.e. role of ordering of the partitions. Partition is a sequence of nonnegative integer numbers. Spinless fermionic wave function of a fractional quantum Hall state can be expanded in the Slater determinant basis indexed by partitions. Symmetric polynomials theory suggests that partitions should be ordered according to the reverse lexicographic order, which corresponds to the natural order. Such ordering of a basis reveals that coefficients of certain spinless FQH states are nonzero only for basis functions indexed by the partitions smaller in natural order than certain partition. We examine whether such property can be of use in examination of other fractional quantum Hall states.

[1] B. A. Bernevig and F. D. M. Haldane, Phys. Rev. B **77**, 184502 (2008)
[2] B. A. Bernevig and F. D. M. Haldane, Phys. Rev. Lett. **100**, 246802 (2008).
[3] B. A. Bernevig and F. D. M. Haldane, Phys. Rev. Lett. **102**, 066802 (2009).
[4] B. Kuśmierz, Y.-H. Wu, and A. Wójs, Acta Phys. Polon. A **126**, 1134 (2014).

Non-linear quantum transport in $n-$type CdMgTe/Cd(Mn)Te *quasi*-ballistic microstructure

E. Bobko[1,2], D. Śnieżek[2], D. Płoch[1], M. Majewicz[2], M. Fołtyn[2], M. Wiater[2], T. Wojtowicz[2], and J. Wróbel[1,2]

[1]*Faculty of Mathematics and Natural Sciences, Rzeszów University, al. Rejtana 16A, 35-959 Rzeszów, Poland*
[2]*Institute of Physics, Polish Academy of Sciences, al. Lotników 32/46, 02-668 Warszawa, Poland*

Modulation doped CdMgTe/Cd(Mn)Te structures combine the high mobility of two dimensional electron gas (2DEG) with the extremely large and tunable Landè g-factor, which makes such a quantum wells the material of choice for the construction of semiconductor spintronic nanodevices. Recently, the effective change of the spin splitting has been realized by the application of a strong external electric field oriented along the growth direction of magnetic quantum well [1]. However, the fabrication of top- and bottom electrostatic gates, which are used for that purpose, may be technologically challenging.

In this paper we show, that the g-factor of a magnetic two-dimensional electron gas can also be *tuned electrically* by an increase of the source-drain voltage, when a device operates in the non-linear transport regime. This finding may greatly simplify the design of a future spintronic structures, since less processing steps will be needed for the final assembly. The only requirement is that the sizes of a conductive channels are reduced below the inelastic coherence length of a 2DEG.

We present the results of low-temperature magneto-transport measurements performed on *quasi*-ballistic microstructure defined lithographically on the $n-$type $Cd_{98.5}Mn_{1.5}Te$ QW having barriers made of CdMgTe. The density of two-dimensional electron gas and its mobility at temperature $T = 4.2$ K were determined to be 3.0×10^{11} cm^{-2} and 2.0×10^5 cm^2/Vs, respectively. The sample was formed as a $\Pi-$shaped multi-terminal device with an overall size of 5 μm. We studied the local and non-local differential magnetoconductance in the linear and non-linear transport regimes. Data were collected as a function of source-drain V_{sd} voltage and magnetic field B up to 6 T. Measurements were carried out in the cryo-free dilution refrigerator Triton 400 at the base temperatures ranging from 0.01 to 0.3 K.

At low magnetic fields ($B < 1$ T) we have observed the Shubnikov-de Haas (SdH) oscillation with the characteristic beating pattern which is a consequence of the giant Zeeman splitting [2]. We show that nodes of such pattern, where the oscillations have a vanishing amplitude, are considerably shifted when V_{sd} is increased up to 4.5 mV. Therefore we conclude, that induced changes of g-factor result from a non-equilibrium population of the spin-splitted Landau levels. Furthermore, at stronger fields ($B > 3$ T) we have observed the very high and narrow magnetoconductance peak related to the transition to quantum Hall ferromagnet (QHFM) state [3]. In the language of edge currents, a QHFM phase corresponds to the unique situation when two channels, carrying electrons with opposite spins, cross in real space. We show that this process can also be controlled by a source-drain voltage.

The research was partially supported by National Science Centre (Poland) under the grant DEC-2012/06/A/ST3/00247, the EU 7th Framework Programme Grant No. REGPOT-CT-2013-316014 and Regional Development Program (Poland), grant WND-RPPK. 01.03.00-18-053/12.

[1] A. Kazakov, *et al*., to be published.
[2] J. Kunc, *et al*., Phys. Rev. B **92**, 085304 (2015).
[3] J. Jaroszyński, *et al*., Phys. Rev. Lett. **89**, 266802 (2002).

Topological crystalline insulator transition and spin texture in (Pb,Sn,Mn)Se

P. Dziawa[1], B.M. Wojek[2], M.H. Berntsen[2], A. Forsman[2], B.J. Kowalski[1], A. Szczerbakow[1], C.M. Polley[3], M. Leandersson[3], T. Balasubramanian[3], J. Domagała[1], T. Wojciechowski[1], W. Knoff[1], O. Tjernberg[2], and T. Story[1]

[1]*Institute of Physics, Polish Academy of Sciences, al. Lotników 32/46, 02-668 Warsaw, Poland*
[2]*KTH Royal Institute of Technology, ICT Materials Physics, Electrum 229, 164 40 Kista, Sweden*
[3]*MAX IV Laboratory, Lund University, 221 00 Lund, Sweden*

$Pb_{1-x}Sn_xSe$ substitutional alloy is the member of new class of quantum materials – topological crystalline insulators (TCIs) [1]. The topological order is protected by (110) mirror symmetry of the rock-salt crystal structure. This phase is manifested by gapless Dirac-like surface states observed upon inversion in band structure and exhibits specific helical spin texture [2, 3]. In these materials the topological non-trivial state with opposite parity in band structure for high symmetry planes is observed for bulk as well as layered materials [4] and can be controlled by pressure [5], temperature or change of chemical composition [3]. In this work we verify possibility of controlling the TCI transition by band gap engineering via incorporation of manganese ions into host matrix. Previous studies of $Pb_{1-x-y}Sn_xMn_ySe$ showed dE_g/dy equal to 30 meV per at.% of Mn [6]. The second crucial point was verification of protection of the helical spin texture in presence of magnetic ions.

Bulk monocrystals of $Pb_{1-x-y}Sn_xMn_ySe$ with $0.28 \le x \le 0.385$ and $y \le 0.022$ were grown by the Bridgman method. The crystalline quality, lattice parameter and chemical composition were studied by x-ray diffraction and energy-dispersive x-ray spectroscopy. In very diluted regime of the manganese ions (y=0.0003) the electron paramagnetic resonance proved that the Mn ions are in 2+ charge state with spin-only S=5/2 local magnetic moment, hence they are built in cation sublattice positions. For purpose to verify our goals we used freshly cleaved (001)-oriented crystals for both angle-resolved and spin-resolved photoemission spectroscopy at 9 K – 300 K and 65 K, respectively. Analysis of the temperature evolution of band structure for whole studied set of samples shows that the TCI transition appears at lower temperatures with respect to $Pb_{1-x}Sn_xSe$. We found that the $dE_g/dT \approx 50$ meV/K is independent on Mn content and does not change for both trivial and TCI states. Studies of spin texture at TCI state were carried out on the sample with very high Sn content (x=0.385 and y=0.01). Spin resolved spectra taken at both sides of X-bar point of surface Brillouin zone exhibit change of spin polarization. This result is analogous to spin texture obtained for $Pb_{1-x}Sn_xSe$ samples [6] and provides clear evidence that magnetic ions in the crystal matrix of topological crystalline insulators do not destroy TCI order. Finally, we propose phase diagram for $Pb_{1-x-y}Sn_xMn_ySe$ crystals as guideline for further works on TCI band gap engineering.

[1] L. Fu, Phys. Rev. Lett. **106**, 106802 (2011)
[2] P. Dziawa, B.J. Kowalski, K. Dybko et al., Nat. Mat. **11**, 1023 (2012)
[3] B. M. Wojek, P. Dziawa, B. J. Kowalski et al., Phys. Rev. B **90**, 161202(R) (2014)
[4] C.M. Polley, P. Dziawa, A. Reszka et al., Phys. Rev. B **89**, 075317 (2014)
[5] P. Barone, T. Rauch, D. Di Sante et al., Phys. Rev. B **88**, 045207 (2013)
[6] B.M. Wojek, R. Buczko, S. Safaei et al., Phys. Rev. B **87**, 115106 (2013)
[7] L. Kowalczyk, A. Szczerbakow, Acta Phys. Pol. **A67**, 189 (1985)

Synthetic Haldane phase of correlated electrons in a chain of semiconductor quantum dots embedded in a nanowire

Błażej Jaworowski [1], Nick Rogers[2], Marek Grabowski[3], Paweł Hawrylak[2]

[1] *Department of Theoretical Physics, Wrocław University of Science and Technology, Wybrzeże Wyspiańskiego 27, 50-370 Wrocław, Poland*
[2] *Department of Physics, Advanced Research Complex, 25 Templeton Str., University of Ottawa, Ottawa, Ontario, K1N 6N5, Canada*
[3] *Department of Physics, University of Colorado at Colorado Springs, Colorado Springs, CO, USA*

Recently, the topological phases of macroscopic quantum matter have gained wide interest. A characteristic features of these phases is the existence of topologically protected edge states. Their robustness suggests their potential applications, e.g. in quantum computing. Some of the topological phases of macroscopic quantum matter can be explained within single-particle picture, whereas others orignate from the strong correlation of electrons. An example of the strongly-correlated topological phase is the Haldane phase , predicted theoretically[1] and observed experimentally[2] in spin-1 antiferromagnetic chains. The ground state of the spin-one chain in Haldane phase is characterized by two edge states with spin-$\frac{1}{2}$.

In this work, we propose a synthetic many-body system of correlated electrons in a chain of semiconductor quantum dots embedded in a nanowire as a candidate for a macroscopic Haldane phase [3]. We consider a chain of N quantum dots embedded in a quantum wire, with 4 electrons per dot . We describe the system using extended Hubbard-Kanamori (HK) model limited to 2 electrons per dot on a degenerate p-shell. The parameters of the HK model , tunneling between dots, direct and exchange interaction within a dot and between dots, are determined from a microscopic calculation for two coupled dots with Ne=8 electrons. We find the ground state and energy spectrum of the N electron HK chain using exact-diagonalization, Lanczos and Density Matrix Renormalization Group [4] methods. We show that the exchange interaction of each two electrons on a degenerate p-shell effectively pairs electrons into spin one objects on each dot and the low energy sector of the HK chain can be mapped onto the low energy sector of a spin one chain. The ground state of the HK chain is shown to correspond to localized states at the edge with effective spin-$\frac{1}{2}$. We note that the spin-$\frac{1}{2}$ edge states can be used as a singlet-triplet qubit [3] encoded in a macroscopic quantum state. Finally, we describe optical transitions between the valence and conduction band states of quantum dots with electrons [5] and identify the signatures of the Haldane phase in absorption spectra. Therefore, our results allow to describe the transfer of quantum information from the singlet-triplet qubit to the photon.

[1] F. D. M. Haldane, Phys. Lett. A 93, 464 (1983)

[2] W. J. L Buyers, R. M. Morra, R. L. Armstrong, M. J. Hogan, P. Gerlach, and K. Hirakawa, Phys. Rev. Lett. 56, 371 (1986)

[3] N. Rogers, M, Grabowski, B. Jaworowski, and P. Hawrylak, to be publsihed.

[4] S. R. White, Phys. Rev. Lett. 69, 2863 (1992)

[5] G. A. Narvaez, and P. Hawrylak, Phys. Rev. B 61, 13753

Three-Dimensional Dirac Semimetal–Insulator Transition in $(Cd_{1-x}Zn_x)_3As_2$ Bulk Crystals

G. Grabecki [1,2], K. Grasza [1], P. Skupiński[1], A. Avdonin[1], I. Yahniuk[3], E. Łusakowska[1], A. Reszka[1], M. Majewicz[1], and T. Dietl[1,4,5]

[1]*Institute of Physics, Polish Academy of Sciences, PL-02 668 Warszawa, Poland*
[2]*Department of Mathematics and Natural Sciences, College of Sciences, Cardinal Wyszynski University, PL 01-938 Warszawa, Poland*
[3]*Institute of High Pressure Physics, Polish Academy of Sciences, PL 01-142 Warszawa, Poland*
[4]*Institute of Theoretical Physics, Faculty of Physics, University of Warsaw, PL-02-093 Warszawa, Poland*
[5]*WPI-Advanced Institute for Materials Research (WPI-AIMR), Tohoku University, Sendai 980-8577, Japan*

Presently it is well established, both theoretically [1] and experimentally [2], that Cd_3As_2 is a three dimensional Dirac semimetal where the valence and conduction bands touch at two points in reciprocal space with a linear dispersion. However, this material is strongly *n*-type with electron concentration usually exceeding 10^{18} cm^{-3} . Since this indicates that the Fermi energy is risen hundreds of meV above the Dirac points, they are not directly accessible by the electron transport measurements. On the other hand, Cd_3As_2 and Zn_3As_2 form a solid solution $(Cd_{1-x}Zn_x)_3As_2$ in the whole range of x. Because Zn_3As_2 is a trivial p-type semiconductor with E_g = 1 eV [3], a transition between the Dirac semimetal and insulator phase is expected around x=0.38[4]. Simultaneously, one expects transition from *n*-type to *p*-type conductivity, which should lower the Fermi energy and enable direct access to the Dirac cones.

In the present work we report on new electron transport measurements performed on bulk crystals of $(Cd_{1-x}Zn_x)_3As_2$, where x changes from 0 to 0.92. They are obtained by the growth from molten phase. The crystal sizes are of the order of several millimeters. For $x < 0.35$ the samples are strongly *n*-type with the Hall electron concentration of the order of 10^{18} cm^{-3}. Their mobilities are above 10^4 cm^2/Vs for all values of x in this range, and they show pronounced Shubnikov-de Haas oscillations for $T < 50$ K. However, for higher Zn content, x = 0.42 , the conductance becomes p-type and it drops by 6 orders of magnitude in comparison with that of x=0.35. Additionally, it strongly decreases with lowering the temperature, indicating insulating behavior. For yet higher Zn content, x = 0.92, we observe restoring of the metallic behavior, but the conductance is p-type in the whole temperature range from 1.8 K to 300 K. In summary, we have observed Dirac semimetal-insulator transition in $(Cd_{1-x}Zn_x)_3As_2$ as a function of x, which opens new possibilities in studies of the topological phases.

[1] J. Bodnar, *Proc. Int. Conf. Phys. Narrow-Gap Semicond*., Warsaw, 1977 (PWN, Warsaw 1978), p. 311; Z. J. Wang, H. M. Weng, Q. S. Wu, X. Dai, and Z. Fang, Phys. Rev. **B 88**, 125427 (2013).
[2] S. Borisenko, Q. Gibson, D. Evtushinsky, V. Zabolotnyy, B. Büchner, and R.J. Cava, *Phys. Rev. Lett.* **113**, 027603 (2014).
[3] H. J. Naake and S. C. Belcher, J. Appl. Phys. **35**, 3064 (1964)
[4] Thong Lu, Xiao Zhang, and Shuang Jia, arXiv:1507.07169v1.

Entanglement spectrum of topological band insulators on the Lieb lattice

M. Brzezińska, P. Potasz, and A. Wójs

Department of Theoretical Physics, Wrocław University of Technology, Wybrzeże Wyspiańskiego 27, 50-370, Poland

Recently, topological insulators have garnered an immense interest due to unique electronic structure and promising applications in the context of quantum Hall effect [1]. Chern insulators are time-reversal symmetry breaking band insulators exhibiting a nonzero Hall conductance. Topologically ordered systems manifest non-local correlations and therefore can be investigated by employing different entanglement measures. The reduced density matrix for a particular subsystem in a real space can be determined from the correlation matrix [2, 3], which is defined as a two-point correlation function.

In this work, we study a free fermion Chern insulator on the two-dimensional Lieb lattice in a cylinder geometry through entanglement spectrum. Within the tight binding approximation, the Lieb lattice has a flat (but trivial) band in the middle of the energy spectrum. However, a topological phase transition can be induced by the presence of spin-orbit coupling and staggered sublattice potential. For various model parameters, we examine the eigenvalues and the trace of the correlation matrix for both trivial and non-trivial phases. The effect of the flux threading on a Chern insulator is shown. Localization of edge states is also discussed.

[1] N. Regnault, and B. A. Bernevig, *Phys. Rev. X* **1**, 021014 (2011).
[2] A. Alexandradinata, T. L. Hughes, and B. A. Bernevig, *Phys. Rev. B* **84**, 195103 (2011).
[3] M. Legner, and T. Neupert, *Phys. Rev. B* **88**, 115114 (2013).
[4] T. L. Hughes, E. Prodan, and B. A. Bernevig, *Phys. Rev. B* **83**, 245132 (2011).
[5] A. M. Turner, Y. Zhang, and A. Vishwanath, *Phys. Rev. B* **82**, 241102(R) (2010).

The effect of magnetic field on edge states in InN/GaN quantum wells

Witold Bardyszewski [1] **and Sławomir P. Łepkowski** [2]

[1] *Faculty of Physics, University of Warsaw, ul. Pasteura 5, 02-093 Warszawa, Poland*
[2] *Institute of High Pressure Physics - Unipress, Polish Academy of Sciences, ul. Sokołowska 29, 01-142 Warsaw, Poland*

It has been recently demonstrated that, under specific conditions, the band structure of InN/GaN quantum wells (QW) may be inverted, resulting in the transition to the so-called topological insulator (TI) state in which, apart from the energy gap in the bulk material there is a continuum of states localized on the edge of the system with energies closing the energy gap.[1] These states give rise to the counter propagating helical channels leading to the so called quantum spin Hall (QSH) effect. In this respect InN/GaN QWs provide a novel example of yet another 2D TI system which may be compared to the existing structures such as HgTe/CdTe and InAs/GaSb QWs realized so far. [2] The band structure inversion in narrow InN/GaN QWs grown along (0001) crystallographic direction is caused mostly by the extremely large built-in electric field originating from piezoelectric effect and spontaneous polarization but also, by the specific band structure of these materials related to their wurtzite structure symmetry. So, although the InN/GaN is a direct gap (type I) quantum well, the wave functions in the conduction and valence band are quite well spatially separated in this structure and therefore one should expect some analogy to the type II broken-gap InAs/GaSb QWs. The topological insulator state is protected by the time reversal symmetry, but it turns out that the helical edge states may persist even at strong magnetic field, as it was demonstrated for the case of HgTe quantum wells. [3] The situation is slightly different in type II broken-gap quantum wells, in which the crossing of Landau levels at some rather low critical value of the magnetic field closes the bulk gap and opens the way for the bulk conduction.

In the present paper we consider the edge states in the infinite stripe geometry of InN/GaN QWs in the magnetic field perpendicular to the stripe plane. Our effective 6x6, two-dimensional Hamiltonian obtained from the full eight-band k.p model incorporates one conduction, one heavy hole and one light hole QW subbands in the vicinity of the energy gap. The magnetic field is accounted for by using the Peierls substitution and by solving the resulting finite difference eigen-problem for a 1000 nm wide stripe of a 14 nm wide QW layer for a range of magnetic fields from B=0 T to B=15 T. In this structure the negative (inverted) energy gap of about 4 meV occurs between the heavy hole and light hole levels at B=0 T. It is observed that the first crossing of the Landau levels originating from the heavy and light-hole bands closes the bulk band gap at about B=6 T. Up to this magnetic field, the dispersion and spin polarization of helical edge states are not very sensitive to the increasing magnetic field. Even after the crossing, up to B=15 T, both edge channels exist, although with much lower degree of spin polarization. One may therefore conclude, that despite the spatial separation of the conduction and valence band states the TI InN/GaN QWs is similar to HgTe system in that the helical edge states are quite robust against the external magnetic field

This work was supported by the Polish National Science Center, Project No. 2012/07/B/ST3/03174.

[1] S. P. Łepkowski and W. Bardyszewski, submitted to *Phys. Rev. B.*
[2] M. Z. Hasan and C. L. Kane, *Rev. Mod. Phys.* **82**, 3045 (2010).
[3] G. Tkachov E.M. Hankiewicz, *Phys. Rev. Lett* **104**, 166803 (2010).

Pressure studies of transition from topological insulator into Anderson topological insulator in HgTe quantum well

I. Yahniuk[1], G. Grabecki[2,3], M. Majewicz[2], J. Wróbel[2], T. Dietl[2], G. Cywiński[1], C. Skierbiszewski[1], S. S. Krishtopenko[4,5], S. A. Dvoretsky[6], N. N. Mikhailov[6,7], F. Teppe[5], W. Knap[1,5]

[1] Institute of High Pressure Physics PAS, 29/37 Sokołowska, ???Warsaw, Poland
[2] Institute of Physics PAS, al. Lotników, PL 02 668 Warsaw, Poland
[3]Department of Mathematics and Natural Sciences, College of Sciences, Cardinal Wyszynski University, PL 01-938 Warszawa, Poland
[4] Institute for Physics of Microstructures RAS, GSP-105, 603950, N. Novgorod, Russia
[5] Laboratoire Charles Coulomb (L2C), UMR CNRS 5221, University of Montpellier, 34095 Montpellier, France
[6] Rzhanov Institute of Semiconductor Physics SB of RAS, 630090 Novosibirsk, Russia
[7] Novosibirsk State University, 630090, Russia
ivan.yahniuk@unipress.waw.pl, grabec@ifpan.edu.pl

One important point in the physics of two-dimensional topological insulators (2DTI) [1] is the unknown role of trivial, i.e., non-helical edge channels that may exist in HgTe QWs, together with the helical ones [2]. They are a result of band bending at the outer edge caused by surface states and/or by contamination by impurities. In the recent work Ma et al. [3] the assume the existence of trivial channels to explain results of microwave impedance microscopy measurements on HgTe QWs. On the other hand, the main evidence against a contribution of the trivial channels in 2DTI is a very high resistance in the wells of the thickness smaller than the critical value, $d < d_c$, i.e., those of direct band structure [1].

In order to resolve this ambiguity we perform new studies of nonlocal resistance of the edge channels in HgTe QW with d = 7.1 nm at different hydrostatic pressures up to 3.6 kbar. Because the pressure would induce a transition between 2DTI and trivial insulator phases [4], one expects the disappearance of nonlocal transport along helical channels, but not via trivial channels. However, we have found that the pressure causes a substantial decrease of the electron mobility, indicating severe deterioration of the sample. Despite of this, a clear edge transport is preserved. This may point to the appearance of a newly predicted Anderson topological insulator phase in our sample [5]. Furthermore, the nonlocal transport vanishes in high magnetic field values strongly dependent on the pressure, the finding in agreement with results of theoretical calculations within the 8-band *kp* model for topological states. Thus our results can consistently be explained by the presence of topological edge channels though the role of pressure-induced defects has to be elucidated.

This work was partially supported by the RFBR (project № 15-52-16017 and № 15-52-16008)

[1] M. König et al. , Science **318**, 766 (2007).
[2] R. J. Haug, H. Munekata, and L. L. Chang, Jpn. J. Appl. Phys. **31**, L127 (1992).
[3] E.Y. Ma et al. , Nat. Commun. **6**, 7252 (2015).
[4] S.S. Krishtopenko et al., Proceedings of XIX International Symposium "Nanophysics and nanoelectronics", Nizhny Novgorod, 2015, vol. 2, p. 547.
[5] Jian Li, Rui-Lin Chu, J. K. Jain, and Shun-Qing Shen, Phys. Rev. Lett. **102**, 136806 (2009)

Electronic properties of bismuth and antimony thin films

M. Bieniek, T. Woźniak, P. Potasz, and A. Wójs

Department of Theoretical Physics, Faculty of Fundamental Problems of Technology, Wrocław University of Technology, Wybrzeże Wyspiańskiego 27, Wrocław, Poland

In the following work topological properties of bismuth and antimony thin films are investigated using density functional theory and tight-binding method. Bismuth bilayer was among first 2-dimensionals systems predicted to exhibit quantum spin Hall effect [1]. Several experiments have confirmed topological nature of edge states in Bi [2], although there is still on-going debate how robust this effect is with respect to number of layers and type of substrate [3]. Contrary to bismuth, free-standing antimony bilayer is known to be trivial semiconductor [4]. When increasing thickness of this material, it undergoes topological phase transition to 2D QSH phase, then to 3D topological insulator and finally to topological semimetal. Phase diagram of this material can be significantly modified by application of strain and electric fields [5], e.g. for sufficient tensile strain turning bilayer Sb to topological insulator.

Motivated by those studies, we investigate topological properties of thin Bi and Sb films. First, electronic structures of Bi and Sb are calculated using density functional theory. Then, sp^3 tight-binding model [6] is fitted to our dft results, paying special attention to band structure around band-gap region and orbital compositions of conduction and valence bands for both Bi and Sb. In next step, Bi-Bi, Sb-Sb structures and Bi-Sb heterostructure are studied. By careful investigation of separated Bi and Sb electronic structure and then effect of their interaction, we extract tight-binding parameters describing interlayer interactions in all systems. Then the effects of spin-orbit coupling strength and interlayer interaction strength on Z_2 invariant and spin textures are presented. Topological nature of edge states in this system is probed in the nanoribbon geometry for both zigzag and armchair edge types.

[1] S. Murakami, *Phys. Rev. Lett.* **97**, 236805 (2006).
[2] F.Yang et al., *Phys. Rev. Lett.* **109**, 016801 (2012); C. Sabater et al., *Phys. Rev. Lett.* **110**, 176802 (2013); I. K. Drozdov et al., *Nature Physics* **10**, 664 (2014);.
[3] Z.-Q. Huang et al., *Phys. Rev. B 88* **109**, 165301 (2013); Z. Liu et al., *Phys. Rev. Lett.* **107**, 136805 (2011); L. Chen et al., *Phys. Rev. B* **87**, 235420 (2013);.
[4] P.-F. Zhang et al., *Phys. Rev. B* **85**, 201410(R) (2012).
[5] F.-Ch. Chuang et al., *APL* **102**, 022424 (2013).
[6] Y. Liu and R. E. Allen, *Phys. Rev. B* **52**, 1566 (1995).

Analysis of topological properties of Chern insulators

Michal Kupczynski and Pawel Potasz[1]

[1] *Wroclaw University of Science and Technology, Wroclaw, Poland*

Chern insulators are band insulators exhibiting a nonzero Hall conductance but preserving the lattice translational symmetry. [1] Unusual protection of quantized conductance is related to nontrivial topology of energy bands characterized by topological invariant, Chern number; topological properties are stable against small perturbations. In this work we investigate different Chern insulator lattice models. We analyze their common features by looking at band structures, edge states behavior, and Berry curvature. We emphasize differences that can be responsible for distinct many body effects when electron-electron interactions are included. In particular, we indicate models that support stabilization of Fraction Chern Insulator (FCI) phases. [3-6]

[1] F. D. M. Haldane, *Phys. Rev. Lett*. **61**, 2015 (1988).
[2] K. Sun, Z. Gu, H. Katsura, and S. Das Sarma, *Phys. Rev. Lett.* **106**, 236803 (2011).
[3] T. Neupert, L. Santos, C. Chamon, and C. Mudry, *Phys. Rev. Lett.* **106**, 236804 (2011).
[4] D. Sheng, Z.-C. Gu, Gu, K. Sun, and L. Sheng, *Nat. Commun.* **2**, 389 (2011).
[5] N. Regnault and B. A. Bernevig, *Phys. Rev. X* **1**, 021014 (2011).
[6] B. Jaworowski, A. Manolescu, and P. Potasz, *Phys. Rev. B* **92**, 245119 (2015).

Ion Implantation and Annealing Based Synthesizing of AIII-BV Nanostructures in SiO_2/Si Matrix

Przemysław Kopyciński[1], Sławomir Prucnal[1,2], Krzysztof Pyszniak[1], Wojciech Grudziński[1], Jerzy Żuk[1]

[1]Maria Curie-Skłodowska University. Pl. M. Curie-Skłodowskiej 1, 20-031 Lublin, Poland
[2] Institute of Ion Beam Physics and Materials Research, Forschungszentrum Dresden-Rossendorf, P.O. Box 510119, 01314 Dresden, Germany

Most of modern electronics manufacturing is based on silicon. But because of its indirect energy band gap silicon cannot be used as an efficient light source. Therefore from economical and technological points of view it is important to find light sources than can be integrated into Si technology.

One of the possible solutions is to integrate AIII-BV semiconductor nanocrystals inside Si-based matrices. For synthesis of such structures sequential ion implantation and annealing techniques can be used.In this work As^+ + $In^+$and As^+ + Ga^+ions were implanted into SiO_2(100nm)/Si. Flash Lamp Annealing (FLA) in the ms range with preheating was employed within a wide range of annealing parameters such as temperature and time. In that way different sizes of InAs and GaAs nanocrystals were obtained.

To investigate optical properties of InAs and GaAs structures we used low-temperature photoluminescence (PL) and micro-Raman spectroscopic techniques including 2D mapping. PL spectra were obtained in a temperature range from 10K up to RT. Raman spectroscopy was performed at room temperature. The Raman spectra confirms very good quality of InAs and GaAs crystals, and deconvoluted PL spectra give interesting information about expected quantum size effect - related blue shift and nanocrystals sizes.

Atomistic Modeling of Excitonic States in Semiconducting Nanostructures: Beyond 10-Million Atoms in Simulation

Michał Zieliński

Institute of Physics, Faculty of Physics, Astronomy and Informatics,
Nicolaus Copernicus University, Grudziadzka 5, 87-100 Torun, Poland

Numerical calculations of excitonic properties of novel nanostructures such as nanowires [1], nanowire quantum dots [2], or crystal phase quantum dots [3] must combine atomistic accuracy with an approachable computational complexity. The key difficulty comes from the fact that excitonic spectra details arise from atomic scale contributions that must be integrated over a large spatial domain containing a million of atoms and more. In this work we present a step-by-step solution to this problem: combined empirical tight-binding, Hartree-Fock and configuration interaction scheme that unites linearly scaling computational time with the essentials of the atomistic modeling. First, we illustrate our method on the example of well-studied self-assembled InAs/GaAs quantum dot, with the emphasis on the dark exciton spectra [4,5]. Next, we study excitonic properties of several nanostructures such as nanowire quantum dot molecules, quantum dashes, and natural quantum dots [6]. Finally, we show results of our approach applied to crystal phase quantum dots [7] containing more than 10 million atoms.

[1] M. B. Bavinck, M. Zieliński, B. J. Witek, T. Zehender, E. P. A. M. Bakkers, and V. Zwiller, *Nano Lett.* **50**, 6206 (2012).
[2] M. Zieliński, *Phys. Rev. B* **88**, 155319 (2013).
[3] M. B. Bavinck, K. D. Jöns, M. Zieliński, G. Patriarche, J.-Ch. Harmand, N. Akopian, and V. Zwiller, *Nano Lett.* **16**, 1081 (2016).
[4] M. Zieliński, Y. Don, and D. Gershoni, Phys. Rev. B **91**, 085403 (2015).
[5] I. Schwartz, E. R. Schmidgall, L. Gantz, D. Cogan, E. Bordo, Y. Don, M. Zielinski, and D. Gershoni, Phys. Rev. **X 5**, 011009 (2015).
[6] M. Zieliński, K. Gołasa, M. R. Molas, M. Goryca, T. Kazimierczuk, T. Smoleński, A. Golnik, P. Kossacki, A.A.L. Nicolet, M. Potemski, Z. R. Wasilewski, and A. Babiński, Phys. Rev. B **91**, 085303 (2015)
[7] P.T. Różański, and M. Zieliński, http://arxiv.org/pdf/1603.02924v1.pdf

Theory of Polariton Condensates

Michał Matuszewski

Institute of Physics, Polish Academy of Sciences, al. Lotników 32/46, Warsaw, Poland

The physics of quantum fluids of light and the related field of nonequilibrium condensation experience dynamic development in the recent years [1]. The experimental realizations of exciton-polariton condensates ten years ago [2] provided vast possibilities for investigating nonequilibrium quantum systems on an entirely new level, important for understanding of fundamentals of nonequilibrium physics. At the same time, prototypes of devices for applications, such as low-threshold polariton lasers, quantum-enhanced interferometers or low-loss polariton circuits, have been realized.

I will briefly describe the basic theory of exciton-polaritons as well as some of the most interesting experimental realizations and future directions. Commonly used theoretical models based on the mean-field generalized Gross-Pitaevskii equation and its extensions including the effects of quantum fluctuations will be discussed.

In the second part of the talk I will describe our work related to the recent observations of instabilities of non-equilibrium exciton-polariton condensates. We demonstrate the first observation of the long-sought reservoir-induced instability in a nonresonantly pumped condensate [3]. Without any free parameters, we find an excellent agreement between the experimental data and numerical simulations of the open-dissipative Gross-Pitaevskii equation, which allows us to dismiss the competing theoretical model based on the complex Ginzburg-Landau equation. In the case of resonant excitation, the observation of the real-space collapse of the polariton fluid was explained by the effective attractive interactions mediated by the lattice phonons [4]. The observation of instabilities in polariton condensates may fundamentally change our understanding of superfluidity, coherence, and critical properties of these systems.

[1] I. Carusotto and C. Ciuti, *Rev. Mod. Phys.* **85**, 299 (2013).
[2] J. Kasprzak, M. Richard, S. Kundermann, A. Baas, P. Jeambrun, J. M. J. Keeling, F. M. Marchetti, M. H. Szymańska, R. Andre, J. L. Staehli, et al., *Nature* **443**, 409 (2006).
[3] N. Bobrovska, M. Matuszewski, K. S. Daskalakis, S. A. Maier, and S. Kéna-Cohen, arXiv:1603.06897.
[4] L. Dominici, M. Petrov, M. Matuszewski, D. Ballarini, M. De Giorgi, D. Colas, E. Cancellieri, B. Silva Fernandez, A. Bramati, G. Gigli, A. Kavokin, F. Laussy, and D. Sanvitto, *Nature Commun.* **6**, 8993 (2015).

Spin-orbitronics of nitride semiconductors

Alberta Bonanni

Institute for Semiconductor and Solid State Physics,
Johannes Kepler University, 4040 Linz, Austria

Besides their indisputable significance for optolectronics and high power electronics, gallium nitride (GaN) and related alloys possess also a number of features attractive for spin-orbitronics, enabling, in particular, spin-charge interconversion *via* spin-orbit coupling associated with inversion asymmetry and leading to a sizable Rashba field and piezoelectric properties.

On degenerate *n*-doped wurtzite GaN:Si films grown on semi-insulating GaN:Mn buffer layers by metal-organic vapor phase epitaxy, we have determined the magnitude of the Rashba parameter α_R=(4.5±1) meV Å from antilocalization magnetotransport studies carried out at millikelvin temperatures [1]. This value of α_R indicates, that in previous studies on electrons inproximity of GaN/(Al,Ga)N interfaces, bulk inversion asymmetry was dominant over structural inversion asymmetry. The comparison of experimental and theoretical values of α_R across a series of wurtzite semiconductors is presented as a test of current relativistic *ab initio* computation schemes [1].

Spin pumping, *i.e.,* the generation of spin currents under ferromagnetic resonance conditions, is an efficient mechanism for the inception of spin current and its conversion into charge current in non-magnetic metals or semiconductors *via* spin Hall effects. We have demonstrated the generation of pure spin current in bilayers of permalloy and *n*-GaN:Si – at room temperature and through spin pumping [2]. We have found for n-GaN:Si a spin Hall angle $\theta_{SH}=3.03\times10^{-3}$, exceeding by one order of magnitude those reported for other semiconductors,and pointing at III-nitrides as particularly efficient spin current generators.

Moreover, we have demonstrated – by direct magnetization measurements – the electrical control of the magnetization in wurtzite (Ga,Mn)N [3]. In this dilute magnetic insulator the Fermi energy is pinned by Mn ions in the mid-gap region, and the Mn^{3+} ions show strong single-ion anisotropy. We have established that (Ga,Mn)N sustains an electric field up to at least 5 MV/cm, indicating that Mn doping turns GaN into a worthwhile semi-insulating material. Under these conditions, the magnetoelectric coupling is driven by the inverse piezoelectric effect that stretches the elementary cell along the *c*-axis and, thus, affects the magnitude of the magnetic anisotropy. In this way, our work bridges two fields of research developed so far independently, namely: the piezoelectricity of wurtzite semiconductors and the electrical control of magnetization in hybrid and composite magnetic structures containing piezoelectric components.

The work was supported by the European Research Council (ERC, Project #227690) and by the Austrian Science Foundation (FWF, Projects #22477, #24471, #26830).

[1] W. Stefanowicz, R. Adhikari, T. Andrearczyk, B. Faina, M. Sawicki, J. A. Majewski, T. Dietl, and A. Bonanni, *Phys. Rev. B* **89**, 205201 (2014).
[2] R. Adhikari, M. Matzer, A. Tarazaga Martin-Luengo, and A. Bonanni, arXiv:1603.06471.
[3] D. Sztenkiel, M. Foltyn, G.P. Mazur, R. Adhikari, K. Kosiel, K. Gas, M. Zgirski, R. Kruszka, R. Jakiela, Tian Li, A. Piotrowska, A. Bonanni, M. Sawicki, and T. Dietl, arXiv:1604.06937.

Adiabatic approximation and fluctuations in exciton-polariton condensates

Nataliya Bobrovska[1], **and Michał Matuszewski**[1]

[1]*Institute of Physics Polish Academy of Sciences, Al. Lotników 32/46, 02-668 Warsaw, Poland*

We study the relation between two models commonly used to describe the dynamics of nonresonantly pumped exciton-polariton condensates: the complex Ginzburg-Landau equation (CGLE) and the open-dissipative Gross-Pitaevskii equation coupled to a separate equation for the reservoir density (ODGPE). We concentrate on the validity of the adiabatic approximation and small density fluctuations approximation that allow one to reduce the coupled condensate-reservoir dynamics to a single partial differential equation. We find that the adiabatic approximation consists of three independent analytical conditions that have to be fulfilled simultaneously. By investigating stochastic versions of the two corresponding models, we verify that the breakdown of these approximations can lead to discrepancies in correlation lengths and distributions of fluctuations. Additionally, we consider the phase diffusion and number fluctuations of a condensate in a box, and show that self-consistent description requires treatment beyond the typical Bogoliubov approximation. In the case of large fluctuations, when the adiabaticity conditions are no longer valid, the reduction of the generalized CGLE to ODGPE model is not possible.

N. Bobrovska, and M. Matuszewski, *Phys. Rev. B* **92**, 035311 (2015).

Stretching magnetism with an electric field in a nitride semiconductor

D. Sztenkiel[1], M. Foltyn[1], G.P. Mazur[1], R. Adhikari[2], K. Kosiel[3], K. Gas[1,4], M. Zgirski[1], R. Kruszka[3], R. Jakieła[1], T. Li[1], A. Piotrowska[3], A. Bonanni[2], M. Sawicki[1], and T. Dietl[1,5,6]

[1]*Institute of Physics, Polish Academy of Sciences, Warszawa, Poland*
[2]*Institut für Halbleiter - und Festkörperphysik, Johannes Kepler University, Linz, Austria*
[3]*Institute of Electron Technology, Warszawa, Poland*
[4]*Institute of Experimental Physics, University of Wrocław, Wrocław, Poland*
[5]*Institute of Theoretical Physics, University of Warsaw, Warszawa, Poland*
[6]*WPI-Advanced Institute for Materials Research, Tohoku University, Sendai, Japan*

The interplay between magnetic and electric properties of magnetic layers is of considerable interest owing to the perspective of exploiting the underlying mechanisms for the next generation of devices for information storage and processing. Several different ways have been exploited for the control of the magnetization vector by an electric field, including gating of thin ferromagnetic layers [1], electric and magnetic coupling in multiferroics [2] or strain in hybrid magnetic/piezoelectric devices [3]. Here we show that the application of an electric field along a polar axis in a wurtzite magnetic semiconductor leads to a sizable change of its crystalline magnetic anisotropy via the inverse piezoelectric effect. We investigate this unforeseen phenomenon experimentally and theoretically in an insulating paramagnetic wz-$Ga_{0,975}Mn_{0,025}N$ as a function of temperature, magnetic, and electric field, as detailed in Fig. 1.

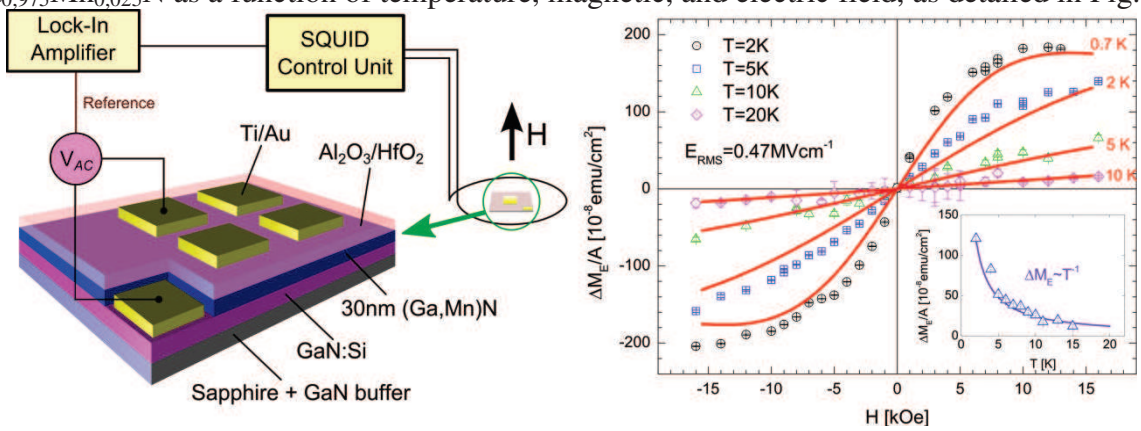

Fig. 1. Left panel: Sample structure and set-up for magnetization measurements in phase with an applied electric field. Right panel: Changes in the magnetization ΔM_E induced by an electric field of 0.47MV/cm applied to (Ga,Mn)N at selected temperatures as a function of the magnetic field applied along the hard axis. Curves: theoretical modeling employing known values of the piezoelectric constant and parameters of single-ion Mn^{3+} anisotropy. In order to account for ferromagnetic Mn-Mn interactions [4], simulations have been performed for effective temperatures (shown near curves). Inset: decrease of ΔM_E with temperature.

References

[1] H. Ohno et al., Nature 408, 944 (2000).
[2] W. Eerenstein, N. Mathur, and J. F. Scott, Nature 442, 759 (2006).
[3] C. Bihler, M. Althammer, A. Brandlmaier, *et al*, Phys. Rev. B 78, 045203 (2008).
[4] A. Bonanni et al., Phys. Rev. B. 84, 035206 (2011).

The work is supported by the Narodowe Centrum Nauki (Poland) through MAESTRO (2011/02/A/ST3/00125), OPUS (2013/09/B/ST3/04175) and FUGA (2014/12/S/ST3/00549) projects as well as by the EC EAgLE project.

Terahertz emission from semiconductor nanowires and non-stoichiometric layers: similarities and differences

Ieva Beleckaitė[1], Ramūnas Adomavičius[1], Renata Butkutė[1], Vaidas Pačebutas[1], Andrius Arlauskas[1], Aloyzas Šiušys[2], Anna Reszka[2], Janusz Sadowski[2,3] and Arūnas Krotkus[1]

[1] *Center for Physical Sciences and Technology, A. Goštauto g. 11, Vilnius, Lithuania*
[2] *Institute of Physics, Polish Academy of Sciences, al. Lotników 32/46, Warsaw, Poland*
[3] *MAX-Lab, Lund University, P.O. Box 118, Lund, Sweden*

Recently, low-dimensional semiconductor nanomaterials have attracted great attention due to their potential for infrared optoelectronics and photovoltaic applications. Also it has been reported that various nanostructures in comparison with bulk semiconductors are able to enhance terahertz (THz) emission from optically excited surfaces. This radiation is determined by the photo-excited electric dipoles which orientation is essential for an efficiency of THz emission. In this work we applied novel measurement techniques for investigation of radiating dipoles in two kinds of semiconductor nanostructures.

In present work, THz emission from molecular beam epitaxy grown Ga-rich GaAs layers and tilted semiconductor nanowires (NWs) was investigated. Experiments were performed using Ti:sapphire oscillator and low temperature grown GaAs antenna for THz electric field detection. THz pulse amplitude dependencies on an angle between the incident laser beam and a normal to the sample surface as well as THz emission azimuthal dependencies in transmission and reflection geometries were performed. We found that in our samples exist two types of THz radiating dipoles. Perpendicular to the semiconductor surface electric dipole is typical for GaAs substrate, whereas parallel dipole occurs due to excess Ga unevenly distribution in non-stoichiometric GaAs layer. In contrast the origin of electric dipole in tilted semiconductor NWs is photoexcited carriers moving along the NW. In this case we have parallel and perpendicular components of the same electric dipole. In tilted NW and some non-stoichiometric GaAs structures parallel to surface dipole is non-vanishing and significant at every sample orientation, whereas in other structures the influence of this dipole depends on azimuthal and excitation angles. Our investigation showed that parallel to the surface electric dipole enhances THz emission and changes intensity ration between reflection and transmission THz beam modes.

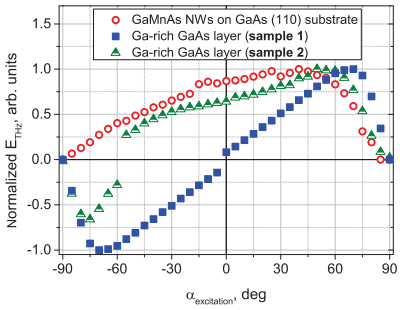

Figure 1: THz pulse amplitude dependencies on an angle between the incident laser beam and a normal to the sample surface for the removed GaMnAs nanowires (NWs) layer and two Ga-rich GaAs layers.

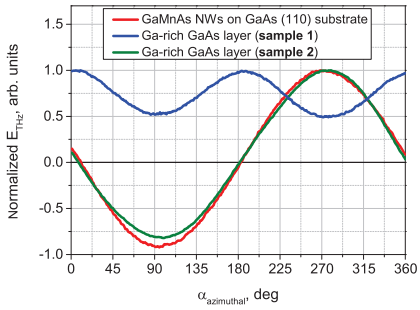

Figure 2: THz emission azimuthal dependencies of the removed GaMnAs NWs layer and two Ga-rich GaAs layer.

Intrasurface Electron Transitions Change of Adsorption Energy at Surfaces of Semiconductors - Mechanism and Consequences to Growth and Doping of Crystals and Layers

Stanisław Krukowski, Pawel Kempisty, Pawel Strąk, Konrad Sakowski
Institute of High Pressure Physics, Polish Academy of Sciences, Sokołowska 29/37, 01-142 Warsaw, Poland

Results of *ab initio* simulations indicate that proper description of semiconductor crystal growth needs considerable modification of the standard Burton, Carbera Frank (BCF) model. These changes include electronic degrees of freedom, not present in the classic formulation. In particular they involve change of pinning of Fermi level at the surface which is determined using extended electron counting rule (ECR) that may be applied to the case of the species adsorbed at the surface. In this work the simulations of adsorption of a large number of molecular and atomic species at various semiconductor surfaces are summarized and discussed. It is shown that during adsorption of ammonia, hydrogen, nitrogen and silicon at GaN(0001), GaN(000$\underline{1}$), AlN(0001) and SiC(0001) surfaces, an additional contribution from intrasurface electron transition changes their adsorption energy. The model of such contribution is presented and critically discussed. According to the new model the adsorption energy is changed by several electronvolts, at change of the pinning of the Fermi level between different surface states. Such change may involve not only the variation of the energy of the adsorbate but also it may lead to different conformation and the location at the surface. From the model it follows that for Fermi level pinned at the surface, the adsorption energy is not dependent on the doping in the bulk but for Fermi level it is. The thermodynamics of the surface-vapor equilibrium is presented with critical analysis regarding the presented formalism based on chemical potential identification of most stable structure of the surface. It is augmented by Langmuir type picture of vapor-surface equilibrium at various level of chemical potential, i.e. vapor temperatures and partial pressures. The results indicate that most of the cases of the growth of semiconductors occurs in the condition for which the Fermi level is not pinned at the surface. Therefore the adsorption energy depends on the Fermi level position in the bulk, i.e. on doping of the bulk semiconductors. Such dependence of the adsorption energy provides basic explanation of the step motion dynamics, incorporation of dopants during growth and surfactant effects. The consequences of these findings on the growth and doping of semiconductor crystals and layers are discussed.

Efficient emission from InAlGaAs single quantum dots with low lattice misfit and AlGaAs indirect bandgap barrier

T. Słupiński, K. P. Korona and J. Borysiuk

Faculty of Physics, University of Warsaw, Warsaw, Poland

We report on the MBE growth of single quantum dots (QD) of quaternary InAlGaAs with AlGaAs barrier and strong emission of red light from single QD. Such QDs might be used as single photon sources in the red range. Indirect bandgap AlGaAs barrier applied allowed to lower photon emission in the barrier and to enhance energy transfer to QDs. Low In content decreased a dot-barrier lattice misfit and, consequently, internal strain in QD, and resulted in an enhanced single QD emission, comparing to e.g. InAs/GaAs.

We discuss the influence of MBE-growth parameters on the intensity of "zero-phonon" emission and on low-temperature (T < 10K) broadening of single QD emission line. We have observed that stronger emission from a single QD is obtained for: (1) InAlGaAs alloys with smaller dot-barrier lattice mismatch and (2) higher MBE growth rate of QD layer, which yields smaller QD size. We have also noticed that lowered lattice misfit had resulted in a relatively wider range of epitaxial growth conditions of efficient emission from single QDs. We discuss those observations by the role of growth-influenced static inhomogeneous distortions of crystal lattice inside the QD on an increased probability of photon + phonon emission, using an analogy to the acoustic phonons effect at increased temperature. Within the picture discussed, a lower photon emission intensity and larger width of emission line from single QD is related to a degree of inhomogeneous strain inside the QD leading to higher Huang-Rhys factor.

MBE growth and properties of quaternary $In_{1-x}(Al_yGa_{1-y})_xAs$ self-assembled QDs in $Al_yGa_{1-y}As$ barrier with low In and high Al content ($1-x = 0.4$, $y = 0.75$) grown on GaAs(001) substrates were studied. The In content was close to the low limit of self-assembled QD formation in Stranski-Krastanov (S-K) growth, usually reported as $1-x \sim 0.2$-0.3. The average size of dots and dot surface density could be controlled by the deposition rate and total excess deposition over h_{crit} – a critical thickness deposited for 2d/3d QD transition. QDs size dependence on metals molecular beam flux intensity (deposition rate) is discussed within a kinetic nucleation and growth model including two competing processes: (1) new dots nucleation after locally overcoming of h_{crit} and (2) size increase of nucleated dots, involving surface diffusion of adatoms.

Efficient single quantum dot emission was observed by microphoto-luminescence (μ-PL) in the red range λ = 650-730 nm (Fig. 1). Low temperature μ-PL single dots emission linewidth ≥0.2 nm observed in InAlGaAs indicates a broadening of single dot emission line, as compared to natural linewidth estimated from time-resolved μ-PL, $\hbar/\tau \sim 1\,\mu eV$ (Fig.1). We relate this broadening to the presence of static lattice disorder inside InAlGaAs QD, considering Fourier components of static inhomogeneous lattice distortions and the matrix element of exciton-lattice coupling in deformation potential approximation. The phonon emission discussed contributes to the μ-PL linewidth and to QD emission intensity by higher Huang-Rhys factor.

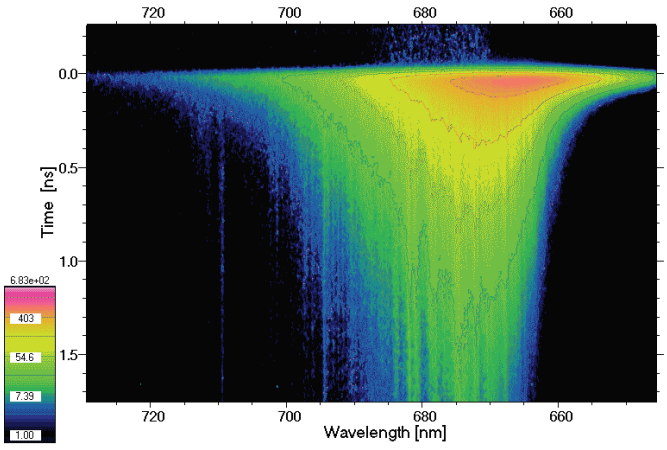

Fig.1. Time-resolved micro-photoluminescence of InAlGaAs/AlGaAs QDs at 4 K. Sharp single dot emission lines show relatively long lifetime $\tau \sim$ 1-1.5 ns, while shorter average lifetime is seen for broad unresolved ensemble emission band.

Acknowledgements: Research is supported by National Research Council (NCN), Poland, grant No. 2012/05/B/ST7/02155

The Role of Phonons for the Optical Control of Excitons and Biexcitons in Semiconductor Quantum Dots

Tilmann Kuhn

Institut für Festkörpertheorie, Westfälische Wilhelms-Universität Münster, Wilhelm-Klemm-Str. 10, 48149 Münster, Germany

Semiconductor quantum dots (QDs) are attractive candidates for a variety of new applications in fields such as quantum cryptography or quantum information processing, where the presence of discrete energy levels is mandatory. Examples of such applications are single-photon sources, sources of entangled photon pairs and qubit devices or quantum gates. The functionality of these applications relies on the preparation of a well-defined quantum state. Therefore, a precise optical control of excitonic and biexcitonic states in semiconductor QDs is a crucial step towards their usage in quantum information technology. Since QDs are embedded in a semiconductor matrix, their interaction with phonons often plays a major role in the preparation process.

In most QDs the fundamental excitons are of heavy hole type consisting of a hole with angular momentum ±3/2 and an electron with spin ±1/2. The excitons can then be divided in two classes, those with total angular momentum ±1, which correspond to dipole-allowed transitions and are therefore called *bright excitons*, and those with total angular momentum ±2, which are dipole-forbidden and therefore called *dark excitons*. The biexciton consisting of two electron-hole pairs has vanishing angular momentum and is dipole-coupled to the bright excitons.

For the four-level system consisting of ground state, bright excitons and biexciton different techniques have been employed to selectively prepare exciton or biexciton states [1]. The most direct way is to use a resonant laser pulse which, in the absence of phonons, for a suitable choice of the pulse area provides a complete inversion, i.e., a complete excitation of the exciton or biexciton. An alternative is the excitation by a chirped laser pulse which, due to the phenomenon of *adiabatic passage,* results in an excitation which is much less sensitive to pulse and material parameters. For both processes the exciton-phonon interaction limits the fidelity, which gives rise to restrictions in the range of pulse parameters and temperature. Using detuned pulses, a phonon-assisted exciton or biexciton generation can be employed, which relies on the exciton-phonon coupling and thus even works better for stronger coupling.

Dark excitons have the advantage of rather long lifetimes. However, they cannot directly be excited optically. It has recently been shown that the combination of a chirped laser pulse and a tilted magnetic field nevertheless allows for an efficient optical generation of dark excitons [2]. A suitably chosen in-plane component of the magnetic field weakly couples bright and dark exciton which, in combination with the adiabatic passage effect, gives rise to a population inversion between ground state and dark exciton. For low temperatures this mechanism turns out to be almost unaffected by phonons. On the other hand, also in the case of dark excitons a parameter regime can be found for which an efficient phonon-assisted dark exciton generation takes place.

[1] D. E. Reiter, T. Kuhn, M. Glässl, and V. M. Axt, J. Phys.: Cond. Mat. **26**, 423203 (2014).
[2] S. Lüker, T. Kuhn, and D. E. Reiter, Phys. Rev. B **92**, 201305(R) (2015).

Self-assembly of Single Crystal Rare-earth Monopnictide Nanostructures in III-V Epilayers

Chris J. Palmstrøm,

University of California, Santa Barbara, Electrical and Computer Engineering and Materials, Santa Barbara, California, United States

Epitaxial rare earth monopnictide (RE-V) nanostructures embedded within a III-V semiconductor matrix are of great interest due to a number of exciting electrical and magnetic properties, including phonon scattering for high ZT thermoelectrics and sub-picosecond carrier lifetimes for terahertz devices. Most work on this nanocomposite system has focused on embedded RE-V nanoparticles, e.g. ErAs or ErSb nanoparticles embedded in GaAs (001) and GaSb (001).

This presentation will focus on the growth of highly anisotropic Er-group-V (Sb and As) nanostructures embedded in a III-V semiconductor matrix by self-assembly during molecular beam epitaxial growth of Er_xIII_{1-x}-V by codeposition. In-situ scanning tunneling microscopy in combination with molecular beam epitaxy allows for atomic scale characterization during different stages of growth. For growth of GaSb(001) with increasing Er concentration, ErSb embedded nanostructures change from nanoparticles to vertical nanorods, nanotrees, horizontal nanorods and nanosheets[1]. The resulting $Er_xGa_{1-x}Sb$ nanocomposites are single crystalline with a continuous Sb-sublattice. The vertical nanorods are continuous throughout the $Er_xGa_{1-x}Sb$ layer, their axes are parallel to the [001] growth direction, and they self-assemble into ordered arrays aligned along the [-110] direction. The horizontal nanorods grow in the [-110] direction.

In the case of GaAs, ErAs nanorods can also form by self-assembly during molecular beam epitaxial growth of $Er_xGa_{1-x}As$ by codeposition. In this case the nanorod formation with the rods growing in the <211> direction was found for growth on GaAs (h11)A surfaces. In contrast, ErAs nanorods do not form on GaAs (h11)B or GaAs (001) surfaces.

Scanning tunneling spectroscopy and angle resolved photoemission spectroscopy were used to measure the electronic bandstructure of embedded RE-V nanostructures of varying dimensions, namely 0D nanoparticles, 1D nanorods, and 2D thin films.

The growth mechanisms for $Er_xGa_{1-x}Sb$ and $Er_xGa_{1-x}As$ that result in embedded vertical and horizontal nanorod formation will be discussed. The atomic scale growth mechanisms are a result of surface diffusion and wetting characteristics which are used to explain the differences for the self-assembly of nanostructures for $Er_xGa_{1-x}Sb$ and $Er_xGa_{1-x}As$.

[1] J. K. Kawasaki, B. D. Schultz, H. Lu, A. C. Gossard, and C. J. Palmstrøm, *Nano Letters* **13**, 2895 (2013)

Phase Separation in IV-VI Alloys – Generation of Thermodynamically Stable Nano-Features

Yaniv Gelbstein

Department of Materials Engineering, Ben-Gurion University of the Negev, Beer-Sheva, Israel. e-mail: yanivge@bgu.ac.il

In the recent years, many efforts were made for generation of nano features in bulk thermoelectric materials for enhancement of the thermoelectric figure merit via the reduction of the lattice thermal conductivity. Taking into account that thermoelectric direct converters from heat to electricity, without involving of any moving parts, exhibit a major stability advantage for long-term operation, compared to many other competing conversion methods, the stability of nano-featured bulk thermoelectric materials is a major issue for consideration.Such converters usually operate under high temperatures and large temperature gradientsconditions, which can affect the stability of the nano-features embedded in the bulk thermoelectric main phases. As an example, one popular production method of nano-featured bulk materials is based on rapid consolidation (e.g. Spark Plasma Sintering) of nano powders obtained by melt spinning or energetic ball milling. Yet, grain coarsening effects can result in gradual deterioration of the nano-structures and thermoelectric performance degradation upon long-term high temperatures operation.

In the current research, an alternative, thermodynamic nano-features generation approach in bulk IV-VI based thermoelectric materials, was considered, using controlled phase separation conditions according to the relevant phase diagrams. Specific systems showing amiscibility gap, including the PbTe-GeTe and PbTe-PbS systems, were heat treated under various required conditions for promoting spinodal decomposition and nucleation and growth reactions. High ZT values of up to 2.2 were obtained due to combined optimal doping and sub-micron phases' decomposition features. Such features were found as thermodynamically stable under long-term investigation at temperatures up to 400^{o}C, resulting in almost unchanged figure of merit values after the various investigated heat treatment durations.

	SATURDAY	SUNDAY
	School Special Tutorial Session	
		Start - 11:45
		Coronado Sul1
		Break
	ARRIVAL	Coronado Sul1
13:00 - 14:30	*LUNCH*	*LUNCH*
	SCHOOL OPENING	
14:30 - 16:15	Blundell Sal1	Malic Sul2
	Break	*Break*
	Blundell Sal1	Malic Sul2
16:15 - 16:45	*Coffee Break*	*Coffee Break*
16:45 - 18:30	Dybko Sal2	Schlom Sul3
	Break	*Break*
	Dybko Sal2	Schlom Sul3
18:30 - 19:30	*BARBECUE*	*DINNER*
		CONCERT + WELCOMING

	MONDAY	TUESDAY	WEDNESDAY	THURSDAY	FRIDAY
	OPENING				
9:00 - 10:45	Wadley Mol1	Xiong Tul1	Ciorga Wel1	Zieliński Thl1	
	Grzybowski - MoO1	Galkowski - TuO1	Kolasiński - WeO1	Matuszewski Thl2	*Start - 10:00*
	Oreszczuk - MoO2	Białek - TuO2	Syperek - WeO2		Kuhn Frl1
	Goryca - MoO3	Grankowska Ciechanowicz - TuO3	Debus - WeO3	Bobrovska - ThO1	
	Heisterkamp - MoO4	Kaczmarski - TuO4	Zhou - WeO4		
10:45 - 11:15	*Coffee Break*	*Coffee Break*	*Coffee Break*	*Coffee Break*	*Coffee Break*
11:15 - 13:00	Vanmaekelbergh Mol2	Nanishi Tul2	Kozuka Wel2	Bonanni Thl3	Palmstrøm Frl2
	Janróz - MoO5	Strak - TuO5	Krzywda - WeO5	Foltyn - ThO2	Gelbstein Frl3
	Mreńca-Kolasińska - MoO6	Kobayashi Tul3	Kazimierczuk - WeO6	Beleckaitė - ThO3	
	Łopion - MoO7		Sawicki - WeO7	Krukowski - ThO4	*CLOSING*
	Dulek - MoO8		Gawarecki - WeO8	Słupiński - ThO5	
13:00 - 14:30	*LUNCH*	*LUNCH*	*LUNCH*	*LUNCH*	*LUNCH*
14:30 - 15:30	*MONDAY POSTER SESSION A*	*TUESDAY POSTER SESSION A*	*WEDNESDAY POSTER SESSION A*	*EXCURSION*	*DEPARTURE*
18:30 - 19:30	*DINNER*	*DINNER*	*DINNER*		
19:30 - 21:00	Dietl Mol3	*Start - 20:00*	Szade Wel3	*Start - 20:00*	
	Majewicz - MoO9	Popielska - TuO6	Potasz - WeO9	*BANQUET*	
	Galicka - MoO10	Binder - TuO7	Rechciński - WeO10		
	Buczko - MoO11	Smoleński - TuO8	Łepkowski - WeO11		
		Klopotowski - TuO9			
		Jadczak - TuO10			
		Molas - TuO11			
21:00 - 22:00	*MONDAY POSTER SESSION B*	*TUESDAY POSTER SESSION B*	*WEDNESDAY POSTER SESSION B*		